The Emergence of Continuum Gravitational Physics from Group Field Theory Models of Quantum Gravity

Roukaya Dekhil

München 2023

The Emergence of Continuum Gravitational Physics from Group Field Theory Models of Quantum Gravity

Roukaya Dekhil

Dissertation
der Fakultät für Physik
der Ludwig-Maximilians-Universität
München

vorgelegt von
Roukaya Dekhil
aus Tunesien

München, den 31.07.2023

Erstgutachter: Dr. Daniele Oriti
Zweitgutachter: Prof. Stefano Liberati
Tag der mündlichen Prüfung: 05.10.2023

Contents

List of Figures

List of Tables

Abstract

Quantum Gravity (QG) theories pursue the goal of reconciling the pillar theories of General Relativity (GR) and Quantum Field Theory (QFT) in theoretical physics and a coherent description of the physical world surrounding us. This prosperous field of research is a crossroad of various disciplines in physics, ranging from the phenomenological to the most abstract mathematical ones.

In this thesis, we devote our focus to the emergence of continuum gravitational physics from the QG background independent approach of Group Field Theory (GFT). In particular, we explore its relation to other QG models such as Spin Foam (SF) in the context of model-building of $4d$ Lorentzian quantum geometries, the interface between quantum entanglement (considered as the preview of emergence) and quantum geometry through the exploitation of spin network states characterizing quantum geometries, and finally the culminating stage of extracting an effective description of the cosmological version of the theory in the language of a field theory propagating on a curved background. More precisely, the three research focal points of this thesis are summarized as follows:

First, we present the construction of a new SF model for $4d$ Lorentzian quantum gravity based on the description of quantum simplicial geometry relying on *edge vector* variables. On the representation theoretic side, quantum states of geometry are built from irreducible representations of the translation group on Minkowski space or functions on the translation group itself. We also show how the new model connects to the Lorentzian Barrett-Crane Barrett-Crane (BC) spin foam model, for a sector of its quantum configurations. The new model manifestly possesses all the relevant degrees of freedom to describe simplicial geometry at the quantum level and thus constitutes a promising proposal for Lorentzian quantum gravity. Hence, it may be seen also as a completion (or a necessary reference point) for known spin foam models based on constrained BF quantization and a formulation of quantum geometry in terms of quantum edge vectors.

We then move on to inspecting the entanglement/geometric characterization of generic superposed quantum geometries. The proposal that spacetime and its geometric properties are emergent entities from purely non-geometric degrees of freedom that are subsequently closely related to entanglement measures has attracted a lot of attention in the sector of quantum information Quantum Information Theory (QIT). We present a straightforward implementation of these techniques in QG models where we focus on a particular

set of QG states. More concretely, we show how studying the entanglement properties of a superposition of QG states, precisely spin network graph states endowed with different combinatorial structures, naturally leads to a generalization of the usual von Neumann entropy obtained for spin network states in Loop Quantum Gravity (LQG) calculations. This is indeed achieved once we borrow different entropic notions and measures from quantum information theory, wherein the studied case of the superposition of states, the von Neumann entropy of entangled regions gives rise to the so-called interaction entropy in QIT already at the kinematical level of the theory.

Lastly, in the absence of any notion of metric background or alternatively, in the presence of diffeomorphism invariance in the theory, the available technology to generate the dynamics is to employ the relational framework. A GFT model where this has been implemented is available and importantly it succeeded in extracting continuum physics in a cosmological context relying on GFT condensates, and more precisely that of a homogeneous Friedmann–Lemaître–Robertson–Walker (FLRW) universe with perturbations included. Starting from such results, we derive the explicit solution to the GFT condensate effective dynamics including the treatment of scalar perturbations. This first step allowed us to investigate further the matter content, and formulate its dynamics in the form of field theory on a curved background. This in turn produced additional emergent properties the field theory possesses in comparison with the classical one, which was further mirrored at the level of the perturbation. Where it the latter case, we attained a modified dispersion relation for the perturbed scalar field.

Abstrakt

QG-Theorien streben danach, die grundlegenden Theorien von GR und QFT in der theoretischen Physik mit einer kohärenten Weltbeschreibung in Verbindung zu bringen. Dieses dynamische Forschungsgebiet ist eine Kreuzung verschiedener physikalischer Disziplinen, die von der phänomenologischen bis hin zur abstrakten mathematischen Physik reichen. In dieser Arbeit widmen wir uns der Entstehung der Kontinuumsgravitationsphysik aus dem QG-Hintergrund unabhängigen Theorie der GFT. Insbesondere untersuchen wir seine Beziehung zu anderen QG-Modellen wie SF im Rahmen der Modellbildung für $4d$ Lorentzsche Quantengeometrien, die Berührung zwischen Quantenverschränkung (als Preview von Entstehung) und Quantengeometrie durch die Ausnutzung von Spin-Netzwerk-Zuständen, die Quantengeometrien charakterisieren, und schließlich die kulminierende Phase der Extraktion einer effektiven Beschreibung der kosmologischen Fassung der Theorie in der Sprache einer Feldtheorie, die sich auf einem gekrümmten Hintergrund ausbreitet. Diese Forschungsschwerpunkte dieser Dissertation lassen sich wie folgt präzise zusammenfassen:

Zunächst stellen wir die Konstruktion eines neuen SF-Modells für $4d$ Lorentz'sche Quantengravitation vor, das auf der Beschreibung einer vereinfachten Quantengeometrie beruht, die sich auf *edge vector*-Variablen stützt. Auf der repräsentationstheoretischen Seite werden Quantenzustände der Geometrie aus irreduziblen Darstellungen der Translationsgruppe auf dem Minkowski-Raum oder Funktionen auf der Translationsgruppe selbst gebildet. Wir zeigen auch, wie das neue Modell mit dem Lorentzschen Barrett-Crane BC-Spinschaum-Modell für einen Sektor seiner Quantenkonfigurationen zusammenhängt. Das neue Modell besitzt offensichtlich alle relevanten Freiheitsgrade, um die vereinfachte Geometrie auf Quantenebene zu beschreiben, und stellt somit einen vielversprechenden Vorschlag für die Lorentzsche Quantengravitation dar. Es kann daher auch als Ergänzung (oder notwendiger Bezugspunkt) für bekannte Spin-Schaum-Modelle angesehen werden, die auf einer eingeschränkten BF-Quantisierung und einer Formulierung der Quantengeometrie in Form von Kantenvektoren basieren.

Anschließend untersuchen wir die Verschränkung/geometrische Charakterisierung von generischen überlagerten Quantengeometrien. Der Vorschlag, dass die Raumzeit und ihre geometrischen Eigenschaften aus rein nicht-geometrischen Freiheitsgraden entstehen, die dann wiederum eng mit Verschränkungsmaßen verknüpft sind, hat im Bereich der Quanteninformation QIT viel Aufmerksamkeit erregt. Wir stellen eine unkomplizierte Umsetzung dieser Techniken in QG-Modellen vor, bei denen wir uns auf eine bestimmte

Gruppe von QG-Zuständen konzentrieren. Konkret zeigen wir, wie die Untersuchung der Verschränkungseigenschaften einer Überlagerung von QG-Zuständen, genauer gesagt von Spin-Netzwerk-Graph-Zuständen mit unterschiedlichen kombinatorischen Strukturen, auf natürliche Weise zu einer Verallgemeinerung der üblichen von-Neumann-Entropie führt, die für Spin-Netzwerk-Zustände in LQG-Berechnungen erhalten wird. Dies wird in der Tat erreicht, wenn wir verschiedene entropische Begriffe und Maße aus der Quanteninformationstheorie entlehnen, wobei der untersuchte Fall der Überlagerung von Zuständen, die von-Neumann-Entropie verschränkter Regionen bereits auf der kinematischen Ebene der Theorie zur so genannten Interaktionsentropie in QIT führt. Darüber hinaus wird ein Vergleich zwischen dem zweiten Quantisierungsformalismus dieses Schemas, der auf der Überlagerung von Zuständen beruht, und dem der LQG-Ergebnisse vorgestellt.

Schließlich besteht die verfügbare Technologie zur Erzeugung der Dynamik in der Verwendung des relationalen Rahmens, wenn kein Begriff des metrischen Hintergrunds oder alternativ dazu die Diffeomorphismusinvarianz in der Theorie vorhanden ist. Ein GFT-Modell, in dem dies umgesetzt wurde, ist verfügbar, und vor allem ist es gelungen, Kontinuumsphysik in einem kosmologischen Kontext zu extrahieren, der auf GFT-Kondensaten beruht, genauer gesagt in einem homogenen FLRW-Universum mit eingeschlossenen Störungen. Ausgehend von diesen Ergebnissen leiten wir die explizite Lösung der effektiven Dynamik von GFT-Kondensaten her, die auch skalare Störungen berücksichtigt. Dieser erste Schritt ermöglichte es uns, den Materiegehalt weiter zu untersuchen und seine Dynamik in Form einer Feldtheorie auf einem gekrümmten Hintergrund zu formulieren. Dies wiederum führte zu zusätzlichen emergenten Eigenschaften, die die Feldtheorie im Vergleich zur klassischen Theorie besitzt, was sich auch auf der Ebene der Störung widerspiegelt. Im letzteren Fall haben wir eine modifizierte Dispersionsrelation für das gestörte Skalarfeld erhalten.

List of Abbreviations

AdS Anti de Sitter 2

AG Analog Gravity 146

BC Barrett-Crane xi

BEC Bose Einstein Condensate 152

BF Background Field B and F ix

CFT Conformal Field Theory 2

CMB Cosmic Microwave Background 4

CPS Coherent Peaked State 76

EFT Effective Field Theory 165

EH Einstein-Hilbert 17

EPRL Engle-Pereira-Rovelli-Livine 17

ETG Extended Theories of Gravity 146

FLRW Friedmann–Lemaître–Robertson–Walker xii

GFT Group Field Theory xi

GL Ginzburg-Landau 181

GR General Relativity xi

LQG Loop Quantum Gravity xii

MGT Modified Gravity Theories 146

QFT Quantum Field Theory xi

QG Quantum Gravity xi

QIT Quantum Information Theory xi

QM Quantum Mechanics 11

SF Spin Foam xi

TN Tensor Networks 182

List of Symbols

$*$	Complex conjugate	σ	Condensate wavefunction
$\delta\phi$	Perturbed matter scalar field	$\star$	Hodge dual
ℓ_P	Planck length	θ	The condensate phase in GFT
η_{IJ}	Minkowski metric	φ	Group Field Theory field
χ	Scalar field	$\vec{\alpha}$	Data associated to open spin network
$\mathfrak{g}$	Lie algebra of the Lie group G	c	Speed of light
Γ	Graph in LQG kinematical sector	d	Spacetime dimension
γ	Graph in GFT kinematical sector	d_j	Dimension of the representation j
$\hat{N}$	Number operator in GFT	e	Tetrad frame
$\hat{V}$	Volume operator in GFT	G	Lie group
$\hbar$	Reduced Planck constant	$g_{\mu\nu}$	Spacetime metric tensor
ι	Intertwiner basis label	I	Intertwiner
$\mathcal{I}$	Intertwiner space	j	Spin representation label
G	Newton constant	M	Spacetime manifold
ϕ_0	Background matter scalar field	S^β	Simplicity constraint operator
ρ	The condensate density in GFT	S_{GFT}	Group Field Theory action

Declaration

This dissertation is based on research done at the Ludwig Maximilian University of Munich (LMU) between September 2020 and July 2023. No part of it or anything substantially the same has been previously submitted for a degree or any other qualification at this or at any other University. This thesis is the result of the author's own work and of the scientific collaboration listed below. The work presented in this dissertation is based on three papers (to appear) listed below.

1. Roukaya Dekhil, Eugenia Colafranceschi, and Daniele Oriti. "Entanglement in superpositions of spin network states with different graph structures" (to appear).

2. Roukaya Dekhil, Matteo Laudonio, Daniele Oriti, Adrian Tanasa. "A new spin foam model of quantum geometry based on edge vectors" (to appear).

3. Roukaya Dekhil, Stefano Liberati, Daniele Oriti. "Cosmological group field theories as a field theory on curved spacetime" (to appear).

Chapter 1

Introduction

The quest for a quantum theory of gravity is still in pursuit in the field of theoretical physics and perhaps at its most glorious stages thanks to the active dialog between the various research fields and the constant developments and flow of information provided by cosmological observations. Indeed, there has been a lot of recent progress to solve the riddle of quantizing GR in the last several decades [3], bringing together the collective effort of several research communities, tackling the various facets of the problem of QG. In particular, the conceptual issues plaguing GR and QFT have called for the intervention and input provided by the philosophy and foundations of the physics community [4–7], since most of the raised questions in this regard are present in very different approaches to QG reflecting the remarkable and unique blueprint of the physics of QG. In parallel to this, the desperate need to be in contact with observations any theory of QG exhibits brings forth the different attempts to derive physical predictions subject to observations [8, 9]. This, in turn, has called for the craft of the phenomenology of QG as well experimental physics [10–13], inspirations from condensed matter physics, and taking initiatives to investigate QG signatures in numerical GR (the army of researchers behind the inquiry of gravitational waves).

Yet the problem of QG *is* still remnant and presents itself as a prosperous field of research, and a promising one when it comes to acquiring a deeper understating of the world surrounding us. Indeed, already contemplating the lessons we have learned from QFT and GR is the very reason why the quest of QG was born. In particular, with the discovery of GR and QFT, the distinctive fundamental notions of matter, space, time, causality, and measurements have been undergoing a great deal of redefinitions since the time of Plato, Copernicus, and Newton. What is interesting in this situation is that, on the one hand, when QFT successfully describes matter (particles) and their *quantum* interactions, whether being of strong, weak, or electromagnetic nature, it fails to provide a similar synthesis for the gravitational sector. On the other hand, GR describes with amazing accuracy the physical phenomena at *large* scales with the revolutionary concept of the smooth *spacetime* fabric, treating time and space on equal footing and how matter behaves in it, however only to some extent, since it exhausts all of its power when it enters the quantum realm.

Now, the main apprehensive approaches to bring together these aspects of the theories rely on the straightforward quantization of GR to extract a corresponding quantum theory of gravity. Some models apply quantization schemes directly to the full spacetime geometry, for instance, canonical loop quantum gravity [14, 15]; others follow path integral formulations of quantum gravity [16, 17] and their modern evolution mostly based on lattice structures e.g. causal dynamical triangulations [18] or group field theories GFT [19] which is *the* framework this thesis is based on. String theory [20], started as a tentative enhancement to the graviton-based formalism to QG, naturally resulting from considering extended string-like (and brane-like) variables. It has as well mirrored striking quantum aspects of the gravitational field despite the absence of a more fundamental description of its microscopic nature. All these approaches agree on the quantum nature of spacetime, but more importantly, they inevitably hint towards a more *fundamental* structure constituting the very core of gravity. Despite this vast landscape of diverse, yet complementary, approaches to the problem of QG, these models commonly indicate the crucial change in perspective towards the quantum nature of spacetime [21, 22], namely that the fundamental nature of our usual notion of continuous spacetime is tightly related to the idea of building blocks as "atoms of space", of no direct gravitational, spatiotemporal or geometric interpretation, and from which it has to *emerge*, whence, giving rise (probably in a suitable approximation) to the usual notion of geometry, gravity, and fields, producing the physics we are familiar with. There are several proposals to the very nature of the emergence of spacetime in this picture, among the most popular ones is the exploitation of the quantum property of *entanglement* [23–25] and adapting a *mean-field theory* approach [21, 26]. The argument supporting the first path is supported by a handful of results in QG and beyond [27–30], we can mention those obtained from the duality between the gravitational theory of asymptotically Anti de Sitter (AdS) spacetime and a Conformal Field Theory (CFT) living on the boundary of the latter, known as the AdS/CFT correspondence (conjecture) [31, 32] as well the one extracted with the background independent GFT approach [33–35]. What distinguishes the calculation carried out from a GFT perspective is that the theory is defined as the quantum field theory *of* spacetime, where the quanta are simplicial complexes, for instance in $4d$ they are tetrahedra, that get entangled by gluing them in an algebraic combinatorial manner. The entanglement of the quantum geometry can be expressed and fully characterized by the technology provided by QIT [36–39]. We will probe this aspect further in this thesis.

The focus in the second route into achieving an emergent continuum spacetime through the mean-field theory approach is based on studying the continuum phase space of QG models, where we restrict our attention to GFT's, inspired by the techniques employed in condensed matter physics [40, 41]. We can see the emergence of spacetime through the lenses of condensed matter physics as a phase transition from some fundamental microscopic degrees of freedom to a continuum *condensate* one [21, 22, 42]. If we take seriously the perspective of quantum geometry being a quantum many-body system, then indeed a phase transition is inevitable for the emergence to occur. In the context of a condensate phase, one can then adapt a mean field approach to extract an effective description to get access to the new As we will see in this thesis, this is the route that (by far) made contact

with the physics at the classical regime and particularly the cosmological sector of it. In reality, it does not only succeed in reproducing the standard continuum limit but it also comes with the natural advantage of providing answers to the very inquiries the classical theories of GR and QFT failed to address. Indeed, the most urgent problem of a consistent theory of quantum gravity is to provide a well-defined predictive theory over a wide range of scales, and hence renormalizable, implying that it should possess a controlled continuum limit. Furthermore, a candidate theory for QG should succeed in providing consistent physical predictions to the theoretical as well as observational constraints posed in the cosmological sector and beyond, with the recent observation of gravitational waves and the confirmation of the existence of black holes [43–45]. Therefore a predictive theory of QG should pass these complementary consistency checks.

Outline of the thesis

We sketched above the general idea of the problem of quantum gravity that is born to reconcile the current theories of GR and QFT. In order to grasp and fully capture the model-building process of any theory of QG, we need to identify and comprehend the various components that enter such a mechanism. We delve into this already in the second chapter of the thesis (chapter 2), where we discuss in more detail the *fundamental* ingredients that any theory QG should take into account by pointing to their necessary role in the existing theories of GR and QFT. In chapter 3 we explore several background independent approaches to QG that are based on *first* discretizing geometry to isolate the supposedly fundamental building blocks of the fabric of spacetime geometries, and *then* quantizing this entity. More precisely we will show how the formulation of GR in a background independent manner is made possible by pointing out its relation to the so-called BF theories. We will indeed present how we can recover GR by constraining a BF theory in $4d$. In turn, this constraint must also be quantized when we transition to the quantum description of the discretized geometry. In fact, this very step of quantizing is the most relevant one to chapter 5 of this thesis, exactly for the reason that this step is what distinguishes a QG from its relative (in a broader way). In this context, we will focus on the covariant quantization approach to GR or shortly SF models, for its relevance to the GFT framework. After this step, we will see that the common lesson we can learn from quantizing GR either canonically or covariantly or by means of introducing a QFT over group manifolds (GFT's) the prominent state that encodes the quantum nature of the discrete geometry is captured by *spin network states.* Therefore, we will spend some time discussing their properties, their geometric interpretations, and the spaces they live in. After this brief journey through the existing models, solved and unresolved issues within them, we propose a new SF model for $4d$ Lorentzian quantum gravity based on an edge vector description (in contrast to the common area variable description) and its implementation within GFT in chapter 5. This is motivated by curing some of the problems that arise from the quantization of the above-mentioned constraints in commonly considered SF models. We then move on to the investigation of the role of entanglement characterizing the most generic quantum state

of geometry, namely that of a superposition of spin network states with different graph structures in chapter 6. In particular, we will show how we can extract information about the connectivity of the quanta of spacetime accomplished through the entropic calculation of the entanglement braiding the quantum fabric of geometry. Note that in this chapter we do not address the more ambitious goal of coarse-graining such states due to the lack of technology to pursue it. However, as we already emphasized above, we do this relying on the mean-field approach to achieving the emergence of continuum physics in chapter 7. We rely on the machinery of the GFT condensate effective (mean-field) cosmology and its success in reproducing a homogeneous isotropic FLRW universe, where in this picture, the classical singularity is washed away by the presence of a quantum bounce. This is the ancillary data starting from which we derive a classical field formulation of GFT on a curved background. More importantly, we perform this procedure at the level of a homogeneous background and then later on when scalar perturbations are introduced. This is of interest to us since we aim to better understand how to bridge the gap between QG and observations, for instance in this case it may allow us to better understand the Cosmic Microwave Background (CMB) spectrum from a QG origin without the need to call for inflationary scenarios.

Chapter 2

The program of Quantum Gravity

In this chapter, we tackle the main conceptual components of the program of quantum gravity and the implications of such ingredients in the model-building process of several approaches. In particular, we will reflect on the nature of such ingredients in section 2.1 and briefly go through the relevant ones to the thesis in section 2.2 and section 2.3. We then discuss how these elements come together with the goal of making contact with classical continuum physics (spacetime and matter) through the notion of emergence in section 2.4. These are the fundamental components that will enter the framework of GFT, which is the one we work with throughout the thesis. Being quantum fields *of* spacetime, defined on group manifolds, we will see how this formalism endorses the necessary ingredients to be advocated as a promising and consistent theory of QG.

2.1 Revision of the conceptual components

Quantum theories of gravity are by far the most interesting and puzzling fields of research in modern theoretical physics. According to our current knowledge, one is able to describe most of the fundamental interactions governing our physical reality using QFT at tiny scales. This powerful framework combines in a simple manner classical field theory, special relativity, and quantum mechanics [46–48]. Despite the debatable and somehow bewildering conceptual (even universal) foundations this theory is based on, such as the superposition- and uncertainty principles, it has so far surpassed several experimental tests to describe matter at the quantum level [ref]. To paint the picture of such peculiar quantum objects that describe our world, let us lay out their properties. Quantum fields are physical entities living on a Hilbert space and are invariant under Poincaré symmetries. They are dynamical degrees of freedom of the theory living on a fixed (non-dynamical) background metric. In this framework, spacetime is then a mere *spectator*. Another interesting feature about QFT is that this *probabilistic* mathematical framework comes to life by means of physical observations through the concept of *observables* and measurements [49]. We may

have conveyed that this is an idealized framework, but in reality, QFT is afflicted with several issues.

On the other end of the spectrum of theories, lies the theory of GR, harnessing the gravitational interaction. The success of GR may be summarized in the famous quote: *Spacetime tells matter how to move; matter tells spacetime how to curve* [50] and this becomes evident once we work out the mathematics of the Einstein equations [51,52]. More precisely, GR reveals the gravitational field as a classical (pseudo)-Riemannian spacetime metric, the dynamics of which are of *deterministic* nature [53,54]. The revolutionary idea of geometrizing gravity replaced the Newtonian perception of space and time as two separate entities [55], where time is considered as absolute and the dynamics of mechanical systems taking place within space, with the *covariance* principle [56]. This is underlined by the gauge invariance of the theory under diffeomorphism transformation. These ingredients are what makes GR a powerful theory, that so far is able to describe the world surrounding us at *large* scales, even more, unraveling the existence of new physical objects in the observable universe such as black holes and gravitational waves [57, 58]. Despite its achievements, just like QFT fails to incorporate the gravitational interactions, GR breaks down at the quantum scale. Indeed, from the above description of QFT, if we put compare it to GR we can see there are paradoxical differences, however complementary they may seem. The quest of reconciling both theories is what defines the research field of QG. Let us spell out several motives as to why we are attracted by putting together the lessons we learned from these pillar theories, starting from which we can identify the main ingredients that should be present in any theory of QG. We do not intend to list all of them, since this also depends on the various perspectives one can adopt, but rather focus on those that are relevant to the scope of this thesis.

There are several incentives to why we would seek a quantum theory of gravity besides the conceptual inconsistencies between QFT and GR. Perhaps the most important ones are the issue of time [5, 21, 59], the unification of all theories (and hence the reductionism path: a coherent quantum theory of all interactions should also include a quantum theory for gravity) and the puzzling phenomena yet to be better understood and answered in the universe (such as the GR singularities, the gravitational field of a quantum field, the thermodynamical behavior of black holes, dark matter, dark energy). There are several reasons as to why one should be and in fact *is* interested in quantizing gravity, or reconciling these two theories of physics [60, 61]. Moreover, the universal coupling of the gravitational field to all known forms of energy enhances the argument that it is only reasonable to argue that gravity has to be implemented in a quantum framework too.
What we can learn from the above reflections on both theories, is that we can unambiguously identify what are the fundamental ingredients that any program of quantum gravity should have. From the QFT side we have the observables symbolizing the operations or the means by which contact to our tangible reality is achieved, discreteness and symmetries are pillars of both theories and the covariance principle as well (as we will discuss below). On the other hand, what GR empathizes is the obvious need to redefine the standard perspective of the background (the stage) on top of which physics takes place. Diffeomorphism

invariance is in fact nothing but a call for adopting a relational perspective on the subject at hand. That being said, the description of the evolution of physical processes can only take place with respect to one another rather than on a fixed absolute reference frame (as is the case of QFT) [62]. In the following sections, we discuss these components and underline the pressing necessity for such ingredients in any fundamental theory of QG [3] to be viable.

Another point we would like to emphasize is, putting aside all the technical as well conceptual issues we are faced with in such a quest, a central problem impeding the process of formulating a QG theory is the absence of a clear *empirical* guideline [63]. This can be understood as the challenges raised by the validity scale of both GR and QFT, where we expect that quantum effects of gravity should undeniably be manifest and relevant in the Planck scale. This scale is a dimensional system of Planck length, l_{P}, Planck time, t_{P}, and Planck mass, m_{P}, respectively. They are given by the expressions

$$l_{\mathrm{P}} := \sqrt{\frac{\hbar G}{c^3}} \approx 1.62 \times 10^{-33}\ \mathrm{cm}\,, \quad t_{\mathrm{P}} := \frac{l_{\mathrm{P}}}{c} = \sqrt{\frac{\hbar G}{c^5}} \approx 5.39 \times 10^{-44}\ \mathrm{s}\,, \tag{2.1.1}$$

$$m_{\mathrm{P}} := \frac{\hbar}{l_{\mathrm{P}} c} = \sqrt{\frac{\hbar c}{G}} \approx 2.18 \times 10^{-5}\ \mathrm{g} \approx 1.22 \times 10^{19} \mathrm{GeV}/c^2\,. \tag{2.1.2}$$

At the level of astrophysical observations, the order of magnitude of these scales is of no relevance (except in the case of black hole physics). However, as argued above, these are *the* scales where quantum gravitational effects are expected to be significant and these are also the scales that we have so far no access to due to the lack of technological advancements. Now that we have roughly a clear idea about the necessary elements and concepts any quantum theory of gravity must be able to consistently address and incorporate, we can further explore them with scrutiny and see how they are relevant in the GFT approach.

2.2 Background independence

In the following, we reflect on the relational background independent ingredient provided by GR. A backup argument for this is provided by the *hole argument* argument stating that the theory does not distinguish reference system objects from dynamical objects. This is translated at the level of the manifold M as the vanishing of the physical meaning to its constituent points, and promoting instead *relative* localization of events. This in turn resonates with the claim of active diffeomorphism invariance of the theory [64]. What this means is that a physical state is not located somewhere [56, 65, 66] but can only be located with respect to another state.

Indeed, in a truly background independent QG formulation (taking into account the diffeomorphism invariance), no reference to any classical metric should enter either the characterization of the quantum state of geometry or the dynamical variables of the theory [67, 68]. The metric should then be treated from an operational perspective and might

be associated with different quantum states of geometry, or a superposition thereof [69]. Now, once we are provided with an operator for the metric, the picture of spacetime at this level must be revisited. To take into account the relationalism induced by the theory's gauge invariance, the quantum states associated with the metric operator can only be interpreted as quantum excitation of spacetime itself. But then the question that is raised at this point is, what is then the physical content these states must bear in order to recover the usual notion of geometry (spacetime)? In the absence of a background defined by a manifold, one answer to this inquiry is to the logical conclusion that the quantum states of spacetime should entail some sort of *non-geometric* (or rather pre-geometric) diffeomorphism invariant information, or conceptions that enables the reconstruction of spacetime. Therefore, they should be of a non-local nature. If we take this seriously, then the quantum geometric information can only be combinatorial and algebraic, capable of translating and reproducing the structure of the manifold as we will encounter in several approaches to QG in the next chapters.

Relationalism in the classical realm. There have been several successful tentatives to highlight the relational character of classical non-relativistic, relativistic, and quantum mechanics [49, 70, 71]. Here we start by illustrating the notion of relationality with the simplest example of the nonrelativistic particle. To this scope, let us consider the action of the particle with a fixed mass $m = 1/2$ for simplicity, this reads

$$S = \int \mathrm{d}t \frac{\dot{q}^2}{4}\,, \tag{2.2.1}$$

where q is the position of the particle and the dot denotes the derivative with respect to t. Usually in non-relativistic physics, the parameter t is perceived as the time of an external clock that does not interfere or interact with the dynamics of the system. As we argued above, this is different in GR since there is no preferred notion of external time. Let us see how we can formulate this for the case of (2.2.1). We then introduce an arbitrary parameter s to obtain an extended two-dimensional configuration space Q_{ext} and we consider the action principle for an extended phase space that can be obtained by promoting the variable t to a dynamical one. This can be precisely implemented provided that solutions to the equations of motion $(t(s), q(s))$ as a function of s can be combined such that at the end of the day, we end up with the same solutions $q(t)$ of the equations of motion of the action (2.2.1). This extended action yields

$$S_{\text{ext}} \equiv \int \mathrm{d}s \mathcal{L}_{\text{ext}} = \int \mathrm{d}s \frac{q'^2}{4t'^2},$$

where the prime denotes a derivative with respect to s now. Let us note that the system described by the above-extended action is in fact invariant under reparametrization $s \mapsto \tilde{s}(s)$. One can push further the analysis and conduct the Hamiltonian formulation of the above action. In fact, the property of being invariant under reparametrization generates

constraints in the Hamiltonian theory. Indeed, one can show that we end up with a primary constraint

$$C_H = p_t + p^2 \approx 0 \tag{2.2.2}$$

where the canonically conjugate variables p and p_t associated to q and t are given by

$$p \equiv \frac{\partial \mathcal{L}}{\partial q'} = \frac{1}{2}\frac{q'}{t'}, \quad p_t \equiv \frac{\partial \mathcal{L}}{\partial t'} = -\frac{1}{4}\left(\frac{q'}{t'}\right)^2, \tag{2.2.3}$$

and where $\approx$ is to denote that the equality is only valid only on the constraint surface denoted by $\mathcal{C}$ [72, 73]. As a result, the extended Hamiltonian is proportional to this constraint,

$$H_{\text{ext}} \equiv p_t p' + pq' - \mathcal{L}_{\text{ext}} = t'\,(q, p, t, p_t)\, C_H \equiv N\,(q, p, t, p_t)\, C_H, \tag{2.2.4}$$

with $t' = N$. Obviously, as the Hamiltonian above entails, all observables are independent of s. Nonetheless, we know that this is artificial and only due to the reparametrization we considered above. We present now how to recast the dynamics as a physical evolution by making use of the notion of *relational observables*. We fix $N = 1$ and study the solutions to the equations of motion written in terms of s. The only non-trivial quantities that do not have vanishing Poisson brackets with the constraints are

$$t' = \{t, C_H\} = 1, \quad q' = \{q, C_H\} = 2p \tag{2.2.5}$$

$$\Rightarrow t(s) \equiv \alpha^s_{C_H}(t) = s + t\,, \quad \text{and} \quad q(s) \equiv \alpha^s_{C_H}(q) = 2ps + q\,. \tag{2.2.6}$$

Let us outline the steps of defining a relational observable from this scheme [70, 74, 75];

- Separate the physical degrees of freedom in system variables and clock ones. In the case of the absence of any preference of what degree of freedom should be used as a clock, we denote this theory to be *clock neutral* then.
- Reformulate the dynamics by inverting the gauge evolution of the chosen clock as a function of s and then plug it back into the dynamics of the system. This produces an explicit dependence on the clock.

Let us illustrate this in more detail. Assuming that our clock system is given by t and p_t. For each value $t(s) = \tau$, the first equation above can be inverted following the steps outlined above and we obtain

$$Q_{q,t}(\tau) \equiv \alpha^s_{C_H}(q)\Big|_{\alpha^s_{C_H}(t)=\tau} = q + 2p(\tau - t), \quad P_{p,t}(\tau) \equiv \alpha^s_{C_H}(p)\Big|_{\alpha^s_{C_H}(t)=\tau} = p\,.$$

One can show that these functions are canonically conjugated, $\{Q_{q,t}(\tau), P_{q,t}(\tau)\} = 1$. In fact, they underline the relation between q and p with t when t reads the value τ, meaning that they answer to the question [74, 75]: What is the position q and momentum p of the particle when the clock t reads τ? Furthermore, they are gauge invariant since their respective commutator with the constraint vanishes and in particular if we choose for

instance the correspondence $t(s) = \tau_0$, we end up with a specific gauge fixing of the gauge constraint.

Now, we can notice that if we fix τ_0, the gauge invariant function $Q_{q,t}(\tau_0)$ can be evaluated at any point of the gauge orbit. In this sense, if we allow the parameter τ to run, we can leaf through the entire constraint surface $\mathcal{C}$ through $Q_{q,t}(\tau)$. It is from this perspective that $Q_{q,t}(\tau)$ represents a gauge-invariant extension of a gauge fixed quantity. This is made clear since τ browses all the possible values of $t(s), Q_{q,t}(\tau)$ and $P_{q,t}(\tau)$ indeed describe the evolution of q and p with respect to t. Therefore, they are relational observables (also known as complete observables). The corresponding observables associated with the clock variables,

$$T_{t,t}(\tau) = \alpha^s_{C_H}(t)\Big|_{\alpha^s_{C_H}(t)=\tau} = \tau$$
$$P_{p_t,t}(\tau) = \alpha^s_{C_H}(p_t)\Big|_{\alpha^s_{C_H}(t)=\tau} = p_t$$

are entailing redundancy. In fact, they do not hold physical information anymore. In principle, one can generalize the above example to the case [75]. *Gauge fixing:* As in the simple example discussed above, it is important to the degrees to notice that the degrees of freedom associated with T are generally redundant and it might be more convenient to find to redundant-free formulation of it. In general, it is not possible to carry out this procedure over the whole phase space because of two reasons

1. The clock and the system degrees of freedom may not be separable in general. This in turn does not allow us to distinguish between the system and the clock degrees of freedom. In this case, a phase space reduction is not possible.

2. It is possible that the Poisson bracket $\{T, C_H\} \neq 0$ is valid only locally meaning that the clock function does not admit a global definition. Therefore, the elimination of clock degrees of freedom cannot be performed over the whole phase space.

To remedy some aspects of these issues, we can make a few assumptions that will come in handy. In particular, we speculate that

- The total phase space can be split into a product of the clock and the system phase spaces: $\mathcal{P} \simeq \mathcal{P}_{\rm C} \times \mathcal{P}_{\rm S}$, with $\mathcal{P}_{\rm C}$ and $\mathcal{P}_{\rm S}$ being the clock and the system phase spaces respectively.

- We will also assume that the two systems do not interact, meaning that

  $$C_H = c_{\rm S} + c_{\rm C} \approx 0$$

  with $c_{\rm C}$ being a function on $\mathcal{P}_{\rm C}$ and $c_{\rm S}$ being a function on $\mathcal{P}_{\rm S}$. Furthermore, we require $\{T, C_H\} = \{T, c_{\rm C}\} = 1$, in order to guarantee that T is a globally good clock.

The relational formalism we just sketched can be in principle straightforwardly generalized to GR.

Relationalism in quantum gravity. We saw in the previous paragraph that relationalism is a concept well-established approach in the field of classical mechanics. This changes drastically when we move the discussion to treat it at the quantum. In particular, the issue of evolution and the very definition of time in the sector of QG has two facets, conceptual subtleties, and technical ones. The conceptual issues start to pop up already when we compare the quantum time t used in Quantum Mechanics (QM) as an absolute parameter with that one in terms of which spacetime is dynamical. If we were to take the program of QG seriously, we need to consider that clocks (in classical mechanics and GR) in such a regime are in fact of quantum nature. However, this becomes incomprehensible and challenging due to the quantum principle that needs to be accounted for [59,76] such as superposition, uncertainty, and observations. In retrospect to this unclear setting, a relational evolution is very poorly understood and it is so far unclear how to define it. On the side of the technical issues, the reflections made on the problem of time in QG rises already as soon as we try to canonically quantize GR. In general, there are two formal paths one can choose, dealing with the quantum clock after having quantized the geometry or before. In this sense, it is a tempus ante/post-quantum approach [77], where relational evolution is established only *before/after* the theory is quantized. In the following, we will explain an alternative way of dealing with the problem of relational evolution, namely that of *effective* relational ones for its relevance to the extraction of continuum physics in chapter 4 and chapter 7.

The principles behind the definition of the emergent effective relational framework are:

1. **Emergence.** The effective dynamics ought to emerge as a *collective* phenomenon. In this context, a formulation in terms of operators corresponding to collective observables and states encoding collective behavior of the underlying degrees of freedom should be available.

2. **Effectiveness.** The relational evolution ought to hold on average, where the operators playing the role of the internal clock should have small quantum (and thermal, when relevant) fluctuations. This is important to reach a semi-classical regime. Moreover, large fluctuations drive effective relational dynamics to be poorly trusted.

The macroscopic physics in such a formalism is depicted by means of expectation values and fluctuations of the collective observables of the theory. This is computed on states that capture some information on the proto-geometric phase defining the conversion to the effective level. To summarize this section in a very simple idea, let us state that the relational strategy amounts to identifying the necessary internal degrees of freedom of the entire system composed of metric and matter fields that can be used as approximate rods and clocks to parametrize the spatial relations and temporal evolution of the remaining degrees of freedom.[1]

[1]This formalism forces us to work with the fact that physical clocks and physical rods will never be *perfect*. Perfect meaning in this context is labeled with the idealized notion of time and space that are present at the level of the coordinate systems.

2.3 Fundamentality and discreteness

In chapter 1 we emphasized that a consistent and well-established theory of quantum gravity must harbor at its core the various *defining* aspects of the theory of the gravitational interaction and that of quantum field theory. In this section we are interested in zooming in into the fabric of the underlying spacetime manifold and gaining a deeper insight into its microscopic structure, bearing in mind the above-raised components of operationality, relationality, and pre-geometric nature of the observed geometry and quantum matter.

In section 2.1 we pointed out that the testability of any QG theory is expected to be relevant at the Planck scale since the gravitational force is then expected to be at its strongest. At this scale, just as in solid-state physics, condensed matter, or molecular physics, there is no reason to believe that the observed smooth manifold defining spacetime still maintains such a structure. In fact, if we learned anything about the structure of matter is that on the macroscopic level, where it does manifest a coherent and sometimes continuous shape, it is only the manifestation of the fine-coarse groaning of more fundamental microscopic structures endorsing such properties. In fact, once we take a closer look and study the fabric of the microstructure, we find out they are not that regularly smooth but rather of finite and discrete nature. The same logic can be applied to the architecture of spacetime (the manifold). So far there is no obvious reason to believe it withholds such a property at the Planck scale. In fact, if we zoom back one may think of what we actually observe is nothing but the successive and strategic refinement of smaller discrete entities, such as *points* (events).

Now, we can illustrate this argument with a more mathematical tool from topological theories [78]. The example is based on the logic of substituting the continuum manifold with a finitary topological space which under the necessary condition of approximating in a clear sense the latter [79]. This of course calls for a definition of a limit where the approximation procedure becomes more precise. We consider a topological space X. One can define a notion of closeness between sets where formally speaking, two sets are close if they are arbitrarily near to each other. In other words, we have the following definition

Definition 1. *A topological space is a set X together with a collection of open subsets T that satisfies the following conditions:*

- The empty set is in T.
- X is in T.
- The intersection of a finite number of sets in T is also in T.
- The union of an arbitrary number of sets in T is also in T.

According to this definition, open subsets can talk to other subsets but in a *finite* way. Systematically speaking, starting from a subset T we can gather enough information by

identifying an open subset that characterizes the space $S(T)$. More precisely, given the open cover T of X, assumed to form a subtopology of X, i.e. to be finite and closed under union and intersection, we consider $x, y \in X$ as equivalent if and only if $\forall t \in T, x \in T \Leftrightarrow y \in T$. Then the space $S(T)$ is the quotient of X with respect to this equivalence relation.
We can also mention another relevant example to our discussion in the next chapter, which is also an equivalent characterization of a finitary space. This discretization example can be provided by an open covering of a given manifold in terms of *simplicial complexes*. This combinatorial geometric notion is defined as a family of sets that is closed under taking subsets, i.e., every subset of a set in the family is also in the family. It is a purely combinatorial description of the geometric notion of a simplicial complex. For instance, in a $2d$ simplicial complex, the sets in the family are the triangles (sets of size 3), their edges (sets of size 2), and their vertices (sets of size 1). This already induces the notion of a nerve of an open covering, which is the simplicial complex having as vertices the open sets of the open covering, and as simplices the finite families of open sets of it whose intersection is non-empty.

As we will encounter in chapter 3 most of the background independent approaches to QG, construct their framework based on these introduced notions of simplicial complexes as substitutes for a continuum spacetime. As we mentioned above, they may actually represent the finite character of spacetime and hence one step closer to a fundamental description thereof. Moreover, before proceeding to the emergence step of the QG program, let us point out that in the case of fixing a discrete substratum to be the fundamental version of spacetime, then (as we suggested above), QG would be analogous to solid state physics where field theoretical methods are used adopting the approximation of a smooth manifold by means of the crystal lattice. The cut-off is then enforced in the so-constructed field theories and it has a clear interpretation in terms of the atomic structure of the space on which these fields live. To address the issue of diffeomorphism invariance, in such a scheme, there are several perceptions one can take which inevitably differentiate QG models and their technical issues [21, 65, 78, 80, 81]. Moreover, identifying the discrete structure of spacetime needs to be complemented by a *quantum* description. In fact, we can make sense of a discretized piece of geometry only if we are provided with its equivalent quantum description from which its physical properties can be extracted in a meaningful manner. This is fundamental to the purpose of QG programs and we will encounter how it is performed in several background independent models in section 3.1.2 (chapter 3), where we first catalog the various discrete structure of geometry and then study how this information is translated in a quantum setting.

2.4 The notion of emergence

In section 2.2 concerning the background independence and the notion of relationality in the classical and QG setting, we stumbled upon the conception of the emergent nature of the relational dynamics, which in its own way tackles some radical issues of the problem

of time. In this section, we generalize this notion to the entire spacetime fabric, not only the time one. Let us first provide a prominent attempt to characterize and define what we mean by emergence, following [4, 21, 82, 83]. Emergence is to be understood as the appearance of properties that are *novel* with respect to a more fundamental description of the same system. They must be endowed with enough substantial and vigorous features, allowing them to generate a new description of the physical system and to fashion new predictions stemming from it. From these lenses, emergence is usually accompanied by some limiting procedure and some levels of approximations in order to provide enough "space" for the novel properties of the system and its consequences to become visible.
In the context of QG, this is already reminiscent of the previous section, where we unraveled several fundamental components that should be considered in any theory of QG. The main role of emergence is then to organize them in a meaningful and precise way, such that each ingredient takes its right "place" at the right "moment". In simpler words, it is the process during which the connection between the complete theory of QG and that of the classical world takes place and comes into existence. However, let us not exaggerate the implications of such a scheme, in fact in practice, the emergence process is usually implemented after having identified a coarse graining procedure, a semi-classical limit. There have been several implementations of this line of reasoning, and in this thesis, we will encounter some of them such as GFT and spin foams. In particular, in such theories, one can identify four levels of emergence as argued by [21], however, we will not go into the details of such levels. The main feature we would like to emphasize in such a program is that they all endorse new types of quantum degrees of freedom which are not geometric in a straightforward way and are in fact of a different nature (usually combinatorial and algebraic) as we already spoiled in the previous sections. The discreteness ingredient we mentioned in section 2.3 and its possible quantum description, is an element shared by most of such theories. For instance, we will see how this can be made explicit with the spin network states of LQG in section 3.3.2 with their dual functional dependence on group elements or group representations associated with graphs, and their histories labeled by the same algebraic data and associated to cellular complexes in section 3.2. More interestingly, the quanta of GFT can be described both as generalized spin networks (section 4.3) and simplicial building blocks of piecewise-flat geometries (whose quantum dynamics merges the idea of spin foam models as we will see in section 4.2) are also theories capturing all the above-mentioned components and it is by so far a well-established theory of QG. In fact, the notion of emergence can be very well formulated in such a framework, respecting the aspect of discreteness, relationalism, operationality, and causality. The emergence, in this case, is understood as effective, and stemming from the collective behavior of the fundamental atoms of spacetime. For more details on this, we refer to the literature, see for instance [59, 84–87]. Or it can also be by employing the quantum properties of the pre-geometric states in the theory, such as entanglement, along with the appropriate coarse graining procedure. In fact, this is a prominent idea in QG approaches such as in the pinpointed duality between entanglement and geometry within the AdS/CFT 1-1 correspondence [24, 88–90].

To be consistent with the above-mentioned programs, it is compulsory to raise several conceptual issues that are usually not addressed in a direct manner. Regarding the relation between entanglement and geometry; the claim made here is that if we take connectivity as entanglement definition implies there is some kind of equity at the fundamental level. We tend to put this by hand and give it a geometrical interpretation without really distinguishing between the true definition of it and the definition we really need in order to make the theory consistent. As for the emergence within any quantum theory of gravity, the question that we are faced with is: how far can we trust this approach? And what can make us so confident that the silent degrees of freedom are not relevant? Is there a parameter that can witness or detect such deficiency? Moreover, it seems that the unidirectionality of the emergence proposal implies descriptive irreversibility. Meaning that, due to the process of emergence, it seems just it is not possible to reverse engineer its action. For instance, this can be illustrated by examples of thermodynamical emergence from the microscopic statistical degrees of freedom.

Chapter 3

On the background independent approaches to quantum gravity

Discretizing GR in vacuum is in itself a very beautifully formulated theory of geometry. As we argued in the previous chapter, a fundamental picture of spacetime ought to be of discrete nature. As we will see in this chapter, it breaks down the smooth fabric of spacetime ($4d$ geometry) to elementary fundamental simplicial building block as we briefly explained in section 2.3 (for a more technical definition of a simplex we refer to section 4). The identification of such discrete geometric structure depends on the dimension we are considering and the chosen triangulation applied to chop the spacetime manifold M into pieces (see figure 3.1c for examples of triangulations). Now, this line of reasoning is usually followed by lattice gauge theories, simplicial geometry, spin foams, and group field theories to provide a background independent QG. All of these approaches share this logic in discretizing the underlying geometry of spacetime, however, the difference between them becomes evident when they reach the step of defining the *quantum* counterpart of such procedure; this is exactly what distinguishes them from one another. As already emphasized in chapter 2, we are interested in SF since they are related to the issue addressed in chapter 5 and their relation to the formalism of GFT (chapter 4), which is the framework we work with throughout this thesis.

The idea behind the SF model approach to quantum gravity is to appropriately discretize the gravitational action (Einstein-Hilbert (EH)), and perform all impositions of the constraints, gauge fixings, as well as path integral quantization of such discretization. We will go through this formalism in section 3.2, where we present the basic tools and concepts in two well-known models of SF, namely the BC and the Engle-Pereira-Rovelli-Livine (EPRL) models, and in particular we will pinpoint how these QG models are differentiated. But first, we need to warm up with the principle notions of discretizing geometry from an *independent background* point of view. This procedure is very well understood and realized in the context of topological BF theory and we will discuss it in section 3.1. Throughout each section, we shall discuss the main steps to build Hilbert spaces and quantum states that can be associated with discretized geometry. To acquire some geometric intuition, we

discuss the case of $3d$ geometry and then proceed to the $4d$ case. Finally, we point out in section 3.3 the common feature shared by all the presented background independent models, namely that of the quantum state of geometry captured by *spin networks*. This will be the basis from which we will study the generic superposed states in chapter 6. The starting point for the discussion in this chapter is the EH (in metric variables) given by

$$S[g_{\mu\nu}] = \frac{1}{2\kappa}\int_M dx^4 R\sqrt{-g}d^4x\,, \tag{3.0.1}$$

where $\kappa = 8\pi G/c^3 = 8\pi\ell_p^2/\hbar$.

3.1 Quantization of discretized geometry

In section 3.1.1 we present the method to carry out the discretization of spacetime in $3d$ as a warm-up to acquire an intuition behind such a procedure. Furthermore, it will enable us to answer several questions before even transitioning to the $4d$ which can be easily done in the $3d$ case. This will allow us to discover the properties of GR at such discretized picture. In particular, we will see that GR in its first order formulation belongs in fact to a larger family of the so-called BF theory type. This can be provided by transforming the metric parametrization of the EH action in GR to first order formulation. We then proceed to the $4d$ case, where the situation becomes peculiar and more interesting since as we will see we would need to identify some constraint to recover GR. After obtaining somewhat a geometric chopped picture of the geometry we proceed with the quantization treatment in section 3.1.2.

3.1.1 Discretizing gravity

In the following, we start by rewriting GR in $3d$ in a first order formalism and present its discretized version as a warm-up and then move to the more interesting case of $4d$ geometries. We will see how the notion of BF theories will allow us to work in a background independent context. We then transition to the quantum realm of each dimension in section 3.1.2.

First order Palatini formulation and BF theory in 3 dimensions.

The starting point for our discussion in the following is to establish the first order formulation of three dimensional geometries, where the derivation is carried out for Lorentzian as well Riemannian gauge groups. The Lorentzian gauge group for its relevance to the physical world and the Riemannian one for its simple structure, the possibility to perform Wick rotations, and its use in QFT, along with enabling a thermodynamic interpretation. Such a connection is made clear once we adopt orthonormal frames instead of metric parameters

to describe the underlying $3d$ geometry. This is precisely described by the triad field e^I_a, where uppercase indices are Lie algebra indices, while lowercase ones are spacetime indices. This enables us to write the metric as a composite object, namely

$$g_{ab} = e^I_a e^J_b \eta_{IJ} \ , \tag{3.1.1}$$

where η_{IJ} is the internal metric in $3d$ and its explicit signature depends on whether we are considering the local gauge group $\mathrm{SO}(2,1)$ for Lorentzian geometry or $\mathrm{SO}(3)$ for Riemannian one. The covariant derivative $d^{(\omega)}$ is carried out with respect to the connection expressed in such a frame. In $3d$, the connection is the spin connection ω^{IJ} and the curvature tensor and its components are respectively defined through

$$F^{IJ} = \mathrm{d}\omega^{IJ} + \omega^I_K \wedge \omega^{KJ} \ , \quad F^{IJ}_{\mu\nu} = \partial_\mu \omega^{IJ}_\nu - \partial_\nu \omega^{IJ}_\mu + \omega^I_{K\mu}\omega^{KJ}_\nu - \omega^J_{K\mu}\omega^{KI}_\nu \ . \tag{3.1.2}$$

This formulation in terms of a triad (orthonormal frame) and connection of EH in (3.0.1) produces the so-called *Palatini* action of the GR action and it reads

$$S[e^{IJ}_a, \omega^{AB}_a] = \frac{1}{2\kappa}\int_M \epsilon_{IJK}\left(e^I \wedge F^{JK}(\omega)\right) = 2\int_M \mathrm{tr}(e \wedge F) \, , \tag{3.1.3}$$

where we set $\kappa = 1$ in the second equality. The equations of motion stemming from (3.1.3) are obtained through applying the variation principle with respect to e and connection ω

$$\delta_e S = 0 \, , \quad \delta_\omega S = 0 \, . \tag{3.1.4}$$

Such equations of motion are equivalent to the Einstein equations in $3d$ and they read

$$F(\omega) = 0 \, , \quad d^{(\omega)}(e) = 0 \, . \tag{3.1.5}$$

The set of dynamical equations in (3.1.5) forces the metricity of the spin connection as well the compatibility between the triad (metric field) e and the connection ω. Notice that it also constrains the curvature $F(\omega)$ to be vanishing everywhere, thus prohibiting any non-flat configuration and local excitation such as gravitational waves.

BF theory and Palatini action. The Palatini action in (3.1.3) is indeed interesting due to its relation to a much larger class of theories, called *Background Field* B and F (*BF*). This family of theories is defined by specifying the choice of the d-dimensional manifold M we work with, a semi-simple group G, a 1-form connection A with values on the Lie algebra of the group $\mathfrak{g}$, its curvature 2-form F and a $(d-2)$-value form B. The action for a BF theory is then expressed in terms of these variables [17, 91] and it is given by the simple expression

$$S[B\,, A] = \int_M \mathrm{tr}\left(B \wedge F(A)\right) \ , \tag{3.1.6}$$

where $\mathrm{tr}(B \wedge F)$ is the d-form produced by taking the wedge product of the differential form part of B and F and using the bilinear form $\langle x, y\rangle = \mathrm{tr}(xy)$ to pair their Lie algebra

valued components (the trace here is taken in the adjoint representation). This action is topological in any dimension and the equations of motion always force the connection to be flat [17]. This is made clear once we derive the dynamical equations after varying the action and we have

$$\begin{aligned}\delta\int_M \mathrm{tr}(B\wedge F) &= \int_M \mathrm{tr}(\delta B\wedge F + B\wedge \underbrace{\delta F}_{\mathrm{d}^{(A)}\delta A}) = \int_M \mathrm{tr}\left(\delta B\wedge F + B\wedge \mathrm{d}^{(A)}\delta A\right)\\ &= \int_M \mathrm{tr}\left(\delta B\wedge F + (-1)^{n-1}\,\mathrm{d}^{(A)}B\wedge\delta A\right) = 0\,,\end{aligned}$$

where in the last step we integrated by parts and neglected the boundary term[1]. Therefore, the equations of motion are

$$F = 0, \qquad \mathrm{d}^{(A)}B = 0\,. \tag{3.1.7}$$

Again, the above set of evolution equations are quite simple and they are merely a hint that BF theories are topological field theories. This becomes more clear when we study the symmetries of the BF theory, where we will see that all solutions for the field B and connection can always be mapped via a gauge transformation, rendering the theory topological. Indeed, suppose that we define a transformation of the A and B fields where A is left unchanged, while B changes by a term which is the external derivative of a $(d-3)$-form, i.e.,

$$A \longmapsto A\,, \quad B \longmapsto B + \mathrm{d}^{(A)}\eta, \tag{3.1.8}$$

for some $(n-3)$-form η with values in $\mathfrak{g}$. The action above in (3.1.6) is invariant under such transformation

$$\begin{aligned}\int_M \mathrm{tr}\left(\left(B+\mathrm{d}^{(A)}\eta\right)\wedge F\right) &= \int_M \mathrm{tr}\left(B\wedge F + \mathrm{d}^{(A)}\eta\wedge F\right) = \int_M \mathrm{tr}\left(B\wedge F + (-1)^n\eta\wedge \mathrm{d}^{(A)}F\right)\\ &= \int_M \mathrm{tr}(B\wedge F)\end{aligned}$$

where we used integration by parts and the Bianchi identity $\mathrm{d}^{(A)}F = 0$. Indeed, this is a gauge symmetry of BF theories since two solutions differing by this transformation are perceived as physically equivalent. Furthermore, for a vanishing curvature for $F = 0$ we end up with a flat connection A, this affects the B field in a way such that $\mathrm{d}^{(A)}B = 0$ can be written locally as $\mathrm{d}^{(A)}\eta$ for some η. Notice that we only discussed the case of the translation symmetry (shifting the field B while keeping A invariant). To completely gauge fixed BF, we also need to take into account the Lorentz transformation, which is necessary to show that all connections are the same up to gauge transformation. This completely fixes the BF theory at hand. As a matter of fact, this becomes clear when we work out the above evolution equation where the $B$is gauge transformed. We see that the field B is an exact form, but its gauge transformations are defined up to any exact form. We are then left with no statement about how many solutions we can obtain for A (besides being

[1] We mention that in principle boundary terms in this action and previous ones can be included and studied, however, for the purpose of this thesis we neglect them and refer to the literature on their implication in QG models [29, 92–94]

flat), and exactly for this reason we need to have the Lorentz gauge transformations. This further implies that one can always gauge away any local degree of freedom of BF theories, proving that the theory contains only global, i.e. *topological* information.

The Palatini action (3.1.3) we encountered above, is in fact nothing but a BF theory once we fix the gauge group G to be $\mathrm{SO}(2,1)$ or $\mathrm{SO}(3)$. This means that GR in $3d$ is indeed nothing but a topological theory [17, 91].
Now, we are interested in discovering what the discretization of such a geometric theory of spacetime will produce. To this aim, we need to introduce some tools and notations that we will employ throughout this section and the overall thesis.

Definition 2. ***n-simplex:*** *is the convex hull of $n+1$ points in $\mathbb{R}^d$, where $d \geq n$. We define then the following geometric notions*

- *0-simplices are vertices, 1-simplices lines,*
- ▲ *2-simplices correspond to triangles, and 3-simplices are associated with tetrahedra.*
- ✧ *4-simplices are simply constructed by gluing 5 tetrahedra along their common triangles, exactly as tetrahedra are gathered through the collection of four triangles glued along their common edges.*

Another notation that is very important as we will see in the quantum definition of discretized geometry is

Definition 3. ***The face of an n-simplex:*** *The convex hull of a non-empty subset of points defining an n-simplex σ is called a face f of σ.*

Definition 4. ***Simplicial complex:*** *is a finite collection of simplices $K = \{\sigma\}$ such that*

- *if σ' is a face of $\sigma \in K$, then $\sigma' \in K$*
- *if $\sigma, \sigma' \in K$ with $\sigma \cap \sigma' \neq \emptyset$, then $\sigma \cap \sigma'$ is a face of σ and σ'*

The definition of a triangulation of a simplicial complex is now presented.

Definition 5. *Triangulation T of simplicial complex:*

- ❥ ***Triangulation:*** *a triangulation T of a continuous manifold M is specified by a pair (K, h) with K a simplicial complex and $h : \cup_{\sigma \in K} \to M$ is a homeomorphism which maps the set of all simplices in K to the manifold.*
- ❥ ***Dual complex:*** *is defined as follows: given a triangulation T, its dual is constructed by identifying each d-simplex with a node and connecting the nodes whenever the corresponding d-simplices have a common a face.*

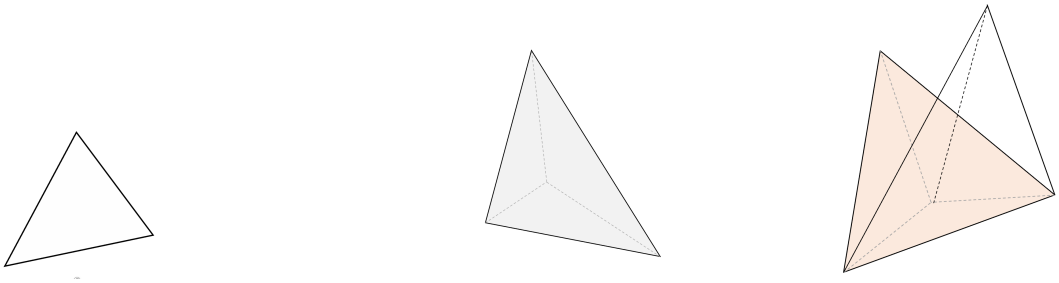

(a) Triangle (face of a tetrahedron).

(b) Tetrahedron within a 4-simplex.

(c) Oriented pair of tetrahedra in the same simplex.

Figure 3.1: Examples of spacetime triangulations.

In this way, n-dimensional objects of the triangulation are dual to $(d-n)$-dimensional ones. In 3d for instance, a face f shared by two tetrahedra becomes dual to a one dimensional object, an edge $e^\star$, and an edge e becomes dual to a face $f^\star$, where we denote the dual of an object by *.

Now we put these notions and definitions at work to extract a discrete version of the three dimensional manifold (spacetime).

Discretizing BF theories and $3d$ gravity The procedure of discretizing BF theories and hence an equivalent formulation of $3d$ GR is well studied and quite understood [17,95]. Let us now describe how this is precisely implemented. We start by considering an oriented geometric triangulation T of the $3d$ manifold M and we generate the discretization as follows:

- ⊙ *B field discretization:* being a 1-form, the (what would be in GR) triad field can be naturally integrated along 1-dimensional objects, i.e along the *edges* e of the triangulation, and when we do so, we obtain a collection of *Lie algebra* elements and hence we write $B^A_e = \int_e B^A$.

- ⊙ *The A-connection discretization:* since it is a 1-form, similarly to the triad field we perform the discretization procedure in such a way that we associate 1-dimensional objects that should be able to measure the curvature located on the edges. Thus, we consider the dual simplicial complex $T^\star$ and the connection A can then be integrated along the dual link $e^\star$ defining therefore *holonomies* $g_{e^\star} \equiv \mathcal{P}\exp\left(\int_{e^\star} A\right)$. These are clearly group elements. We presented some properties that the holonomies enjoy in Appendix A.1.

- ⊙ *The Curvature F:* The discretized curvature in this picture is then naturally reproduced as the product of the group elements $g_{e^\star}$ associated with the links of the boundary of the dual face $f^\star$, and it is thus associated with the dual face itself; $g_{f^\star} = \prod_{e^\star \subset \partial f^\star} g_{e^\star}$. This is in turn dual to the edges of the triangulation T, so we have

the simplicial curvature associated with them, as we wanted. The logarithm of the group element g_{f^*} $\log(g_{f^*})$ gives a Lie algebra element that we denote by F_e, that we can think of as the substantial discretization of the curvature field on the edges of T.

This is the discretization prescription of variables (B_e, F_e) that is dual to the edges of a given triangulation T which we summarized in table 3.1.

Continuous variables	Discretized variables
$\int_M$	$\sum_{e\in T}$
The B field	$B_e^A \equiv \int_e B^A$
The connection A	$g_{e*} \equiv \mathcal{P}\exp\left(-\int_{e*} A\omega\right)$
The curvature F_e	$g_{f^\star} = \prod_{e^\star\subset\partial f^\star} g_{e^\star}$
The measure $D[B]$	$\prod_e dB_e^A$
The measure $D[A]$	$\prod_e dg_{e*}$
$S[B\,, A] = \int_M \mathrm{tr}\,(B\wedge F(A))$	$S[B, A] = \sum_{e\in T} \mathrm{tr}\,(B_e F_e)$

Table 3.1: On the left-hand side of the table we have the continuous variables of BF theory and on the right-hand side, we can read off the discretized version of it. Examples of triangulations of the continuous manifold are given in figure 3.1c.

The discretized action is then given by the discrete sum over the edges of the triangulation T and it yields

$$S[B, A] = \sum_{e\in T} \mathrm{tr}\,(B_e F_e)\ . \tag{3.1.9}$$

There is also the necessary check that this action is endowed with all of the discrete counterparts of the symmetries of the continuum action [17, 95]. The partition function associated with an arbitrary triangulation T can be written as

$$Z(T) = \int \prod_e \mathrm{d}B_e \prod_{e^\star} \mathrm{d}g_{e^\star} \exp\left\{ i \sum_e \mathrm{tr}\,(B_e F_e)\right\} = \int \prod_{e^\star} \mathrm{d}g_{e^\star} \prod_{f^\star} \delta\,(g_{f^\star})\,, \tag{3.1.10}$$

where in the second equations we end up with a δ-function on the group element $g_{f^\star}$ representing the holonomy of the connection around a dual face $f^\star$ after exploiting the fact that Lie algebra variables B_e act essentially as Lagrange multiplier.
This procedure can be naturally generalized to the case of $4d$ gravity as we will see in the next paragraph. In fact, it is a direct implementation of the prescription presented in table 3.1.

Discretizing $4d$ Gravity, Plebanski and Plebanski-Holst action

Now that we went through the description of GR in terms of the triad variable e and the connection, which is depicted by the first order Palatini formulation, we proceed to the

case of four dimensional spacetime. Once we have the first order formulation of the $4d$ gravity we study its relation to BF theory. Let us then start by promoting the triad to its four dimensional counterpart, i.e. we then replace it with the tetrad field e^I_a and write the spacetime metric $g_{ab} = e^I_a e^J_b \eta_{IJ}$. Hence, after implementing this parametrization, the action (3.1.3) produces the Palatini action of GR in $4d$

$$S[e^{IJ}_a, \omega^{AB}_a] = \int \epsilon_{IJKL}\; e^I \wedge e^J \wedge F^{KL}(\omega)\,, \tag{3.1.11}$$

where ω^{IJ} is the Lorentz connection this time, taking values in the Lie algebra of the Lorentz group $\mathfrak{so}(3,1)$ (or $\mathfrak{so}(4)$ for a Riemannian manifold). The equations of motion are obtained by varying with respect ω and e and they read

$$\epsilon_{IJKL}\, e^J \wedge F^{KL}(\omega) = 0\,, \quad d_\omega(e^I \wedge e^J) = 0\,. \tag{3.1.12}$$

Notice their algebraic simplicity. If the tetrad field is invertible meaning that a non-degenerate metric can be constructed, then the above equations are equivalent to Einstein's equation. However, the field equations, as well as the action (3.1.11) continue to make sense for degenerate tetrads. For example, the no-geometry state $e = 0$ (diffeomorphism invariant vacuum) solves the equations and makes perfect sense in terms of the new variables. Moreover, the symmetries of the action are, just as in the $3d$ case, the usual diffeomorphism invariance and the invariance under the internal gauge group, i.e., the Lorentz group SO(3, 1) (or SO(4) for Riemannian geometries).

It is important to mention that it is possible to show that there is another possible combination of the tetrads and the curvature that enjoy the same set of symmetries of the Palatini action [96] that leads to the same classical evolution equations of GR in vacuum. This is given by the term proportional to

$$\int e \wedge e \wedge F\,. \tag{3.1.13}$$

This is called the *Holst term*, and it can supplement the Palatini action such that

$$S[e,\omega] = \int e \wedge e \wedge \star F[\omega] + \frac{1}{\gamma}\int e \wedge e \wedge F[\omega]\,, \tag{3.1.14}$$

where $\star$ stands for the Hodge star product [96, 97]. The above coupling constant is chosen as the inverse of the Barbero-Immirzi parameter γ[2], defined in LQG as a free parameter of the theory [14, 98]. The two terms can be collected into the *Plebanski-Holst* action:

$$S[e,\omega] = \int \left(\star e \wedge e + \frac{1}{\gamma} e \wedge e\right) \wedge F[\omega]\,. \tag{3.1.15}$$

[2]It is worth mentioning that this term has no particular influence on the equations of motion and it can be shown to be vanishing on-shell [96].

This formulation is equivalent to GR in the classical framework. However, as we will discover in section 3.1.2 it becomes relevant when we enter the quantum description of the theory in section 3.2.
Similarly to the $3d$ case, we can write down the BF formulation of the action (3.1.11) which can be produced once we write the B field satisfying the quadratic *Plebanski* constraint [51, 96, 99]

$$B^{IJ} = \epsilon^{IJ}_{KL}\, e^K \wedge e^L \,. \tag{3.1.16}$$

This condition imposed on the B field in this setting, restricts the topological theory to one with local degrees of freedom, i.e. to that of GR in first order formulation. In this sense, we can start off from a BF theory, implement the above constraint and we end up with the familiar GR action. It is then reasonable to consider GR as a topological, dynamically *constrained* BF theory. More precisely the above constraint imposed on the B field is consistently incorporated through the *Plebanski action* [16] that yields

$$S[B,\omega,\mu] = \int_M \left[B^{IJ} \wedge F_{IJ}(\omega) - \frac{1}{2}\mu_{IJKL} B^{KL} \wedge B^{IJ} \right] , \tag{3.1.17}$$

where B and F are both two-forms with values in the algebra $\mathfrak{so}(3,1)$ (or $\mathfrak{so}(4)$) and the field strength $F^{IJ} = \mathrm{d}^{(\omega)}\omega^{IJ}$ for a connection 1-form valued again in the respective algebra. Here the constraint is imposed thanks to the Lagrange multiplier μ obeying the symmetries

$$\mu_{IJKL} = \mu_{[IJ][KL]} = \mu_{[KL][IJ]}, \quad \mu_{IJKL}\,\epsilon^{IJKL} = 0.$$

The equations of motions are thus obtained by varying with respect to ω, B, and μ. More importantly, the variation with respect to μ forces

$$\epsilon_{IJKL}\, B^{IJ}_{ij} B^{KL\ ij} = 0 \,, \tag{3.1.18}$$

implying that B_{ij} is a *simple bivector*. It is exactly for this reason that this constraint goes as *the quadratic simplicity constraint* in the literature [16, 99]. The geometric solution to the above constraint corresponds to the following configurations for the bivector

$$B^{IJ}_{\pm} = \pm \frac{\epsilon^{IJ}{}_{KL}}{2} e^K \wedge e^L \,, \tag{3.1.19}$$

where $e^A = e^A_a\ \mathrm{d}x^a$ is a real tetrad field. For completeness, let us mention that the simplicity constraint can also be defined to include the Barbero-Immirzi parameter γ present in the Holst action (3.1.14) and we denote this constraint by $S_\gamma(B)$. This naturally forces the B field to take the form [100]

$$B = \pm \left(1 + \star\gamma^{-1}\right) e \wedge e \,, \tag{3.1.20}$$

where $\star$ defines the Hodge dual. The constraint on the bivector can then be imposed on the BF analog of the Holst action in (3.1.14) that is identified as the *Plebanski-Holst* action given by

$$S[B,\omega,\mu] = \int \left[\mathrm{tr}(B \wedge F[\omega]) + \mu \cdot S_\gamma(B) \right] , \tag{3.1.21}$$

where the field B is given by (3.1.20), which reduces to (3.1.18) if we take the limit $\gamma \to \infty$. The actions (3.1.21) and (3.1.11) do not change the principles of discretizing the geometry at the classical level of the theory, however, their differences lie within the operation of implementing the constraints at the quantum level. Let us then first proceed to derive the discretization scheme thereof following the same steps as in the $3d$ case, but now one dimension higher.For this purpose, we work with a triangulation T of spacetime, where the spin-connection of the BF theory is again naturally discretized along the links $e^\star$ of the dual complex, in such a way that we end up with a Lie algebra element associated with each dual link $e^\star$, or analogously to each tetrahedron τ connecting two 4-simplices, namely

$$\omega_{e^\star}^{IJ} = \int_{e^\star} \mathrm{d}x^i \omega_i^{IJ} \in \mathfrak{g}\,. \tag{3.1.22}$$

and so similarly to the $3d$ (see table 3.1 for a summary) case but one dimension higher we have the following discretization prescription:

- *Connection:* we consider path-ordered exponential of the discretized connection $\omega_{e\star}$, namely $g_{e\star} \equiv \mathcal{P}\omega_{e\star}$ and match the curvature to the faces $f^\star$ of the dual complex (corresponding to triangles $\Delta \in T$) by the logarithmic operation that yields

$$F_\Delta = \log\left(g_{f^*}\right) \in \mathfrak{g}\,, \tag{3.1.23}$$

  with $g_{f^\star}$ is the product of group variables corresponding to the links circling the face $f^\star$, dual to the triangle Δ.

- *Discretization of B:* B is a two form, it can be naturally discretized on triangles $\Delta \in T$:

$$B_\Delta^{IJ} \equiv \int_\Delta \mathrm{d}x^i\ \mathrm{d}x^j B_{ij}^{IJ}\,. \tag{3.1.24}$$

This then can be used as inputs to produce the partition function associated with the triangulation T for the unconstrained, discretized BF theory:

$$Z(T) = \int \prod_\Delta \mathrm{d}B_\Delta \prod_{e^\star} \mathrm{d}g_{e^\star} \exp\left\{ i \sum_\Delta \mathrm{tr}\left(B_\Delta F_\Delta\right)\right\}. \tag{3.1.25}$$

In this setting, GR is recovered once we correctly implement the discrete counterpart of the simplicity constraint S_γ. This is translated into imposing a delta function forcing the constraint on the B field configurations $S_\gamma\left(B_\Delta\right) = 0$, this then yields

$$Z(T) = \int \prod_\Delta \mathrm{d}B_\Delta \prod_{e^*}\ \mathrm{d}g_{e^*} \delta\left(S_\gamma\left(B_\Delta\right)\right) \exp\left\{ i \sum_\Delta \mathrm{tr}\left(B_\Delta F_\Delta\right)\right\}\,. \tag{3.1.26}$$

where $\delta\left(S_\gamma\left(B_\Delta\right)\right)$ encapsulates the imposition of the discretized constraint that reduces the BF theory to GR. As we will see in section 3.2, it is exactly the quantization of this constraint through the presence of the delta function, that gives rise to different quantum gravity models.

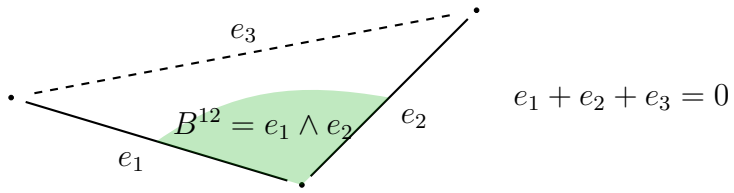

Figure 3.2: Closure of a triangle based on three edges. Illustrated is also a bivector B^{12} constructed out of the wedge product of two edge vectors, e_1 and e_2.

3.1.2 Quantization procedure of discrete gravity

So far we managed to successfully provide a discretized version of spacetime in $3d$ and $4d$ in terms of triangles and tetrahedra as fundamental building blocks, where their dynamics are captured by the discretized partition functions in (3.1.10) and (3.1.26). Now, we want to construct the quantum picture associated with such discretized simplicial geometries which is the main goal of any QG theory. To achieve this, we start by showing how all the elements of the triangulation are given a quantum description and how quantum states are constructed. This simplifies the identification of the fundamental building blocks for the transition amplitudes as we will see below. In the next section, we give an explicit derivation of the partition function and transition amplitudes for the theory based on these building blocks provided by the spin foam model.

Quantization of $3d$ simplicial geometry

We start by presenting the quantum version of the discretized geometry discussed above motivated by quantum simplicial geometry. More precisely, we provide the logic behind constructing the Hilbert space associated with the set of edges, triangles, tetrahedra, and the corresponding quantum states, spanning such a space. The key idea is then to *quantize* the basic variables of the theory and to obtain a state associated with each 2-dimensional surface in the simplicial manifold. This is obviously given by a collection of triangles glued together along common edges where an amplitude for each 3-dimensional manifold is then provided by a group of 3-simplices, tetrahedra, glued together along common triangles. Finally, we can generate the path integral expression for the transition amplitudes. In order to systematically implement this program, we follow a very simple line of reasoning: we write down the classical constraint that is imposed on the elementary discrete edges to close and form a triangle and then we lay out its quantum counterpart, starting from which we can perform the same steps for the tetrahedron.

Once we have fixed a triangulation T, we saw that in $3d$ the geometry of the $d-1$ boundary data are simply given by triangles. These objects can then be glued together to build the fundamental structure of the discretized simplex which are tetrahedra as illustrated in figure 3.3.

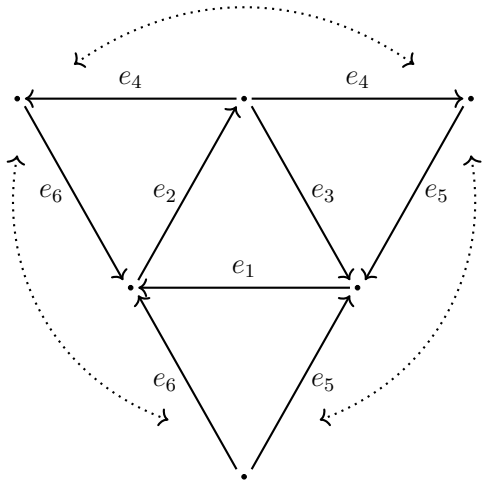

Figure 3.3: Closure of a tetrahedron τ on its four faces by identifying the common edges in each pair of faces (triangles).

Now, a single tetrahedron can be understood as the convex envelope of four points in $\mathbb{R}^3$ [101]. With reference to figure 3.2, we see that a set of triads $\vec{e}_1, \vec{e}_2, \vec{e}_3$ of independent vectors defines completely the triangle, such that

$$\sum_{i=1}^{3} \vec{e}_i = 0\,, \tag{3.1.27}$$

and we call this equation at the classical level of the geometric description the *closure constraint*. The fundamental parameter used in expressing geometric quantities is the discrete variable that can be associated with the triad field e. We saw when we derived the discretization of BF theory in $3d$ (section 3.1.1) that the discretization is performed by associating to each edge an SU(2) group element. There is then a natural algebraic way to construct its quantum analog. Now the quantization program can be implemented canonically, by promoting the above algebra variables to operators, which once assigned a representation, can act on a given Hilbert space (representation space V^{j_2}) [3]. In the current situation, it will act on the Hilbert space of the quantum tetrahedron.
Let us then implement the sketched quantization procedure in the case of the discretized $3d$ geometry.

- *Quantum vector:* we choose a representation j_e and turn its Lie algebra into an operator acting on the representation space V^{j_e}. This gives us the Hilbert space

[3] In fact, we can associate to each edge an element of the canonical basis of the SU(2) Lie algebra, J_i in some representation j. Doing this, the operator corresponding to the square of the edge length $e_a \cdot e_a$ for the edge a is given by the SU(2) Casimir $C = L^2 = J_a \cdot J_a$, which is diagonal on the representation space V^{j_a}, $L_a = j_a(j_a + 1)$. Therefore we see that the representation label j gives the *quantum* length L of e to which the corresponding representation is assigned, thus the Hilbert space V_j can be interpreted as the Hilbert space for a 3-vector with squared length $j(j + 1)$.

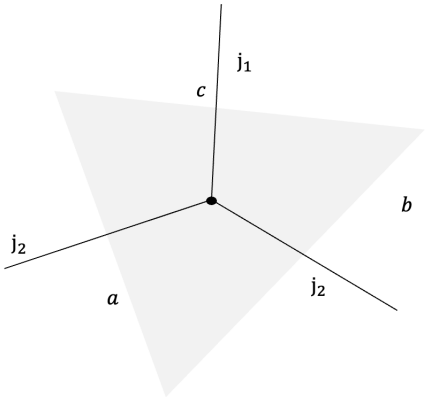

Figure 3.4: Spin network state describing the quantum triangle *abc* with edges labeled by spin representations $j_1\,, j_2\,, j_3$. The closure of the triangle is translated to requiring the invariance of the tensored state of the respective edges. This defines the *vertex* state.

and a set of operators acting on it and they are associated with each edge of the triangle. The edge Hilbert space is given by the direct sum of all Hilbert space that can reproduce a possible fixed edge *length*: $\mathcal{H}_e = \oplus_{j_e} V^{j_e}$. It is important to stress that this is the fundamental Hilbert space starting from which we can construct the one for the triangle as well as the one for the tetrahedron.

- *Quantum triangle:* As we have already introduced above, a classical triangle is given by a set of three vectors that close together (3.1.27). The quantum state that we can give to triangles is obviously constructed based on three copies of the quantum edge vector extracted above. However, we need to define the *quantum* counterpart of the *closure* constraint imposed so that the edges close, meaning that we have to constrain the space of three edges given by the tensor product $V^{j_1} \otimes V^{j_2} \otimes V^{j_3}$. The closure constraint is translated to a very well-known invariant tensor in the representation theory of SU(2), namely the *intertwiner* between the three representations j_1, j_2, j_3, i.e. the $3j$ symbol:

$$\varphi_\Delta = I^{j_1 j_2 j_3}_{m_1 m_2 m_3} = \begin{pmatrix} j_1 & j_2 & j_3 \\ m_1 & m_2 & m_3 \end{pmatrix} . \tag{3.1.28}$$

  The resulting quantum state is unique and is usually called a *vertex* (see figure 3.4). The full Hilbert space for the quantum triangle Δ (abc) is then given by[4]:

$$\mathcal{H}_\Delta = \oplus_{j_a, j_b, j_c} \mathrm{Inv}\left(V^{j_1} \otimes V^{j_2} \otimes V^{j_3}\right) . \tag{3.1.29}$$

Now, classically, a generic $2d$ surface is constructed out of glued triangles along their common edges. In the quantum picture, this is translated into gluing the corresponding

[4]If one takes into account the triangle inequalities, this can be converted at the quantum level to inequalities for the representation parameters j_a, given by $|j_1 - j_2| \leq j_3 \leq j_1 + j_2$. When this holds, there is then only one possible choice for the state of the quantum triangle [102].

states of the quantum triangles where the gluing is basically defined through the tracing over the common representation space of tensored triangles. The amplitude in this case, is automatically associated with a quantum tetrahedron τ. This can be naturally provided by the construction mentioned above in terms of quantized edges and their Hilbert spaces. A tetrahedron τ can be seen as a cobordism $S^3 \to \mathbb{C}$ given by 4 boundary triangles (meaning 6 boundary edges as illustrated in figure 3.3 and figure 3.1b) [103, 104]. In this case, we can associate it with the amplitude

$$\tau(j) : \otimes_i \varphi_{\Delta_i} = \otimes_i \mathrm{Inv}\left(V^{j_{1_i}} \otimes V^{j_{2_i}} \otimes V^{j_{3_i}}\right) \to \mathbb{C}. \tag{3.1.30}$$

The above amplitude is quite simple and it preserves all the information we need about τ. Indeed, the representations associated with the six edges of the tetrahedron obey the triangle inequalities and are invariant under the group of rotations SU(2). Consequently, it can be obtained by explicitly constructing the four invariant tensors ($3j$-symbols) for the four triangles[5], thus getting a scalar as a result. The amplitude can be then expressed for the case of a *fixed* spin value as

$$\tau(j) = I^{j_1 j_2 j_3}_{m_1 m_2 m_3} I^{j_3 j_4 j_5}_{m_3 m_4 m_5} I^{j_5 j_1 j_6}_{m_5 m_1 m_6} I^{j_6 j_2 j_4}_{m_6 m_2 m_4} = \{6j\}\,, \tag{3.1.31}$$

i.e. by the $6j$-symbol and for a generic choice of spin labels, we end up with the more general amplitude

$$\tau = \left(\prod_i \sum_{j_i} \Delta_{j_i}\right) \{6j\}\,. \tag{3.1.32}$$

For a generic simplicial complex, the amplitude is simply given by a product of $6j$-symbols, one for each tetrahedron, where we also similarly sum over representations for all the edges in it. The above outlined quantization procedure of the classical discretized partition function in $3d$ is summarized in table 3.2.

Classical discrete parameters	*Quantization*	*Hilbert space*
Edge vector e_i of a triangle Δ	j_e	$\mathcal{H}_e = \oplus_{j_e} V^{j_e}$
Triangle Δ	$\varphi_\Delta = I^{j_1 j_2 j_3}_{m_1 m_2 m_3}$	$\mathcal{H}_\Delta = \oplus_{j_i} \mathrm{Inv}\,(V^{j_1} \otimes V^{j_2} \otimes V^{j_3})$
Tetrahedron τ	$\otimes_i \varphi_{\Delta_i}$ (3.1.30)	$\tau = \left(\prod_i \sum_{j_i} \Delta_{j_i}\right) \{6j\}$

Table 3.2: Quantization prescription of the edges, triangles and tetrahedra. The implementation of the classical closure constraints in already performed. The resulting fundamental elementary state of quantum geometry is depicted in figure 3.4.

[5] This is an operation that mimics the closure of the four triangles to build up the boundary sphere S^3.

$4d$ quantum discretized geometry

In the four dimensional case, we are dealing with one dimension higher for the boundary geometry. We are dealing then with tetrahedra instead of triangles which are glued among their common faces. This construction is the basic entity characterizing the geometry triangulation T, namely 4-simplices. Similarly to the case of $3d$ geometry, we start by describing the classical geometric objects we need to reproduce the continuum geometry and then proceed to its quantum counterpart (see table 3.2 for a concise outline of the $3d$ case).
The main difference with the $3d$ geometry is that a classical tetrahedron can be described through a set of four *bivectors* that are normal to each of its triangular faces. Analogously to the $3d$ case, in order to proceed with its quantization we rely on the isomorphism between the space of bivectors for Riemannian or Lorentzian signature with the respective Lie algebra elements.

First, let us start by stating that the analog of the closure constraints in (3.1.27) is then applied to the bivectors on the faces of a given tetrahedron. This forces the closure of the tetrahedron and it reads as

$$\sum_{i=1}^{4} B_i^{IJ} = 0\,, \tag{3.1.33}$$

There is an additional constraint that we need to impose on the bivectors which is the geometric condition that they have to lie in the same three dimensional hypersurface [101, 102]. This can be specified by finding a vector X that must be normal to all four bivectors, illustrated in figure 3.6. This condition makes the bivector *simple*, and we call it the *linear simplicity constraint*. It is of great importance to mention that, the quadratic simplicity constraint admits two sectors of solutions of the topological and gravitational sectors [1]. However, the linear simplicity constraint has solutions only in the gravitational sector, making it a slightly stronger condition than the quadratic one, but it picks out the correct solution sector. As we will see later on, once we discuss spin foam models in section 3.2, this constraint can be imposed in different ways, birthing different QG models. The quantization of a tetrahedron then proceeds exactly in the same way as the $3d$ case. In the following we denote Hilbert spaces of triangles with the subscript Δ and representation with t. We can explicitly describe it in the Lorentzian (and Riemannian) cases as follows:

1. We use the isometry $\bigwedge^2 \mathbb{R}^4 \simeq \mathfrak{so}(4) \simeq \mathfrak{spin}(4)$ and in the Lorentzian case the isometry $\bigwedge^2 \mathbb{R}^{3,1} \simeq \mathfrak{so}(3,1)$. This naturally allows us to associate the bivector attributed to a triangle Δ with a generator of the algebra:

$$B^{IJ}(t) \to *J^{IJ}(t) = \epsilon^{IJ}_{KL} J^{KL}\,. \tag{3.1.34}$$

2. We then promote these variables into operators. This is (as in the $3d$ case) carried out by associating to the different triangles Δ an irreducible representation (irrep) ρ_t

of the group and the corresponding representation space using the geometric quantization map as in the $3d$ case so that the generators of the algebra act on it. This of course depends on the group at hand and its harmonic analysis. Again, as we will see later on, this very step will differentiate QG models.

3. *The Hilbert space of a quantum triangle:* the group we are working with is in the Lorentzian case $\mathrm{SL}(2,\mathbb{C})$, the double cover of the Lorentz group $\mathrm{SO}(3,1)$ (and in the Riemannian Spin(4) being the double cover of SO(4)). In the Lorentzian case, the irreps in the *principal* series are characterized by a pair (ρ,ν) of a natural number ν and a real number ρ. For the case of SO(4) the unitary representations are labeled by two half integers (j_1,j_2). The Hilbert spaces of the *un-constrained* quantum triangle in these cases yield
$$\mathcal{H}=\oplus_{\nu,\rho}\mathcal{H}^{(\nu,\rho)} \tag{3.1.35}$$
in order to impose the quantum constraint to reproduce a bivector we rely on the map (3.1.34) which produces a condition on vanishing Casimir [105–107]
$$J\left(\rho_t\right)\cdot *J\left(\rho_t\right)=\epsilon_{IJKL}J^{IJ}\left(\rho_t\right)J^{KL}\left(\rho_t\right)=C_2\left(\rho_t\right)=0\,. \tag{3.1.36}$$
where t labels a triangle. For the Lorentzian case, we end up with the representation labeled by $(\rho,0)$ corresponding to time-like triangles and $(0,\nu)$ corresponding to spacelike triangles that solve the constraint (in SO(4) case we have only representation of the form (j,j)) as explained in the appendix A.1. The associated Hilbert spaces for both cases read respectively
$$\mathcal{H}_\Delta=\oplus_\nu\mathcal{H}^{(\nu,0)}\cup\oplus_\rho\mathcal{H}^{(0,\rho)}\,,\quad \mathcal{H}_\Delta=\oplus_j\mathcal{H}^{(j,j)}\,. \tag{3.1.37}$$

4. *Tetrahedron Hilbert space:* the Hilbert space for the tetrahedron is obtained from that of its triangles, in particular, it is assembled by four of them, mimicking the classical picture where we need four triangles to close in order to obtain τ. Therefore we are considering each tetrahedron, with given representations assigned to its triangles, to be a tensor product: $\mathcal{H}_{\Delta_1}\otimes\mathcal{H}_{\Delta_2}\otimes\mathcal{H}_{\Delta_3}\otimes\mathcal{H}_{\Delta_4}$ of the four representation spaces for its faces where the tensored spaces decompose pairwise into those labeled with the balanced (simple) representations only. We still have to impose the closure constraint we associate to the tetrahedron through an intertwiner between the four simple representations associated with its faces acting as the map
$$B^{\rho_1\rho_2\rho_3\rho_4}:\mathcal{H}_{\Delta_1}\otimes\mathcal{H}_{\Delta_2}\otimes\mathcal{H}_{\Delta_3}\otimes\mathcal{H}_{\Delta_4}\to\mathbb{C} \tag{3.1.38}$$
and this is illustrated in figure 3.5. Therefore the Hilbert space of a quantum tetrahedron is given by:
$$\mathcal{H}_\tau=\mathrm{Inv}\left(\mathcal{H}_{\Delta_1}\otimes\mathcal{H}_{\Delta_2}\otimes\mathcal{H}_{\Delta_3}\otimes\mathcal{H}_{\Delta_4}\right)\,, \tag{3.1.39}$$
with $\mathcal{H}_{\Delta_i}$ being the Hilbert space for the i-the triangle Δ defined above. Each state in this Hilbert space is then a group intertwiner called the Barrett-Crane intertwiner. We will discuss this invariant quantity when we again encounter the BC model in section 3.2.

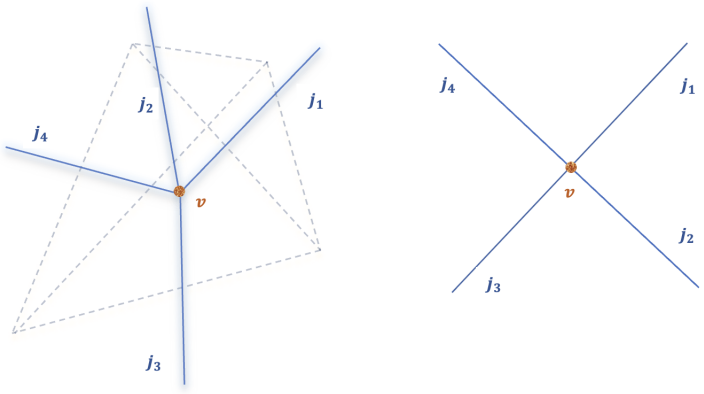

Figure 3.5: The vertex depicting a quantum tetrahedron in $4d$ with four outgoing links labeled by spin representations. The links are dual to the faces (triangles) of the tetrahedron and the invariance at the vertex is translated to the closure of the four of them.

5. *4-Simplex amplitude:* the quantum amplitude for a 4-simplex σ, interpreted as an elementary dynamical variation affecting the geometry, thus expressing the dynamics of the theory, is indeed the fundamental building block for the partition function and the transition amplitudes of the quantum theory. As in the $3d$ case, this amplitude is built out of the tensors associated with the tetrahedra in the 4-simplex. This clearly allows us to immediately take into account the conditions to describe the geometry of the simplicial manifold, at both the classical and *quantum* level and has to be invariant under the gauge group (again, to reproduce GR it is the groups $\mathrm{SL}(2,\mathbb{C})$ or $\mathrm{Spin}(4)$). This can be obtained by contacting the five required tetrahedra to get

$$A_\sigma : \otimes_i \,\mathrm{Inv}\left(\mathcal{H}^{1_i} \otimes \mathcal{H}^{2_i} \otimes \mathcal{H}^{3_i} \otimes \mathcal{H}^{4_i}\right) \to \mathbb{C}\,, \tag{3.1.40}$$

This amplitude is for fixed representations associated with the triangles, meaning we are also fixing the area of the corresponding triangles. Finally, the full amplitude takes into account all representations, where (3.1.40) plays the role of weight for each configuration.

The quantization of the classical constraints produces different spin foam models as we will discuss in section 3.2. As we already emphasized, the transition to the quantum picture is achieved through implementing such a constraint at the level of the representation labels decorating the fundamental building blocks. Below in table 3.3 we report the main ingredients to perform such quantization in $4d$.

3.2 Covariant quantization program

We have seen that in BF theory the partition function can be computed by triangulating spacetimes in $3d$ and $4d$ considering all the ways of labeling dual faces by irreducible

Classical discrete parameters	*Quantization*	*Hilbert space*
Triangle Δ	$\varphi_\Delta = I^{j_1 j_2 j_3}_{m_1 m_2 m_3}$	$\mathcal{H}_\Delta = \oplus_\nu \mathcal{H}^{(\nu,0)} \cup \oplus_\rho \mathcal{H}^{(0,\rho)}$
Tetrahedron τ	$B^{\rho_1\rho_2\rho_3\rho_4}$ (3.1.38)	$\mathcal{H}_\tau = \mathrm{Inv}\left(\otimes_i^4 \mathcal{H}_{\Delta_i}\right)$

Table 3.3: Quantization prescription of the discretized partition function (3.1.26) in $4d$. The implementation of the classical closure and simplicity constraints is already performed and made evident by selecting the balanced representation of the principle series of $\mathrm{SL}(2,\mathbb{C})$. The resulting fundamental elementary state of quantum geometry (the tetrahedron) is illustrated in figure 3.5. Notice that we reported here only the Lorentzian quantum geometry data.

.

representations and dual edges by intertwiners. The amplitude is then constructed such that for each of such labeling, we view an amplitude as the product of amplitudes for dual *faces*, dual *edges*, and dual *vertices*. To formalize this concept and directly relate it to the EH action, we introduce the formalism of *spin foams* (SF). Spin foam models resulted from the line of research that follows the path integral quantization technique. It started off as an attempt to write down a Feynman path integral for GR [108–110] and was later on motivated by the lack of a concrete successful description for the dynamics of the quantized $3d$ geometries provided by the spin network states [102, 111, 112]. This also means the picture of a $4d$ quantum geometry is lacking (and still is). It is at this stage that spin foams propose an approach to address such a problem of properly imposing the quantum dynamics of geometries.
Analogously to spin networks is defined as a graph Γ with edges labeled by spins and vertices labeled by intertwining maps, a SF is a $2d$ piecewise linear cell complex with faces decorated by spins and edges labeled by intertwining operators. As we will see later in section 3.3 when we discuss the notion of spin networks, we can conceptualize SF either abstractly or embedded in spacetime. In both cases, a generic *slice* of a SF at a fixed time gives a *spin network*. Edges of this spin network come from faces of the SF. The vertices on the other hand of the spin network come from edges of the SF. In this picture, as we move the slice along the timeline, the topology of this spin network dynamically changes only when the slice passes a vertex of the spin foam.

General structure of the spin foam model

Let us start with the definition of what is a spin foam. It is very analogous to the definition of a spin network that we will study extensively in section 3.3, but everything is one dimension higher. More precisely [17]:

Definition 6. *(Spin foam) Given a spin network $\Psi = (\Gamma, \rho, \iota)$, a spin foam $F : \emptyset \to \Psi$ is a triple $(\sigma, \tilde{\rho}, \tilde{\iota})$*

- *σ is a 2 -dimensional oriented complex such that Γ (the graph) borders σ, $\tilde{\rho}$ is a*

labeling of each face f of σ by an irreducible representation ρ_f of a group G,

- *$\tilde{\iota}$ is a labeling of each edge e not lying in Γ by an intertwiner mapping the irreducible representations (irreps) of the faces incoming to e to the tensor product of the irreducible representations of the faces outgoing from e,*

- *for any edge e' of Γ we have; $\tilde{\rho}_f = \rho_{e'}$ if f is incoming to e' and $\tilde{\rho}_f = \rho^*_{e'}$ if it is outgoing from it, and for any vertex v in Γ, $\tilde{\iota}_e = \iota_v$ with appropriate dualization.*

As we emphasized earlier, we now explore two SF models that differ due to the imposition of the simplicity constraint of the bivectors at the quantum level. In section 3.2.2 we see how the linear simplicity constraint appearing in the Plebanski-Holst action is implemented, whereas in section 3.2.1 we present the main point of the Barrett Crane (BC) model imposing the quadratic simplicity constraint. Furthermore, it is important to emphasize that the techniques we developed in quantizing BF theory can not be borrowed and implemented a the level of SF. This can be explained by the fact that the path integral of spin foam theory is regularized on a triangulation and consequently fixing it [16]. This means that at the level of its 2-complex, the degrees of freedom are *truncated*. Indeed, we can discretize and quantize the topological theory first. The B-fields are assigned to the faces of the 2-complex, triangles, and encode their geometry. However, the connection is *regularized* by considering only its holonomy responsible for the parallel transport along the (half-)edges of the 2-complex (from one tetrahedron to another). As explained above, the topological theory partition function consists of a collection of delta functions imposing flatness of each face of the 2-complex.

3.2.1 The Lorentzian Barrett Crane model

In the following, we want to sketch the main idea behind the Barrett-Crane model since the main results obtained in chapter 5 are an extension of this formalism. The BC model is one of the most extensively studied spin foam models for quantum gravity from a covariant formulation [102,113,114]. Let us present the main features that led to such a construction, referring for more extensive and detailed analysis to the literature [16,115–117]. We focus on the Lorentzian BC model in $4d$ since it is the main spin foam model related to the setting in chapter 5, the discussion can be simply generalized to cover the Riemannian case. The BC model can be formally viewed as a spin foam quantization of Plebanski's formulation of GR. For now, we focus only on this action, leaving the Plebanski-Holst action treatment to section 3.2.2 when we discuss the EPRL model.

Classical geometry description: We saw that in $4d$, we can write the EH action in a first order formulation captured by the Plebanski action in (3.1.21) which is basically a constrained BF. The recovery of GR as a subclass of the BF family theories is based on the identification of the B field with the bivector associated with the triad field, namely

$$B^{IJ} = \pm\epsilon^{IJKL} e_K \wedge e_L, \quad \text{and} \quad B^{IJ} = \pm e^I \wedge e^J \,, \tag{3.2.1}$$

The BC model provides an attempt for the quantum translation of these geometric constraints and a framework for their implementation in a consistent QG model. The starting point is the formalism developed in 3.1 where GR is reproduced in a simplicial geometric setting by constraining the BF theory in four dimensions. This description paves the way to introduce a background independent attempt to quantize it. As already spoiled several times, what makes a QG model different from its relatives is how to quantize the above constraint imposed onto the bivectors. In the following, we perform this for the simple expression (3.2.1). We carry out the same steps of quantization provided by the map (3.1.34) for the bivector [2,115,118], where the gauge group is the Lorentzian one (the Riemannian case is similarly constructed):

$$B = *(e \wedge e) \,. \tag{3.2.2}$$

Let us go a bit into the details to understand how to implement such a very simple constraint at the quantum level. To do so, we start by describing the *classical* set of constraints imposed on the B-field in the BF theory which is now imposed automatically on the bivector:

- The bivectors change sign when the orientation of the triangles Δ within a given tetrahedron τ is changed.
- The bivector is simple.
- The bivectors associated with neighboring triangles sum to simple bivectors, if both of them share an edge.
- The four bivectors associated with the faces of a tetrahedron sum to zero:

$$\sum_i^4 B_i^{IJ} = 0 \,. \tag{3.2.3}$$

Quantum bivector and tetrahedron: The quantization procedure of these constraints is similar to the one derived in section 3.1.2 and it amounts in providing a consistent description of the quantum bivector. The Barrett-Crane quantization proceeds by associating to each triangle Δ an irrep of the Lorentz group in *the principal unitary series*, with the identification

$$B^{IJ}(t) \leftrightarrow *L^{IJ}\left((\rho,\nu)_\Delta\right) \,, \tag{3.2.4}$$

where L is the generator of the Lorentz algebra and $(\rho,\nu)_\Delta$ are the representations labels such as ν being a half-integer number, and ρ a real positive number labeling them (for the detailed input provided by group theory of the Lorentz group, we refer the reader to Appendix A.1). The corresponding representation space (on which the generator L acts) are attached to each triangle Δ, and assigned to each tetrahedron τ an invariant

tensor (intertwiner) in the space given by the tensor product of the four representation spaces associated with its faces, intertwining, therefore, the triangle Hilbert spaces. This is basically the action of gluing the set of triangles to build a given tetrahedron. This identification then allows a *quantum* translation of the classical constraints listed above as:

- If a triangle changes orientation, the representations are then interchanged with their dual.
- The representations that we associate to the bivector are only the *simple* (balanced) ones: $(0,\nu)$ or $(\rho,0)$. This is translated as setting this restriction through $C_2 = L\left((\rho,\nu)_\Delta\right)\cdot *L\left((\rho,\nu)_\Delta\right) = \nu\rho = 0$, where C_2 is the second invariant Casimir of the algebra (see Appendix A.1). These selected representations can be realized in the spaces of square integrable functions on the hyperboloids in Minkowski space $\mathbb{M}^4$. We will consider only the representations that are associated with spacelike tetrahedra (simple bivector with $\nu = 0$) since they are the only ones relevant to our discussion for the BC model.[6] The Hilbert space is then given by
$$\mathcal{H}^{(0,\rho)} = L^2[Q_1] = \bigoplus_\mu R_{0\,,\rho}\,\mathrm{d}\rho\,\rho^2\,. \tag{3.2.5}$$
- The representations associated with adjacent triangles sum to simple representations (fulfilling $C_2 = 0$), if Δ and Δ' share an edge; this also implies that the tensor for a tetrahedron τ must be decomposed into its Clebsch-Gordon series where the contributions in the entries of such a sum are non-zero for simple representations *only*.
- The tensor associated with a τ is an invariant tensor under the action of $\mathrm{SO}(3,1)$. Thus we associate an intertwiner I_τ to each of these building blocks.

This set of conditions allows the identification of a unique state Ψ_τ for each tetrahedron in the triangulation T. Geometrically, the simplicity constraint is translated to have the bivectors lying in the same hypersurface illustrated by figure 3.6. This is exactly given by the invariant tensor called the *Barrett-Crane intertwiner*.

The partition function. Using the same BF derivation for the partition function, we consider the L^2 square integrable functions on the hyperboloids in Minkowski space $\mathbb{M}^4$ and realize the BC constraint by using a suitable *projector* on it [105, 114]. The geometric

[6] This reason is laid down as follows: for the quantization procedure, the algebra associated with the two spectra of the balanced irreps have different Poisson structures. For instance, the spacelike simple Lie algebra elements include the subalgebra $\mathfrak{su}(2)$, for which there exists a quantization condition that the symplectic form is integral and as a consequence, this naturally leads to a discrete series of representations. On the other hand, the corresponding cohomology class for the time-like elements vanishes, so there is no known quantization condition so far. This produces an arbitrariness of the parameter [114].

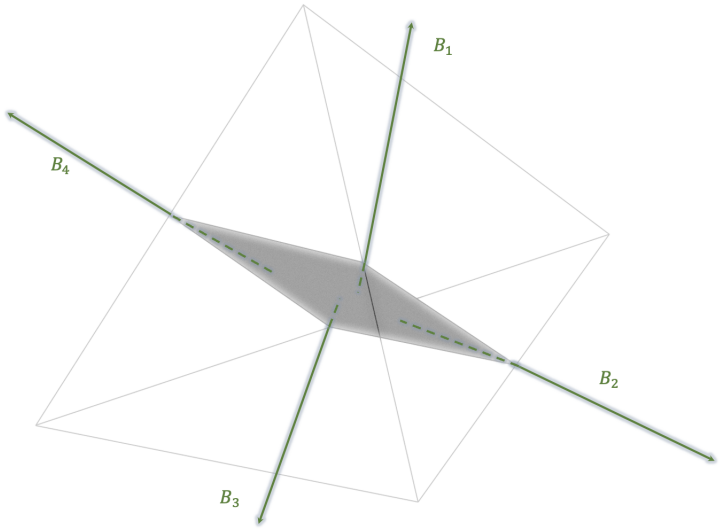

Figure 3.6: Geometric interpretation of the simplicity constraint. The gray surface is the hypersurface where all the four bivectors normal to the faces of the triangles must be embedded.

meaning of such a projection is to restrict to spacelike triangles that are defined through time-like bivectors (see Appendix A.1). The above constraints are then implemented as follows:

1. *Upper hyperboloid* Q_1: The simple representations are then considered once we restrict the Hilbert space to the irreps in the principle series which are realized once we impose invariance under the SU(2) group action on the representations associated the each face of the triangle (defined by the corresponding bivector).

2. *Closure constraint of* τ*:* Relying on the same set of SU(2) invariant representations, we further demand invariance under the action of the Lorentz group of the product of the four representation functions corresponding to the four triangles of τ.

In both cases, the employed projectors realize the simplicity constraint. Now, let us see the intertwiner that can be constructed by considering the tensor product of spacelike triangles labeled by the quantum labels of the balanced representations within the principle series. The tetrahedron-intertwiner yields [102, 114]

$$B^{\rho_1\rho_2\rho_3}_{j_1k_1j_2k_2j_3k_3j_4k_4} = \int_{SL(2,\mathbb{C})/SU(2)\sim Q_1} dx D^{\rho_1}_{00j_1k_1}(x) D^{\rho_2}_{00j_2k_2}(x) D^{\rho_3}_{00j_3k_3}(x) D^{\rho_4}_{00j_4k_4}(x), \qquad (3.2.6)$$

where the $D^\rho(g)$ are matrix elements of the representation ρ of the group element g as explained in Appendix A.1 and x are the coordinate on Minkowski space. Notice that here, the required invariance under the action of SU(2) turns the integral over $\mathrm{SL}(2,\mathbb{C})$ into an integral over the homogeneous space Q_1 (as we anticipated above)[7]. This invariant

[7]Of course, in the Lorentzian case, where the integration domain is noncompact, we are not at all certain that the integral is well defined or even makes sense. We will discuss this in detail later in chapter

tensor represents, as we said, the state of a tetrahedron whose faces are labeled by the given representations; it can be represented graphically as in figure 3.3.

Now we have all the ingredients to compute the transition amplitude associated with the BC model. It can be obtained by contacting the five tetrahedra as in (3.1.40). This amplitude is for fixed representations associated with the triangles, i.e. for fixed triangle areas; the full amplitude involves a sum over these representations with the above amplitude as a weight for each configuration. The resulting model is then given by the partition function based on continuous representations where the measure is provided by the Plancherel one,

$$Z = \left(\prod_f \int_{\rho_f} d\rho_f \rho_f^2\right) \left(\prod_{v,e_v} \int_{Q_1} dx_{e_v}\right) \prod_e A_e\left(\rho_k\right) \prod_v A_v\left(\rho_k, x_i\right) , \tag{3.2.7}$$

with the amplitudes[8] for edges (tetrahedra) and vertices (4-simplices) being given by

$$A_e\left(\rho_1, \rho_2, \rho_3, \rho_4\right) = \int_{Q_1} dx_1 dx_2 K^{\rho_1}\left(x_1, x_2\right) K^{\rho_2}\left(x_1, x_2\right) K^{\rho_3}\left(x_1, x_2\right) K^{\rho_4}\left(x_1, x_2\right) ,$$

where K^ρ is the invariant kernel resulting from the contraction of two simple representations and it is naturally invariant under SU(2). It is then associated with each triangle in each 4-simplex. The face amplitude is given by the product of the Plancharel measure

$$\left(\prod_f \int_{\rho_f} d\rho_f \rho_f^2\right) . \tag{3.2.8}$$

Whereas the vertex amplitude is given by [2, 119]

$$A_v\left(\rho_k, x_i\right) = K^{\rho_1}\left(x_1, x_2\right) K^{\rho_2}\left(x_2, x_3\right) K^{\rho_3}\left(x_3, x_4\right) K^{\rho_4}\left(x_4, x_5\right) K^{\rho_5}\left(x_1, x_5\right) \tag{3.2.9}$$

$$K^{\rho_6}\left(x_1, x_4\right) K^{\rho_7}\left(x_1, x_3\right) K^{\rho_8}\left(x_3, x_5\right) K^{\rho_9}\left(x_2, x_4\right) K^{\rho_{10}}\left(x_2, x_5\right) . \tag{3.2.10}$$

The explicit expression of K that will turn out to be very useful for the computations in chapter 5 reads as

$$K^{\rho_k}\left(x_i, x_j\right) = \frac{2\sin\left(\eta_{ij}\rho_k/2\right)}{\rho_k \sinh \eta_{ij}} , \tag{3.2.11}$$

where η_{ij} is the hyperbolic distance between the points x_i and x_j on the hyperboloid Q_1. This vertex is depicted by the figure 5.4 in chapter 5.
It is interesting to mention that the amplitudes describe an interaction among the representation labeled by ρ gluing different 4-simplices and tetrahedra in the triangulation every time they share a triangle, and an interaction among the different tetrahedra in each

5.

[8] Note that the integration measure here is given by the Plancharel one for the corresponding group and $\mathrm{SL}(2,\mathbb{C})$ we have infinite dimensional space for the group representations.

4-simplex.
The outlined Lorentzian QG model encountered several improvements to include the geometric information coming from the normal vectors to the tetrahedron that we will also discuss in chapter 5 [100, 120–122].

3.2.2 The EPRL spin foam model

We saw in section 3.1, the Plebanski formulation of GR provided us with a topological description for the $4d$ geometry by expressing it as a constrained BF. We also encountered the basic variables of the BF theory are a 2-form B conjugated to a connection A (with curvature F) in this case. Imposing the linear simplicity constraint on the B field reduces the BF action to the Holst one in (3.1.14). We saw that the corresponding partition function is then given by (3.1.26).
The task is then to implement a quantum version of the constraints in order to recover the gravitational *physical* degrees of freedom. As we already previously mentioned, this is not a straightforward task due to the simplicial framework the action is formulated in. As a matter of fact, there is so far no canonical quantization procedure in such discretized scheme. However, this is a price that has to be paid for requiring background independence.
To address the Holst contribution properly, we examine the linear simplicity constraint in a rather different way. Consider a space-like hypersurface Σ of the manifold M where we choose to fix the internal gauge to be the *temporal* gauge[9]. The normal to Σ is then simply given by $n_I = (1, 0, 0, 0)$. This gauge fixing clearly breaks the Lorentz symmetry of the theory, reducing it to an SO(3) rotational symmetry, and is actually equivalent to selecting a preferred Lorentzian frame. This allows us to separate the bivector components into boost and rotational parts and we can then establish the relation

$$K^I = n_J B^{IJ} = n_J(\star e \wedge e)^{IJ}\,, \quad L^I = n_J(\star B)^{IJ} = \frac{1}{\gamma} n_J(\star e \wedge e)^{IJ}\,, \tag{3.2.12}$$

from which we can deduce

$$K^I = \gamma L^I\,. \tag{3.2.13}$$

Moreover, the anti-symmetric properties of B^{IJ} are sufficient to deduce that the components of the boost and rotational parts of the bivector (K^0 and L^0 normal to Σ) vanishes. This enables us to view K and L as $3d$ vectors where (3.2.13) reduces to:

$$\vec{K} = \gamma \vec{L}\,, \quad K^i = B^{i0}\,, \quad L^i = \frac{1}{2}\epsilon^i_{jk} B^{jk}\,. \tag{3.2.14}$$

Now translating this to the quantum versions amounts to promoting the above boost and rotation to operators acting on the Hilbert space and then *weakly* imposing the constraint,

[9] As we will see this is also the gauge of the canonical quantization in LQG. In fact, it is very common to refer to the EPRL model and more generally SF as the covariant completion of LQG.

highlighting the relation between the Casimir operators, this amounts to explicitly writing the Casimirs as

$$K^2 - L^2|\rho, k, j, m\rangle = \left(\gamma^2 - 1\right) L^2|\rho, k, j, m\rangle\,, \quad \vec{L}\cdot\vec{K}|\rho, k, j, m\rangle = \gamma L^2|\rho, k, j, m\rangle. \tag{3.2.15}$$

This can be interpreted as a set of conditions imposed on the eigenvalues of the operators, namely

$$\rho^2 - k^2 + 1 = \left(\gamma^2 - 1\right) j(j+1),$$
$$\rho k = \gamma j(j+1)$$

which are solvable for large enough quantum numbers (to reproduce in the continuum limit the continuous simplicity constraint) [123]

$$\rho = \gamma j \quad k = j\,. \tag{3.2.16}$$

The irreps of $\mathrm{SL}(2,\mathbb{C})$ relevant in the Lorentzian model are then acting on the Hilbert space $\mathcal{H}^{(\gamma j, j)}$. Hence again, there is a one-to-one correspondence between SU(2) irreps and the $\mathrm{SL}(2,\mathbb{C})$ ones used in the theory. The key ingredient of the EPRL model is this isomorphism map. It embeds the spin j of the SU(2) representation into the lowest spin sector of the unitary irrep restricted to the principal series of $\mathrm{SL}(2,\mathbb{C})$ labeled by $(\nu,\rho) = (j, \gamma j)$. Moreover, the EPRL prescription enforces this map at every vertex of the 2-complex, enforcing the restriction of the irreps to γ-simple ones given by the matrices $D^{\gamma j, j}_{jmjn}(g)$. If the 2-complex has a boundary, the spin foam partition function maps states from the LQG kinematical Hilbert space into the complex numbers. The EPRL spin foam partition function is given as a state sum over SU(2) spins j_f on the faces and intertwiners I_e on the edges of the 2-complex, i.e.

$$\mathrm{Z} = \sum_{j_f, i_e} \prod_f A_f\left(j_f\right) \prod_e A_e\left(i_e\right) \prod_v A_v\left(j_f, i_e\right)\,, \tag{3.2.17}$$

defined in terms of the face amplitude A_f, and the edge amplitude A_e and the vertex amplitude A_v. Requiring the correct convolution property of the path integral at a fixed boundary, the form of the face amplitude $A_f\left(j_f\right) = 2j_f + 1$ and the edge amplitude $A_e\left(i_e\right) = 2i_e + 1$ are fixed [123, 124]. This allows us to define the Lorentzian edge and vertex amplitudes:

$$A_e\left(i_e\right) = 2i_e + 1\,,$$
$$A_v\left(j_f, i_e\right) = \sum_{l_f, k_e} \left(\prod_e d_{k_e} B_4^L\left(j_f, l_f, i_e, k_e\right)\right) \{15j\}\left(l_f, k_e, i'\right)\,,$$

where we have the Lorentzian boost function

$$B_4^L\left(j_a, l_a, i, k\right) \equiv \sum_{m'_a} \begin{pmatrix} j_a \\ m'_a \end{pmatrix}^{(i)} \begin{pmatrix} l_a \\ m'_a \end{pmatrix}^{(k)} \int_0^\infty d\mu(r) \prod_a d^{(\gamma j_a, j_a)}_{j_a l_a m'_a}(r)\,.$$

The EPRL SF is a model for the quantum geometry of $(3+1)$-spacetime with a Lorentzian signature. Electric and magnetic components of bivectors can be mapped into the boost and rotation generators of $\mathfrak{sl}(2,\mathbb{C})$. Again, the simplicity constraint translates at the quantum level into relations between the stabilizer SU(2) spin labels with representation labels of $\mathrm{SL}(2,\mathbb{C}) : |\nu| = j$ and $\rho = \gamma j$. In this sense, the weak imposition of the simplicity constraint in the EPRL model is basically carried out by introducing a cut-off in the infinite summation over the $\mathrm{SL}(2,\mathbb{C})$ irreps.

In the GFT case imposing the constraint is different and it takes into account the information that the normal vector to the hypersurface, where all bivectors lie, as an additional degree of freedom. In fact, since simplicity forces the tetrahedra to be on the same $3d$ surface, it forces invariance of each bivector under rotations belonging to the stabilizer of the normal X [120, 125]. When this normal is chosen to be time-like, the *stabilizer* is a subgroup $\mathrm{SU}(2)_X \in \mathrm{SL}(2,\mathbb{C})$. We will discuss this point in chapter 4.

The notions outlined above of the Lorentzian quantum geometry provided by EPRL will be used to extract cosmological dynamics in chapter 7 from a GFT setting. Let us summarize the cavities of both models since we will address them in the following chapters:

3.1 The cavities in BC and EPRL

- The first step towards deriving a quantum discrete version in the case of Lorentzian GR, is to first work the from the BF theory the constraints that will reproduce the dynamical equations of GR. This is basically restricting the B field to the tetrad one through the general constraint (when we take γ to infinity we recover the BC bivector instead of the EPRL one)

$$B = \pm \left(1 + \star\gamma^{-1}\right) e \wedge e \,, \tag{3.2.18}$$

- The quantization procedure is to associate the bivector with Lie algebra elements formally written as $B = \star L$.

- Imposing the simplicity constraint at the level of the balanced representations, after having solved the Casimirs. This allows us to identify the Hilbert spaces and quantum states. For the EPRL model, we get the pair of labels $(\gamma j, j)$ whereas for BC they are labeled by ρ. The limitations in the BC model are the following:

  1. The *ultra locality* issue: the 4-simplices are identified through the triangle areas; we also have the bivectors associated with the same triangle in different simplices that are not identified.
  2. The presence of *degenerate* geometries. For instance, they can correspond to the no-geometry state $e = 0$ (diffeomorphism invariant vacuum).

- ▷ The EPRL model includes only the upper and lower hyperboloids in the Minkowskian space, this is mainly due to the weak imposition of the simplicity constraint.

We will provide an alternative model to address such issues in chapter 5, where the formulation for the geometry is based on the edge vectors defining the bivector instead of the bivector itself as in these models. Indeed, a description based solely on bivectors of the quantum geometry is not good enough to encode all degrees of freedom of the discretized geometry.

3.3 Spin network states as quantum states of discrete geometries

Spin networks defined as graphs decorated by quantum data appear in several contexts and approaches to quantum gravity, as we saw in the previous sections. Indeed, they are present in quantum gauge theories, QG, topological quantum field theories, and CFT. Here we are interested in their role in background independent QG. As we will discuss below and in the next chapter 4, they provide an orthonormal basis of states for the quantum geometry of space; in this role, they in fact enter the QG approaches of LQG [15,111,126,127], spin foam models [91,128] and GFT [19,85,129–131]. In fact, all of these approaches share the same standpoint that spin network states are indeed states of quantum geometry. However, as we will see below, what differentiates one theory from the other is the structure of the Hilbert space and the reorganization of the spin network degrees of freedom. In this section, we will show how such quantum states of geometry enter each QG model. This is important to study the more general case of a superposition of such states in the GFT formalism that we address in chapter 6. There, we focus on studying a superposition of spin networks with different combinatorial structures from the lenses of quantum information theory.

3.3.1 Origins of spin network states

Spin networks were first introduced by Penrose as a purely combinatorial object and were proposed as a substitute for a spacetime manifold [119,132]. In this original formulation, they are trivalent graphs with edges labeled with irreducible representations of a group and intertwining operators. In fact, Penrose tried to replace the notion of continuum space avoiding the path of providing an approximation of it, but instead, he aimed for a complete new reformulation of the theory. This new description in fact relies on the discrete concepts which are then considered as *primary concepts*, based on the idea evoked in chapter 2 of the possibility that our picture of spacetime as a manifold breaks down at the Planck scale, hence promoting the conception of discrete structures. This is the same perception of finding the basic building blocks of the theory. In this picture, the continuous quantities

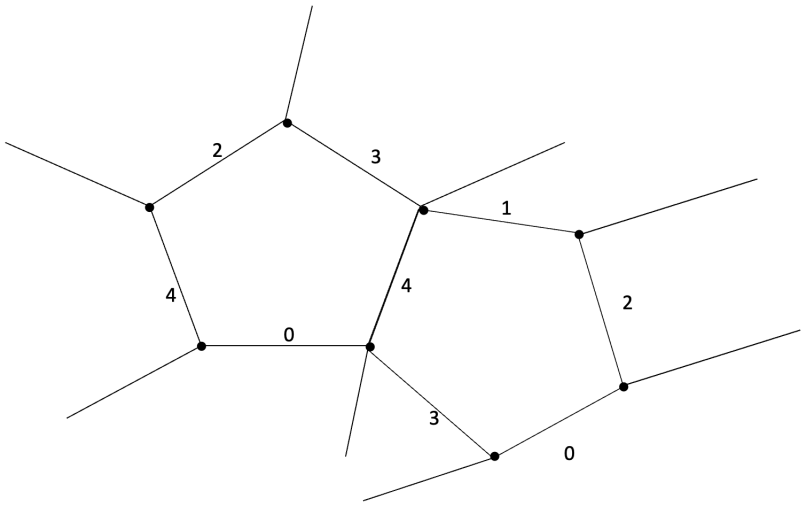

Figure 3.7: Penrose spin network in terms of units of $\hbar$.

are then expected to emerge in the limit where the *complexity* of the model increases. However, this demands a definition of the notion of complexity in this context.

In developing the theory of spin networks, Penrose was inspired more by the QM theory of angular momentum than by the details of the geometry of GR. We now lay down the basic notions he introduced to define his model of quantum states of geometry. The Penrose model is defined by a set of *units*, each one representing a block with a well-defined total angular momentum $j = \frac{n\hbar}{2}$, where $n \in \mathbb{N}$ is the *spin number*; a unit with spin-number n is called an n-unit. Now these units are associated with line pieces that converge to each other to form a node. This can be seen in figure 3.7. What is interesting is that the units do not carry any meaning in terms of the usual motions of particles but Penrose describes them as basic systems responsible for carrying the angular momentum around. They interact at nodes where the conservation of total angular momentum is satisfied. In fact, the only relevant information is the combinatorics and the spin assignment to each link in the unity.
Moreover, in this context, every spin network is assigned an integer, called *norm* which is a purely combinatorial quantity. Another requirement such a norm should satisfy is that, for it to be non-zero, the labeling of the network must be applied such that: at each vertex, the QM rules for the combination of total angular momenta are respected. At the level of the graph, this is equivalent to grouping an a-unit, a b-unit, and a c-unit subject to the following two conditions:

- $a + b + c \leq 2\max\{a, b, c\}$ (triangle inequality) and
- $a + b + c$ even (conservation of the fermionic number mod 2).

The norm is defined through the notion of a *value* of a closed spin network defining a graph without open edges. We conceptualize it as follows: starting from a closed spin

network, we replace every n-unit with n parallel strands within a network say, γ where at each node, pairs of strand ends (belonging to different units) are then connected together. The QM conservation of angular momentum guarantees that all strands that are flowing into a node are connected. This is illustrated as follows: There are several ways in which the strands can be routed (r stands for the different routing), such that each one results in a number N of loops (closed) contained in what we call the *stranded* diagram. In this setting, the value $V[\gamma]$ of the closed spin network γ is then nothing but

$$V[\gamma] = \left(\prod_{edges} \frac{1}{n!}\right) \sum_{r} \epsilon(-2)^{N}, \tag{3.3.1}$$

where ϵ is a sign that tells us how the points between several and different strands at the nodes are connected. The norm of a generic *open* spin network β is then given by the modulus of $V[\beta\#\overline{\beta}]$, where $\beta\#\overline{\beta}$ is the closed spin network obtained by connecting β with a copy $\overline{\beta}$ of itself through the coupling of the corresponding free-end units.

Penrose went on to prove we can have a quantum probability interpretation starting from such a notion of the norm. What is compelling in this theory is that he was actually able to prove that in the limit of large spin numbers, one can recover a notion of *directions in space*. Penrose theory of spin networks is one of the first attempts that hinted to reconsider the structure of spacetime and its relation to the QM principles. It was indeed further improved when Rovelli and Smolin discovered that spin networks can be used to describe kinematical states in LQG [111], as we will see in section 3.3.2.

3.3.2 Spin networks in Covariant Loop quantum gravity

In order to clearly understand how the spin networks enter the SF amplitudes and the Hilbert spaces they live in, we need first to discuss the canonical quantization approach to GR, as provided by LQG. In fact, if we take a generic slice of a given SF, we get a spin network, describing therefore the geometry of space at a *given time*. This is the key difference between Penrose original formulation of spin networks. What we are discussing in the following is sort of an upgrade of the $3d$ Penrose spin networks to ones that capture space at a given "moment". LQG is a background independent approach to the problem of QG that belongs to the line of research that is invested in extracting the canonical quantization of GR [73, 133]. The starting point in this program is the Hamiltonian formulation of the Einstein Hilbert action [51] through rewriting it with the geometric tools provided by the 3+1 formalism [134, 135]. This allows a natural setup to introduce the notion of time evolution and hence specify the role of the time derivative needed to obtain conjugate variables within a Hamiltonian formulation. Therefore, in the following we will sketch the main steps in deriving the kinematical Hilbert space of LQG and the elements of such space, representing the geometric quantum states of the quantized spacetime. We then

discuss the lack of a dynamical physical Hilbert space and explain how SF (in particular the EPRL one) is perceived as the dynamical completion of LQG[10].

Tetrad formulation of classical GR As in the case of discretizing spacetime in section 3.1 we introduce the frame field provided by four co-vectors e^I_a and consider the four dimensional spacetime metric as a composite object similar to (3.1.1) in $4d$. In this manner, the tetrad frame can also be decomposed in terms of lapse and shift variables where in this case it takes a simpler form

$$e^I_0 = e^I_\mu \tau^\mu = N n^I + N^a e^I_a, \quad \delta_{ij} e^i_a e^j_b = g_{ab}\,, \quad i,j = 1,2,3, \tag{3.3.2}$$

where the triad e^i_a represents the spatial counterpart of the tetrad. The LQG approach to quantizing gravity is crucially dependent on choosing the so-called *time gauge*[11]. This is equivalent to imposing

$$e^I_\mu n^\mu = \delta^I_0 \qquad e^0_\mu = (N,0) \longrightarrow e^I_0 = \left(N, N^a e^i_a\right)\,. \tag{3.3.3}$$

This gauge fixing restricts the Lorentz gauge group to the rotation subgroup that leaves the time normal vector to the hypersurface invariant, namely $SU(2) \subset SL(2,\mathbb{C})$. We can furthermore define the *densitized triad* and the Ashtekar-Barbero connection [14, 127] respectively

$$E^a_i = e e^a_i = \frac{1}{2}\varepsilon_{ijk}\varepsilon^{abc} e^j_b e^k_c\,, \quad A^i_a = \gamma \omega^{0i}_a + \frac{1}{2}\varepsilon^i_{jk}\omega^{jk}_a\,, \tag{3.3.4}$$

where γ is the Immirzi parameter, the new internal index i corresponds to the adjoint representation of $SU(2)$ and ω is the spin-connection of the $3d$ hypersurface Σ_t being the spacelike hypersurface at time t. These two extended variables, are in fact conjugate variables and can be used to write down the alternative expression for the ADM action [52, 73] in the tetrad frame, namely

$$S\left(A,E,N,N^a\right) = \frac{1}{\gamma}\int \mathrm{d}t \int_\Sigma \mathrm{d}^3x \left[\dot{A}^i_a E^a_i - A^i_0 D_a E^a_i - NH - N^a H_a\right]\,, \tag{3.3.5}$$

where we can identify the constraints[12] appearing above as

$$\begin{aligned} G_j &\equiv D_a E^a_i = \partial_a E^a_j + \varepsilon_{jk\ell} A^j_a E^{a\ell}\,,\\ H_a &= \frac{1}{\gamma} F^j_{ab} E^b_j - \frac{1+\gamma^2}{\gamma} K^i_a G_i\,,\\ H &= \left[F^j_{ab} - \left(\gamma^2+1\right)\varepsilon_{jmn} K^m_a K^n_b\right] \frac{\varepsilon_{jk\ell} E^a_k E^b_\ell}{\det E} + \frac{1+\gamma^2}{\gamma} G^i \partial_a \frac{E^a_i}{\det E}\,. \end{aligned} \tag{3.3.6}$$

[10] Let us mention here that, a canonical analysis of first order Palatini action exists. However, there is no canonical quantization formulation of it. The covariant quantization, in this case, is then the BC model then

[11] In this sense, time-gauge amounts to adjusting the time axis in the frame field to the one that is singled out by the foliation of spacetime. This is what induces the breaking of the Lorentz invariance of the theory in $4d$.

[12] The invariance under local Lorentz transformations gives rise to new gauge symmetry in the action and hence additional constraints.

The vector constraint H_a is responsible for generating the $3d$ diffeomorphisms on the hypersurface Σ_t, whereas the scalar one H is devoted to the time evolution. The new formulation in terms of tetrads has brought up an extra constraint, the *Gauss constraint* (G_j), that is responsible for generating gauge transformations. Notice that this gauge transformation is the result of the time gauge implemented at the triad and is not to be confused with the diffeomorphisms of GR. Indeed, one can show that E^b_j and A^i_a transform respectively as an $SU(2)$ vector and as an $SU(2)$ connection under this transformation [112, 127].The change of variables we performed and the partial gauge fixing (the time gauge) is the reason behind this change in the gauge symmetry group.
It will be useful later on to deal with the smeared version of these canonical variables in the quantization procedure. The densitized triad is a 2-form and thus, it is natural to smear it on a surface, namely

$$E_i(S) \equiv \int_S n_a E^a_i \mathrm{d}^2\sigma \,, \quad n_a = \varepsilon_{abc} \frac{\partial x^b}{\partial \sigma_1} \frac{\partial x^c}{\partial \sigma_2} \,, \tag{3.3.7}$$

with n_a is the normal to the surface. With this smearing, we identify the quantity $E_i(S)$ as the flux of E across a surface S. The connection is a 1-form, so we can smear it on a one dimensional path. To this end, if we consider a path e and a corresponding parametrization

$$x^a(s) : [0,1] \to \Sigma_t \,, \tag{3.3.8}$$

we can associate a given connection A^i_a with an element of SU(2) such that $A_a \equiv A^i_a \tau_i$, with τ_i[13] being the generators of $SU(2)$. We can therefore integrate A_a along the path e given as a line element, namely

$$A^i_a \longrightarrow \int_e A \equiv \int_0^1 \mathrm{d}s A^i_a(x(s)) \frac{\mathrm{d}x^a(s)}{\mathrm{d}s} \tau_i \,. \tag{3.3.9}$$

Then, as we encountered in section 3.1 we can make use of the notion of holonomy of A along the path e as

$$h_e = \mathcal{P} \exp\left(\int_e A\right) = \sum_{n=0}^{\infty} \iiint_{s_n>0} A\left(e\left(s_1\right)\right) \cdots A\left(e\left(s_n\right)\right) ds_1 \cdots ds_n \,, \tag{3.3.10}$$

with the path-ordered product $\mathcal{P}$ and the parametrization $s \in [0,1]$. We avoided the explicit description of the properties of holonomies in section 3.1 and also here we list them in Appendix A.1.

Kinematical Hilbert space of Loop Quantum Gravity

The formulation introduced above is clearly related (but not yet equivalent) to the BF formulation of GR discussed in section 3.1. The $3d$ hypersurface is in fact GR in $3d$ in

[13]The τ_i are the Pauli matrices and should not be confused with the tetrahedron symbol τ that we encounter when are dealing with discretized geometry. Furthermore, for the integration of such connection along a path, we use the same notation as in section 3.1, namely a path is associated with e.

the temporal gauge. However, the quantization procedure here is different as we will see shortly. The usual procedure for canonical quantization of a gauge theory relies on the role played by the metric that enables the definition of a measure for the kinematical Hilbert space. However, for the present case of GR in $4d$, this notion is absent and there is no background metric at the disposal to define the integration measure. The challenge then is to define such a measure on the space of connections without relying on a background metric, which is naturally provided by the so-called *cylindrical functions*.
A graph γ is defined to be the collection of paths $e \subset \Sigma_t$ meeting at most at their endpoints. Given such a graph $\gamma \subset \Sigma_t$ with N_e being the number of edges that it contains, an element $\psi_{\gamma,f} \in \mathrm{Cyl}_\gamma$ is labeled by a smooth function f and a graph γ. This smooth function f is defined as $f : \mathrm{SU}(2)^{N_e} \to \mathbb{C}$ and it is given by a functional of the connection defined as

$$\psi_{\gamma,f}[A] := f\left(h_{e_1}[A], h_{e_2}[A], \cdots, h_{e_{N_e}}[A]\right) \ , \tag{3.3.11}$$

where e_i for $i = 1, \cdots, N_e$ are the edges of the corresponding graph. Taking the union of all these functionals constitutes the notion of cylindrical functions of generalized connections denoted Cyl, such that

$$\mathrm{Cyl} = \cup_\gamma \mathrm{Cyl}_\gamma \ . \tag{3.3.12}$$

This represents the algebra of the physical observables from which we will show to define the kinematical Hilbert space $\mathcal{H}_{kin}$. This space of functionals once endowed with a proper scalar product can be turned into a Hilbert space. In fact, one can show that the full kinematical Hilbert space is provided by the direct sum $\mathcal{H}_{kin} = \bigoplus_{\gamma \subset \Sigma_t} \mathcal{H}_\gamma$, where $\mathcal{H}_{kin}$ is the kinematical Hilbert space overall gauge connections A on Σ_t, once we use the inner product provided by the Ashtekar and Lewandowski [91, 127],

$$\mathcal{H}_{kin} = L_2\left[A, \mathrm{d}\mu_{AL}\right] \ , \quad \mu_{AL}\left(\psi_{\gamma,f}\right) = \int \prod_{e \subset \gamma} dh_e f\left(h_{e_1}, h_{e_2}, \cdots h_{e_{N_e}}\right) \ , \tag{3.3.13}$$

with $\mathrm{d}\mu_{AL}$ introduced as the Ashtekar-Lewandowski measure. We start by introducing an orthogonal basis on the space using the Peter-Weyl theorem.This implies that any function $\psi_{(\gamma,f)}[A] \in \mathcal{H}_\gamma$ can be decomposed in unitary irreducible representation of the group

$$\psi_{(\Gamma,f)}[A] = \sum_{j_e, m_e, n_e} \hat{f}^{j_1,\ldots,j_n}_{m_1,\ldots,m_n,n_1,\ldots,n_n} D^{(j_1)}_{m_1 n_1}\left(h_{e_1}[A]\right) \ldots D^{(j_n)}_{m_n n_n}\left(h_{e_n}[A]\right) \ . \tag{3.3.14}$$

What we have accomplished with this program so far is the definition of a well-behaved kinematical Hilbert space for GR[14]. Following the Dirac quantization scheme, we can proceed with quantizing the constraints appearing in (3.3.5)

$$\mathcal{H}_{kin} \xrightarrow{\hat{G}_i=0} \mathcal{H}^0_{kin} \xrightarrow{\hat{H}^a=0} \mathcal{H}_{Diff} \xrightarrow{\hat{H}=0} \mathcal{H}_{phys} \, . \tag{3.3.15}$$

[14]It carries a representation of the canonical Poisson algebra, and as a bonus, this representation is unique.

This can be summarized as follows:

⊙ *Quantum Gauss constraint:* Its solution are quantum states that are gauge invariant under SU(2). Imposing gauge-invariance then means requiring the cylindrical function to be invariant under the action of the group at the nodes, which can be easily implemented via *group averaging*. This amounts to inserting on each edge a projector selecting the gauge invariant part of $\bigotimes_e V^{(j_e)}$, namely defined as

$$\mathcal{P} = \int \mathrm{d}g \prod_{e\in n} D^{(j_e)}(g)\,, \quad \prod_e D^{(j_e)}_{m_e n_e}(h_e) \in \bigotimes_e V^{(j_e)}\,. \tag{3.3.16}$$

Denoting the intertwiner[15] by i_α as a ket in the basis of $\mathcal{P}$, with $\alpha = 1, \ldots, \dim V^{(0)}$, V^0 being the singlet space, and i^*_α the dual. This leads us to the notion of *spin network states*. These states are labeled with a graph γ, with an irreducible representation $D^{(j)}(h)$ of spin-j of the holonomy h along each link, and with an element i of the intertwiner space $\mathcal{H}_n \equiv \mathrm{Inv}\left[\bigotimes_{e\in n} V^{(j_e)}\right]$ and are defined as

$$\psi_{(\gamma, j_e, i_n)}[h_e] = \bigotimes_e D^{(j_e)}(h_e) \underset{n}{\otimes} i_n\ . \tag{3.3.17}$$

Imposing the gauge invariance in this manner allows us to present the solutions for the Gauss constraints, namely $\hat{G}_i\psi = 0$ where the spin network basis forms a complete basis of the Hilbert space of solutions $\mathcal{H}^0_{kin}$ of it. $\mathcal{H}^0_{kin}$ decomposes as a direct sum over spaces on a fixed graph that subsequently decomposes as a sum over intertwiner spaces, namely

$$\mathcal{H}^0_{kin} = \underset{\gamma\subset\Sigma}{\oplus} \mathcal{H}^0_\Gamma\ , \tag{3.3.18}$$

$$\mathcal{H}^0_\gamma = L_2\left[SU(2)^L/SU(2)^N, \mathrm{d}\mu_{Haar}\right] = \oplus_{j_l}\left(\otimes_n \mathcal{H}_n\right)\ . \tag{3.3.19}$$

These equations are of the same nature as equations that simulate a Fock-decomposition of a Hilbert space.

⊙*Spatial diffeomorphism quantum constraint:* Due to the notion of linear functional on $\mathcal{H}^0_{kin}$, namely $\eta(\hat{\phi}\psi) = \eta(\psi), \quad \forall\psi \in \mathcal{H}^0_{kin}$, with $\eta \in \mathcal{H}^{0*}_{kin}$ (the space of linear functionals), we can define a projector $\mathcal{P}_{Diff}$ on $\mathcal{H}_{Diff}$ in a way that we sum over all diffeomorphism except those that correspond to the trivial ones in $TDiff_\gamma$. Hence the expression for the projector yields

$$\langle\psi|\psi'\rangle_{Diff} \equiv \langle\psi\,|\mathcal{P}_{Diff}|\,\psi'\rangle = \sum_{\phi\in \mathrm{Diff}/\mathrm{TDiff}_\gamma} \left\langle\hat{\phi}\psi|\psi'\right\rangle\ . \tag{3.3.20}$$

This step amounts to ordering the spin network states into equivalence classes of graphs under diffeomorphisms which we will call *knots*.

[15] A suitable method to build them amounts to add first two irreps only, then the third, and so on, that lead to a virtual decomposition of links.

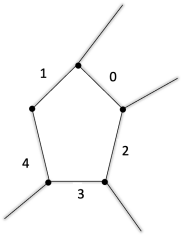

(a) An example of a spin network with all modes considered. The numbers refer to the spin labels decorating the edges of the graph.

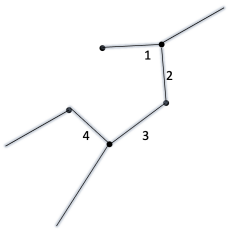

(b) An example of a spin network without the zero mode link. The numbers refer to the spin labels decorating the edges of the graph.

Figure 3.8: Spin network in loop quantum gravity.

⊙ *Quantum Hamiltonian constraint:* Till now there is no clear way to correctly implement the proper quantization procedure on the Hamiltonian constraint encoding the dynamics of GR. A way to do this is by using Thiemann's trick using the properties of the geometrical operator of the volume, and other established entities [127].

Quantum geometric operators

The main physical prediction of the above-outlined quantum gravity model relies on the crucial role that some geometric operators play. It is worth mentioning that these operators are not Dirac observables in general. Interestingly for special situations, they can be, for instance, the area operator is a Dirac observable in LQG black hole computations, i.e. it commutes with all the constraints and not just the Gauss one [112].

- *Quantizing the area operator* given a surface S characterized by its normal n_a and the densitized triad the discretized area is given by [134]

$$A(S) = \int_S d\sigma_1 d\sigma_2 \sqrt{E_i^a E^{bi} n_a n_b}\,. \tag{3.3.21}$$

  For a surface intersected only once by the holonomy path. We introduce a decomposition of S in N two-dimensional cells and write the integral as the limit of a Riemann sum.

$$A(S) = \lim_{N\to\infty} A_N(S) = \lim_{N\to\infty} \sum_{I=1}^{N} \sqrt{E_i(S_I) E^i(S_I)}\ , \tag{3.3.22}$$

  where $E_i(S_I)$ is the flux going through the I'th cell. Promoting it to an operator amounts to defining the area operator, namely $\hat{A}(S) = \lim_{N\to\infty} \hat{A}_N(S)$. The operator $\hat{E}^i$ now acts on a generic spin network state, labeling a generic graph γ. Therefore once the decomposition is sufficiently fine so that each S_I is punctured once and only once and hence taking a further refinement has no effect. The limit now amounts to

simply the sum of the contributions of the finite number of punctures p of S created by the links of the graph which reads

$$\hat{A}(S) = \lim_{N\to\infty} \sum_{I=1}^{N} \sqrt{\hat{E}_i(S_I)\hat{E}^i(S_I)}\psi_{(\gamma,f)} = \sum_{p\in S\cup\gamma} \hbar\sqrt{\gamma^2 j_p(j_p+1)}\psi_\gamma \ . \tag{3.3.23}$$

This expression presents the spectrum of the area operator. It also implies that it acts diagonally on spin network states, thus allowing them to be eigenstates of the area operator.

- *Volume operator:* Similarly to the area operator, we consider a partition of the region into cubic cells ϵ. This would allow us to write the definition of the volume in terms of the flux and it reads [126]

$$V(R) = \lim_{\epsilon\to 0} \sum_I \sqrt{\frac{1}{48}\epsilon_{ijk} \sum_{\alpha\beta\gamma} E_i(S_I^\alpha)E_j(S_I^\beta)E_k(S_I^\gamma)} \ . \tag{3.3.24}$$

Notice the presence of the epsilon tensor implying that the three fluxes must be different and that the volume does not act on links. Hence the volume operator acts only on the *nodes* of the graph. In fact, its matrix elements vanish between different intertwiner spaces. The volume operators turn out to be diagonalized by spin network states as well. We do not go into detail in the calculation of the spectrum of the volume operator, for which we refer to the literature.

3.2 Spin networks in Covariant Loop Quantum Gravity

▷ A spin network is a graph $\gamma \subset \Sigma$ with edges e labeled by irreps of G, namely **spins** $j_e \in \frac{\mathbb{N}}{2}$, and vertices v labeled by **intertwiners** $\iota_v \in I_v$, i.e. G-invariant tensors of (the tensor product of) the representations attached to all edges converging at a vertex.

▷ A spin network state $|\Gamma, \vec{j}_e, \vec{\iota}_v\rangle$ is the state corresponding to the following wavefunction on the space of generalized connections:

$$S_{\gamma,\vec{j}_e,\vec{\iota}_v}(\vec{h}_e) = \bigotimes_{v\subset\Gamma} \iota_v \bigotimes_{e\subset\Gamma} \sqrt{2j_e+1} D^{j_e}(h_e) \tag{3.3.25}$$

where $h_e \in G$ is the holonomy of the Ashtekar connection A_a^i along the edge e of γ. That is, a spin network is a wavefunction defining a probability amplitude on the holonomies.

▷ Spin network states (defined on *graphs*) are gauge invariant states and provide a basis of the space of solutions of the Gauss constraint.

▷ Spin network states diagonalize the area and the volume operator and can be understood as representing quantum twisted geometries: every link is dual to

a surface $S \subset \Sigma$ intersecting it, and the spin attached to the link is related to the area of such surface according to; every node is dual to an elementary portion of space, and the intertwiner attached to it is related to its volume.

- ▷ The invariance under spatial diffeomorphisms for spin networks gives rise to spin-knot states.
- ▷ Spin network states invariant under spatial diffeomorphisms and defined on closed graphs (thereby gauge invariant) represent kinematical states of the theory, whose evolution is implemented via the scalar constraint.
- ▷ A consistent covariant dynamical description of these $3d$ quantum geometries in LQG is provided by SF[a]. In this context, SF describes the transition amplitude from a geometric state S to S' where the vertices take into account any topological change (interaction). Therefore the states describing the boundary of the 4-simplex are provided by LQG spin network graphs.

[a]Recall that LQG is based on canonical quantization where the states in this formalism describe the geometry of space at a fixed time (due to the time gauge).

Chapter 4

Group field theories

In the previous chapter 3, we discussed the program of the background independent approaches to the problem of quantum gravity. The elegant formulation of GFT as a QFT *of* spacetime makes it peculiar and a powerful theory to provide a promising attempt to quantize gravity. In this chapter, we will present the basic notions and definitions that underline this approach since it is the framework we work with throughout this thesis. We start by pointing out the powerful technology provided by GFT. Perhaps one of the most powerful ones is the purely algebraic and combinatorial aspect of the theory. This is made evident below where we will see how the GFT action describes the combinatorially non-local dynamics of the scalar function of group elements. Expanding the action (in the form of a partition function) of such a field requires only the representation associated with the group of the field domain. The resulting Feynman diagrams encode the interaction of the theory and are in fact purely topologically combinatorial. This analysis is based on the harmonic resolution of the functions on the group and its representations. The field theory in this context does not encode any reference to any notion connected to spacetime. It is only after having specified the group (that might correspond to the gauge group in GR) and how many copies of it must be considered (giving the right dimensionality) that we could even start thinking of a quantum theory of spacetime. It is in this sense that GFT presents all the aspects of a background independent approach to the problem of QG. Moreover, GFT is considered as the completion of the spin foam proposal in QG as we will see in section 4.2, where we discuss its general relation to this class of QG theories and examine how the BC and EPRL models are reproduced from a GFT setting. In section 4.3 we take a different route (and rather non-perturbative approach) within GFT to induce connectivity within the quantum states of geometry, mimicking therefore the continuum notion at the quantum level. This can be precisely expressed by entangling the fundamental degrees of freedom of the theory giving rise to the idea of *entanglement graphs*. We then end this chapter in section 4.4 with a possible coarse graining scheme that the GFT approach implements in order to extract physical predictions in the cosmological sector of physics. Before embarking on this endeavor, let us briefly discuss the basic setup of GFT.

A GFT is the theory of a quantum field φ defined on d copies of a group manifold G, i.e.

$$\varphi : G^d \to \mathbb{C}\,, \tag{4.0.1}$$

$$g^1, \dots, g^d \mapsto \varphi(g^1, \dots, g^d)\,, \tag{4.0.2}$$

where d is the dimension of spacetime which should *emerge* from the GFT model. The GFT action enjoys a non-local interaction term and the full dynamics are encoded in the expression

$$S_{\text{GFT}}\left[\varphi^*, \varphi\right] = \int \left[\mathrm{d}g_I\right]^2 \varphi^*\left(g_I\right) \mathcal{K}\left(g_I, g_I'\right) \varphi\left(g_I'\right) \tag{4.0.3}$$

$$+ \sum_i \frac{\lambda_i}{D_i} \int \left[\mathrm{d}g_I\right]^{D_i} \varphi^*\left(g_{I_1}\right) \dots \mathcal{V}_i\left(g_{I_1}, \dots, g_{I_{D_i}}\right) \dots \varphi\left(g_{I_{D_i}}\right) + \text{ c.c. }, \tag{4.0.4}$$

where i specifies the type of interactions of the field φ, characterized by a different number D_i of fields involved and where the integration is carried out over d copies of the group manifold based on the Haar measure of the product space G^d such that $\mathrm{d}g_I \equiv \mathrm{d}g_1 \dots \mathrm{d}g_d$. The kinetic and interaction kernels $\mathcal{K}$ and $\mathcal{V}$, respectively. They are in general functions which are specified by the given model, and they encode, in particular, specific constraints that need to be imposed on the GFT field in order to establish a direct connection with existing QG models.

Moreover, it is important to emphasize that the presence of combinatorial non-local interactions in the action is responsible for the gluing of GFT quanta of discrete geometric structures. In fact, the fundamental $(d-1)$-simplices combine into d-complexes of arbitrary topology, which can be envisaged as discrete pieces of the continuum spacetime emerging from them (in some appropriate limit) [85, 136]. As we will see later when we discuss the GFT dynamics in section 4.2 these d-complexes are dual to the Feynman diagrams in the perturbative expansion of the GFT partition function, i.e.

$$Z = \int D\varphi D\varphi^* e^{-S_{GFT}[\varphi,\varphi^*]} = \sum_\Gamma \frac{\lambda^{N(\Gamma)}}{\text{sym}(\Gamma)} Z(\Gamma), \tag{4.0.5}$$

where Γ is the Feynman graph, $N(\Gamma)$ is the number of interaction vertices in Γ, $\text{sym}(\Gamma)$ is a symmetry factor and $Z(\Gamma)$ is the Feynman amplitude associated to Γ. At the boundary of the Feynman diagrams one can show that the states are described by spin-networks as used for instance in LQG (summarized in Box 3.2) and the Feynman amplitudes coincide with SF amplitudes [16]. This can be made explicit once we perform the Peter-Weyl decomposition of the group functions, as we will see in section 4.2. Let us finally mention that GFT can be regarded as a generalization of random tensor models [137–139], where the combinatorial structures of the latter are enriched with the input coming from the group-theoretic data. As we will clarify in section 4.3, precisely this additional information delivered from the group theory side is responsible for the interpretation of the graphs associated with GFT states as *patterns* of entanglement among field quanta.

4.1 General construction of the kinematical sector of GFT

In this section, we explore the multitude of possible representations that we can make use of to express the GFT field. We focus on the $4d$ case. This is important for section 4.2 since we will show that depending on the representation we associate to the field, the pairing with the corresponding SF is made easier, and the problem of the quantum simplicity constraint is better addressed and formulated. In fact, to make the connection with the previous chapter on discretizing geometry, we can think of the group elements g_I entering the field definition as the equivalent of the bivector associated with each triangle of the tetrahedron. The closure procedure and gluing of simplices reproduced by a geometric entity are addressed by the dynamics and symmetries of GFT. The above definition of the GFT field was expressed in the group basis. In the following, we present other representations, that may provide more insight into the physical (kinematical as well dynamical) properties of the models. Throughout the thesis, it will prove therefore useful to oscillate between such representations.

• **GFT in representation basis.** We define the transform of a square integrable ($\mathcal{L}^2$) function f on the Lie group G in terms of unitary representations U as follows [124,140–143]

$$f(U) = \int \mathrm{d}g f(g) U_{g^{-1}} \,. \tag{4.1.1}$$

For several groups including the ones we will be considering throughout the thesis, we can invert the above formula obtaining [105, 144]

$$f(g) = \int_{\tilde{G}} \mathrm{d}\mu \left(U^\lambda\right) \mathrm{tr}\left(f\left(U^\lambda\right) U^\lambda_g\right) \,, \tag{4.1.2}$$

and we integrate over all equivalence classes λ of the irreducible unitary representations U of the group G, denoted by $\tilde{G}$. The quantity $\mu\left(U^\lambda\right)$ is the Plancherel measure. Let us give two explicit examples of this decomposition into unitary representations for the GFT over the groups SU(2) and $\mathrm{SL}(2,\mathbb{C})$.

⊙ SU(2) GFT: similarly to what we encountered in section 3.3, this group is a semi-simple compact Lie group, so its unitary irreducible representations are finite dimensional and labeled by half-integers $j \in \{0, 1/2, 1, \ldots\}$ (see Appendix A.1). The dimension of the representation spaces is $d(j) = 2j+1$. The above formula becomes in the case of this group

$$f(g) = \sum_j d(j) \sum_{m,n=-j}^{j} f^j_{mn} D^j_{mn}(g) \,. \tag{4.1.3}$$

where D^j_{mn} are the Wigner matrices and m, n are the magnetic indices related to the spin j. The delta function on the group $\delta(g)$, with transform $\delta\left(U^j\right) = \mathbb{I}_{d(j)}$, can be decomposed

in terms of the group character χ^j.

$$\delta(g) = \sum_j d(j)\chi^j(g), \quad \chi^j(g) \equiv \operatorname{tr} D^j(g)\,. \tag{4.1.4}$$

Therefore, for a GFT field φ defined on d copies of SU(2) we have the general decomposition rule in this group

$$\varphi\left(g_I\right) = \sum_{j_1,\ldots,j_d} \left(\prod_{i=1}^{d} d\left(j_i\right)\right) \operatorname{tr}_{\vec{j}}\left[\varphi^{\vec{j}} \bigotimes_{i=1}^{d} D^{j_i}\right]. \tag{4.1.5}$$

where the vector notation stands for the collection of different spin labels $\vec{j} = j_1\,, \cdots, j_d$.

⊙ $\mathrm{SL}(2,\mathbb{C})$ GFT: The representation theory of $\mathrm{SL}(2,\mathbb{C})$ is rather complicated in comparison to SU(2) as we encountered in the discussion regarding SF. The non-compactness of the group causes also a problem for the GFT case, as we will discuss in chapter 5. The unitary irreps of $\mathrm{SL}(2,\mathbb{C})$ are labelled by the pair (ρ,ν). To define the measure, we rely on the Plancherel inversion formula and it reads for a function $f \in L^2(\mathrm{SL}(2,\mathbb{C}))$,

$$f(g) = \int_0^\infty \mathrm{d}\rho \sum_{\nu\in\mathbb{Z}/2} 4\left(\rho^2+\nu^2\right) \sum_{j=|\nu|}^{\infty} \sum_{l=|\nu|}^{\infty} \sum_{m=-j}^{j} \sum_{n=-l}^{l} f^{\rho\nu}_{jmln} D^{(\rho,\nu)}_{jmln}(g)\,. \tag{4.1.6}$$

Therefore, for a GFT field defined on d copies of $\mathrm{SL}(2,\mathbb{C})$ we have

$$\varphi\left(g_I\right) = \left[\prod_{i=1}^{r} d \int_0^\infty \mathrm{d}\rho_i \sum_{\nu_i\in\mathbb{Z}/2} 4\left(\rho_i^2+\nu_i^2\right) \sum_{j_i=|\nu_i|l_i=|\nu_i|}^{\infty} \sum_{m_i=-j_i}^{\infty} \sum_{n_i=-l_t}^{j_i}\right] \tag{4.1.7}$$

$$\times\, f^{\rho_i\cdots}_{j_1 m_1 \ldots j_r m_d l_1 n_1 \ldots l_d n_d} \prod_{i=1}^{d} D^{(\rho_i,\nu_t)}_{j_t m_t l_l n_t}\left(g_I\right)\,. \tag{4.1.8}$$

• **GFT in the noncommutative (NC) Lie algebra basis.** As we will see later on in chapter 5, this basis will play a convenient role to derive the new GFT model in terms of edge vectors, addressing therefore the subtleties summarized in Box 3.1. Now, let us see how we can express the GFT field in terms of this dual basis. This can be carried out by means of noncommutative Lie algebra variables [100, 122]. The latter is obtained from the group-based representation via a noncommutative Fourier transform. What is peculiar about this Fourier transform is that, it unitarily maps functions on the group G to functions on the corresponding Lie algebra $\mathfrak{g}$, where the group Fourier transform is defined through the plane waves [145–147],

$$e : G \times \mathfrak{g} \to \mathbb{C}\,, \quad (g,B) \mapsto e_g(B). \tag{4.1.9}$$

The Lie algebra $\mathfrak{g}$ can be always identified with $\mathbb{R}^{d_G}$ as a vector space, the e_g can be understood as elements of the continuum space of functions on $\mathbb{R}^{d_G}, \mathcal{C}\left(\mathbb{R}^{d_G}\right)$. Denoting

the closure of their linear span as $\mathcal{C}_\kappa\left(\mathbb{R}^{d_G}\right)$, the composition rules of these plane waves can be used to define a noncommutative product on the algebra of functions $\mathcal{C}_\kappa\left(\mathbb{R}^{d_G}\right)$, namely by extending

$$\star : \mathcal{C}_\kappa\left(\mathbb{R}^{d_G}\right) \times \mathcal{C}_\kappa\left(\mathbb{R}^{d_G}\right) \to \mathcal{C}_\kappa\left(\mathbb{R}^{d_G}\right), \tag{4.1.10}$$

$$(e_{g_1}, e_{g_2}) \mapsto e_{g_1} \star e_{g_2} \equiv e_{g_1 g_2}\,, \tag{4.1.11}$$

to the whole space $\mathcal{C}_\kappa\left(\mathbb{R}^{d_G}\right)$. This defines the noncommutativity of the Lie algebra through the star product $\star$. Since we will be mostly working with the SU(2) group let us write down the GFT in its NC algebra basis [148]. The plane waves are defined as $e_g(B) \equiv \exp[i\,\mathrm{tr}(Bg)]$, with $B \equiv \mathbf{B}\cdot\boldsymbol{\sigma}$, in a basis σ^i (with σ^i being Pauli matrices) of $\mathfrak{su}(2)$. The trace is taken in the fundamental representation. The $\star$-product above is then defined on two copies of $\mathcal{C}_\kappa(\mathbb{R}^3)$, since $\mathfrak{su}(2)$ can be identified with $\mathbb{R}^3$. Using the plane waves, the Fourier transform $\mathcal{F}$ of a function f is given by

$$\mathcal{F}(f)(B) \equiv \tilde{f}(B) \equiv \int_G \mathrm{d}g e_g(B) f(g)\,. \tag{4.1.12}$$

More importantly, it is possible to define a delta function on the Lie algebra as

$$\delta_B\left(B'\right) \equiv \int \mathrm{d}g\, e_{g^{-1}}(B) e_g\left(B'\right)\,, \tag{4.1.13}$$

that has the following action on functions

$$\int \mathrm{d}B'\left(\delta_B \star f\right)\left(B'\right) = \int \mathrm{d}B'\left(f \star \delta_B\right)\left(B'\right) = f(B)\,, \tag{4.1.14}$$

$$\left(f \star \delta_B\right)\left(B'\right) = \left(f \star \delta_{B'}\right)(B)\,. \tag{4.1.15}$$

Now, the quantities presented above are defined for functions on a single copy of a Lie group which can easily be extended on several copies of the same group. This is obviously required to achieve a GFT description. For example, in the case of a d group copies, the GFT field decomposition yields

$$\tilde{\varphi}\left(B_I\right) \equiv \int \mathrm{d}g_I \left[\prod_{i=1}^{d} e_{g_i}\left(B_i\right)\right] \varphi\left(g_I\right)\,, \tag{4.1.16}$$

where now, for each group element g_I, we have a group element $B_I \in \mathfrak{g}$ and $I = 1, \ldots, d$. The interpretation of these algebra variables will become clear in the following section.

4.2 GFT dynamics and spin foams

In the following, we point out the relation of the GFT formalism to that of SF. In particular, we will focus on the BC- and the EPRL models in $4d$, since these are exactly the SF that

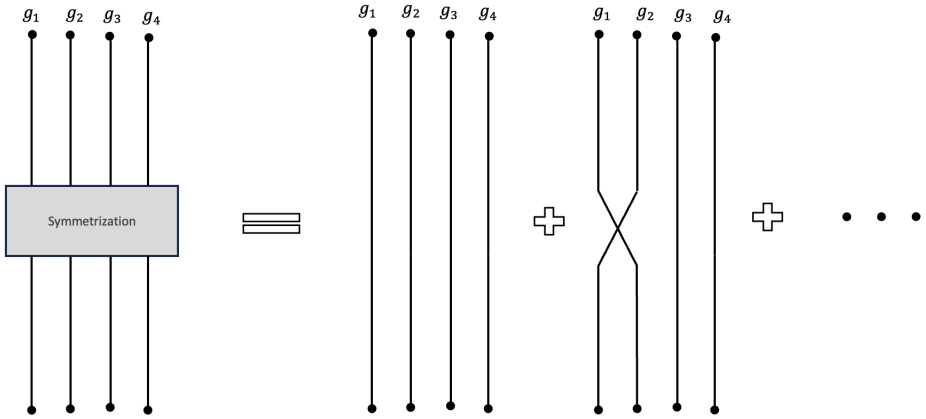

Figure 4.1: Group field theory propagator: each of the four strands carries a (simple) representation of the group and the box stands for a symmetrization of the four arguments, i.e. for a sum over given permutations of the ordering of the arguments [1].

will be at the basis of the results extracted in chapter 5 and chapter 7. In the standard theory of quantum fields, the basic QFT can be expressed in coordinate space as well as momentum one. It is also endowed with a partition function, from which one successfully extracts the Feynman diagrams that encode the dynamics the QFT is endowed with. The same line of reasoning can be exactly implemented in the GFT formalism, but in a rather richer way than the standard QFT one, due to the multifold algebraic tools group theory brings to the game. It is a group theory of group manifolds (these are then the equivalent of the coordinates) and its dynamics are dictated as in standard QFT by a kinetic term $\mathcal{K}$, from which one can study the *propagator* of the theory, and an interaction term $\mathcal{V}$ that depicts how the elementary building blocks interact with each other. This picture, precisely tells us how the group elements (that are dual to simplices as we saw in section 3.1.2) get glued together. To proceed, let us first try to build some intuition behind what kind of propagator- and vertex- structure we are dealing with in this picture we then move on to stressing the relation between GFT and SF through the perturbative expansion of (4.0.5) relying on the different representation of the GFT that we use as input in this partition function.

• **Building an intuition for Feynman diagrams** ▷ The GFT propagator is illustrated in figure 4.1 and can be represented by four straight parallel lines, depicting the four arguments of the field (g_1, g_2, g_3, g_4). This propagator has a group variable at the two ends of each line. On the other hand, the vertex is a more involved structure, it is endowed with a combinatorial structure, since it is responsible for the gluing and pairing of the arguments of the GFT fields building a 4-simplex σ, with five vertices and four lines coming out of each of them (five tetrahedra-propagators with four triangles-lines each).

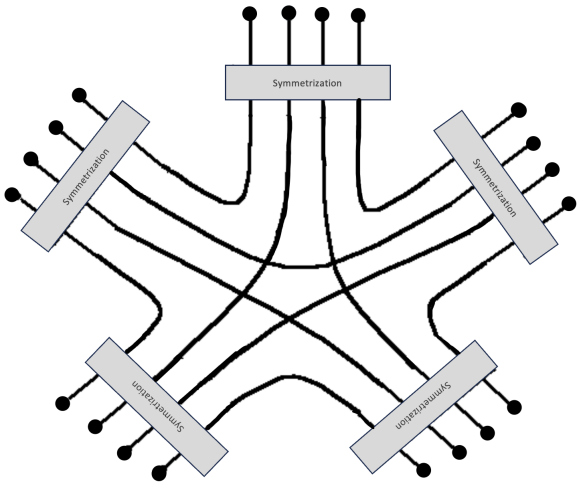

Figure 4.2: Group field theory vertex depicting the combinatorial nature of the interaction of the 4-simplex [1].

▷ The Feynman diagrams are obtained in this case, by connecting a number of vertices with the propagators (see figure 4.1) constructing fat graph. This is done for all admissible *permutation* of the lines in the propagator, reflecting the combinatorial character of the interactions.

▷ Assigning an orientation to the vertices and propagators, every single strand of the propagator gets glued to another one in the five open sites of the vertex, illustrated in figure 4.2. Furthermore, the GFT field is endowed with a permutation symmetry affecting the group elements labels. This is translated at the level of the propagator to be assigned to all various terms resulting from the different ways in which the four carried indices can be permuted (see figure 4.1).

▷ In this picture, the sum over Feynman graphs Γ can be re-written as a sum over fat graphs γ with an amplitude for each fat graph given by

$$Z(\lambda) = 1 + \sum_{\gamma} v(\gamma) \cdot \lambda^{N(\gamma)} Z(\gamma)\,, \quad v(\gamma) = \frac{l(\gamma)}{N(\gamma)! \cdot (5! N(\gamma) \cdot (4!)^{e(\gamma) N(\gamma)}}\,, \tag{4.2.1}$$

where $v(\gamma)$ provides us with the number of inequivalent ways of labeling the vertices of γ with $N(\gamma)$ symbols and $e(\gamma)$ is the number of links in γ. So in principle, each of these stranded fat graphs can go through different propagators and vertices, where we don't exclude the possibility of forming a cycle by closing on itself. This process of cycling (generating faces) is labeled in the GFT momentum space by the representation assigned to the strand, giving rise to a *labeled* 2-complex i.e. a SF. Therefore, we see that there is a 1-1 correspondence between the Feynman graphs of our field theory and that of SF. In turn, we are able to interpret such a perturbation as a sum over SF (labeled 2-complexes) where the amplitude $Z(\Gamma)$ plays the role of amplitude for each SF, and it is the partition

function itself specifies a SF model. It is worth noticing that, unlike the SF point of view of fixing the triangulation, the above partition function generates all possible triangulations of a given topology and those entering all topologies as well. Indeed, this corresponds to all the possible pairing of lines, translating to all possible gluing of faces (triangles). It is in this sense that the GFT framework provides a completion to SF. Let us now put some mathematics to these words.

It is also important to underline the fact that GFT generates a sum over topologies as well as a sum over different triangulations of the same topology and not a fixed one. This then takes into account the full space of the degrees of freedom defining thus a full background independent theory of spacetime [1].

• **General construction of the GFT Feynman diagrams** The identification of GFT with a specific SF model relies on the way we can decompose the field theory as a scalar function of a group. This is of course very well studied in group theory and depends on the group domain G. This is manifest once we decompose the GFT by expanding it in Fourier modes [109, 149–151] provided by the Peter-Weyl theorem

$$\varphi\left(\mathbf{g}\right) = \sum_{\mathbf{r}} f_{\mathbf{n}}^{(\mathbf{r})\mathbf{m}} \prod_{u} \sqrt{\dim r_u}\, U^{(r_u)}{}_{m_u}{}^{n_t}\left(g_u\right) \,, \tag{4.2.2}$$

where the bold notation refers to a collection of group elements $\mathbf{g} = g_1\,, \cdots, g_u$, their respective quantum number in the irreducible representation labeled by r and $f_{\mathbf{n}}^{(\mathbf{r})\mathbf{m}}$ are the mode coefficients in such a basis. Inserting this expansion in the action (4.0.3), we can read out both the propagator and vertex. The calculation is straightforward due to the simple form provided by the Peter-Weyl decomposition of the group field. Indeed this allows us to use the orthogonality relation of the representation matrices. Now, the propagator resulting from the kinematics of such field decomposition

$$\mathcal{K}[\psi] = \frac{1}{2\cdot 4!} \sum_{\mathbf{r}} \left[f_{\mathbf{n}}^{(\mathbf{r})\mathbf{m}}\right]^{*} f_{\mathbf{n}}^{(\mathbf{r})\mathbf{m}} \,, \tag{4.2.3}$$

produces the propagator of the field

$$P^{r_1 m; r_2' n} = \sum_{\sigma\in S_4} \delta_{\mathbf{r}_1 \sigma(\mathbf{r}_2)} \delta^{\mathbf{m}_1}_{\sigma[\mathbf{m}_2]} \delta^{\sigma[\mathbf{n}_2]}_{\mathbf{n}_1} \tag{4.2.4}$$

with $\delta^{\mathbf{b}}_{\mathbf{a}} = \prod_{t=1}^{4} \delta^{b_t}_{a_t}$ and σ the permutation acting on the group elements labels. To express the interaction term $\mathcal{V}$ in terms of the coefficients f in a simple manner, we make use of further representation-theoretic notion. If $g_{12} \in G$ defines a parallel transport on the edge from node 1 to node 2 then $g_{21} = (g_{12})^{-1}$ defines parallel transport along the inverse edge from 2 to 1. In this picture, a unitary representation $U^{r,m_1}_{m_2}$ of the element g_{21}, to consider the *parallel* propagator from 2 to 1 in the complex conjugate of the representation r such that

$$\left(U(g_{21})^{r,m_1}_{m_2}\right)^{*} = \left(U(g_{21})^{r,m_1}_{m_2}\right)^{-1} \,. \tag{4.2.5}$$

For simplicity, let us focus on the case of a fixed representation on all edges. In general, the $\left(U^{(r)}\right)^*$ are not associated with $U^{(r^*)}$ of its own equivalence class, but instead, it is only *unitarily* equivalent to it[1]. This calls for the introduction of a new quantity. We define $\varepsilon^{(r)}_{mn}$ to be a unitary matrix such that

$$U^{(r)*} = \varepsilon^{(r)\dagger} U^{(r^*)} \varepsilon^{(r)} \tag{4.2.6}$$

and we allow $\varepsilon^{(r)mn} = \left(\varepsilon^{(r)}_{mn}\right)^*$, which is the inverse of $\varepsilon^{(r)}_{mn}$ such that $\varepsilon^{(r)}_{mx}\varepsilon^{(r)nx} = \delta^n_m$.
Now, before we proceed to the vertex expression, notice that from (4.2.6) we are led to conclude that $\varepsilon^{(r)}_{mn}$ is an invariant tensor, hence an intertwiner, where m is a covector index of the representation r^* and n is a covector index of the representation r. We can then make use of their properties and in particular, we have

$$U^{(r)n}_{m_1}\left(h_1 h_2^{-1}\right) = U^{(r)x}_{m_1}(h_1)\left[U^{(r)x}_{n}(h_2)\right]^* = U^{(r)x}_{m_1}(h_1)\,\varepsilon^{(r)}_{xy} U^{(r^*)y}_{m_2}(h_2)\,\varepsilon^{(r)nm_2}. \tag{4.2.7}$$

Adopting when needed the relation $r_{ij} = r^*_{ji}$ for $i > j$ we are able to write the interaction term for the fields as [149]

$$\mathcal{V} = \sum_{\mathbf{r}_\cdot,\mathbf{I}_\cdot} A^{(\mathbf{r}_\cdot)}\mathbf{I}_\cdot \cdot \left[\prod_{i\neq j}\sqrt{\dim r_{ij}}\right] U^{(r_{ij})}{}_{m_{ij}x_{ij}}\left(h^j_i\right)\prod_k W^{m_{k1}\ldots m_{kk-1}m_{kk+1}\ldots m_{k5}}_{I_k}\prod_{i<j}\varepsilon^{(r_{ij})}_{x_{ij}x_{ji}}. \tag{4.2.8}$$

The invariance of ε induces the resulting tensors $W^{\mathbf{m}_k}_{I_k}$ to be also invariant and they are considered as intertwiners that are coupling the incident representations r_{ki}. The above equation is then the expression of the interaction term on the field in spin representation, where bivalent vertices are characterized by intertwiners $\varepsilon^{(r_{ij})}_{x_{ij}x_{ji}}$ (which is $\sqrt{\dim r_{ij}}$ times the unique normalized bivalent intertwiner). Thus, the orientations of the edges are present only through the ordering of the indices in this ε. Now let us write the expression for $\mathcal{V}$. If we use the reality of φ to replace φ by φ^* in (4.0.3) the integrals can be carried out using the above derived expression for $\mathcal{K}$ and $\mathcal{V}$

$$\mathcal{V} = \frac{1}{5!}\sum_{\mathbf{r}_{\cdot,\cdot},\mathbf{I}_\cdot} A^{(\mathbf{r}_\cdot)\mathbf{I}_\cdot}\prod_k\left[b^{(\mathbf{r}_k)\mathbf{m}_k}\mathbf{x}_k\right]^* W^{\mathbf{m}_k}_{I_k}\prod_{i<j}\varepsilon^{(r_{ij})}_{x_{ij}x_{ji}}.$$

The term $\mathcal{V}$ is even simpler when expressed in terms of the spin-network coefficients in an expansion of the gauge-invariant field $\varphi^*(\mathbf{h}) = \int_G \varphi(g\mathbf{h})dg$. A spin-network-type expansion of this field can be obtained by inserting into the expansion of the field the projector

$$\int_G \prod_{t=1}^4 U^{(r_t)}{}_{m_t}{}^{n_t}(g)dg = \sum_I \left[W^{(\mathbf{r})m_1m_2m_3m_4}_I\right]^* W^{(\mathbf{r})n_1n_2n_3n_4}_I.$$

[1]For example, all representations of SU(2) are equivalent to their conjugates, however on the other hand, unitary irreps of non-integer spins are not real and are indeed not equal to their conjugates.

The field then has the simpler form

$$\varphi^*(\mathbf{h}) = \sum_{\mathbf{r},I} c^{(\mathbf{r})I}{}_{\mathbf{n}} W_I^{(\mathbf{r})\mathbf{m}} \prod_{t=1}^{4} \sqrt{\dim r_t} U^{(r_t)n_t}{}_{m_t}(h_t) \tag{4.2.9}$$

and the interaction term is then given by

$$\mathcal{V} = \frac{1}{5!} \sum_{\mathbf{r}_{..},\mathbf{I}_{.}} A^{(\mathbf{r}_{..})\mathbf{I}_{.}} \prod_k \left[c^{(\mathbf{r}_{k.})I_k} \mathbf{x}_k \right]^* \prod_{i<j} \varepsilon^{(r_{ij})}_{x_{ij}x_{ji}},$$

which tells us that it is simply A times the result of contracting together the indices of five c^* in the pattern of a 4-simplex. This formula allows us then to express the functional integral of the path integral action of the GFT action as an ordinary integral over the coefficients f. (which are finite in number if the spin foam model has been regulated by cutting off the sum over representations).

• **The relation between the extended GFT model and BC and EPRL spin foam models.** In the previous discussion, we came across the bridging relations between GFT and SF. Now we would like to explicitly express this for two SF models. The GFT field describing quantum pieces of $4d$ spacetime is encoding the theoretic-algebraic information about the bivector associated with each face of a given tetrahedron (one of the four triangles). As we discussed above, the interaction term in the GFT action in (4.0.3) takes care of the gluing of such fundamental building blocks of the quantum geometry, further underling the highly non-local combinatorial aspect of the dynamics. In the following, we focus on the Riemannian definition of geometry and then move on to the Lorentzian case. Recall that in section 3.2.1 we encountered that the information specified by the normal vector to the set of bivectors is indeed crucial [145]. Precisely for this reason, one can then promote the normal vector to the tetrahedron to a kinematical variable $X \in S^3 \simeq \mathrm{SU}(2)$ by adding it as an independent argument in representing tetrahedron [120,122,145], achieving an enhancement to the properties of the field under closure and simplicity constraints. Henceforth, in this extended formulation, GFT field can be expressed in the Lie algebra representation, where the group now is Spin(4), as

$$\varphi(B_1, \ldots, B_4) \to \varphi(B_1, \ldots, B_4; X), \quad X \in \mathrm{SU}(2), \tag{4.2.10}$$

where a rotation by $h \in \mathrm{Spin}(4)$ acts also on the normal X and in this representation, the closure constraint can be easily implemented. The invariant under rotation expressed in the Lie algebra representation reads

$$\varphi(B_1, \ldots, B_4; X) = \varphi(B_1, \ldots, B_4; h \triangleright X) \star E_h(B_1) \ldots E_h(B_4), \tag{4.2.11}$$

Using the properties of the group Spin(4), we can decompose the action of $h \in \mathrm{Spin}(4)$ on $X \in \mathrm{SU}(2)$ by using the isomorphism $\mathrm{Spin}(4) \simeq \mathrm{SU}(2) \times \mathrm{SU}(2)$, so that an element $h \in \mathrm{Spin}(4)$ can be written as $h = (h^+, h^-)$, with h^+ and h^- being elements of two copies

of SU(2). This allows us to redefine the invariance of the normal vector X (4.2.11) in terms of a projector that can which can be imposed in the following way

$$(C_h\varphi)(B_1,\dots,B_4;X)=\int \mathrm{d}h\varphi(B_1,\dots,B_4;h\triangleright X)\star E_h(B_1)\dots E_h(B_4)\,. \tag{4.2.12}$$

The action on the normal X is then given by [147]

$$h\triangleright X=h^+n\left(h^-\right)^{-1}\,. \tag{4.2.13}$$

Now let us introduce the plane waves associated with the decomposition of the bivector and its dual in terms of SU(2) ones relying on the same isomorphism articulated above

$$E_h(B)\equiv e_{h^-}\left(B^-\right)e_{h^+}\left(B^+\right)\,, \tag{4.2.14}$$

where $B=(B^-,B^+)$ is the corresponding decomposition of the Lie algebra $(4)\simeq\mathfrak{su}(2)\times\mathfrak{su}(2)$. Moving to *the group representation*, the closure constraint is translated as

$$\varphi(g_1,\dots,g_4;X)=\varphi\left(g_1h^{-1},\dots,g_4h^{-1};h\triangleright X\right)\,, \tag{4.2.15}$$

as one can show by making use of an NC Fourier transform. This completely addresses the issue of the normal vector to the set of bivectors. At this stage, we can proceed with the implementation of the simplicity constraint. At the discrete level and relying on the above decomposition of the bivector, a more compact and general way of expressing it yields

$$XB_i^-X^1+\beta B_i^+=0,\quad \forall i=1,2,3,4,\quad \beta\equiv\frac{\gamma-1}{\gamma+1}. \tag{4.2.16}$$

We already mentioned that this constraint should not be imposed too strongly at the quantum level to cover some of the full phase space of the gravitational degrees of freedom as in the case of the EPRL model. It is, nonetheless, very practical to combine them in a more general equation, namely

$$\left(S^\beta\triangleright\varphi\right)(B_1,\dots,B_4;X)=\varphi(B_1,\dots,B_4;X)\star S_X^\beta(B_i)\,, \tag{4.2.17}$$

where $S_X^\beta(B_i)$ encrypts the different ways in which the constraint can be imposed on the GFT field and it is given by

$$S_X^\beta(B)=\sum_{J=(j^+,j^-)}\sum_j d(J)d(j)\omega(J,j,\beta)\Theta^J(x)\star\chi^j\left(XB^-X^{-1}+B^+\right)\,. \tag{4.2.18}$$

The quantity χ^j above is the character for $\mathfrak{su}(2)$, defined from a Fourier transform of the SU(2) character $\chi^j(g)=\operatorname{tr}D^j(g)$

$$\chi^j(B)=\int \mathrm{d}g\chi^j(g)e_g(B),\quad \forall x\in\mathfrak{su}(2),\quad \forall g\in\mathrm{SU}(2)\,, \tag{4.2.19}$$

and where denote by Θ^J the character of the Lie algebra Spin(4), defined in terms of its $\mathfrak{su}(2)$ decomposition such as

$$\Theta^J(B) \equiv \chi^{j^-}\left(B^-\right)\chi^{j^+}\left(B^+\right), \quad \forall B = \left(B^+, B^-\right) \in \mathfrak{spin}(4).$$

The coefficients $\omega(J, j, \beta)$ are responsible for the details of the implementation procedure. They define the relations between $J = (j^+, j^-)$ and j. For instance, if we take to be equal to the identity $\omega(J, j, \beta) = 1$, it is then clear that S^β reduces also to the identity. On the other hand, letting $\gamma \to \infty$, which corresponds to the BC model, the coefficients read

$$\omega(J, j, \beta) = \delta_{j+j^-}\delta_{j0} \quad \text{(BC)} \tag{4.2.20}$$

which delivers as a constraint $\delta\left(XB^-X^{-1} + B^+\right)$. As for the EPRL model, we have

$$\omega(J, j, \beta) = \delta_{j-|\beta|j^+}\delta_{j(1-\beta)j^+} \quad \text{(EPRL)} \tag{4.2.21}$$

we refer to the original literature on the detailed derivation of this compact and concise expression [100]. Before proceeding to the Lorentzian description of the above program, let us add that, the imposition of both constraints C_h and S^β guarantees the *geometricity* of the quantum entities that we are building. For these reasons, let us stress this fact by introducing the combined constraint

$$G^\beta = C_h \circ S^\beta = S^\beta \circ C_h\,, \tag{4.2.22}$$

which is called the *geometricity* constraint. Moreover, it is worth emphasizing that it is possible to show that the closure and simplicity constraint do in fact commute, an important feature that is required for the addition of the normal vector to be guaranteed.

• ***GFT and the Lorentzian BC model*** As we encountered in section 3.2.1, the BC model has succeeded so far in providing a consistent (despite its rigid) formulation of quantum geometry with Lorentzian signature *only* for *spacelike* tetrahedra and thus defined through time-like normal. We show now how we recover the BC counterpart in the GFT framework, where we explicitly point out the BC intertwiner, which will be useful for chapter 5. We consider then the BC imposition of simplicity, for a timelike normal $X \in \mathrm{H}^3 \simeq \mathrm{SL}(2,\mathbb{C})/\mathrm{SU}(2)$. In group representation, this yield

$$\varphi\left(G_1, \ldots, G_4; X\right) = \varphi\left(G_1 g_1, \ldots, G_4 g_4; X\right), \quad \forall g_I \in \mathrm{SU}(2)_X\,, \quad \forall G_I \in \mathrm{Spin}(4)_X\,. \tag{4.2.23}$$

Similarly to what we discovered in section 3.2.1, in terms of Lie algebra elements, the above condition forces the second Casimir of the group to vanish

$$C_2 \equiv K_I L^I \equiv B \cdot \star B = 0\,.$$

At the level of representations labeled by (ρ, ν) the choice $\nu = 0$ is identified with spacelike bivectors. This respects indeed the requirement to be orthogonal to a timelike normal

meaning that the simplicity constraint takes care of that. Moving to the closure condition, we analogously impose it as above. It is when both of these geometric conditions are respected that we end up with geometric spacelike tetrahedra. These are naturally represented by functions $\varphi(G_I;X)$ which in spin representation read

$$\varphi(G_I;[a]) = \left[\prod_i \int \mathrm{d}\rho_i 4\rho_i^2 \sum_{j_i m_i}\right] \varphi^{\rho_i 0,00}_{j_i m_i} \prod_i D^{(\rho_i,0)}_{j_i m_i 00}(g_i a)\ , \tag{4.2.24}$$

where $[a]=X$ is a representative of $Q_1 \simeq \mathrm{SL}(2,\mathbb{C})/\mathrm{SU}(2)$. Integrating over the normal we obtain

$$\varphi(G_I) \equiv \int_{\mathrm{H}^3} \mathrm{d}X \varphi(G_I;X) = \int \mathrm{d}\rho_I \sum_{j_I,l_I} \sum_{m_I,n_I} \varphi^{\rho_I}_{j_I m_I} \left[\prod_{i=1}^4 \left(4\rho_i^2\right) D^{(\rho_i,0)}_{j_i m_i l_i n_i}(g_I)\right] B^{\rho_I}_{l_I n_I}\ , \tag{4.2.25}$$

where $B^{\rho_I}_{l_I n_I}$ is the BC intertwiner, i.e.

$$B^{\rho_I}_{l_I n_I} \equiv \int_{\mathrm{H}^3} \mathrm{d}X \prod_{i=1}^4 D^{(\rho_i,0)}_{j_i m_i 00}(X)\,.$$

• ***GFT and the EPRL model.*** Analogously to the BC case explained above, we proceed by applying the same steps for the EPRL model. In this case, the simplicity constraint at the quantum level is established through relations between the stabilizer SU(2) spin labels with the representation labels of $\mathrm{SL}(2,\mathbb{C})$: $|\nu| = j$ and $\rho = \gamma j$. We can then use these relations to form an equivalent description of the resulting field in terms of $\mathrm{SU}(2)/\mathrm{SU}(2)_{\mathrm{diag}}$, with the SU(2) embedding in $\mathrm{SL}(2,\mathbb{C})$ being described by the map (4.2.11), however with $G_1,\dots,G_4 \in \mathrm{SL}(2,\mathbb{C})$. After further imposing the closure constraint, we obtain functions on $\mathrm{SU}(2)^4/\mathrm{SU}(2)_{\mathrm{diag}}$. This reads in the spin representation basis

$$\varphi(g_I) = \sum_\iota \sum_{j_I} \sum_{m_I,n_I} \varphi^{j_1,\dots,j_4;\iota}_{m_1,\dots,m_4} \left[\prod_{i=1}^4 \sqrt{d(j_i)} D^{j_i}_{m_i n_i}(g_I)\right] \mathcal{I}^{j_1,\dots,j_4;\iota}_{n_1,\dots,n_4} \equiv \sum_{\vec{\alpha}} \varphi_{\vec{\alpha}} \psi_{\vec{\alpha}}(g_I)\,, \tag{4.2.26}$$

where $\vec{\alpha} = \{j_I, m_I, \iota\}$ and $\mathcal{I}^{j_1,\dots,j_4;\iota}_{n_1,\dots,n_4}$ is an SU(2) intertwiner obtained from the right-diagonal invariance imposed on the field.
It is worth emphasizing that the only crucial difference between the BC and EPRL decomposition of the filed is that the intertwiner space in the BC case is *one-dimensional*. Moreover, the above equation shows that the degrees of freedom of the GFT field, $\vec{\alpha} = \{j_I, m_I, \iota\}$ are exactly spin-network data, showing a direct connection of SU(2) models with LQG.

This summarizes the completion of the GFT approaches to the several covariant quantization proposals to gravity. There is another path that relies on interesting properties of the quantum geometries that can shed more light on the continuum problem every QG approach is confronted with, namely quantum *entanglement*. This perspective is based on

the argument that the emergence of spacetime is traced back to their entangled fundamental quantum states. In the next section, we will see how this is systematically implemented in GFT. This will be further generalized in the results of chapter 6.

4.3 GFT spin-network states as entanglement graphs

In the following, we discuss how to glue pieces of quantum geometries relying on GFT entanglement graphs. To easily grasp the techniques of how we can do this procedure, we need tools from quantum information theory as we will see below. Furthermore, it is of great importance to pinpoint how the structure of the considered Hilbert space enters the entropic calculations which quantifies the entanglement between quantum geometries. This is extensively studied in the LQG approach and GFT but as we will see, due to the different Hilbert space structure of the two theories, the corresponding entanglement measure is different. We start here by exposing the essential tools of entanglement graphs characterized by the spin-network states in the GFT Hilbert space.

The kinematical states of GFT. spin-networks can be interpreted in several quantum gravity models as discretized spatial geometries [119]. As anticipated, we focus mainly on GFT states [152], where spin-network graphs are understood as the collection of individual vertices (representing building blocks of space, where the *particles* picture thereof is described by the GFT Fock space) correlated with each other. As already mentioned, a closely related formalism to that of GFT is LQG. The equivalent states to those considered as GFT particles arise in this case from the discretization of the base manifold and quantizing it canonically as we encountered in section 3.3.2.

More specifically, as we encountered in section 3.3.2 and section 4.1 for both approaches the elementary portion of space is a quantum $(d-1)$-simplex dual to a d-valent vertex, whose edges are decorated by elements of a group G [85,153] (see figure). The phase space of the quantum simplex is realized by the Hilbert space $\mathcal{H} = L^2\left(G^d/G\right)$, where the group G is usually chosen to be $G = SU(2)$. As we explain in the following, in GFT the picture of a connected set of such building blocks of space is comprehended by correlating the degrees of freedom living on the dual vertices. As we saw in the previous section, the quantum state of the geometry of the simplex can be fully described in the spin representation. In fact, according to the Peter-Weyl theorem a vertex wave function can be decomposed into irreducible representations of the group $G = SU(2)$ in terms of the spin-network basis

$$\varphi(\vec{g}) = \sum_{\vec{j}\vec{n}\iota} \psi^{\vec{j}\iota}_{\vec{n}} S_{\vec{j}\vec{n}\iota}(\vec{g}), \tag{4.3.1}$$

where the vector notation refers to a collection of edge variables: group variables $\vec{g} = \{g_1, \ldots, g_d\}$, spins ($SU(2)$ irreducible representations) $\vec{j} = \{j_1 \ldots j_d\}$, and magnetic numbers $\vec{n} = \{n_1, \ldots, n_d\}$ (which can be thought of as quantum numbers attached to the edge

free-ends); and the symbol ι is the intertwiner quantum number encoding the gauge invariance of the individual vertex. In fact, it labels a basis in the invariant Hilbert space under the action of SU(2)

$$\mathcal{I}^{\vec{j}} = \mathrm{Inv}_{\mathrm{SU}(2)}[V^{j_1} \otimes \cdots \otimes V^{j_d}]\,, \tag{4.3.2}$$

where V^{j_i} is the representation space of the edge carrying the spin j_i. The functions $S_{\vec{j}\vec{n}\vec{\iota}}(\vec{g})$ appearing in the harmonic decomposition of (4.3.1) are the spin-network basis wave functions [105, 134] and throughout this section and in chapter 6

$$S_{\vec{j}\vec{n}\iota}(\vec{g}) = \sum_{\vec{m}} I^{\vec{j}\iota}_{\vec{m}} \prod_i \sqrt{d_{j_i}} D^{j_i}_{m_i n_i}(g_i)\,, \tag{4.3.3}$$

where $I^{\vec{j}\iota}_{\vec{m}} \in \mathcal{I}^{\vec{j}}$ is the normalized intertwiner tensor, $D^{j_i}_{m_i n_i}(g_i)$ is the Wigner matrix representing the group element g_i and $d_{j_i} = 2j_i + 1$ is the dimension of the representation space V^{j_i}. A spin-network basis state $|\vec{j}\vec{n}\iota\rangle$ is then defined by the wave function $\langle \vec{g}|\vec{j}\vec{n}\iota\rangle = S_{\vec{j}\vec{n}\iota}(\vec{g})$ and possesses a clear geometrical interpretation. In fact, recall that as we saw in section 3.3.2, the spin-network basis diagonalizes the area and volume operators of LQG [134, 153] which somehow refines our geometric intuition about such quantum gravity states. At the level of the Hilbert space of the single vertex, the Peter-Weyl decomposition yields

$$\mathcal{H} = L^2\left(G^d/G\right) = \bigoplus_{\vec{j}} \left(\mathcal{I}^{\vec{j}} \otimes \bigotimes_{i=1}^{d} V^{j_i}\right)\,, \tag{4.3.4}$$

and the state of the single vertex then reads

$$|\varphi\rangle = \bigoplus_{\vec{j}} \sum_{\vec{n}\iota} \varphi^{\vec{j}}_{\vec{n}\iota} |\vec{j}\vec{n}\iota\rangle. \tag{4.3.5}$$

If we are interested in considering the case of N-vertices, we are faced with two different approaches. We list them now:

1. In the framework of LQG, we usually start from a graph Γ based on L edges and N vertices. We systematically construct the corresponding space of square integrable functions by taking L copies of the group G associated with each link, namely $\mathcal{H}_\Gamma = L^2(G^L/G^N)$. If the case where the graph is completely connected, then the Hilbert space consists only of that of the intertwiners $\mathcal{H}_\Gamma = L^2(G^L/G^N) = \bigoplus_{\vec{j}} \mathcal{I}^{\vec{j}}$.

2. However, in the GFT formalism, the focus is mainly based on the vertices structure (which are not gauge invariant structures). Therefore, the graph emerges from their quantum correlations through the procedure of gluing. More specifically, if we consider N distinguishable vertices, the corresponding GFT Hilbert space (for distinguishable particles) is nothing more than the tensor product of all the single-vertex Hilbert spaces associated with each one of them

$$L^2\left(G^{d\times N}/G^N\right) := \underbrace{\mathcal{H} \otimes \cdots \otimes \mathcal{H}}_{N} = \mathcal{H}_N\,, \tag{4.3.6}$$

where $\mathcal{H}$ is defined by (4.3.4).

The gluing of vertices in the GFT picture, corresponds in the spin representation, to entanglement between the degrees of freedom living on the edges, and the resulting spin-network graphs are referred to as *entanglement graphs* [36]. A N-open vertices-state living on this Hilbert space (4.3.6) is denoted by $|\psi_N\rangle$ and is obtained by taking the $N-$ tensor product of single-vertex states in (4.3.5) yielding

$$|\varphi_N\rangle = \bigotimes_N \bigoplus_{\vec{j}} \sum_{\vec{n}\iota} \psi^{\vec{j}}_{\vec{n}\iota} |\vec{j}\vec{n}\iota\rangle \,. \tag{4.3.7}$$

By taking the direct sum of the Hilbert spaces associated with all possible number of vertices N one ends up with the GFT pre-Fock space that reads

$$\text{pre-}\mathcal{F}(\mathcal{H}) = \bigoplus_{N=1}^{\infty} \mathcal{H}_N \,. \tag{4.3.8}$$

It is possible from this formulation to build a Fock space of the theory which is naturally obtained by symmetrizing every term of the direct sum over the vertex labels

$$\mathcal{F}(\mathcal{H}) = \bigoplus_{N=1}^{\infty} \text{sym} \left(\underbrace{\mathcal{H} \otimes \cdots \otimes \mathcal{H}}_{N} \right) . \tag{4.3.9}$$

The second-quantization formulation of GFT is then provided by promoting the GFT field to an operator $\hat{\varphi}$ and $\hat{\varphi}^\dagger$ that satisfy the following bosonic commutation relations, i.e.

$$[\hat{\varphi}(\vec{g}), \hat{\varphi}^\dagger(\vec{g}')] = \int dh \prod_{i=1}^{d} \delta(h g^i (g^{i'})^{-1}), \qquad [\hat{\varphi}(\vec{g}), \hat{\varphi}(\vec{g}')] = [\hat{\varphi}^\dagger(\vec{g}), \hat{\varphi}^\dagger(\vec{g}')] = 0, \tag{4.3.10}$$

where the r.h.s. of the first equation is the gauge-invariant Dirac delta distribution on G^d. The GFT Fock space is then generated from the repeated action of the creation operator on the vacuum state $|0\rangle$. This vacuum state is identified with the state annihilated by $\hat{\varphi}(\vec{g})$. In this second quantization language, the modes appearing in the Peter-Weyl decomposition of (4.3.1), for which we use again the simple notation $\varphi_{\vec{\alpha}} \coloneqq \varphi^{\vec{j}}_{\vec{n},\iota}$ where $\vec{\alpha} \coloneqq \{\vec{j}, \vec{n}, \iota\}$, are similarly promoted to creation and annihilation operators which satisfy

$$[\hat{\varphi}_{\vec{\alpha}}, \hat{\varphi}^\dagger_{\vec{\alpha}'}] = \delta_{\vec{\alpha},\vec{\alpha}'}, \qquad [\hat{\varphi}_{\vec{\alpha}}, \hat{\varphi}_{\vec{\alpha}'}] = [\hat{\varphi}^\dagger_{\vec{\alpha}}, \hat{\varphi}^\dagger_{\vec{\alpha}'}] = 0 \,. \tag{4.3.11}$$

In this setting, achieving an entangled state can be realized by projecting states living on (4.3.6) onto maximally entangled state of a pair of edge-spins. This induces a connected set of links between the vertices. For instance, two edges e^i_x and e^i_y can be glued to form a link ℓ^i_{xy} by projecting the state $|\psi\rangle$ onto the maximally entangled state:

$$|\ell^i_{xy}\rangle := \bigoplus_j \frac{1}{\sqrt{d_j}} \sum_n (-1)^{j+n} \, |j\,, n\rangle \otimes |j\,, -n\rangle \ , \tag{4.3.12}$$

to obtain a more general entangled state that includes N-vertices with possible open links. Let us now introduce some tools from the theory of quantum information to methodically implement this correlating procedure for an arbitrary number of labeled vertices, which can be generalized to unlabeled ones. The basic idea we chase here is to view two connected vertices through a link adjacent to each other.

Adjacency matrix and gluing procedure. In order to systematically implement this within the graph structure, let us introduce some notions from graph theory that will facilitate the task, underlying thus the combinatorial patterns for distinguishable and indistinguishable vertices. For these and other notions of graph theory, we refer to [154].

Definition 7. *Labeled graph: is a graph γ where there is an ordered set of vertices $V = \{v \,|v = 1, \dots, N\}$ connected according to a certain pattern. A labeled graph composed of N vertices can be described by a $N \times N$ matrix A, called adjacency matrix, whose entries encode the adjacency relations among vertices: A_{xy} takes value 1 if vertex x is connected to vertex y, and 0 otherwise. Since A encodes all information about γ (which simply consists of who is glued to whom) we refer to a graph by using both notations, i.e. $\gamma \equiv A$.*

Two graphs are said to be *isomorphic* if they differ only by the labels decorating their vertices, so in principle, two labeled graphs $\gamma = A$ and $\gamma' = A'$ with the same number of vertices N are isomorphic if there exist a permutation operation π on N elements such that $A' = P_\pi A P_\pi^{-1}$, where P_π is the matrix obtained by permuting the columns of the identity matrix according to π [36, 155].

Definition 8. *An unlabeled graph $[\gamma]$ is the combinatorial pattern represented by $[A]$, where $\gamma \equiv A$.*

In the above definition, we encounter the notion of equivalent classes for the adjacency matrices, we clarify this now. For this purpose, given an adjacency matrix A, we denote by $[A]$ the equivalence class of matrices obtained by permuting rows and columns of A:

$$[A] = \{A' | A' = P_\pi A P_\pi^{-1},\ \pi \in S_N\}, \tag{4.3.13}$$

where S_N is the set of possible permutations of N elements. Consequently, it is obviously two isomorphic graphs belong to the same equivalence class of adjacency matrices. Furthermore, two unlabeled graphs $[\gamma]$ and $[\gamma']$ are said to be isomorphic if and only if they have a common adjacency matrix and two isomorphic graphs have exactly the same set of adjacency matrices.

The properties encoded in the adjacency-matrix encoding of a graph can also take into consideration the collection of edges outgoing from a given edge carrying different colors or labels. This can be naturally implemented in the case of spin networks. Therefore, in the following, we denote by e_x^i the edge carrying the color i departing from vertex x and by ℓ_{xy}^i the link formed by fusing the edges e_x^i and e_y^i. This can be made clear in figure 4.3.

If the pair of vertices can be connected through the edge ℓ_{xy}^i, we can collect and store this information about all possibly connected vertices within a certain graph in the matrix

$$A_{xy} = \begin{pmatrix} a_{xy}^1 & 0 & \dots & 0 \\ 0 & \ddots & & \\ \vdots & & \ddots & \\ 0 & & & a_{xy}^d \end{pmatrix}, \tag{4.3.14}$$

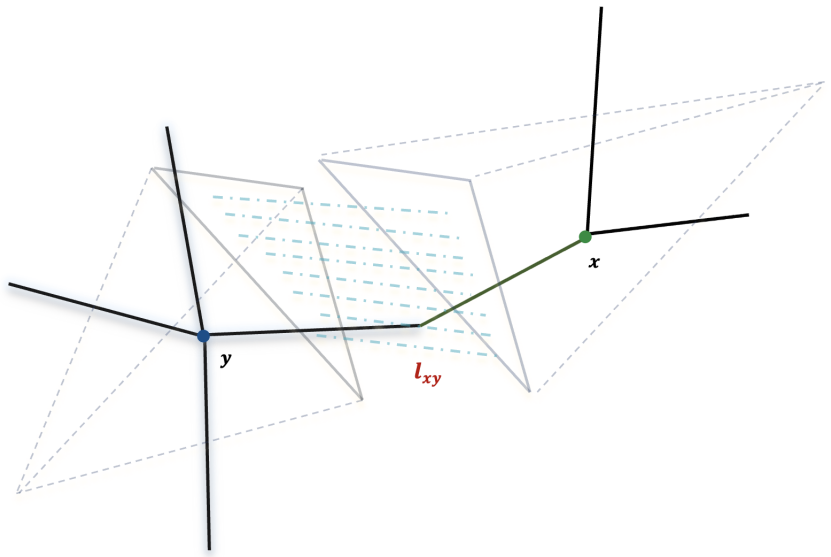

Figure 4.3: Gluing two links emanating from two vertices x and y. The glued link ℓ_{xy} is the resulting common link after the entangling procedure. At the level of the tetrahedra, this gluing procedure results in identifying common faces. The fusion of these faces is symbolized by the parallel dashed lines between the tetrahedra.

where the entries are denoted by a^i_{xy} and are equal to 1 (0) if vertices x and y are connected (not connected) along their edges labeled by i. We also define the following substructures of a labeled-graph γ described by such generalized adjacency matrix

* $L = \{\ell^i_{xy} \ | x, y \in V : (A_{xy})_{ii} = 1\}$ set of internal links of γ,
* $\partial\gamma = \{e^i_x \ | x \in V : (A_{xy})_{ii} = 0 \ \forall \ y \in V\}$ set of boundary edges of γ,
* $E = L \cup \partial\gamma$ set of all edges of γ.

These are the notions that we will use throughout this section and in chapter 6, where we generalize the notion of a single entanglement graph to the case of a superposition.

Starting from such a class of states, it is then possible to construct labeled graph states according to a pattern γ whose connectivity is encoded in the so-called adjacency matrix within the GFT formalism. This is carried out by mainly implementing it at the level of the gluing procedure defined through the map [36]:

Definition 9. *The gluing map of (open) links connecting two vertices x and y is carried out by the map*

$$P_\ell : L^2(G^2) \to L^2(G^2/_R G), \tag{4.3.15}$$

where the two copies of the group G are attached to the edges e^i_x and e^i_y to be fused together, ℓ is a short notation for ℓ^i_{xy} and R is the factorization over the right action of the group.

The link map P_ℓ is defined as

$$P_\ell := \int \mathrm{d}h \mathrm{d}g_x^i dg_y^i \, |g_x^i\rangle \langle g_x^i h| \otimes |g_y^i\rangle \langle g_y^i h| \,. \tag{4.3.16}$$

In fact, this gluing operation is equivalent to the realization of an averaging through the right action of the group on the two open edges carrying g_x^i and g_y^i [36, 156]

$$\int \mathrm{d}h \psi(\dots, g_x^i h, \dots, g_y^i h, \dots) = \psi_\ell(\dots, g_x^i (g_y^i)^{-1}, \dots). \tag{4.3.17}$$

Clearly the convolution depending on the group element h forces $\psi(\vec{g}_1, \dots, \vec{g}_N)$ to depend on g_x^i and g_y^i through the product $g_x^i (g_y^i)^{-1}$ representing the group variable associated to the internal link ℓ_{xy}^i. The expansion of a graph wave function defined with N vertices underlining the gluing operation through this procedure can be captured in the expression

$$\Psi_\gamma(\{g_\ell\}) = \int \prod_{x<y} \mathrm{d}h_i^{xy} \psi(\{g_i^x h_i^{xy}\}) = \sum \psi_{\vec{n}}^{\vec{\jmath}\vec{\iota}} \mathcal{I}_{\vec{m}}^{\vec{\jmath}\vec{\iota}} \int \prod_{x<y} \mathrm{d}h_i^{xy} \prod_{x,i} \sqrt{d_{j_i^x}} D^{j_i^x}_{m_i^x n_i^x} \left(g_i^x h_i^{x t_i(x)}\right) , \tag{4.3.18}$$

with h_i^{xy} is the gluing element, connecting the vertices x and y, here we define the quantity $t_i(x)$ as the target tensor that encodes the information delivered from the adjacency matrix that dictates the connectivity of the graph, $\mathcal{I}_{\vec{p}}^{\vec{\jmath}\vec{\iota}} := \prod_x \mathcal{I}_{p^x}^{j^x \iota^x}$ and $\psi_{\vec{n}}^{\vec{\jmath}\vec{\iota}} := \psi_{\vec{p}\vec{n}}^{\vec{\jmath}} \mathcal{I}_{\vec{p}}^{\vec{\jmath}\vec{\iota}} \prod_{x,i} \sqrt{d_{j_i}^x}$ and the sum is over all repeated indices. By performing the integral over the gluing elements, we obtain

$$\begin{aligned} \Psi_\gamma(\{g_\ell\}) = \sum \Psi_{\partial\gamma\{n_i^x\}}^{\{j_i^{x t_i(x)}\}\vec{\iota}} \mathcal{I}_{\vec{m}}^{\{j_i^{x t_i(x)}\}\vec{\iota}} \prod_{x,i:x<t_i(x)} \sqrt{d_{j_i^{x t_i(x)}}} D^{j_i^{x t_i(x)}}_{m_i^x m_i^{t_i(x)}} \left(g_i^x g_i^{t_i(x)^{-1}}\right) \\ \times \prod_{x,i:t_i(x)=0} \sqrt{d_{j_i^x}} D^{j_i^x}_{m_i^x n_i^x}(g_i^x) \,. \end{aligned} \tag{4.3.19}$$

In the spin-network basis, gluing edges is equivalent to entangling the degrees of freedom attached to their free ends. We can show this once we compute the entanglement measure, quantifying such correlations.

GFT Hilbert space structure. The LQG can be perceived as a GFT Hilbert space, however, governed by a different organization of its elements (and excluding the zero modes). A generic LQG state is in fact associated with all possible graphs $\{\Gamma\}$ (embedded in the spacial manifold) and lives on the Hilbert space given by $\mathcal{H}_{LQG} = \bigoplus_\Gamma \mathcal{H}_\Gamma$ where $\mathcal{H}_\Gamma$ is the individual Hilbert space underlying a graph γ. Such superposed states correspond to states in the GFT Hilbert space $\mathcal{H}_{GFT} = \bigoplus_{N=0}^\infty \mathcal{H}_N$, for more details see [131, 157]. It is of great importance at this level to address the differences between the Hilbert spaces of the theories.

* Starting from the GFT Hilbert space $\mathcal{H}$ defined in (4.3.6) we take a direct sum over the number of vertices, as opposed to the set of graphs in LQG, and we do not impose any cylindrical equivalence (and, thus, in particular, one keeps the zero modes in the Hilbert space). See figure 3.8b and 3.8a.

* States associated with different graphs end up being organized very differently in $\mathcal{H}_{GFT} = \mathcal{F}(\mathcal{H})$ compared to the LQG space: states associated to graphs with a different number of vertices are orthogonal, whereas states associated to different graphs but with the same number of vertices are, generically, *not orthogonal*.

* This distinguishes the GFT Fock space $\mathcal{F}(\mathcal{H})$ in the sense that it decreases the importance of the exact graph structure, as compared to the LQG Hilbert space.

* The GFT formalism is not only considered as the second quantized version of LQG but it is actually a *completion* of the LQG definition of the quantum dynamics of spacetime. We already saw this at the level of the dynamics in section 4.2. To be more precise, there is a simple and straightforward map that transforms the canonical spin network states into group field theory states which are exactly provided by the group averaging one, or the link map defined above. This clearly preserves the quantum geometric information. Starting from the GFT field we can always obtain a corresponding LQG wave function ψ_Γ, namely

$$\psi_\Gamma = \sum_{\{m_i^j\}} \varphi^{\vec{j}_i,\vec{\iota}_i}_{\vec{m}_i} \prod_{l_{\gamma_i}} \delta_{j_i^a,j_j^b} \delta_{m_i^a,m_j^b}. \tag{4.3.20}$$

  This indeed clarifies the embedding of $\psi_\Gamma \in \mathcal{H}_{LQG}$ into $\mathcal{H}_{GFT}$. Indeed, (4.3.20) manifests states associated with the graph Γ as possible elements of the GFT Hilbert space contains, among its elements, states. It is also worth mentioning that the Hilbert space $\mathcal{H}_{LQG}$ is a Hilbert subspace of $\mathcal{H}_{GFT}$, this is evident once we see that the scalar product on the first is in fact the one induced by the latter [156].[2]

These properties can be traced back to the fact that GFT graphs do not provide a direct definition of the kinematical Hilbert space, and they rather emerge as entanglement patterns among building blocks defined in the pre-Fock space. This is a crucial property that makes the GFT graph states a more powerful tool to extract more information about the entanglement from such pre-geometric states, from which spatial-temporal entities should emerge. As we will see later when we compute the entanglement entropy of the more general case of a superposition of states in chapter 6, while the LQG and GFT (pre-Fock) Hilbert space structure might agree to some extent on some entropic terms entering the entanglement measure, the fact that the GFT states are not necessarily orthogonal results

[2]Notice that this statement is representation-independent. This can be formulated as follows; it is only reasonable to consider that any closed LQG states can be broken down in such a way that they can be written as a linear combination of states describing *disconnected* open spin-network vertices of an arbitrary number. It is exactly the extra conditions implementing the gluing that ensures their reconstruction [131].

in the rise of an additional expression that can be interpreted in quantum information theory as an *interaction information* [158, 159].

4.4 Effective cosmologies from Group Field Theories

In this section, we focus on a certain class of coherent states that the GFT formalism employs to extract an effective cosmological prediction from a QG origin. We will go through the assumptions we are making in the model and mention several physical predictions that will be useful for us in chapter 7. The assumptions that will allow us to do so enter the GFT approach at the kinematical level as well the dynamical one.

For the remainder of this section let us focus on the simplest case of GFT field in the group representation decomposed in the spin-network basis using (4.3.1)

$$\varphi\left(g_I\right)=\sum_{\iota}\sum_{j_I}\sum_{m_I,n_I}\varphi^{j_1,\dots,j_4;\iota}_{m_1,\dots,m_4}\left[\prod_{i=1}^{4}\sqrt{d\left(j_i\right)}D^{j_i}_{m_i n_i}\left(g_I\right)\right]\mathcal{I}^{j_1,\dots,j_4;\iota}_{n_1,\dots,n_4}\equiv\sum_{\vec{\alpha}}\varphi_{\vec{\alpha}}\psi_{\vec{\alpha}}\left(g_I\right)\,. \tag{4.4.1}$$

where we denoted as usual the quantum labels with the abbreviated vector notation $\vec{\alpha}=\left\{\vec{j},\vec{m},\iota\right\}$. The wave function above, as already emphasized, depicts a discrete portion of what would be identified as spacetime after taking the continuum limit. As mentioned in chapter 1, attaining a physical structure that could be understood as spacetime can be achieved once we understand the continuum limit as the emergence of classical physical properties from the characterizing behavior of the underlying microscopic pre-geometric and pre-matter degrees of freedom. The resulting physical quantities obtained in such a way will be referred to as *effective* ones.

The above quantum states bear the seeds of the geometry we aim to reproduce at the effective level and they were intensively studied in various quantum gravity models [77, 86, 160, 161]. To better understand the phenomena of the emergence of matter degrees of freedom along the geometrical ones, we are faced with the necessity of considering additional degrees of freedom that would play the role of pre-matter. As we will mention below, the simplest set of degrees of freedom that fulfills such a task is that of scalar fields and in this thesis, we focus only on this class. Implementing scalar fields as pre-matter degrees of freedom can be carried out in two ways, where we can make the distinction between a set of fields that represent a relational reference frame (clock and rods) and another playing the role of matter content [75, 77, 162, 163]. This can be observed already at the level of the corresponding defined GFT operators and then later on at the effective level, once we try to match the obtained physics to the classical ones [164]. In the next paragraphs, we explain more in detail how this can be precisely done in GFT.

4.4.1 Kinematics of relational GFT.

The scheme discussed above can be precisely implemented once we couple the pre-geometric data encoded in the GFT field to the scalar fields ones [165]. Following this line of reasoning, one can introduce the so-called pre-matter data alongside the purely geometric degrees of freedom encoded in the discretized simplex. Clearly, this must be performed in such a way that the perturbative expansion of the GFT partition function (see section 4.2) matches the discrete path-integral of the simplicial gravity model minimally coupled with the massless scalar fields one wants to reproduce. In the following, we work with a set of five massless scalar fields, where four of them will play the role of a relational reference frame minimally coupled to our GFT, whereas the fifth will be considered as the matter field.
At the level of the GFT, minimally coupling n massless scalar field, the group field operator takes the form $\hat{\varphi}\left(g_I, \chi^a\right) \equiv \hat{\varphi}\left(g_I, \chi^1, \ldots, \chi^n\right)$, for running from $a = 1, \ldots, n$. Of course, the commutation relation in (4.3.10) changes as well and it reads as

$$\left[\hat{\varphi}\left(g_I, \chi^a\right), \hat{\varphi}^\dagger\left(g'_I, (\chi')^a\right)\right] = \mathbb{I}_G\left(g_I, g'_I\right) \delta^{(n)}\left(\chi^a - (\chi')^a\right) . \tag{4.4.2}$$

The additional degrees of freedom encoded in the scalar field induce a change on the level of the kinematical structure of the Fock space and it is reflected also in the second quantized operators, which now involve integrals over all the possible values of $\chi^a \in \mathbb{R}^n$. For instance, the number operator is expressed now as

$$\hat{N} = \int \mathrm{d}^n\chi \int \mathrm{d}g_I \hat{\varphi}^\dagger\left(g_I, \chi^a\right) \hat{\varphi}\left(g_I, \chi^a\right) . \tag{4.4.3}$$

A crucial quantity for describing cosmological geometries is the volume operator and it is given by

$$\hat{V} = \int \mathrm{d}^n\chi \int \mathrm{d}g_I \; \mathrm{d}g'_I \hat{\varphi}^\dagger\left(g_I, \chi^a\right) V\left(g_I, g'_I\right) \hat{\varphi}\left(g'_I, \chi^a\right) , \tag{4.4.4}$$

whose matrix elements $V\left(g_I, g'_I\right)$ are defined from those of the first quantized volume operator in the group representation. Similarly to the defined geometric operators such as the volume and area operator, we are able to construct a set of observables naturally associated with the pre-matter fields, through polynomials and derivatives with respect to χ^a for each $a = 1, \ldots, n$. In particular, the two fundamental, self-adjoint ones that can be derived in this way are the scalar field- and the momentum operator,

$$\hat{\chi}^b \equiv \int \mathrm{d}^n\chi \int \mathrm{d}g_I \chi^b \hat{\varphi}^\dagger\left(g_I, \chi^a\right) \hat{\varphi}\left(g_I, \chi^a\right) , \tag{4.4.5}$$

$$\hat{\Pi}_b = \frac{1}{i} \int \mathrm{d}^n\chi \int \mathrm{d}g_I \left[\hat{\varphi}^\dagger\left(g_I, \chi^a\right) \left(\frac{\partial}{\partial\chi^b} \hat{\varphi}\left(g_I, \chi^a\right)\right)\right] , \tag{4.4.6}$$

Notice that thanks to the relational scheme to describe the dynamics and evolution of observables at the quantum level, the expectation values of the above operators (4.4.5) and (4.4.6) on appropriate semi-classical and continuum states would be associated to the scalar field itself and conceivably its momentum.

GFT quantum gravity states and relationalism The relational program encapsulating as well the evolution of small inhomogeneities in GFT in a cosmological setting (as we will see later on), relies heavily on the class of quantum gravity states we work with. These states should conceal some proto-geometric interpretation in terms of approximate continuum geometries. Such semi-classical states are expected to be formed following an appropriate coarse-graining procedure of the underlying microscopic degrees of freedom. In the GFT framework, this aspect is associated with the collective behavior, encoding the hydrodynamic description of the underlying quantum gravity model. One of the simplest forms of states describing such collective behavior is encoded by the condensate ones, where each fundamental quantum is attributed the same coherent wave function (assumption QL.1):

$$|\sigma\rangle = \mathcal{N} e^{||\sigma||^2/2} e^{\int \mathrm{d}g_I \mathrm{d}^n\chi^a\, \sigma(g_I,\chi^a)\hat{\varphi}^\dagger(g_I,\chi^a)} |0\rangle \ . \tag{4.4.7}$$

The normalization condition of this state captures a very interesting physical quantity which is the number of particles in terms of expectation value N.

$$||\sigma||^2 = \int \mathrm{d}g_I \int \mathrm{d}^n\chi^a\, |\sigma(g_I,\chi^a)|^2 = \langle\sigma|\, \hat{N}\, |\sigma\rangle = \langle \hat{N}\rangle \ . \tag{4.4.8}$$

Moreover, this coherent state is a superposition of infinitely many spin-network degrees of freedom captured by a single collective function. An additional important property of this state is that they are eigenstates of the GFT field operator $\hat{\varphi}$

$$\hat{\varphi}\,(g_I,\chi^a)\,|\sigma\rangle = \sigma\,(g_I,\chi^a)\,|\sigma\rangle \ . \tag{4.4.9}$$

Before proceeding to the effective relational dynamics our GFT model produces, it is important to present the symmetry assumptions we assume this class of states should be endowed with. These can be listed as follows:

- *diagonal left-invariance:* The condensate wave function is diagonal left-invariant: $\sigma\,(g_I,\chi^a) = \sigma\,(hg_I,\chi^a)$, $\forall h \in \mathrm{SU}(2)$. Geometrically, this can be interpreted as an average over the relative embedding of the tetrahedron in the corresponding algebra [164, 166]. This gives rise to an isometry between the domain of the condensate wave function to the space of all the spatial metrics at a point (minisuperspace).

- *Isotropy:* this symmetry condition (assumption QL.3) renders the wave function effectively dependent on only one spin label j:

$$\sigma\,(g_I,\chi^a) = \sum_{j=0}^{\infty} \sigma_j\,(\chi^a)\, \mathcal{I}^{*jjjj,\iota_+}{}_{m_1m_2m_3m_4} \mathcal{I}^{jjjj,\iota_+}_{n_1n_2n_3n_4} \sqrt{d(j)^4} \prod_{i=1}^{4} D^j_{m_in_i}\,(g_I)\,, \tag{4.4.10}$$

  where $d(j) = 2j+1$ and $\iota_+$is the largest eigenvalue of the volume operator compatible with j. Therefore, the condensate wave function in spin representation reads as

$$\sigma_{\vec{\alpha}}\,(\chi^a) \equiv \sigma_{\{j,\vec{m},\iota_+\}}\,(\chi^a) = \sigma_j\,(\chi^a)\, \overline{\mathcal{I}}^{jjjj,\iota_+}_{m_1m_2m_3m_4} \ . \tag{4.4.11}$$

  The dependence of the condensate wave function on a single spin simplifies the complications at the computational level to bridge the transition between the microscopic and the effective level of the theory [86, 161, 167].

The implementation of the effective relational description of physical quantities in the GFT formalism is thoroughly discussed in [77]. The relational evolution of geometric observables with respect to a scalar field clock and rods was constructed by making use of the concept of Coherent Peaked State (CPS). This gives a class of states which - as the name entails - is coherent, equipped with a wave function that has strong peaking properties on the scalar field variables (assumption QL.2). Working with a spacetime dimension d, with $d \leq n$„ the condensate wave function is then adjusted as follows

$$\sigma_{\epsilon^\mu,\pi_\mu;x^\mu}\left(g_I,\chi^a\right)=\left[\prod_{\mu=0}^{d-1}\eta_{\epsilon^\mu}\left(\chi^\mu-x^\mu,\pi_\mu\right)\right]\tilde{\sigma}\left(g_I,\chi^a\right)\,, \tag{4.4.12}$$

where $\eta_{\epsilon^\mu}\left(g_I;\chi^\mu-x^\mu,\pi_\mu\right)$ is the peaking function [77, 164, 168]. The equation for each $\mu=0,\ldots,d-1$, would encode the distribution of spatial geometric data for each point x^μ of the physical manifold coordinatized by the frame fields χ^μ. The peaking function is taken to be a Gaussian associated with a small width. The most studied case is usually related to a single field variable, namely a clock. [77] showed that in order to correctly implement such assumptions the parameter $\epsilon \ll 1$ should not tend to zero. This results in suppressed quantum fluctuations and as discussed in [77, 168], it should satisfy $\epsilon\pi_0^2 \gg 1$ where π_0 (being the clock momentum) determines the non-trivial phase of the Gaussian. By construction, the expectation value of the intrinsic version of the second quantized field operators $\hat{\chi}^\mu$ in (4.4.5) on the above states is approximately given by

$$\langle\hat{\chi}^\mu\rangle_\sigma \equiv \frac{\langle\hat{X}^\mu\rangle_\sigma}{\langle\hat{N}\rangle_\sigma} \simeq x^\mu\,, \tag{4.4.13}$$

which allows us to identify the change with respect to x^μ as physical. These are the fundamental states that we will work with when we extract physical predictions in cosmology. Since the most important operator in cosmological application in quantum gravity models, is the volume operator (which in our work should be capturing isotropic perturbations), we will further make the assumption that the reduced wave function is isotropic as well as the peaking properties of the condensate

$$\sigma_{\epsilon,\delta,\pi_0,\pi_x;x^\mu}\left(g_I,\chi^\mu,\phi\right)=\eta_\epsilon\left(\chi^0-x^0;\pi_0\right)\eta_\delta\left(|\boldsymbol{\chi}-\mathbf{x}|;\pi_x\right)\tilde{\sigma}\left(g_I,\chi^\mu,\phi\right)\,, \tag{4.4.14}$$

where $|\boldsymbol{\chi}-\mathbf{x}|^2=\sum_{i=1}^d\left(\chi^i-x^i\right)^2$. Furthermore, it is assumed that the parameter δ is complex; $\mathbb{C}\ni\delta=\delta_r+i\delta_i$, but with a positive real part $\delta_r>0$. As we will see below, considering a complex width for the rods peaking function, enables us at the perturbative level to obtain equations that are dependent on a derivative kernel endowed with an emergent Lorentzian signature.

4.4.2 Dynamics of relational GFT

The first step in deriving the dynamics of the theory (after having implemented the relational reference frame), is to impose the same field symmetries of the classical action for

the scalar fields (playing the role of rods and clocks) since it should be preserved at the quantum level as well (assumption QL.4). Hence, the set of symmetries the GFT action should preserve is invariance under Lorentz transformations or Euclidean rotations, shifts, and reflections. This assumption produces a simpler form for the interaction $\mathcal{V}$ and kinetic terms $\mathcal{K}$, which read for the EPRL model

$$\mathcal{K} = \int \mathrm{d}g_I \; \mathrm{d}g'_I \int \mathrm{d}^d\chi \mathrm{d}^d\chi' \mathrm{d}\phi \mathrm{d}\phi' \bar{\varphi}\left(g_I, \chi\right) \mathcal{K}\left(g_I, h_I; \left(\chi - \chi'\right)^2_\lambda, \left(\phi - \phi'\right)^2\right) \varphi\left(h_I, \left(\chi'\right)^\mu, \phi'\right), \tag{4.4.15}$$

$$\mathcal{V} = \int \mathrm{d}^d\chi \mathrm{d}\phi \int \left(\prod_{a=1}^{5} \mathrm{d}g_I^a\right) \mathcal{U}\left(g_I^1, \ldots, g_I^5\right) \prod_{\ell=1}^{5} \varphi\left(g_I^\ell, \chi^\mu, \phi\right), \tag{4.4.16}$$

where $\left(\chi - \chi'\right)^2_\lambda \equiv \mathrm{sgn}(\lambda) M^{(\lambda)}_{\mu\nu} \left(\chi - \chi'\right)^\mu \left(\chi - \chi'\right)^\nu$ and where $\mathcal{K}$ and $\mathcal{V}$ are respectively the kinetic and interaction kernels encoding information about the EPRL-like model and, in particular, about the specific Lorentzian embedding of the theory. Moreover, recall that for the purpose of this thesis, we are in the case where we are neglecting interactions and hence, we work only with the dynamics attained from K.
The extraction of effective mean-field dynamical equations from the full quantum equations of motion has been derived in [77]. By effective mean field dynamics, we mean the imposition of the quantum equations of motion averaged on the states that we consider to be relevant for an effective relational description of the cosmological system (assumption EL.1). In line with what we mentioned so far, these states would be the coherent states $|\sigma_{\epsilon^\mu}; x^\mu, \pi_\mu\rangle$ and the dynamical equations of the GFT field are obtained as follows

$$\left\langle \sigma_{\epsilon^\mu}; x^\mu, \pi_\mu \left| \frac{\delta S_{\mathrm{GFT}}\left[\hat{\varphi}, \hat{\varphi}^\dagger\right]}{\delta \hat{\varphi}^\dagger\left(g_I, x^\mu\right)} \right| \sigma_{\epsilon^\mu}; x^\mu, \pi_\mu \right\rangle = 0\,. \tag{4.4.17}$$

Here, S_{GFT} is the classical GFT action, whose specific form is given in [156]. Notice when assuming that the effective dynamics are only captured by an averaged form of the equations of motion is rather a strong truncation of the microscopic quantum dynamics. This further implies that the quantum fluctuations are in fact neglected, which can affect the treatment of small perturbations[3].

These are the kinematical and dynamical ingredients we are considering in this thesis. Let us mention that the physical predictions thereof will be carried out for the case of small background densities (early time cosmology) as well as large ones (late time cosmology). The prescribed inhomogeneities are implemented at the level of the GFT condensate, as we will shortly present below, where we solve the extracted effective dynamics of the GFT condensate at the level of the background along with the inhomogeneous one.

[3]In fact, the Landau-Ginzburg analysis in the other case of the extended BC model (instead of the EPRL one) restricted to spacelike tetrahedron and various non-local interactions such as the simplicial one suggests that the quantum fluctuations are largely suppressed and that thus the tree-level theory is sufficient to capture large scale continuum physics in GFT [41].

Effective evolution equations. The evolution equation in (4.4.17) of the GFT condensate can be computed as was done in [164] and one can also perform scalar perturbations which we will present shortly. Considering the lowest order in the parameters[4] $|\delta|$ and ϵ contributions in the evolution equation (4.4.17), the effective dynamics for the GFT reduced wave function are encoded in the equation

$$\partial_0^2\tilde{\sigma}_j\left(x,\pi_\phi\right)-i\gamma\partial_0\tilde{\sigma}_j\left(x,\pi_\phi\right)-E_j\left(\pi_\phi\right)\tilde{\sigma}_j\left(x,\pi_\phi\right)+\alpha^2\nabla^2\tilde{\sigma}_j\left(x,\pi_\phi\right)=0\,, \tag{4.4.18}$$

where we have dropped the superscript $^\mu$ for the argument of the reduced wave function $\tilde{\sigma}_j, x\equiv x^\mu$ and where ∂_0^2 and $\nabla^2\equiv\sum_i\partial_i^2$ represent derivatives with respect to rods and clock values, respectively. This evolution equation is represented in the momentum space of the scalar matter field ϕ_0 and after considering both assumptions EL.3 and EL.4. The quantum gravity parameters appearing in the above equation where $z_0\equiv\epsilon\pi_0^2/2$, and $z\equiv\delta\pi_x^2/2$ are functions of the clock and rods momenta, read as

$$\gamma\equiv\frac{\sqrt{2\epsilon}z_0}{\epsilon z_0^2}\,,\qquad r_s^{(\lambda)}\equiv\frac{\tilde{K}_\lambda^{(s)}}{\tilde{K}_\lambda^{(0)}}\,,\qquad E_j^2\equiv\frac{1}{\epsilon z_0^2}-r_{j;2}^{(\lambda)}\left(\pi_\phi\right)\left(1+3\lambda\alpha^2\right)\,, \tag{4.4.19}$$

$$\alpha^2\equiv\frac{1}{3}\frac{\delta z^2}{\epsilon z_0^2}\,,\qquad \alpha_r=\frac{\pi_x^2}{6}\frac{\delta_r^2-\delta_i^2}{\epsilon z_0^2}\,,\qquad \alpha_i=\frac{\pi_x^2}{3}\frac{\delta_r\delta_i}{\epsilon z_0^2}\,, \tag{4.4.20}$$

where α_r and α_i are the real and imaginary part of α^2. The obtained evolution equation (4.4.18) is the fundamental equation determining the form of the reduced condensate wave function $\tilde{\sigma}$, which consequently affects the matter content of the theory. The separation into real and imaginary parts of the evolution equation in (4.4.18) following the steps in [164] and after applying the Madelung representation for $\tilde{\sigma}_j$ yields

$$\ddot{\rho}_j+\alpha_r\nabla^2\rho_j-\left[\left(\theta_j'\right)^2+\eta-\gamma\theta_j'-\alpha_r\left(\boldsymbol{\nabla}\theta_j\right)^2-\alpha_i\nabla^2\theta_j\right]\rho_j-2\nabla\rho_j\cdot\nabla\theta_j=0\,, \tag{4.4.21}$$

$$\theta_j''\rho_j+2\theta_j'\rho_j'-\gamma\rho_j'+\alpha_r\left[2\nabla\rho_j\cdot\nabla\theta_j+\nabla^2\theta_j\rho_j\right]-\beta_j\rho_j+\alpha_i\left[\nabla^2\rho_j-\left(\boldsymbol{\nabla}\theta_j\right)^2\rho_j\right]=0\,, \tag{4.4.22}$$

where we have dropped the arguments of the condensate parameters for notation simplicity. The additional parameters appearing in the above equations read as

$$\eta_j\equiv\frac{1}{\epsilon z_0^2}-r_{j;2}\left(\pi_\phi\right)\left(1+3\lambda\alpha_r\right)\,,\quad \beta_j=3\lambda\alpha_i r_{j;2}\,. \tag{4.4.23}$$

For the perturbation treatment, we consider the perturbative framework with respect to the spatial gradient encoding slightly inhomogeneous relational quantities. This is implemented at the level of the mean field expression for the density and phase factor

$$\rho_j=\rho_0+\delta\rho\,,\quad \theta_j=\theta_0+\delta\theta\,, \tag{4.4.24}$$

[4] $|\delta|$ and ϵ are the expansion parameters that enter the expansion of the dynamical equation of the reduced wave function and they characterize the peaking properties of the condensate (4.4.14).

with $\rho_0 = \rho_0(x^0, \pi_\phi)$ and $\theta_0 = \theta_0(x^0, \pi_\phi)$ being background (zeroth-order) quantities and with ρ and θ being small corrections to them. We dropped the spin index j for notation simplicity. The remainder of this section will revolve around studying the zeroth- and the first-order (in $\delta\rho, \delta\theta$) form of equations (4.4.21) and explicitly solving them.

Zeroth order: background equations. At the zeroth-order, the above set of equation (4.4.21) becomes

$$\ddot{\rho}_0\left(x^0, \pi_\phi\right) - \left[\left(\dot{\theta}_0\left(x^0, \pi_\phi\right)\right)^2 + \eta_j(\pi_\phi) - \gamma\dot{\theta}_0\left(x^0, \pi_\phi\right)\right]\rho_0\left(x^0, \pi_\phi\right) = 0, \tag{4.4.25}$$

$$\ddot{\theta}_0\left(x^0, \pi_\phi\right)\rho_0 + 2\dot{\theta}_0\left(x^0, \pi_\phi\right)\dot{\rho}_0\left(x^0, \pi_\phi\right) - \gamma\dot{\rho}_0\left(x^0, \pi_\phi\right) - \beta\rho_0\left(x^0, \pi_\phi\right) = 0\,. \tag{4.4.26}$$

This can be written as

$$\ddot{\theta}_0\left(x^0, \pi_\phi\right) + \left(\dot{\theta}_0\left(x^0, \pi_\phi\right) - \frac{\gamma}{2}\right)\frac{\partial_0(\rho_0^2)\left(x^0, \pi_\phi\right)}{\rho_0^2\left(x^0, \pi_\phi\right)} - \beta = 0\,, \tag{4.4.27}$$

$$\frac{\ddot{\rho}_0\left(x^0, \pi_\phi\right)}{\rho_0\left(x^0, \pi_\phi\right)} = \left(\dot{\theta}_0\left(x^0, \pi_\phi\right)\right)^2 + \eta_j(\pi_\phi) - \gamma\dot{\theta}_0\left(x^0, \pi_\phi\right)\,. \tag{4.4.28}$$

In fact, the GFT condensate degrees of freedom can be associated with conserved charges due to several symmetry-invariance, as was already studied in [166]. These properties enable us to express the above equations in terms of constants of motion, denoted with Q_j and $\mathcal{E}_j$, and this yields

$$\dot{\theta}_0\left(x^0, \pi_\phi\right) = \frac{\gamma}{2} + \frac{Q_j(\pi_\phi)}{\rho_0^2\left(x^0, \pi_\phi\right)}\,, \tag{4.4.29}$$

$$(\dot{\rho}_0)^2\left(x^0, \pi_\phi\right) = \mathcal{E}_j(\pi_\phi) - \frac{Q_j^2(\pi_\phi)}{\rho_0^2\left(x^0, \pi_\phi\right)} + \mu_j^2(\pi_\phi)\,\rho_0^2\left(x^0, \pi_\phi\right)\,, \tag{4.4.30}$$

where $Q_j = \rho_j^2\dot{\theta}_j$ is the constant of motion resulting from the $U(1)$ symmetry of the GFT condensate, $\mathcal{E}_j$ is usually interpreted as the energy associated with the condensate and finally $\mu_j^2 = \eta_j(\pi_\phi) - \gamma^2/4$ is a parameter carrying rods and matter information contents. When we proceed with solving the dynamical equations for the background condensate, we will rely on the different forms in (4.4.29) and (4.4.27) upon convenience.

First order: perturbation equations. The perturbations equation of first order derived in [164] is given by the set of coupled evolution equations

$$\begin{aligned}&\delta\ddot{\rho}(x, \pi_\phi) + \alpha_r\nabla^2\delta\rho(x, \pi_\phi) - \eta(\pi_\phi)\,\delta\rho(x, \pi_\phi) \\ &- \left[\delta\dot{\theta}(x, \pi_\phi)\left(2\dot{\theta}_0\left(x^0, \pi_\phi\right) - \gamma\right) - \alpha_i\nabla^2\delta\theta(x, \pi_\phi)\right]\rho_0\left(x^0, \pi_\phi\right) = 0\,,\end{aligned} \tag{4.4.31}$$

$$\begin{aligned}&\delta\ddot{\theta}(x, \pi_\phi)\,\rho_0\left(x^0, \pi_\phi\right) + \ddot{\theta}_0\left(x^0, \pi_\phi\right)\delta\rho(x, \pi_\phi) + 2\delta\dot{\theta}(x, \pi_\phi)\,\dot{\rho}_0\left(x^0, \pi_\phi\right) + 2\dot{\theta}_0\left(x^0, \pi_\phi\right)\delta\dot{\rho}(x, \pi_\phi) \\ &- \gamma\dot{\rho} + \alpha_r\left[\nabla^2\theta(x, \pi_\phi)\right]\rho_0 - \beta\rho(x, \pi_\phi) + \alpha_i\nabla^2\rho(x, \pi_\phi) = 0\,.\end{aligned} \tag{4.4.32}$$

In chapter 7 we briefly discuss the regime in which the above set of dynamical equations decouple and how they can affect the perturbed matter content at the background level (section 7.2), as well the perturbed one (section7.3). We will present the explicit solution of the background density and phase satisfying the dynamical equations in (4.4.29) and the perturbed ones obeying those in (4.4.31) and how to use this technology to express the GFT prediction about the early and late time universe as field theory on curved spacetimes, recovering, therefore, the standard notions of physics in the cosmological sector.

Chapter 5

A new spin foam model of quantum geometry based on edge vectors

As we encountered in chapter 3, one of the various background independent approaches to the problem of finding a complete theory of quantum gravity is the formalism of the so-called spin foams [16, 95, 98, 169, 170]. In the broad spectrum of quantum gravity theories [14, 91, 171], SF is considered a successful approach to put in motion the dynamics of the quantum geometry of spacetime. In fact, one of the interesting crossed-roads between the different approaches to QG is when state sum model [172] for gravity was introduced [173, 174] (initially inspired from statistical mechanics [175]) which then converged to SF. In fact, the latter implements, in a precise way, the idea of a sum over geometries, exploiting the duality between simplicial complexes and spin network states [95, 101]. It was demonstrated by Barrett and Crane that, one can think of this model, once applied to the $4d$ simplicial geometries, as a discretization of a constraint BF model as we saw in section 3.1 (introduced by Plebanski [114]), where it was also shown that its partition function can be linked to the gravity one (through the Plebanski action). Of course, this was possible upon the identification of the B field with the bivector specifying the face of the tetrahedron. However, this success comes with a price as we argued when we listed the subtleties with this model in Box 3.1. The first problem that they face is the well-known obstacle of providing a classical limit, where their asymptotics [176] is not dominated by the Regge action. The second misfortune is that they contain an abundant contribution from degenerate geometries [116]. One of the possible way-out to such issues was pointed out by Barrett and Crane and a proposal to surpass them was first formulated by Barrett and Yetter in [115] as well as [176]. One way to address such issues is to make sense of such degenerate contributions. More precisely, this can be traced back to the lack of a quantum operator exploiting the geometrical content of edge vectors in $4d$ since the classical description of such geometries is built from constraining bivectors (the wedge product of two vectors) with an indirect assumption that edge *lengths* exist, except in degenerate configurations. However, the studies of the degenerate configurations led to the conclusion that the geometry of the length is absent and hence is at the core of such degeneracies [176].

It is Yetter and Crane that emphasized in [115] one possibility to remove the degeneracy would be to use decorations on the *edge vectors* of the triangulation instead of the bivectors. Therefore, they proposed a model based on infinite dimensional unitary irreducible representations of the Lorentz group acting on vectors in Minkowski space studied by Dirac [177]. Here, the quantization of Minkowski space is realized as the Hilbert space associated with the translation group. Crane and Yetter proposed to combine these Hilbert spaces to construct the quantization of a bivector, or analogous that of a triangle.

The goal of this chapter is to exploit the proposal of Barrett and Crane and this in turn constitutes our new proposal for the SF which aims at removing such conceptual and technical problems with the main objective to provide a more natural classical limit. In this chapter, we then tackle the main issue

- How can we define a quantum geometry based on the edge length data entering the discretized picture of $4d$ Lorentzian geometry?
- What are the corresponding transition amplitude and its explicit relation to the BC and the GFT framework?

Therefore we can list the following steps to be clarified in this chapter to address the above questions

1. Identify the classical of Lorentzian geometry where the fundamental variable is the edge vector instead of the bivector. This is carried out at the level of the triangle and tetrahedron which are then used to compute the 4-simplex amplitude.
2. Provide a quantization procedure for this formulation in terms of edge vectors using the expansors introduced by Dirac, exploiting them as unitary irreducible representations of $\mathrm{SL}(2,\mathbb{C})$.
3. We then compute the edge-based amplitude and point out the relation of this new SF model to the BC one and GFT formalism.

This chapter is organized as follows. In section 5.1 we start by a mathematical warm-up on the theory of infinite dimensional representation of the Lorentz group that will eventually be associated with the edge vectors as well as the bivectors on the 2-simplex of the new model. Following the motivation highlighted above, we identify the displacement vector on the edge as a function of the translation group on the Minkowski space, and hence we sketch the mathematics behind it. In this case, we relate the Lorentzian harmonic oscillators via their coherent states to the representations of the group of translations. We are then equipped with the necessary tools to identify the quantum description of a classical triangle based on the geometric entity of an edge vector (and its unitary representation),

as we argued below. This will be the main result in section 5.2. We further explore the difference between a quantum triangle whose wave function (and Fourier transform) is based on the *quantum edge vectors* and that whose geometry is captured by the *bivector*. We previously mentioned the construction of Crane and Yetter provided in [115], where they realized the construction of the quantum bivector as it will be described in section 5.2 and then explain that a general four dimensional triangulation can be obtained as the proper merge of the representations. This will be implemented in section 5.3. The gluing is realized by taking the tensor product of bivector Hilbert spaces and identifying the representation labels associated with edges and faces. As we will argue through this part of the thesis, starting from such construction based on edge vectors and the introduction of the translation group representations, one ends up with additional terms stemming from these degrees of freedom in the final amplitude in comparison with the BC amplitude. This will be the main discussion of the results of section 5.4. In section 5.4.3 we provide the GFT counterpart of such amplitudes.

5.1 Relevant representation theory of translation and Lorentz groups

The group theoretic quantization of edge vectors and their combinations to define simplicial geometry is a central point of our construction. The possibility to quantize simplicial geometry in group theoretic terms, thus obtaining a purely algebraic state sum model associated with simplicial lattices is, more generally, the key fact at the core of the spin foam formalism for quantum gravity [16, 98] and of the group field theory formalism as well [145, 149]. This group-theoretic quantization is based, as we will show, on the translation group. The precise relation between the representation theory of the translation group and that of the Lorentz group, on the other hand, is the basis for relating our description of quantum geometry, as well as the amplitudes of the new model, to that of the known spin foam models. The latter, in fact, is based on a description of simplicial geometry in terms of bivectors associated with triangles and a quantization of the same in terms of the representation theory of the Lorentz group. The tools from the representation theory of the translation group and the way they relate to the Lorentz group are interesting in themselves, from a mathematical point of view. Therefore, we illustrate them in some detail in this section, before proceeding to the construction of the new spin foam model. Specifically, the relevant representations are the unitary infinite dimensional representations of both groups. We start from those of the Lorentz group [105, 177, 178], the mathematical basis of known spin foam models for Lorentzian $4d$ gravity. We first present the representations of the principal series [114, 144] derived for the $\mathrm{SL}(2,\mathbb{C})$ group (which is the covering group of the Lorentz group) then we recall how Dirac initially introduced the infinite dimensional representations for a non-compact group. Dirac's construction in terms of expansors [177, 179] is then presented; it is particularly relevant to our discussion since it leads to the infinite dimensional representations of the translation group. The underlying relation between the

representations in the principle series for the Lorentz group and those of the translation group becomes evident once we exploit properties of the harmonic oscillator basis, which we deal with in detail in the last part of this section. We remark that one can work in the spinor basis as well, in order to realize the irreducible representations of the Lorentz group, as studied in [179].

5.1.1 Infinite dimensional unitary representations of the Lorentz group

A short summary of the realization of the infinite dimensional unitary representations of the Lorentz group and its algebra in the space of homogeneous functions as well the Plancharel decomposition of the various classes of such representations are listed in the Appendix A.1. In the following we present the alternative representation of the Lorentz group in terms of expansors, first introduced by Dirac in [177,179] that we will rely on in to describe a *quantum edge vector*. Finite dimensional representations of the $\mathrm{SL}(2,\mathbb{C})$ group, i.e. tensor and spinor representations, are the ones mostly used in theoretical physics, and specifically in particle physics. However, these are not unitary and the problem of identifying finite unitary representations remains unsolved [141,178]. On the other hand, the case of the infinite dimensional representations of the Lorentz group has been extensively studied in [105,144,179], and unitary irreducible representations were first derived in [177].

Expansors. Let us now introduce an alternative realization of the representations of the Lorentz group. Historically, these were introduced by Dirac in [177] and further studied in [179] in terms of so-called *expansors*. They are tensors-like objects in a manifold with an infinite enumerable number of components. They also possess an invariant positive definite quadratic form for their squared length. Such representations are realized on the space of homogeneous polynomials on Minkowski space $\mathbb{M}^4$. The notions introduced in what follows will help to establish the relation between the representations of the Lorentz group and that of the translation group (geometrically, between the quantum bivectors and the quantum edge vectors). We focus on homogeneous polynomials (of degree n) of the real vector ξ_μ built from monomials $\xi_x^i \xi_y^j \xi_x^k \xi_t^{-1-h}$, with $i,j,k,h \in \mathbb{N}$. Notice that, due to the negative power of the time coordinate ξ_t, the combination of such monomials is infinite dimensional. The homogeneous polynomial can be written in the form of a power series as

$$P(\xi_\mu) = \sum_{ijkh} A_{i\,j\,k\,h}\, \xi_x^i \xi_y^j \xi_z^k \xi_t^{-1-h}\,, \tag{5.1.1}$$

where the coefficient A is called *expansor*. These coefficients are regarded as the coordinates of vectors in an infinite dimensional space. On this space of homogeneous functions, one can define the unitary representations of the Lorentz group, with unitarity condition enforced

by the scalar product:

$$P_1 \cdot P_2 = \sum_{ijkh} A_{i\,j\,k\,h} B_{i\,j\,k\,h}\,, \tag{5.1.2}$$

that also provides a notion of norm given by the square length of the polynomial $|P|^2 = \sum_{ijkh} A^2_{i\,j\,k\,h}$. In order to derive the representation of the Lorentz group on such expansors, one first considers the infinitesimal Lorentz transformations on the basis coordinates ξ. Demanding that the square length $\xi_0^2 - \xi_1^2 - \xi_2^2 - \xi_3^2$ remains invariant under these transformations, one obtains the corresponding transformation for the expansors. It is precisely these induced linear transformations on the expansors that identifies them as the unitary representation of the Lorentz group. We present now their relation to the representation of the translation group.

5.1.2 The Harmonic oscillator representation of the translation group

Dirac emphasized that the expansors can be interpreted as a tensor product of four harmonic oscillators. This is crucial in the case of integral n-values, where one can make a variable transformation that is familiar in quantum mechanics, relating the expansors in (5.1.1) with harmonic functions [177]. This can be seen explicitly considering the transformation map:

$$\begin{aligned} x_a &= \frac{1}{\sqrt{2}}\Big(\xi_a + \frac{\partial}{\partial \xi_a}\Big)\,, \qquad \frac{\partial}{\partial x_a} = \frac{1}{\sqrt{2}}\Big(\frac{\partial}{\partial \xi_a} - \xi_a\Big)\,, \\ x_t &= \frac{1}{\sqrt{2}}\Big(\xi_t - \frac{\partial}{\partial \xi_t}\Big)\,, \qquad \frac{\partial}{\partial x_t} = \frac{1}{\sqrt{2}}\Big(\frac{\partial}{\partial \xi_t} + \xi_t\Big)\,, \end{aligned} \tag{5.1.3}$$

for $a = x, y, z$. It is important to stress that this map underlines the correct commutation relations between all the above-introduced operators. In the new $x-$variables, the homogeneous polynomial on Minkowski space (5.1.1) can be represented as a combination of polynomials in (5.1.3) which are basically a general composition of four Hermite functions:

$$P(x_\mu) = \sum_{ijkh} A_{i\,j\,k\,h}\, \Psi_{i\,j\,k\,h}(x_\mu)\,, \tag{5.1.4}$$

where the expansors are the coefficient of such combination (expansion):

$$\begin{aligned} \Psi_{ijkh}(t,x,y,z) &= \frac{1}{\pi n! \sqrt{2^{i+j+k+h}}} \Big(x_i - \partial_{x_i}\Big)^i \Big(x_j - \partial_{x_j}\Big)^j \Big(x_k - \partial_{x_k}\Big)^k \Big(x_h - \partial_{x_h}\Big)^h e^{-\frac{1}{2}(x_t^2 + x_a x^a)} \\ &= \psi_h(t)\,\psi_i(x)\,\psi_j(y)\,\psi_k(z)\,. \end{aligned} \tag{5.1.5}$$

In these terms, the scalar product (5.1.2) simplifies thanks to the orthogonality of the Hermite functions and it takes the integral form:

$$P_1 \cdot P_2 = \int \mathrm{d}x^4\, \psi_{h_1}(t)\,\psi_{i_1}(x)\,\psi_{j_1}(y)\,\psi_{k_1}(z)\;\psi_{h_2}(t)\,\psi_{i_2}(x)\,\psi_{j_2}(y)\,\psi_{k_2}(z) \tag{5.1.6}$$

$$= \frac{i_1! j_1! k_1!}{h_1!}\,\delta_{i_1 i_2}\,\delta_{j_1 j_2}\,\delta_{k_1 k_2}\,\delta_{h_1 h_2}\,. \tag{5.1.7}$$

The alternative representation of the ξ variables that Dirac introduced is related to the theory of the four dimensional harmonic oscillator. Indeed, the four x-parameters can be treated as the coordinates of a four-dimensional harmonic oscillator, whereas the respective four operators ∂_{x_μ} are the conjugate momenta p_{x_μ}. To illustrate further the duality between the expansors and the harmonic oscillator, a state of the oscillator with components $0, 1, 2, 3$ occupying the ith, jth, kth, hth quantum states respectively, is represented by Ψ_{ijkh} given in (5.1.5). Following the map (5.1.3) one can get back the ξ-representation and the function $\Psi_{i\,j\,k\,h}(x_\mu)$ goes over to $\xi^i_x \xi^j_y \xi^k_z \xi^{-1-h}_t$. In this sense, the state of the oscillator with components sitting in a quantum state (5.1.4) is naturally identified with an expansor with one non-vanishing component, whereas a stationary state corresponds to a homogeneous expansor. Note that the degree of the expansor corresponds to the the energy of the state of the harmonic oscillator, not including the zero-point energy.
Recalling the expressions of the ladder operators (the annihilation and creation operators) associated with a four dimensional harmonic oscillator, we recognize that they can be written as the inverse relation of (5.1.3):

$$\begin{aligned} a_i^\dagger = \xi_i = \frac{1}{\sqrt{2}}(x_i - \partial_i)\,, \qquad a_0^\dagger = -\partial_{\xi_t} = \frac{1}{\sqrt{2}}(t - \partial_t)\,, \\ a_i = \partial_{\xi_i} = \frac{1}{\sqrt{2}}(x_i + \partial_i)\,, \qquad a_0 = \xi_t = \frac{1}{\sqrt{2}}(t + \partial_t)\,, \end{aligned} \tag{5.1.8}$$

where $i = 1, 2, 3$ are the space-like indices and the 0 index stands for the time like one. Notice how the Lorentzian signature is reflected in the relation between the creation and annihilation operators and the coordinates on Minkowski space. For completeness, the ladder operators always satisfy the canonical commutators

$$[a_\mu\,,\, a_\nu^\dagger] = \delta_{\mu\nu}\,, \tag{5.1.9}$$

where the space-like creation operators $a_i^\dagger$ are represented by the space coordinates of Minkowski space ξ_i, but the time-like creation operator $a_0^\dagger$ is represented by its momentum (up to a sign), and vice-versa for the annihilation operators. Following this line of reasoning, the momenta p_μ can be perceived as the generators of the *group of translations* on Minkowski space. A basis of infinite dimensional representations for the translation group is thus given by eigenvectors of the harmonic oscillator ladder operators. In QM it is well known that such a set of eigenvectors is those that mostly resemble the classical behavior of the oscillator, i.e. *coherent states* [180]. In particular, there exists a coherent ket for the annihilation operator and a coherent bra for the creation operator, given by:

$$a\,|\,\alpha\rangle = \alpha\,|\,\alpha\rangle\ , \quad \langle\alpha\,|\,a^\dagger = \langle\alpha\,|\,\alpha^*\,, \qquad \text{with} \quad \alpha \in \mathbb{C}\,. \tag{5.1.10}$$

The action of the creation operator on the coherent ket or that of the annihilation operator on the coherent bra can be derived by expanding the coherent state as a combination of the eigenstates of the harmonic oscillator, captured by the expression:

$$|\,\alpha\rangle = e^{-\frac{1}{2}|\alpha|^2} \sum_{n=0}^{\infty} \frac{\alpha^n}{\sqrt{n!}}\,|\,n\rangle\,. \tag{5.1.11}$$

As we previously emphasized, we are interested in describing bivectors in terms of four dimensional edge vectors and their representations. Such edge vectors are elements of $\mathbb{M}^4$ and thus upon quantization can be regarded as a tensor product of coherent states $|\,\alpha_\mu\rangle = |\,\alpha_t, \alpha_x, \alpha_y, \alpha_x\rangle$. This is in return an eigenvector simultaneously of the three dimensional translation group, with generators $p_i = -i\partial_{\xi_i} = -ia_i$, *and* for the time-like position operator $\xi_t = a_0$. We refer to [180] for more details on the coherent states of the harmonic oscillator. The key point for our later construction is that they provide an eigenbasis for the translation group on Minkowski space, whose generators are identified as ladder operators of the harmonic oscillator (5.1.8). However, such representations are not unitary, as the coherent states are not orthogonal

$$\langle\alpha\,|\,\beta\rangle = e^{-\frac{1}{2}(|\alpha|^2+|\beta|^2-2\alpha^*\beta)}\,. \tag{5.1.12}$$

On the other hand, since generic states of the harmonic oscillator can be decomposed as a combination of coherent states, they form an overcomplete basis and satisfy the closure relation (resolution of the identity):

$$\int \mathrm{d}\alpha\,|\,\alpha\rangle\langle\alpha\,| = \pi\,. \tag{5.1.13}$$

The homogeneous polynomials in (5.1.1) or (5.1.4) are thus functions on Minkowski space or equivalently functions on the translation group. In practice, we consider a vector $e = (\lambda_t, \lambda_x, \lambda_y, \lambda_z)$ in Minkowski space parametrized by the coordinates $\lambda_\nu \in \mathbb{M}^4$. The Hilbert space associated with such a vector is the space of square integrable functions on four copies of $\mathbb{R}$, $L^2[e] := L^2[\lambda]$. In this picture, the coordinates $\lambda_\nu \in F(\mathbb{R}^4)$ are identified with the generators of the functions on Minkowski space, i.e. of the Hilbert space $L^2[\lambda]$. We thus refer to the *vector wave function* (or alternatively to the quantization of the vector e), as the general function:

$$f(\lambda_\nu)\ \in L^2[\lambda] \cong F(\mathbb{M}^4)\,. \tag{5.1.14}$$

A basis for the four dimensional harmonic oscillator is realized as a tensor product of independent oscillators. Therefore, we define the four dimensional ladder operators as a linear combination of creation and annihilation operators such that

$$\begin{aligned} a^\dagger(\lambda) &= a_0\lambda_t + a_1^\dagger\lambda_x + a_2^\dagger\lambda_y + a_3^\dagger\lambda_z\,,\\ a(\lambda) &= a_0^\dagger\lambda_t + a_1\lambda_x + a_2\lambda_y + a_3\lambda_z\,. \end{aligned} \tag{5.1.15}$$

The first operator appearing in the above equations is the operator associated with the position on Minkowski space identified by the vector e, which will be assigned the coherent bra $\langle\alpha_\nu\,|$ as eigenvector, with eigenvalue α_ν^*; the second one is the operator associated to the momentum (or equivalently to translations) on Minkowski space identified by the vector e, that has the coherent ket $|\,\alpha_\nu\rangle$ as eigenvector, with corresponding eigenvalue α_ν.
The wave function (5.1.14) of the quantum vector can thus be expanded in Fourier modes of the translation group ('momentum space') or likewise in the harmonic decomposition of

the position group ('configuration space'):

$$\begin{aligned} \textit{Translation:} \quad f(\lambda) &:= \int \mathrm{d}\alpha' \mathrm{d}\alpha \, \langle \alpha_\nu \, | a(\lambda) | \, \alpha'_\nu \rangle \, f_{\alpha_\nu, \alpha'_\nu} \,, \\ \textit{Position:} \quad f'(\lambda) &:= \int \mathrm{d}\alpha \mathrm{d}\alpha' \, \langle \alpha_\nu \, | a^\dagger(\lambda) | \, \alpha'_\nu \rangle \, f'_{\alpha_\nu, \alpha'_\nu} \,, \end{aligned} \tag{5.1.16}$$

where the terms $\langle \alpha_\nu \, | a(\lambda) | \, \alpha'_\nu \rangle$ and $\langle \alpha_\nu \, | a^\dagger(\lambda) | \, \alpha'_\nu \rangle$ are matrix elements that play the role of plane waves in the operation relating the Fourier transform of functions belonging to the Hilbert space $L^2[\lambda]$ to the spaces of Fourier modes on the translation (or position) group. Furthermore, note that the two decompositions are related to each other since the two plane waves $\langle \alpha_\nu \, | a(\lambda) | \, \alpha'_\nu \rangle$ and $\langle \alpha_\nu \, | a^\dagger(\lambda) | \, \alpha'_\nu \rangle$ are the complex conjugate of each other[1]. This is, in the end, a reformulation of standard Fourier analysis on Minkowski space in group-theoretic terms that will turn out to be useful in the following.
As we will exploit in section 5.2.2, an explicit realization of the plane waves $\langle \alpha_\nu \, | a(\lambda) | \, \alpha'_\nu \rangle$ and $\langle \alpha_\nu \, | a^\dagger(\lambda) | \, \alpha'_\nu \rangle$ can be provided in terms of solutions of the harmonic oscillator.

The four dimensional Lorentzian harmonic oscillator As was shown in [180–182], an infinite dimensional realization for the balanced representations $R_{0\,\mu}$ of the Lorentz group can be obtained as the space of solutions of the Laplace equation. Again, this is accomplished by taking the Laplacian to be the Casimir C_1 of the Lorentz algebra, with eigenvalue $-(1+\mu^2)$. This relation is particularly interesting for us, because it provides the quantization of a simple bivector, as we encountered in the BC model and EPRL one (section 3.2), and its underlying connection to the quantum vector.
By a simple change of variables (see Appendix A.2), the remaining Casimir C_1 in (A.1.6) for balanced representations can be expressed in terms of hyperbolic parameters as:

$$C_1 = J^2 - N^2 = \frac{1}{\sinh^2\eta}\partial_\eta(\sinh^2\eta\,\partial_\eta) + \frac{1}{\sinh^2\eta}\left(\frac{1}{\sin\theta}\partial_\theta(\sin\theta\,\partial_\theta) + \frac{1}{\sin^2\theta}\partial_\varphi^2\right), \tag{5.1.17}$$

which is the Laplacian on the hyperboloid Q_1 introduced in section 5.1.1 for the Plancherel decomposition of the Lorentz representations. In section 5.1.2 we explained that the ladder operators of the harmonic oscillator can be used as generators of the translation (and position) group. Therefore, we can use the coordinates on Minkowski space ξ_μ and their momenta, recast as the ladder operators of the harmonic oscillator coordinates (5.1.8), to realize the Lorentz generators (rotations and boosts)

$$J_a := -i\varepsilon_{abc}\,\xi_b\partial_{\xi_c} = -i\varepsilon_{abc}\,a_b^\dagger a_c \,, \quad N_a := -i(\xi_t\partial_{\xi_a} + \xi_a\partial_{\xi_t}) = -i(a_0 a_a - a_0^\dagger a_a^\dagger)\,. \tag{5.1.18}$$

One can check that the above operators satisfy the usual $\mathfrak{so}(1,3)$ commutation relations

$$[J_a\,,\,J_b] = i\varepsilon_{abc}\,J_c \,, \quad [J_a\,,\,N_b] = i\varepsilon_{abc}\,N_c \,, \quad [N_a\,,\,N_b] = -i\varepsilon_{abc}\,J_c\,. \tag{5.1.19}$$

[1] By making further assumptions on the wave functions, one can derive the relation between the Fourier modes $f_{\alpha_\nu,\alpha'_\nu}$, $f'_{\alpha_\nu,\alpha'_\nu}$. For instance, requiring the wave function to be real, $\bar{f}(\lambda) = f(\lambda)$, one would obtain the condition $\bar{f}_{\alpha_\nu,\alpha'_\nu} = f'_{\alpha_\nu,\alpha'_\nu}$.

Since we would like, in the following, to express the balanced representations of the Lorentz group in terms of representations of the translation group (and vice-versa), we would like to derive the eigenstates of (5.1.17) (representations of the Lorentz group) as a combination of the eigenstates of the harmonic oscillator (representations of the translation group). In particular, we show in this subsection that the eigenfunctions of (5.1.17) are the non-radial contribution of the eigenfunctions of the four dimensional harmonic oscillator.

To proceed, we recall that the target space used by Dirac [177] (the space of homogeneous polynomials) to construct the infinite dimensional representations of the Lorentz group, can be re-expressed as the Hilbert space of four dimensional Lorentzian harmonic oscillators. Here the polynomials (5.1.1) take the form (5.1.4). Therefore, the set of homogeneous polynomials on Minkowski space can be derived as the general solution of the Schrödinger equation

$$\mathcal{H}\,\Psi = E\,\Psi\,, \tag{5.1.20}$$

where the Hamiltonian operator

$$\mathcal{H} = -\frac{1}{2}\Delta + \frac{1}{2}(t^2 - x^2 - y^2 - z^2)\,, \tag{5.1.21}$$

is the Hamiltonian of the four dimensional Lorentzian harmonic oscillator and Δ is the four dimensional flat D'Alambertian operator $\Delta = \partial_t^2 - \partial_x^2 - \partial_y^2 - \partial_z^2$. In the appendix A.2 we show how to solve such Schrödinger equation in different coordinate basis, inspired by [180], and derive the eigenbasis in terms of the variables of the *hyperbolic basis*:

$$\Psi_{n_r,\mu,\ell,m}(r,\eta,\theta,\phi) = (-1)^{n_r}\sqrt{\frac{n_r!}{\Gamma(n_r+\mu+1/2)}}r^{\mu-1}e^{-\frac{1}{2}r^2}L_{n_r}^{(i\mu)}(r^2)\frac{1}{\sinh\eta}Q_\ell^{i\mu}(\coth\eta)Y_\ell^m(\theta,\phi), \tag{5.1.22}$$

associated to the energy $E = 2n_r + i\mu + 1$, where $L_n^{(\alpha)}$ are the Laguerre polynomials, Q_λ^α are the Legendre functions of the second kind and Y_m^ℓ are the spherical harmonics. In the appendix A.2, we also show how this wave function is related to the homogeneous polynomials proposed by Dirac, expressed in terms of the harmonic functions:

$$\Psi_{n_r,\mu,\ell,m}(r,\eta,\theta,\phi) = \sum_{n_t,n_x,n_y,n_z} \mathcal{C}_{n_r,\,\mu,\,\ell,\,m}^{n_t,\,n_x,\,n_y,\,n_z}\,\Psi_{n_t,n_x,n_y,n_z}(t,x,y,z)\,, \tag{5.1.23}$$

where the coefficients are given by

$$\begin{aligned}\mathcal{C}_{n_r,\,\mu,\,\ell,\,m}^{n_t,\,n_x,\,n_y,\,n_z} &= \langle n_t,n_x,n_y,n_z|n_r,\mu;\ell,m\rangle \\ &= \sum_{n_R,n_\rho}\frac{i^{m+|m|}(-1)^{\tilde{n}_x+n_\xi}(\sigma_m i)^{n_y}}{2^{(1-\delta_{m,0})/2}}\,e^{i\varphi}\;\mathcal{C}_{n_\rho,\tilde{n}_z,n_R}^{\frac{1+|m|}{2},\frac{1}{4}+\frac{q_z}{2},\frac{\ell}{2}+\frac{3}{4}}\,\mathcal{C}_{\tilde{n}_x,\tilde{n}_y,n_\rho}^{\frac{1}{4}+\frac{q_x}{2},\frac{1}{4}+\frac{q_y}{2},\frac{1+|m|}{2}} \qquad (5.1.24)\\ &\times\,\mathcal{C}_{\tilde{n}_t+\bar{n}_t/2,\,n_R,\,n_r}^{1/4+q_t/2,\,\ell/2+3/4,\,(1+i\mu)/2}\,, \qquad (5.1.25)\end{aligned}$$

which are a combination of the $\mathfrak{su}(1,1)$ Clebsh-Gordan coefficients (A.2.14). As we had anticipated, the non-radial part of the solution, yielding the equation (A.2.5), reads

$$\Psi_{\mu,\ell,m}(\eta,\theta,\phi) = \frac{1}{\sinh\eta}\,Q_\ell^{i\mu}(\coth\eta)\,Y_\ell^m(\theta,\phi)\,, \tag{5.1.26}$$

and it is the solution to the Laplace equation with Laplacian (5.1.17) and eigenvalue $-(1+\mu^2)$. Therefore, it is the infinite dimensional representation of the Lorentz group associated with a time-like bivector (normal to a spacelike triangle). These solutions can indeed be used to construct the (time-like) balanced D-matrices (A.1.3):

$$D^{0,\mu}_{\ell,m;\ell',m'}(g) = \langle 0,\mu;\ell,m\,|U(g)|\,0,\mu;\ell',m'\rangle \tag{5.1.27}$$

$$= \int \mathrm{d}r\mathrm{d}\eta\mathrm{d}\Omega r^3 \sin^2(\eta)\,\overline{\Psi}_{\mu,\ell,m}(\eta,\theta,\phi)\Psi_{\mu,\ell',m'}(\eta',\theta',\phi')\,, \tag{5.1.28}$$

where the primed coordinates $\{\eta',\theta',\phi'\}$ encode the action of the Lorentz transformation g.

We further note that, the wave function $\Psi_{n_t,n_x,n_y,n_z}(t,x,y,z)$ is an infinite dimensional realization of the harmonic oscillator eigenstate $|\,n_t,n_x,n_y,n_z\rangle$. We recall that the coherent states of the harmonic oscillator, which are a linear combination of the eigenstates $|\,n_t,n_x,n_y,n_z\rangle$, were identified as the eigenbasis of the translation group (5.1.10). We can thus extend the relation (5.1.11) to the wave functions

$$\Psi_{\alpha_t,\alpha_x,\alpha_y,\alpha_z}(t,x,y,z) = e^{-\frac{1}{2}\sum_\nu|\alpha_\nu|^2}\sum_{\{n_\nu\}}\frac{\alpha_t^{n_t}\alpha_x^{n_x}\alpha_y^{n_y}\alpha_z^{n_z}}{\sqrt{n_t!n_x!n_y!n_z!}}\,\Psi_{n_t,n_x,n_y,n_z}(t,x,y,z)\,, \tag{5.1.29}$$

which, together with (5.1.23), provides the relation between the wave functions associated with the infinite dimensional representations of the Lorentz group and the wave functions associated with the infinite dimensional representations of the translation group, given by

$$\Psi_{n_r,\mu,\ell,m}(r,\eta,\theta,\phi) = \sum_{n_t,n_x,n_y,n_z}\int \mathrm{d}^4\alpha_\nu\, e^{-\frac{1}{2}\sum_\nu|\alpha_\nu|^2}\mathcal{C}^{n_t,n_x,n_y,n_z}_{n_r,\mu,\ell,m}$$

$$\times\,\frac{\alpha_t^{*\,n_t}\alpha_x^{*\,n_x}\alpha_y^{*\,n_y}\alpha_z^{*\,n_z}}{\pi^4\sqrt{n_t!n_x!n_y!n_z!}}\Psi_{\alpha_t,\alpha_x,\alpha_y,\alpha_z}(t,x,y,z)\,. \tag{5.1.30}$$

These relations will be crucial for relating the new spin foam model based on edge vectors, quantized in terms of representations of the translation group, and the Barrett-Crane spin foam model in section 3.2.1 based on a description of simplicial geometry in terms of bivectors, quantized in terms of representations of the Lorentz group.

5.2 Quantum triangle

We now start our new spin foam construction for quantum simplicial geometry with the analysis of a single triangle embedded in Minkowski space, first at the classical, then at the quantum level. We recall how to combine geometric edge vector data on a triangle and their classical constraints as in the spirit of section 3.1.2 and section 3.2.1. We then build the corresponding quantum version of the constraints, using the group-theoretic tools of section 5.1 that define a quantum edge vector. Since both edge vectors and bivectors can be used to describe a geometric triangle, we illustrate the construction based on both of them and point out the differences between the two at the quantum level.

5.2.1 Classical triangle

Classical triangle. The geometry of a classical triangle in Minkowski space is completely determined by using only two among its constituent three edge vectors $e_1, e_2, e_3 \in \mathbb{M}^4$, as illustrated in figure 5.1, with the latter set satisfying the *closure condition*, namely the relation: $e_1 + e_2 + e_3 = 0$. Working with the larger, constrained set of variables ensures that the description is not affected by any specific choice of a pair of edge vectors. To spell out, for later use, these obvious facts, consider three edge vectors in Minkowski space given by:

$$e_1 = (\zeta_t, \zeta_x, \zeta_y, \zeta_z) \ , \quad e_2 = (\lambda_t, \lambda_x, \lambda_y, \lambda_z) \ , \quad e_3 = (\omega_t, \omega_x, \omega_y, \omega_z) \, , \tag{5.2.1}$$

parametrized by the coordinates $\zeta_\mu, \lambda_\mu, \omega_\mu \in F(\mathbb{M}^4)$. All the geometric properties of the corresponding triangle are determined by any pair of these edge vectors, plus the closure condition:

$$e_1 + e_2 + e_3 = 0 \quad \Rightarrow \quad \zeta_\mu + \lambda_\mu + \omega_\mu \, . \tag{5.2.2}$$

Classical bivector. A classical bivector, associated with the same triangle in Minkowski space, is obtained by taking the wedge product of two edge vectors. A bivector contains less information than the one required to specify the geometry of the associated triangle. In fact, if we consider again three edge vectors $e_1, e_2, e_3 \in \mathbb{M}^4$, the bivector geometry is determined by the two conditions:

1. *closure relation*: every edge vector of the three vectors of the triangle is given by the sum of the other two $e_1 + e_2 = e_3$;
2. *skew-symmetry*: the normal to the plane spanned by the constrained three vectors, in which the triangle lies, is given by the restriction to the wedge (or external) product of any two edge vectors (up to a change of orientation).

The first condition alone would reduce the information contained in the three (edge) vectors to that characterizing a classical triangle, while the second restricts it further (again, in a way that remains independent of any specific choice of two edge vectors). Given the three edge vectors (5.2.1), the bivector represented in Fig.(5.1) is thus constructed as:

$$b := e_1 \wedge e_2 = e_1 \wedge e_3 = e_3 \wedge e_2 \, . \tag{5.2.3}$$

We can now present the quantization prescription to the above-described classical geometric entities.

5.2.2 Quantization

We now proceed to the quantization of a triangle and a bivector, following the suggestions in [115], and relying on the relations we obtained in section 5.1.2. Recall that, we identified

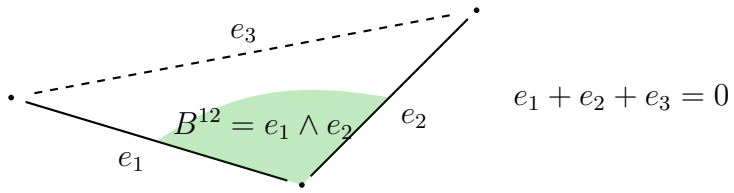

Figure 5.1: Triangle with edge vectors $e_1, e_2, e_3 \in \mathbb{M}^4$ and closure relation (5.2.2). In blue is the bivector part.

in (5.1.14) the quantum states of an edge vector in Minkowski space with the (square integrable) functions of the translation group. This was then realized as the Hilbert space of the four dimensional harmonic oscillator. Now, let us consider a triangle t with edge vectors that satisfy the closure condition (5.2.2). The space of states associated with the quantum triangle is therefore the tensor product of the Hilbert spaces associated with any two of its edge vectors, for instance; $e_1, e_2 \subset t$:

$$L^2[e_1, e_2] := L^2[e_1] \otimes L^2[e_2]\,, \quad e_1 + e_2 + e_3 = 0\,. \tag{5.2.4}$$

subject to the closure condition. To ensure proper geometric interpretation, our construction should not be affected by the choice of the pair of vectors e_1, e_2. To ensure this, we introduce the operator that maps the quantum space of a triangle in terms of the edge vectors e_1, e_2 into the quantum space of the exact same triangle in terms of the edge vectors e_1, e_3. Let such *switching operator* be defined as the map:

$$\sigma : L^2[e_1, e_2] \to L^2[e_1, e_3]\,. \tag{5.2.5}$$

Thus, the proper quantum space of a triangle is thus the space $L^2[e_1, e_2]$ equipped with the closure condition and invariant under the action of the switching operator σ. This makes certain that we properly encode the full geometric data of the triangle in our states.

The quantum bivector. As we have seen, one can restrict the classical configuration space of a triangle to its anti-symmetric part, to obtain the geometry of the associated bivector. At the quantum level, this procedure is realized by taking the skew-symmetric part of the tensor product (5.2.4), which is invariant under the σ operator. This subspace, denoted by $T^A[e_1, e_2]$, is therefore naturally identified as the Hilbert space of a bivector. Moreover, as discussed in section 5.1, by constructing bivectors (at both classical and quantum levels) directly from wedging edge vectors, we restrict our attention only to the simple bivectors[2]. At the quantum level, this can be equivalently translated into associating

[2]Geometrically, this simplicity condition on the bivectors ensures that the two edge vectors and the normal vector are not planar, and, purely as a condition on bivectors:

$$\langle b\,, *b\rangle = 0\,. \tag{5.2.6}$$

These are indeed the well-known simplicity constraints on which the usual spin foam construction in terms of bivectors is based.

the bivectors with duals of Lie algebra elements $b = *L \in \mathfrak{so}(3,1)^*$ and quantizing them by replacing the (dual) Lie algebra with a sum over their representation category. The simplicity constraint amounts to restricting to the balanced representations $R_{0\rho}$ or R_{j0} of the principle series, whose Plancherel decomposition is given in the set of equations (A.1.4); the choice of one or the other of the two classes of balanced representations corresponds to considering spacelike or timelike triangles, respectively (see [114, 125]). We can then establish that, once we associate an element of the dual Lorentz Lie algebra $\mathfrak{so}^*(1,3)$ to each wedge product of a pair of translations on Minkowski space $\mathbb{M}^4 \wedge \mathbb{M}^4$, we identify an isomorphism between the Hilbert space of a wedged vectors (bivector) with the space of functions on such Lie algebra. This isomorphism reads:

$$T^A[e_1, e_2] := L^2[e_1] \wedge L^2[e_2] \cong F(\mathfrak{so}^*(1,3)) \,. \tag{5.2.7}$$

Using this Hilbert space of a quantum bivector, we can construct explicitly the operator corresponding to it, along the lines suggested in [115], and provide different representations for the same Hilbert space. This is relevant in what follows since we are interested in deriving the Fourier expansion of the wave functions associated with the quantum bivector. Let us recall that in section 5.1.2 we identified the set of representations of the translation group on Minkowski space as the space of solutions of the 4-d Lorentzian harmonic oscillator. In this case, the position and momentum operators in the Minkowski coordinates ξ_μ are interpreted as generators of translations and the respective momenta. Once expressed in the harmonic oscillator basis via the map (5.1.15), such generators are the familiar creation and annihilation operators. In this formulation, (5.1.8), expressed as a combination of the ladder operators, provides an explicit infinite dimensional realization of the isomorphism $\mathbb{M}^4 \wedge \mathbb{M}^4 \cong \mathfrak{so}^*(1,3)$. The elements of the dual Lorentz algebra (bivectors) are then given by the wedge product of creation and annihilation operators (translations). One can extend such a scheme to a general simple bivector. To this end, consider a pair of edge vectors:

$$e_1 = (\zeta_t, \zeta_1, \zeta_2, \zeta_3) \;, \quad e_2 = (\lambda_t, \lambda_1, \lambda_2, \lambda_3) \,. \tag{5.2.8}$$

One can associate to such edges the position and momentum (or translation) operators; these are realized as functional operators on the Hilbert space $L^2[\zeta] \,, L^2[\lambda]$ of the edge vectors. Similarly to (5.1.15) when represented in the harmonic basis, elements living on these Hilbert spaces are expressed as a combination of the creation and annihilation operators of the harmonic oscillator:

$$\begin{aligned} a_1^\dagger &:= a_t\zeta_t + a_x^\dagger\zeta_x + a_y^\dagger\zeta_y + a_z^\dagger\zeta_z \,, \qquad a_2^\dagger := a_t\lambda_t + a_x^\dagger\lambda_x + a_y^\dagger\lambda_y + a_z^\dagger\lambda_z \,, \\ a_1 &:= a_t^\dagger\zeta_t + a_x\zeta_x + a_y\zeta_y + a_z\zeta_z \,, \qquad a_2 := a_t^\dagger\lambda_t + a_x\lambda_x + a_y\lambda_y + a_z\lambda_z \,. \end{aligned} \tag{5.2.9}$$

According to the map (5.1.8), the annihilation operators a are then associated with the generators of translations on Minkowski space, while the creation operators $a^\dagger$ can be seen as the quantization of their dual momenta (position operators ξ on Minkowski space). In a similar manner, the wedge product of the two edge vectors $e_1 \wedge e_2$ can be assigned an operator that acts on the Hilbert space $L^2[\zeta, \lambda]$

$$b_{e_1 \wedge e_2} := -i a_1^\dagger \wedge a_2 = -i(a_1^\dagger a_2 - a_2^\dagger a_1) \,. \tag{5.2.10}$$

The operator $b_{e_1\wedge e_2}$ is understood as the quantization of the simple bivector $e_1 \wedge e_2$. Note that for $\zeta_\mu = \delta_{\mu,0}$ and $\lambda_\mu = \delta_{\mu,i}$ we have $b_{e_1\wedge e_2} = N_i$, while for $\zeta_\mu = \delta_{\mu,i}$ and $\lambda_\mu = \delta_{\mu,j}$ we instead obtain $b_{e_1\wedge e_2} = \varepsilon_{ijk} L_k$. Moreover, we can alternatively express the bivector operator (5.2.10) in the $\mathfrak{so}(1,3)$ basis, namely in terms of rotations and boosts as:

$$b_{e_1\wedge e_2} = \sum_a \Big(\alpha_a N_a + i\beta_a L_a\Big)\,, \tag{5.2.11}$$

where

$$\alpha_a = (\zeta_t\lambda_a - \zeta_a\lambda_t)\ , \quad \beta_a = -i\varepsilon_{abc}\,\zeta_a\lambda_b\,. \tag{5.2.12}$$

According to [115], the Hilbert space $L^2[\zeta,\lambda]$ associated with the quantum bivector (5.2.10) has to be invariant under the switching operator. We prove this fact for the bivector operator (5.2.11).

Proposition 1 (Invariance under the switching operator)**.** *Consider a triplet of vectors e_1, e_2, e_3 on Minkowski space parametrized by the coordinates ζ, λ, ω, such that they form the boundary of a triangle: $\zeta + \lambda = \omega$. The Hilbert space of the bivector (5.2.10) does not depend on which pair of edge vectors that are used to construct the bivector (5.2.10). Therefore, it is invariant under the switching operator*

$$\sigma : L^2[\zeta,\lambda] \ \to\ L^2[\zeta,\omega] \qquad \textit{for}\ \ \zeta+\lambda=\omega\,, \tag{5.2.13}$$

up to a sign that reflects the orientation of the vector normal to the triangle.

Proof. We show that the quantum bivector in (5.2.11) is invariant under such switching operator and thus agrees with [115]. According to the closure condition $\zeta + \lambda = \omega$, the third edge of the triangle is given by

$$e_3 = (\omega_t, \omega_1, \omega_2, \omega_3) = (\zeta_t + \lambda_t, \zeta_1 + \lambda_1, \zeta_2 + \lambda_2, \zeta_3 + \lambda_3)\,, \tag{5.2.14}$$

and a basis for the associated position and momentum operators is given by

$$\begin{aligned} a_3^\dagger &= a_t\omega_t + a_x^\dagger\omega_x + a_y^\dagger\omega_y + a_z^\dagger\omega_z\,,\\ a_3 &= a_t^\dagger\omega_t + a_x\omega_x + a_y\omega_y + a_z\omega_z\,, \end{aligned} \qquad \to \quad a_3^\dagger = a_1^\dagger + a_2^\dagger\ , \quad a_3 = a_1 + a_2\,. \tag{5.2.15}$$

A direct computation shows that the quantization of the bivector $e_1 \wedge e_3$ is equivalent to that of $e_1 \wedge e_2$ since they obey the condition $e_1 + e_2 + e_3$. Thus, the associated Hilbert spaces are isomorphic (invariant under the switching operator).

$$b_{e_1\wedge e_3} := -i(a_1^\dagger a_3 - a_3^\dagger a_1) = -i\Big(a_1^\dagger(a_1+a_2) - (a_1^\dagger + a_2^\dagger)a_1\Big) = -i(a_1^\dagger a_2 - a_2^\dagger a_1) := b_{e_1\wedge e_2}\,. \tag{5.2.16}$$

□

Notice that such realization provides the quantization of a triangle on Minkowski space with edges parametrized by the coordinates ζ, λ, ω. It also confirms that, once we restrict the Hilbert space of the quantum triangle to the skew-symmetric part, we establish the proper quantization of a bivector, which is given as the wedge product of any two of the triangle edge vectors.

Wave function. Following the above construction of a quantum triangle and a quantum bivector, we can now derive the associated wave functions, i.e. give a more explicit realization of their quantum states. Let us then consider a pair of vectors e_1, e_2, parametrized respectively by the coordinates $\zeta, \lambda \in F(\mathbb{M}^4)$. We refer to the *triangle wave function* (or the quantization of the triangle t), as the function:

$$f(\zeta, \lambda) \ \in L^2[\zeta, \lambda] \,. \tag{5.2.17}$$

According to the construction above, the proper quantization is realized if the two coordinates of the edge vectors satisfy the closure relation $\zeta + \lambda + \omega$ for a given edge e_3 parametrized by ω, such that the wave function (5.2.17) is invariant under the switching operator (5.2.5). On the other hand, we refer to the *bivector wave function* (or the quantization of a bivector b), as the function:

$$g(\zeta, \lambda) \ \in T^A[\zeta, \lambda] = F(\mathbb{M}^4 \wedge \mathbb{M}^4) \,, \tag{5.2.18}$$

that are the sub-class of the functions (5.2.17). Note that they are elements of the skew-symmetric part of the Hilbert space $L^2[\zeta, \lambda]$. By the same token, a more standard formulation of the Hilbert space of bivector can be characterized in terms of the (Lorentzian) Euler angles (5.2.11), rather than in terms of the coordinates on the two vectors. The Hilbert space, in this case, takes the form $L^2[b] := L^2[\alpha, \beta] = F(\mathfrak{so}^*(1,3))$, where the generators (the coordinates functions) are now the Euler angles $\{\alpha_a, \beta_a\} \in F(\mathfrak{so}^*(1,3)) \cong F(\mathbb{R}^6_\star)$ (here, the subscript $\star$ stands for a non-trivial (star) product for the functions on $\mathbb{R}^6$, given by the non-trivial product of the algebra $\mathfrak{so}(1,3)$). Obviously, the Hilbert space is not affected by the choice of coordinates and the two formulations are isomorphic, as $\mathbb{M}^4 \wedge \mathbb{M}^4 \cong \mathfrak{so}^*(1,3)$ and related by the map (5.2.12). Notice that as we identify bivectors as non-commutative geometric entities, whose quantization is provided by assigning them Lie algebra elements is actually obtained, starting from commutative functions of commutative edge vectors (which as we have seen are elements of the translation group). This can be already depicted from the antisymmetric combination of the ladder operators that define the bivector in terms of edge vectors.

We can use the operator associated with the bivector constructed above, to expand the wave function in the Fourier modes. This can be realized both in terms of the edge vectors $(\lambda_1\,, \lambda_2)$ or in the Euler angle parametrizations $(\alpha\,, \beta)$:

$$\begin{aligned} f(\lambda_1, \lambda_2) &:= -i \int \mathrm{d}\alpha \mathrm{d}\alpha' \, \langle \alpha_\nu \, | a^\dagger(\lambda_1) a(\lambda_2) - a^\dagger(\lambda_2) a(\lambda_1) | \, \alpha'_\nu \rangle \, f_{\alpha_\nu \,, \alpha'_\nu} \,, \\ f(\alpha, \beta) &:= \sum_{n_r=0}^{\infty} \int \mathrm{d}\mu \mu^2 \sum_{\ell, \ell', m, m'} \langle n_r, \mu; \ell, m \, | \sum_a \Big(\alpha_a \, N_a + i \beta_a \, L_a \Big) | \, n_r, \mu; \ell', m' \rangle f^{n_r, \mu; \ell, m}_{n_r, \mu; \ell', m'} \,, \end{aligned} \tag{5.2.19}$$

with $\ell, \ell' \in [0, \infty)$, $\ell \leq m \leq \ell$ and $\ell' \leq m' \leq \ell'$. It is important to notice that, in contrast to the bivector, a Fourier expansion for the triangle wave function (5.2.17) is simply achieved by taking the tensor product of two vector wave functions (5.1.14), provided they satisfy

the triangle closure condition.
Let us introduce the compact notations for some terms appearing in (5.2.19)

$$b(\lambda_1,\lambda_2) = -i(a^\dagger(\lambda_1)a(\lambda_2) - a^\dagger(\lambda_2)a(\lambda_1))\,, \quad b(\alpha,\beta) = \sum_a \left(\alpha_a\, N_a + i\beta_a\, L_a\right), \tag{5.2.20}$$

where the expectation value of these operators appearing in (5.2.19) (with respect to the coherent states) plays the role of a plane wave in the Fourier transform. An explicit expression for the bivector wave function (5.2.18) is obtained by the infinite dimensional representations of such plane waves. This allows us to write the following expression for the bivector operator:

$$\begin{aligned}\langle \alpha_\nu\, |b(\lambda_1,\lambda_2)|\, \alpha'_\nu\rangle &= \int \mathrm{d}x^4\, \overline{\Psi}_{\alpha_\nu}(t,x,y,z)\, \Psi_{\alpha'_\nu}(t',x',y',z')\,,\\ \langle n_r,\mu;\ell,m|b(\alpha,\beta)|n_r,\mu;\ell',m'\rangle &= \int \mathrm{d}r\mathrm{d}\eta\mathrm{d}\Omega r^3 \sinh^2(\eta)\overline{\Psi}_{n_r,\mu;\ell,m}(r,\eta,\theta,\phi)\Psi_{n_r,\mu;\ell',m'}(r',\eta',\theta',\phi'),\end{aligned} \tag{5.2.21}$$

where the primed coordinates encode the action of the operator b, in the basis (5.2.10) or (5.2.11). We further emphasize that the plane waves appearing in the above Fourier decomposition can simultaneously be recast in terms of the eigenfunctions of the harmonic oscillator expressed in the Minkowski basis (A.2.2) (as well as in the hyperbolic basis (A.2.5)), and likewise in terms of the eigenfunctions of the coherent states. This can be made evident using the relations (5.1.29), (5.1.30) or their inverses.
For what will come later, it is important to stress that the bivector wave functions, as elements of the algebra $\mathbb{R}^6 \cong \mathfrak{so}^*(1,3)$, are equipped with a sum:

$$f(b+b') = \begin{cases} f(\lambda_1+\lambda'_1,\lambda_2+\lambda'_2)\,,\\ f(\alpha_1+\alpha'_1,\beta_2+\beta'_2)\,. \end{cases} \tag{5.2.22}$$

It is also interesting to recall that the Lie algebra $\mathfrak{so}^*(1,3)$ is endowed with a nontrivial Poisson structure; indeed, as a quantum group, it is isomorphic to $\mathbb{R}^6_\star$, which is endowed with the star $\star$ product. In the Fourier decomposition, this product appears as a non-trivial combination of plane waves (5.2.21) as we presented in section 4.1. This is equivalently reflected in the canonical commutators of the creation and annihilation operators $(a^\dagger, a)$ as well in the Lorentz commutation relations (5.1.19).

5.3 Quantum tetrahedron

At this level, we are well equipped with the essential material to provide a quantum description of a tetrahedron, both in terms of edge vectors and bivectors. This is the building block of quantum geometry in spin foam models and group field theories, as well as in the simplicial sector of canonical LQG. It is also the starting point for the quantum geometric construction of spin foam amplitudes. In the following we first recall the classical description; then, we provide the quantum version of the same description and the definition of quantum states.

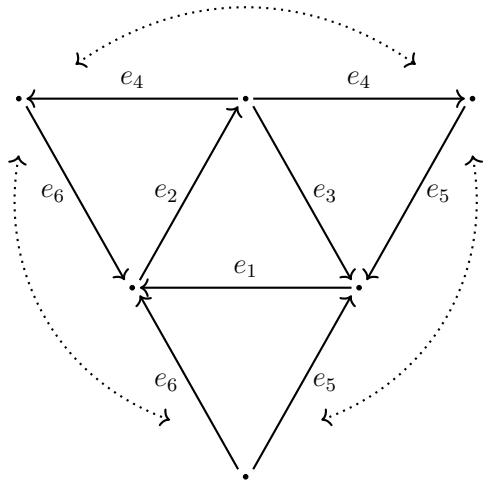

(a) Combination of four triangles into a tetrahedron. The four triangles are labeled by t_i and the six edges (shared pairwise by triangles) by e_j.

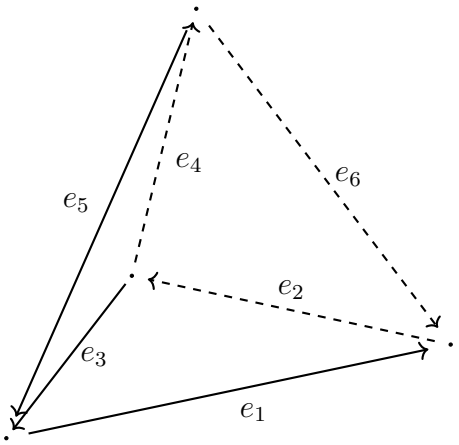

(b) Tetrahedron from three edge vectors, e_1, e_3, e_5.

Figure 5.2: Combinatorics of τ and its closure constraints from edge vectors.

5.3.1 Classical tetrahedron

Classical tetrahedron via edge vectors. Let us consider six edge vectors $e_a \in \mathbb{M}^4$, for $a = 1, \dots, 6$, that satisfy the four closure conditions:

$$e_1 + e_2 + e_3 = 0 \ , \quad e_4 + e_5 + e_3 = 0 \ , \quad e_1 + e_5 + e_6 = 0 \ , \quad e_2 + e_4 + e_6 = 0 \, . \tag{5.3.1}$$

Obviously, they specify the full geometric information about the tetrahedron. The four closure conditions are not independent of each other: any one of them can be written as a linear combination of the other three relations. It is then clear that the geometry of a tetrahedron is completely determined by three of these six edge vectors, attached to a common vertex, such that, taken in pairs, they enter three of the four closure conditions (5.3.1) [102], as we encountered in section 3.1.1. For instance, using figure (5.2a), the geometry of a tetrahedron τ_e in Minkowski space is encoded in the vector triplet $e_1, e_3, e_5 \subset \tau_e$ with the three conditions (as in figure (5.2b)):

$$e_1 + e_2 + e_3 = 0 \ , \quad e_4 + e_5 + e_3 = 0 \ , \quad e_1 + e_5 + e_6 = 0 \, , \tag{5.3.2}$$

Note that the *normal vector* to the tetrahedron in its $4d$ embedding can be obtained easily in this edge-based formulation. Indeed, we can express it as the Hodge dual of the wedge product of any triplet of independent edge vectors, and this yields:

$$n_{\tau_e} = *(e_i \wedge e_j \wedge e_k) \ , \qquad \text{for} \qquad e_i + e_j + e_k \neq 0 \, . \tag{5.3.3}$$

The existence of the normal n_{τ_e} is ensured by the fact that, in three dimensions, there exists always a triplet of independent edge vectors, thus the wedge product (5.3.3) does not vanish.

Classical tetrahedron: bivectors. Alternatively to the above description based on the edge vectors, one can characterize a classical tetrahedron τ_b in Minkowski space in terms of the four bivectors b. This description is obtained from the skew-symmetric geometry of the four triangles specified by the closure conditions in (5.3.1). In order to properly encode the geometric data in the tetrahedron τ_b, the four bivectors have to satisfy the following two constraints:

1. *Dependence relation*: the wedge product of each pair of bivectors $b_i, b_j \subset \{b_1, b_2, b_3, b_4\}$ vanishes: $b_i \wedge b_j = 0$;
2. *Closure relation*: each of the four bivectors is given by the sum of the other three: $b_1 + b_2 + b_3 + b_4 = 0$.

The first condition ensures that each bivector shares one and only one vector with each of the others (thus it is indeed a simple bivector constructed from the edge vectors of a geometric tetrahedron), while the second property is a direct consequence of the fact that the tetrahedron geometry is encoded in the closure of the four triangles (5.3.1).
We point out the crucial difference between the geometric construction exploiting the full data of the triangle, and that based solely on bivectors. One can observe that the bivector-based tetrahedron τ_b encodes less geometric information with respect to the edge-based one τ_e. Specifically, one cannot reconstruct the normal vector from the bivectors alone, the knowledge of which on the other hand is relevant for understanding how the intrinsic geometric data transform under $4d$ Lorentz transformations in the embedding Minkowski space. This becomes evident when we start with the edge vectors formulation and recover the condition on the bivectors. Let us see this explicitly. Given the four triangles specified by the closure conditions (5.3.1), one can define the four bivectors:

$$b_1 = e_2 \wedge e_3 \ , \quad b_2 = e_3 \wedge e_5 \ , \quad b_3 = e_6 \wedge e_5 \ , \quad b_4 = e_2 \wedge e_6 \ . \tag{5.3.4}$$

The first relation (the dependence relation) for the construction of τ_b is easily established from edge vectors, once we rely on the fact that at most a triplet of the six edge vectors e_a are linearly independent in four dimensions, namely:

$$b_i \wedge b_j = (e_a \wedge e_b) \wedge (e_b \wedge e_c) = e_a \wedge (e_b \wedge e_b) \wedge e_c = 0 \, , \tag{5.3.5}$$

for $a \neq b$, $a \neq c$ and $b \neq c$. As for the closure relation, the closure of the four triangles (5.3.1) implies the gluing of the boundary of the tetrahedron. This is translated into the fact that the four bivectors (5.3.4) sum up to zero:

$$\begin{aligned} b_1 + b_2 + b_3 + b_4 &= e_2 \wedge e_3 + e_3 \wedge e_5 + e_6 \wedge e_5 + e_2 \wedge e_6 \\ &= (e_2 - e_5) \wedge e_3 + (e_2 - e_5) \wedge e_6 = (e_2 - e_5) \wedge (e_3 + e_6) \\ &= (e_2 - e_5) \wedge (e_2 - e_5) = 0 \, . \end{aligned} \tag{5.3.6}$$

We thus recover the bivector picture of the tetrahedron τ_b. This is obtained by imposing further restrictions on the edge vectors in order to access the skew symmetric sector of the

geometry described by the bivectors. However, the converse clearly does not work. There is no notion of the normal vector (5.3.3) in terms of such entities. In turn, this is needed to ensure $4d$ covariance of the bivector description (including the constraints ensuring that they come from edge vectors). A similar point was raised in [114], where an extended formulation of the Barrett-Crane model was realized to encode the normal vector.

5.3.2 Edge-based quantization of the tetrahedron

Quantum tetrahedron from edge vectors. The new SF model is based on the quantum states for quantum tetrahedra. Therefore, our next step is to construct the corresponding Hilbert space of wavefunctions.
As we discussed, the geometry of a tetrahedron is completely determined by three of its edge vectors meeting at one of the four vertices, where the closure conditions (5.3.2) must hold. Identifying the quantum space of a single edge vector with the space of (square integrable) functions on the translations group, we naturally define the quantum space of a tetrahedron τ_e in Minkowski space as the tensor product of three of them, equipped with the proper closure conditions:

$$L^2[e_1,e_3,e_5] := L^2[e_1]\otimes L^2[e_3]\otimes L^2[e_5]\ , \quad \begin{cases} e_1+e_2+e_3=0\,, \\ e_4+e_5+e_3=0\,, \\ e_1+e_5+e_6=0\,. \end{cases} \tag{5.3.7}$$

Here the tensor product of each pair of spaces $L^2[e_i,e_j]$ for $i\neq j=1,3,5$ is the quantum space of a triangle (see section 5.2), and it is automatically invariant under the switching operator (5.2.5). Moreover, one can reconstruct τ_b in terms of the three bivectors by reducing the degrees of freedom of each triangle to its skew symmetric part. At the level of Hilbert spaces, this translates into

$$T^A[e_1,e_2,e_3] := T^A[e_1,e_3]\otimes T^A[e_1,e_5]\otimes T^A[e_3,e_5] \cong F(\mathfrak{so}^*(1,3))^{\times 3}\,. \tag{5.3.8}$$

However, as we already observed at the classical level, some geometric information, namely the data of the normal vector to τ_b, is not encoded in the skew symmetric part of the Hilbert space given in (5.3.8). It is instead included in the sub-space of (5.3.7) obtained by the triple antisymmetric product:

$$L^2[n_\tau] = L^2[e_1]\wedge L^2[e_3]\wedge L^2[e_5] \subset L^2[e_1,e_3,e_5]\ , \quad L^2[n_\tau]\not\subseteq T^A[e_1,e_2,e_3]\,, \tag{5.3.9}$$

i.e. it can be reconstructed from quantum edge vector data.

Tetrahedron wave function. We can now provide the construction of the wave functions associated to the tetrahedron τ_e (as well as τ_b). These functions are the elements

of the Hilbert space (5.3.7), and therefore are defined as functions on three copies of the translation group on Minkowski space:

$$f(\lambda_a, \lambda_b, \lambda_c) \ \in F(\mathbb{M}^4)^{\times 3}\,, \tag{5.3.10}$$

where the coordinates of three edges of the tetrahedron meeting at one of its four vertices satisfy the closure conditions for three different triangles, e.g. $a = 1$, $b = 3$ and $c = 5$ in the notation of Fig.(5.2a) and Fig.(5.2b).
One more symmetric way to construct these functions is to extend the Hilbert space (5.3.7) and consider as a first step a set of six edges e_i, for $i = 1, \dots, 6$. This set of vectors should close to form four triangles according to the constraints (5.3.1). Therefore, the elements of this extended Hilbert space would be functions of the form $f(\lambda_1, \lambda_2, \lambda_3, \lambda_4, \lambda_5, \lambda_6) \in F(\mathbb{M}^4)^{\times 6}$ subject to the quantum closure constraint:

$$\hat{\mathcal{C}}_t(\lambda_1, \dots, \lambda_6) = \delta(\lambda_1 + \lambda_2 + \lambda_3)\, \delta(-\lambda_3 + \lambda_4 + \lambda_5)\, \delta(-\lambda_5 + \lambda_6 - \lambda_1)\,, \tag{5.3.11}$$

where the subscript t stands for the closure of three of the four triangles t of τ_e. Obviously, the closure of the fourth triangle is automatically obtained. The closure condition (5.3.11) ensures that the quantum tetrahedron expressed in terms of the edge vectors encodes all the properties of the tetrahedron wave function (5.3.10).
As in the classical prescription, by reducing the Hilbert space (5.3.7) to its skew-symmetric part (5.3.8), we obtain the standard formulation of a quantum tetrahedron in terms of bivectors, which are however automatically simple, i.e. functions of the (quantum) edge vectors. Notice that, similarly to the case of triangles, the wave function of the tetrahedron can be written as a function of the (commutative) quantum edge vectors (elements of the translation group).
In this case, one can consider a set of three bivectors. We then write down the wave function for τ_b as an element of the quantum space (5.3.8):

$$f(x_1, x_2, x_3) \ \in F(\mathfrak{so}^*(1,3))^{\times 3}\,, \tag{5.3.12}$$

where the three bivectors coordinates obey the closure condition $x_1 + x_2 + x_3 + x_4 = 0$ for some $x_4 \in F(\mathfrak{so}^*(1,3))$. The coordinates (the variables x) of the bivectors can be identified, for instance using (5.2.11), as the Euler angles of the Lorentz group:

$$x_i := \{\alpha_i^a,\, \beta_i^a\} \ \in F(\mathbb{R}^6_\star) \cong F(\mathfrak{so}^*(1,3))\,. \tag{5.3.13}$$

Once again, the same expression for the tetrahedron wave function can be achieved by extending the Hilbert space and considering a constrained sub-space implementing the skew-symmetry condition. In this scenario, we work on four copies of the space of functions in the dual Lorentz algebra, whose elements are the functions $f(x_1, x_2, x_3, x_4) \in F(\mathfrak{so}^*(1,3))^{\times 4}$ constrained by the condition $(\hat{\mathcal{C}}_\tau * f) = f$. This imposes the following closure constraint on the bivector coordinates:

$$\hat{\mathcal{C}}_{\tau_b}(x_1, x_2, x_3, x_4) = \delta(x_1 + x_2 + x_3 + x_4)\,. \tag{5.3.14}$$

Recall that the subscript τ_b stresses that this constraint enforces the closure of the boundary of the tetrahedron τ_b. As we already indicated in the discussion of the classical tetrahedron, the constraint on the bivector coordinates in (5.3.14) is inherited by the closure of the triangles in (5.3.11). Similarly, we can identify the sub-space of $F(\mathfrak{so}^*(1,3))^{\times 4}$, constrained by the condition in (5.3.14), as a sub-space of the tetrahedron extended Hilbert space $L^2[e_1, e_2, e_3, e_4, e_5, e_6]$ obeying the condition (5.3.11):

$$(\hat{\mathcal{C}}_t * f)(\lambda_1, \ldots, \lambda_6) \;\Rightarrow\; (\hat{\mathcal{C}}_{\tau_b} * f)(x_1, x_2, x_3, x_4)\,. \tag{5.3.15}$$

As already pointed out, the above relation is not an equivalence, since it is clear that a part of the tetrahedron geometry τ_e can not be recovered from the bivector description. One can expand the tetrahedron τ_b wave function (5.3.12) in the Fourier decomposition as we did for the bivector wave function given in (5.2.19). Let us introduce the compact notation $T^{\alpha'_\nu}_{\alpha_\nu}(\lambda_1, \lambda_2)$ for the translation group plane waves $\langle \alpha_\nu \,|a^\dagger(\lambda_1)a(\lambda_2) - a^\dagger(\lambda_2)a(\lambda_1)|\, \alpha'_\nu\rangle$. The decomposition of (5.2.19) then reads:

$$f(\lambda_1, \lambda_2) = -i \int \mathrm{d}\alpha \mathrm{d}\alpha'\, T^{\alpha'_\nu}_{\alpha_\nu}(\lambda_1, \lambda_2)\, f^{\alpha_\nu}_{\alpha'_\nu}\,, \tag{5.3.16}$$

Hence, the tetrahedron τ_e wave function (5.3.12) decomposes in the Fourier modes as:

$$\begin{aligned} f(\lambda_1, \ldots, \lambda_6) = \int \mathrm{d}\alpha^6 \mathrm{d}\alpha'^6\, & T^{\alpha'_{1;\nu}}_{\alpha_{1;\nu}}(\lambda_2, \lambda_3)\, T^{\alpha'_{2;\nu}}_{\alpha_{2;\nu}}(\lambda_3, \lambda_5)\, T^{\alpha'_{3;\nu}}_{\alpha_{3;\nu}}(\lambda_6, \lambda_5) \\ & \times T^{\alpha'_{4;\nu}}_{\alpha_{4;\nu}}(\lambda_2, \lambda_6)\, f^{\alpha_{1;\nu}, \alpha_{2;\nu}, \alpha_{3;\nu}, \alpha_{4;\nu}}_{\alpha'_{1;\nu}\, \alpha'_{2;\nu}\, \alpha'_{3;\nu}\, \alpha'_{4;\nu}}\,. \end{aligned} \tag{5.3.17}$$

where the different labels appearing in $T^{\alpha'_\nu}_{\alpha_\nu}(\lambda_i, \lambda_j)$ are those that decorate the quantum vectors obeying a certain combinatorial relation (this is dictated by the constraint (5.3.11)). This of course encoded in the combinations of the ladder operators and can be exactly extracted by evaluating the matrix elements appearing in (5.2.21) (relying as well on the material in the appendix (A.2)). In section 5.4 we will see how this is realized for the example of a timelike bivector.

5.4 A new spin foam model based on edge vectors

At this point, we could finally propose an explicit description of a new SF model for four dimensional geometries based on the coordinates of the edge vectors. We discussed the main steps and tools to compute the SF amplitude in section 3.2. The main difference in our case is then, that our tetrahedron Hilbert space and quantum states are associated to several copies of the translation group associated with the set of edges defining the four triangles of the tetrahedron. To this end, in section 5.4.1 we use the quantum space of the tetrahedron τ_e provided in section 5.3 given in terms of the edge vectors, as the quantum state of the new model. We refer to figure 5.3 for an example of the construction of the boundary geometry. We then present the explicit calculation starting from the new

model, explaining how we are able to recover a rather combinatorial (noncommutative) combination of the BC vertex in section 5.4.2. This is basically done only in the case of a spacelike tetrahedron. We finally produce the GFT model in section 5.4.3 that is associated with this edge-based SF model, where now the field theory is defined over three copies of the translation group with the proper closure conditions imposed on three triangles.

5.4.1 A new spin foam amplitude

Properly combining states of the fundamental building blocks (tetrahedron) of the discretized geometry would then allow the amplitude computation of the new spin foam model. The basic idea behind it is very simple. We use functions on the group of translation on Minkowski space as quantum states such that, the gluing of quantum states is explicitly realized by identifying the coordinates of these functions (degrees of freedom associated to edge vectors). In particular, we define the amplitude of a general four dimensional triangulation Γ as a combination of the amplitudes of 4-simplices $\mathrm{s} \subset \Gamma$, along with identifying their boundary tetrahedra $\tau \subset \Gamma$:

$$\mathcal{A}_\Gamma = \prod_s \mathcal{A}_\mathrm{s} \prod_\tau \mathcal{A}_\tau \,. \tag{5.4.1}$$

Here, the amplitude of a single 4-simplex is expressed as:

$$\begin{aligned}\mathcal{A}_\mathrm{s} = \int [\mathrm{d}\lambda]^{10} \Big(\prod_{\alpha=1}^{3} \prod_{a=1}^{4-\alpha} \hat{\mathcal{C}}_{t_{\alpha;a}}(\{\lambda_{\alpha;i}\}) \Big) \star \Big(\delta(\lambda_{1;1}-\lambda_{2;4}) \star \delta(\lambda_{1;1}-\lambda_{4;5})\Big) \\ \Big(\delta(\lambda_{1;2}-\lambda_{2;6}) \star \delta(\lambda_{1;2}-\lambda_{5;3})\Big) \Big(\delta(\lambda_{1;3}-\lambda_{2;2}) \star \delta(\lambda_{1;3}-\lambda_{3;6})\Big) \\ \Big(\delta(\lambda_{1;4}-\lambda_{3;5}) \star \delta(\lambda_{1;4}-\lambda_{5;1})\Big) \Big(\delta(\lambda_{1;5}-\lambda_{3;1}) \star \delta(\lambda_{1;5}-\lambda_{4;4})\Big) \\ \Big(\delta(\lambda_{1;6}-\lambda_{4;3}) \star \delta(\lambda_{1;6}-\lambda_{5;2})\Big) \Big(\delta(\lambda_{2;1}-\lambda_{3;4}) \star \delta(\lambda_{2;1}-\lambda_{5;5})\Big) \\ \Big(\delta(\lambda_{2;3}-\lambda_{3;2}) \star \delta(\lambda_{2;3}-\lambda_{4;6})\Big) \Big(\delta(\lambda_{2;5}-\lambda_{4;1}) \star \delta(\lambda_{2;5}-\lambda_{5;4})\Big) \\ \Big(\delta(\lambda_{3;3}-\lambda_{4;2}) \star \delta(\lambda_{3;3}-\lambda_{5;6})\Big) \,,\end{aligned} \tag{5.4.2}$$

where $\lambda_{\alpha;i}$ is the coordinate of the i^{th} edge of the tetrahedron α, for $\alpha = 1,\dots,5$ and $i = 1,\dots,6$, and $t_{\alpha;a}$ stands for the triangle a of the tetrahedron α, for $a = 1,2,3,4$. The $\star$ symbol refers to the non-commutative product of the functions on $\mathbb{M}^4$, inherited from the noncommutativity of the ladder operators. Note that in the expression above we have decorations on all of the ten edges of the 4-simplex. Indeed, for simplicity, we constructed the 4-simplex amplitude (5.4.2) starting by the extended Hilbert spaces of the five tetrahedra, each of them is given as a constrained version of the functions on its six edge vectors. As we pointed out in section 5.3, it is enough to impose *three* triangle-closure conditions for each tetrahedron. Hence, in this formulation, the full geometry of the 4-simplex is recovered by providing the closure of only six of the ten triangles in it (we refer to Fig.(5.3) for the edges and triangles combinatorics of a 4-simplex). According to this

figure, the expression of the amplitude appearing in (5.4.2) is achieved once we require the closure of the set of triangles $a = 1, 2, 3$ of the tetrahedron $\alpha = 1$, of the triangles $a = 1, 2$ of the tetrahedron $\alpha = 2$ and the last triangle $a = 1$ of tetrahedron $\alpha = 3$. This is just an example of how one can fix the combinatorics. The 4-simplex amplitudes are combined together by identifying the edge decorations. To realize the gluing we use the amplitude $\mathcal{A}_\tau$ given by;

$$\mathcal{A}_\tau = \int [\mathrm{d}\lambda]^6 \prod_{i=1}^{6} \delta(\lambda_{\alpha;i} - \lambda_{\beta;i}) \,. \tag{5.4.3}$$

The presence of the closure condition for the six triangles implies that the amplitude (5.4.2) reproduces the expression of the 4-simplex amplitude in the standard formulation (in terms of bivectors) as we already emphasized for a single tetrahedron in (5.3.15). The 4-simplex amplitude (5.4.2) thus reduces to the following form:

$$\mathcal{A}_{\mathrm{s}} = \int [\mathrm{d}x]^{10} \left(\prod_{\alpha=1}^{4} \hat{\mathcal{C}}_{\tau_\alpha}(\{x_{\alpha;a}\}) \right) \star \prod_{\alpha=1}^{4} \prod_{a=1}^{4} \delta(x_{\alpha;a} - x_{\alpha+a;5-a}) \,, \tag{5.4.4}$$

where this time $x_{\alpha;a}$ is the coordinate of the a^{th} triangle of the tetrahedron α, with $\alpha = 1, \ldots, 5$ and $a = 1, \ldots, 4$, and we used again the symbol $\star$ to implement the non-trivial product between the delta functions. As for the amplitude (5.4.2), the sub-leading geometry is obtained by the closure of four out of the five tetrahedra τ_b. The four closures are encoded in the functions $\hat{\mathcal{C}}_{\tau_b}$. Similarly, the tetrahedron amplitude (5.4.3) simply provides the identification of the triangle decorations of two tetrahedra:

$$\mathcal{A}_\tau = \int [\mathrm{d}x]^4 \prod_{a=1}^{4} \delta(x_{\alpha;a} - x_{\beta;a}) \,. \tag{5.4.5}$$

5.4.2 Recovering the Barrett-Crane model

In the following, we show explicitly how the new model reduces to a nontrivial combination of BC amplitudes. We carry out this computation since it is the only available well-studied amplitude in such a model. We show this for the case of timelike bivectors (spacelike edge vectors). Therefore, we start with the usual description of the quantum bivector and work our way through using the tools in section 5.1 to explicitly express it in terms of spacelike edge vector coordinates.

The quantum minkowskian timelike bivector Let us recall that, the quantization of bivectors in Minkowski space $\mathbb{M}^4$ is based on considering the elements of the dual Lorentz Lie algebra $\mathfrak{so}^*(1,3)$. Since upon exponentiation (integration), the Lorentz algebra is mapped into the Lorentz group, one can wonder how our construction based on quantum vectors is explicitly related to the usual Lorentz representation we introduced in

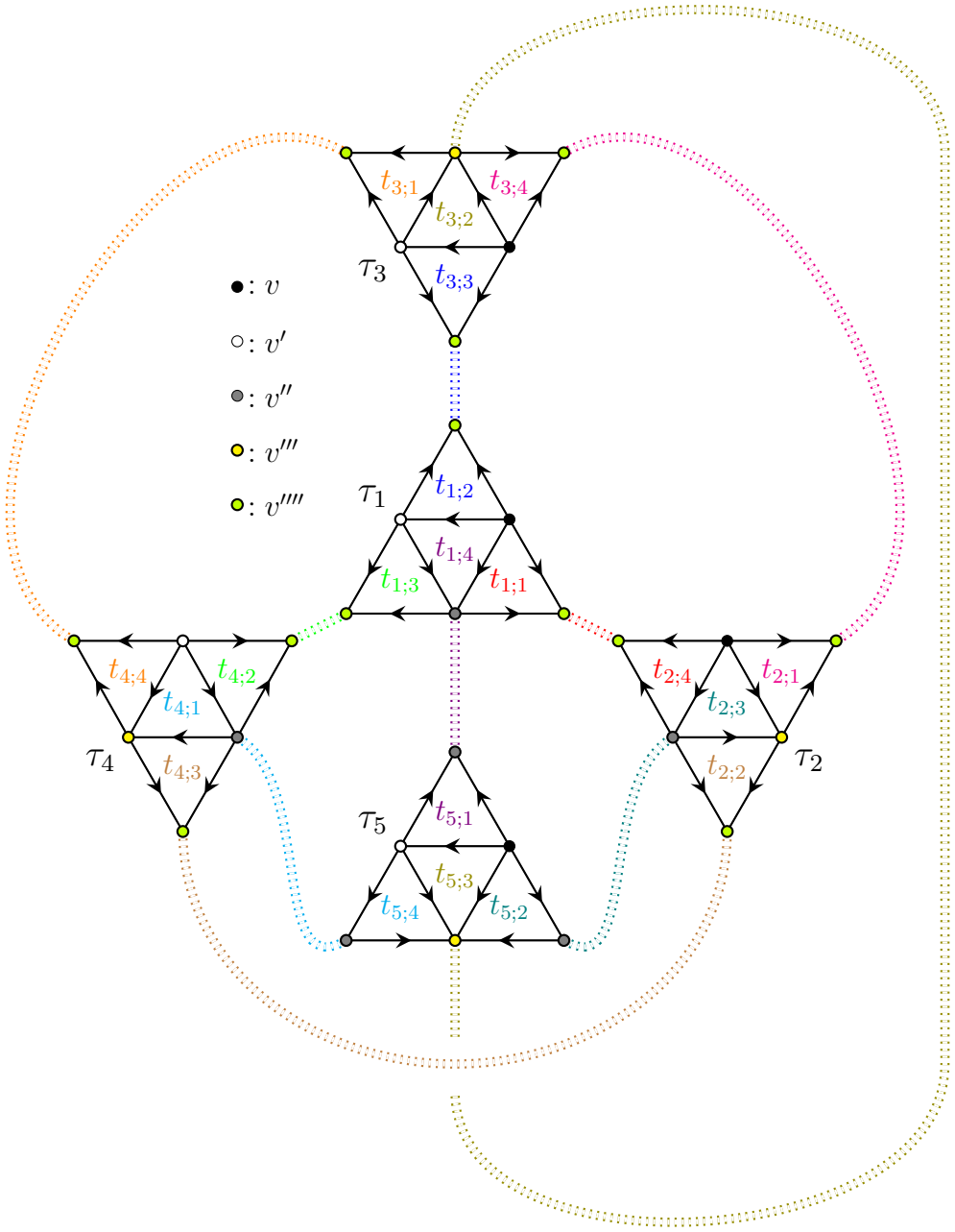

Figure 5.3: 4-simplex boundary construction: five tetrahedra share five vertices. Each of the four faces of each tetrahedron is identified with one of the faces of the other four tetrahedra. We use the same color and a double dotted line for the identified faces.

section 5.1. To make this connection clear, let us start with a unitary representation for a general Lorentz group element:

$$U(g) = e^{\sum_a (\alpha_a N_a + i\beta_a L_a)} . \tag{5.4.6}$$

Following the scheme outlined in section 5.2 to construct the bivector wave function, one can define the Hilbert space of the square integrable functions on the Lorentz group $L^2[\mathrm{SO}(1,3)] \cong F(\mathrm{SO}(1,3)) \ni f(g)$. Similarly to the bivector (Fourier decomposed) wave functions we derived in (5.2.19), the unitary operator (5.4.6) can be used to expand the wave functions in the Fourier decomposition according to the expression:

$$f(g) := \sum_{n_r=0}^{\infty} \int \mathrm{d}\mu\mu^2 \sum_{\ell,\ell'} \sum_{m,m'} \langle n_r, \mu; \ell, m \,|U(g)|\, n_r, \mu; \ell', m' \rangle \, f^{n_r,\mu;\ell,m}_{n_r,\mu;\ell',m'} . \tag{5.4.7}$$

However, this time let us stress that the plane waves used for the above harmonic expansion are more familiar since their non-radial contribution coincides with the irreducible representations of the Lorentz group (the standard D-matrices), namely that they satisfy the following equality

$$D^{0,\mu}_{\ell,m;\ell',m'}(g) := \langle \mu; \ell, m \,|U(g)|\, \mu; \ell', m' \rangle , \tag{5.4.8}$$

for $j = 0$, as we consider only the balanced *timelike* representations. According to the representation theory of the Lorentz group, the wave function and its harmonic expansion (5.4.7) encodes the proper gravitational degrees of freedom for a timelike region, provided that the function is invariant under rotations. This condition is implemented as:

$$\int \mathrm{d}u \, f(gu) = f(g) , \tag{5.4.9}$$

for all the rotations $u \in \mathrm{SO}(3)$. This condition correctly restricts the Hilbert space of the Lorentz group to the space of functions on the upper hyperboloid Q_1, introduced in the Plancharel decomposition in section 5.1. In this case, the Fourier decomposition (5.4.7) reduces to the expansion in terms of timelike infinite dimensional irreducible representations of the group, namely by setting the angular momentum quantum numbers (l, m) equal to 0:

$$f(g) := \sum_{n_r=0}^{\infty} \int \mathrm{d}\mu\mu^2 \, \langle n_r, \mu; 0, 0 \,|U(g)|\, n_r, \mu; 0, 0 \rangle \, f^{n_r,\mu}_{n_r,\mu} , \tag{5.4.10}$$

where we identify the non-radial part of the kernel as[3]:

$$D^{0,\mu}_{0,0;0,0}(g) := \langle \mu; 0, 0 \,|U(g)|\, \mu; 0, 0 \rangle . \tag{5.4.11}$$

Furthermore, let us recall that the explicit expression for these plane waves in the hyperbolic basis given by (A.2.5) and since we are interested in the timelike sector and restricting the

[3]The extension to the full harmonic oscillator basis $|\, n_r, \mu; \ell', m' \rangle$ is trivial, as the plane wave given by $\langle n_r, \mu; \ell, m \,|U(g)|\, n_r, \mu; \ell', m' \rangle$ is diagonal in the radial contribution.

plane wave to the case where $n_r = 0$ (for simplicity), we obtain the explicit expression for the $D-$ matrix in the hyperbolic basis:

$$D^{0,\mu}_{0,0;0,0}(g) = \langle 0,\mu;0,0\,|U(g)|\,0,\mu;0,0\rangle = \int \mathrm{d}\eta\, Q_0^{1-\mu^2}(\coth\eta)\, Q_0^{1-\mu^2}(\coth\eta')\,, \qquad (5.4.12)$$

where η' is obtained by the action of the transformation g on the Legendre function Q with the coordinates η. Notice that this is the canonical D matrix encoding the quantum geometry of a timelike bivector in the hyperbolic basis, which we will express in what follows in the harmonic oscillator basis.
Let us now translate these results for quantum bivectors, expressed in terms of the canonical D-matrices (in different parametrizations), to the Minkowskian one, which is basically that of the translation group. This is indeed achieved since we can expand the function on the Lorentz group and also in the Fourier modes of translations using the coherent states of the harmonic oscillator. This yields the harmonic decomposition

$$f(g) := \int \mathrm{d}\alpha\mathrm{d}\alpha'\, \langle \alpha_\nu\,|U(g)|\,\alpha'_\nu\rangle\, f_{\alpha_\nu,\,\alpha'_\nu}\,. \qquad (5.4.13)$$

In this case, the plane wave that appears in the decomposition is:

$$\langle \alpha_\nu\,|U(g)|\,\alpha'_\nu\rangle = \int \mathrm{d}x^4\, \overline{\Psi}_{\alpha_\nu}(t,x,y,z)\left(U(g)\,\Psi_{\alpha'_\nu}\right)(t,x,y,z)\,, \qquad (5.4.14)$$

which is related to the standard Lorentz representations obtained through the Plancharel decomposition (5.4.7), by the change of basis (5.1.29), (5.1.30):

$$\begin{aligned}\langle \alpha_\nu\,|U(g)|\,\alpha'_\nu\rangle = e^{-\frac{1}{2}(|\alpha|^2+|\alpha'|^2)} \sum_{\{n_\nu,n'_\nu\}} \sum_{n_r=0}^{\infty} \sum_{\ell,\ell'} \sum_{m,m'} \\ \frac{\alpha_t^{n_t}\alpha_x^{n_x}\alpha_y^{n_y}\alpha_z^{n_z}(\alpha'_t)^{*n'_t}(\alpha'_x)^{*n'_x}(\alpha'_y)^{*n'_y}(\alpha'_z)^{*n'_z}}{\pi^8\sqrt{n_t!n_x!n_y!n_z!n'_t!n'_x!n'_y!n'_z!}}\, D^{0,\mu}_{\ell,m;\ell',m'}(g)\,. \end{aligned} \qquad (5.4.15)$$

Once again we restrict the Fourier expansion to the timelike sector on Q_1. In terms of edge vector coordinates, the upper hyperboloid is obtained by the intersection of a pair of co-linear light cones centered at the timelike points parametrized by $P_i = (0, x_i, y_i, z_i) \in \mathbb{M}^4$ of Minkowski space:

$$\begin{cases} t^2 = A\Big((x-x_1)^2+(y-y_1)^2+(z-z_1)^2\Big)\,, \\ t^2 = A\Big((x-x_2)^2+(y-y_2)^2+(z-z_2)^2\Big)\,, \end{cases} \quad \Rightarrow \quad t^2-x^2-y^2-z^2 = R^2\,, \qquad (5.4.16)$$

with $R^2 = 2A\Big((x_1-x_2)^2+(y_1-y_2)^2(z_1-z_2)^2\Big)$ being the hyperbolic distance between two points. We can therefore restrict the space of the translation group to the null edge vectors with unitary time coordinate

$$e = (1,\lambda_x,\lambda_y,\lambda_z)\,, \quad |e|^2 := 1-\lambda_x^2+\lambda_y^2+\lambda_z^2 = 0\,. \qquad (5.4.17)$$

Note that, this can be regarded as the gauge condition[4] on the edge vectors that allows recovering the timelike simple bivectors spanning the tangent space of the hyperboloid Q_1, for more details on hyperbolic geometry we refer to [183]. It is easy to check that this condition correctly implies that the bivector in such parametrization is timelike: $|b|^2 > 0$. With this condition, the constrained Lorentz wave function in (5.4.10) is automatically decomposed as a combination of timelike edge vectors (or equivalently, generators of translations).

Now we arrive to the last map we need to implement in our construction. Note that (5.4.6) provides the relation between the bivector wave function (5.2.18) and the one on the Lorentz group. This type of relation between functions on the Lorentz group and functions on the dual Lorentz algebra is encoded in the non-commutative (NC) Fourier transform. This is basically an intertwining map between the group and algebra representation (and vice-versa), ensuring their unitary equivalence. Recall that it is given by the integral transform:

$$\hat{f}(x) = \int \mathrm{d}g\, e_\star(g\,,\,x)\, f(g)\,, \tag{5.4.18}$$

where $e_\star(g\,,\,x)$ is the star NC exponential for the Lorentz group, it is also referred to as the noncommutative plane waves. Its representative equations can be derived by requiring that, the intertwined function spaces define a representation of the same underlying quantum algebra, and applying the action of unitary operators on the various representations. Moreover, it is important to note that deriving an explicit expression of this NC plane wave depends on the choice of a quantization map. For more details see [100, 148].

Since we are restricting the Lorentz wave functions to those that are invariant under rotations given in (5.4.10), the non-commutative Fourier transform allows to express the bivector functions in (5.2.18) in terms of timelike canonical D-matrices (derived in (5.4.11)) and it yields:

$$\hat{f}(x) = \int \mathrm{d}g\mathrm{d}\mu\, \mu^2\, e_\star(g\,,\,x)\, D^{0,\mu}_{0,0;0,0}(g)\, f^\mu_\mu\,. \tag{5.4.19}$$

More importantly, a similar expansion can be obtained for the bivector wave function in terms of the edge vector coordinates. Here, the group element $g \in \mathrm{SO}(1,3)$ is parametrized as in (5.4.6), whereas the exponent is the bivector operator given by (5.2.10) i.e. as a linear combination of the ladder operators, expressed in terms of the coordinates $(\lambda_1, \lambda_2) \in \mathbb{M}^4$:

$$\hat{f}(\lambda_1, \lambda_2) = \int \mathrm{d}g\mathrm{d}\mu\, \mu^2\, e_\star(g\,,\,x\,(\lambda_1, \lambda_2))\, D^{0,\mu}_{0,0;0,0}(g)\, f^\mu_\mu\,, \tag{5.4.20}$$

with $U(g) = e^{-i(a^\dagger(\lambda_1)\,a(\lambda_2) - a^\dagger(\lambda_2)\,a(\lambda_1)}$ and $\ell, \ell' = 0$ for timelike bivectors $|b|^2$, that are obtained by the skew symmetric product of the translation-generators (the ladder operators) and must satisfy the condition (5.4.17). Thus, the NC edge vector-based construction of a quantum triangle and then a tetrahedron proceeds naturally, once we follow the step defined in section 5.2.-5.3.

[4] Furthermore, we note that the condition (5.4.17) can be written in terms of the Euler coordinates of a bivector (5.2.11), whose coordinates are explicitly given in (5.2.12).

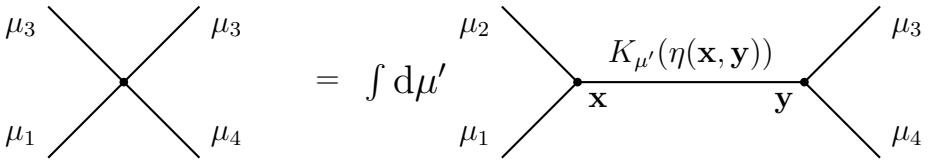

Figure 5.4: The tetrahedron amplitude of the Barrett-Crane model [2]

.

Recovering Barrett-Crane results. Maybe one of the most important relations we derived so far is expressed in the expansion (5.4.20). In fact, we show that now, we relate the new SF amplitude (5.4.1) to the one proposed by Barrett and Crane [114] for the case of timelike bivector-based geometry.
Using the expansion above in terms of NC Fourier transform based on edge coordinates, the new amplitude of a single 4-simplex yields:

$$\mathcal{A}_{\mathrm{s}} = \int [\mathrm{d}\lambda]^{10}\,[\mathrm{d}h]^{5}\mathrm{d}^{5}\mu \prod_{\alpha=1}^{5}\prod_{a=1}^{4}\prod_{i=1}^{6} \mu_\alpha^2\, e_\star(h_\alpha\,,\, x_{\alpha;a}(\lambda_{\alpha;i},\lambda_{\alpha;i}))\, D^{0,\mu_\alpha}_{0,0;0,0}\Big(g(x_{\alpha;i})g^{-1}(x_{\alpha+i;5-i})\Big)\,, \tag{5.4.21}$$

and it is given in terms of the bivector coordinates x (in the Euler angle parametrization), expressed as a combination of the coordinates of the edge vectors λ. Recall that $\lambda_{\alpha;i}$ stands for the coordinate of the i^{th} edge of the tetrahedron α, for $\alpha = 1,\dots,5$ and $i = 1,\dots,6$. The $\star$ symbol refers to the non-commutative product of the functions on $\mathbb{M}^4$.
In this picture, the timelike canonical D matrices given in (5.4.11), associated with the timelike irreducible representations of the Lorentz group, can be computed explicitly as in (5.4.12) and expressed as the term

$$D^{0\mu}_{0,0;0,0}(g_1 g_2^{-1}) = K_\mu(d_\eta(\mathbf{x}_{g_1},\,\mathbf{x}_{g_2})) = \frac{\sin(\mu d_\eta)}{\mu \sinh d_\eta}\,, \tag{5.4.22}$$

where d_η is the hyperbolic distance between two points $\mathbf{x}_{g_i}$ on the hyperboloid Q_1 associated to the Lorentz transformations g_i. It is obvious now that based on (5.4.21), the amplitudes associated with a tetrahedron and to a 4-simplex can be expressed as a combination of the terms (5.4.22). This construction is realized by representing the terms (5.4.22) as the graph dual to tetrahedra. In particular, we associate a set of coordinates $\mathbf{x} \in Q_1$ on the hyperboloid Q_1 to a given vertex of the graph, one parameter μ is attached to each edge of the graph, and the term (5.4.22) is associated to each internal edge of the graph. We refer to Fig.(5.4). By merging together several of these graphs dual to tetrahedra, one can construct the *relativistic spin networks*, which are graphs with no boundary dual to 4-dimensional triangulations. The relativistic spin networks were first introduced by Barrett and Crane in [114], further studied in [2, 184], and were also derived as the Feynman diagrams of a group field theory in [91, 117].

Notice that in our case, the amplitude obtained in (5.4.21) presents itself as a highly nontrivial combination of such terms, i.e. BC amplitude-like terms, for the case of time like bivectors. The main difference is that, once we reformulate the model using the

edge vectors and exploiting their relation to the translation group, we get a rather more sophisticated transition amplitude for the quantum geometries. Indeed, this is implicitly encoded in the NC plane waves appearing in (5.4.21).
We thus have proved that, our new spin foam amplitude (5.4.1) reduces to the one proposed by Barrett and Crane when we restrict the space of quantum states (quantum tetrahedra) to the anti-symmetric part. However, as pointed out already, that our construction, inspired from [115], provides the complete information on the full geometry of *timelike tetrahedra*, including the information of spacelike normal vector. This is clear once we instead of inserting the data of a timelike bivector, we consider that of a spacelike one. This can be made evident when we follow the same steps presented in the beginning of this section when we take into account the matrix elements in (5.4.8) for the case of time like edge vectors. Indeed, the outlined quantization procedure in this paper explicitly demands that matching edges have the same lengths, all the triangles of the 4-simplex to close as well as, the bivectors on faces to correspond to the edges.

5.4.3 Group field theoretic formulation based on edge vectors

In this last part, we emphasize that the new SF amplitude (5.4.1) can be obtained as the Feynman graph of GFT [19,84] as we discussed in chapter 4. In this case, the fundamental field of the theory is the tetrahedron wave function given by (5.3.10) expressed as a function on three copies of the translation group $F(\mathbb{M}^4)^{\times 3}$ with the proper closure conditions for the three triangles. More explicitly, it is given as a function on six copies of the translation group constrained by the closure condition in (5.3.11).
The action that governs the GFT model, $\mathcal{S}_{GFT} = \mathcal{S}_{\mathcal{K}} + \mathcal{S}_{\mathcal{V}}$ is given by an interaction term, that encodes the combinatorics of a 4-simplex, and a propagator, playing the role of identifying such terms. This is explicitly given by (4.0.3). Therefore, the interaction term is expressed exactly as a combination of five fields with the kernel given by the 4-simplex amplitude in (5.4.2), and similarly, the amplitude of the quadratic term of the action, the propagator, is given by (5.4.3). The Feynman diagrams of the model are thus obtained as a combination of such amplitudes and are naturally represented as graphs dual to 4-geometries (see section 4.2). In this sense, the Feynman amplitude associated with a general complex is therefore equivalent to the SF amplitude (5.4.1). In the following, we present briefly a formulation of the theory.

Four dimensional group field theory with edge vectors

Let us construct a GFT based on the edge vectors of a $4d$ triangulation. We provide first the general setting and then derive the amplitude associated with a triangulation, showing the equivalence between this result and that obtained in ordinary GFT's.

Kinematics. Consider a four dimensional group field theory, whose fundamental degrees of freedom are encoded in some functions $\hat{\Phi}$ on six copies of the group $\mathbb{R}^4$; these are associated with the tetrahedra that compose the triangulation of a $4d$ manifold. We would like to express these tetrahedra in terms of the edge vectors.

As we did for the vector and bivector wave function in section 5.2-5.3, we associate to each edge vector e_i of the tetrahedron τ a set of (four) coordinates $\lambda_i \in F(\mathbb{R}^4)$. Therefore, the fundamental field of our GFT (which we also called a tetrahedron wave function) is expressed as:

$$\hat{\Phi}(\lambda_1, \lambda_2, \lambda_3, \lambda_4, \lambda_5, \lambda_6) \ \in L^2[\lambda_1, \lambda_2, \lambda_3, \lambda_4, \lambda_5, \lambda_6] \cong F(\mathbb{R}^4)^{\times 6}\,. \tag{5.4.23}$$

We recall that according to the construction in [115], the bivector wave function is well defined only if the two vectors are part of a triplet that satisfies the closure condition of a triangle boundary. Accordingly, also the tetrahedron wave function (5.4.23), given as a combination of four bivectors, is well-defined only for a six-tuple of vectors that satisfy the proper closure conditions. Relying on the combinatorics depicted in Fig.5.2a, we also obtain the closure constraint that must be satisfied by the fields

$$\hat{\Phi} = (\hat{\mathcal{C}}_t \star \hat{\Phi})\,, \tag{5.4.24}$$

where we used the symbol $\star$ to recall that the functions satisfy a nontrivial star product and recall that $\hat{\mathcal{C}}_t$ is the closure constraint given by (5.3.11). We note that among the six edges of the tetrahedron, four of them are sufficient to encode the tetrahedron combinatorics. Indeed, one can describe the tetrahedron just by using the four bivectors as we already established in (5.3.15). This yields

$$(\hat{\mathcal{C}}_t\, \hat{\Phi})(\lambda_1, \ldots, \lambda_6) \equiv (\hat{\mathcal{C}}_\tau\, \hat{\Phi})(x_1, x_2, x_3, x_4) = \delta(x_1 + x_2 + x_3 + x_4) \star \hat{\Phi}(x_1, x_2, x_3, x_4)\,, \tag{5.4.25}$$

In (5.4.6) we emphasized the relation between the bivector wave function (5.2.18) and the function on the Lorentz group. Usually, this connection is realized by the Plancharel expansion for the functions on the Lorentz group. For instance, the function $\Phi(g_1, g_2, g_3, g_4) \in F(\mathrm{SO}(1,3)^{\times 4})$ is the fundamental field of a $4d$ GFT based on the Lorentz group, and it is related to (5.3.15) by the standard non-commutative Fourier transform on the Lorentz group. Following this line of reasoning, the tetrahedron closure (5.3.6), implied by the closure of the four triangles (5.3.11), is implemented by a gauge projector on the field such that $\forall h \in \mathrm{SO}(1,3)$ we have

$$(\mathcal{P}\,\Phi)(g_1, g_2, g_3, g_4) = \int \mathrm{d}h\, \phi(hg_1, hg_2, hg_3, hg_4) \quad \overset{\star Fourier}{\longrightarrow} \quad b_1 + b_2 + b_3 + b_4 = 0\,. \tag{5.4.26}$$

Therefore, one can relate the ordinary group field theory to our formulation through the chain of maps

$$\Phi \in F(\mathrm{SO}(1,3)^{\times 4}) \ \overset{\star Fourier}{\longrightarrow} \ \hat{\Phi} \in F(\mathbb{R}^6_\star) \cong F(\mathfrak{so}^*(1,3)) \ \overset{eq.(5.3.15)}{\longrightarrow} \ \underset{\mathcal{C}:\,(5.1.25)}{\overset{eq.(5.3.15)}{\longrightarrow}} \ \hat{\Phi} \in F(\mathbb{R}^4 \wedge \mathbb{R}^4). \tag{5.4.27}$$

Following the construction of the bivector wave function (5.2.18), one can expand also the tetrahedron wave function (5.4.23) in the Fourier decomposition. Let us write the decomposition (5.2.19) as

$$\hat{\Phi}(\lambda_1, \lambda_2) = -i \int \mathrm{d}\alpha \mathrm{d}\alpha' \, T^{\alpha'_\nu}_{\alpha_\nu}(\lambda_1, \lambda_2) \, \hat{\Phi}^{\alpha_\nu}_{\alpha'_\nu} \,, \tag{5.4.28}$$

Then, the tetrahedron wave function (5.4.23) decomposes in the Fourier modes as

$$\hat{\Phi}(\lambda_1, \ldots, \lambda_6) = \int \mathrm{d}\alpha^6 \mathrm{d}\alpha'^6 \, T^{\alpha'_{1;\nu}}_{\alpha_{1;\nu}}(\lambda_2, \lambda_3) \, T^{\alpha'_{2;\nu}}_{\alpha_{2;\nu}}(\lambda_3, \lambda_5) \, T^{\alpha'_{3;\nu}}_{\alpha_{3;\nu}}(\lambda_6, \lambda_5) \tag{5.4.29}$$

$$\times \, T^{\alpha'_{4;\nu}}_{\alpha_{4;\nu}}(\lambda_2, \lambda_6) \, \hat{\Phi}^{\alpha_{1;\nu}, \alpha_{2;\nu}, \alpha_{3;\nu}, \alpha_{4;\nu}}_{\alpha'_{1;\nu} \, \alpha'_{2;\nu} \, \alpha'_{3;\nu} \, \alpha'_{4;\nu}} \,. \tag{5.4.30}$$

Again, up to the closure condition (5.3.11), this expansion is equivalent to the Fourier decomposition of the tetrahedron wave function expressed in terms of the four bivectors, which, upon non-commutative Fourier transform, is related to the Plancharel decomposition of the function on the Lorentz group, see (5.4.27).

Dynamics. Once we have determined the fundamental field and its symmetry, let us introduce the action that governs the group field theory model

$$\mathcal{S}_{GFT} = \mathcal{S}_{\mathcal{K}} + \mathcal{S}_{\mathcal{V}} \,, \tag{5.4.31}$$

with the coupling constant set to 1 for simplicity. The action expressed in terms of the star product then yields:

$$\mathcal{S}_{GFT} = \int \mathrm{d}\lambda^6 \, (\hat{\Phi} \star \hat{\Phi})(\{\lambda_i\}) + \int \mathrm{d}\lambda^{12} \, (\hat{\mathcal{K}} \star (\hat{\Phi} \cdot \hat{\Phi}))(\{\lambda_i; \lambda_j\}) \tag{5.4.32}$$

The *kinetic term* whose amplitude is given by the *propagator*

$$\hat{\mathcal{K}} = \prod_{i=1}^{6} \delta(\lambda_i \lambda_{i+6}^{-1}) \,, \tag{5.4.33}$$

enforces the identification of the edges of a pair of tetrahedra (fields). While

$$\begin{aligned}
\mathcal{S}_{\mathcal{V}} = \int \mathrm{d}\lambda^{10} \, & (\hat{\mathcal{C}} \, \hat{\Phi})(\lambda_1, \lambda_2, \lambda_3, \lambda_4, \lambda_5, \lambda_6) \star (\hat{\mathcal{C}} \, \hat{\Phi})(\lambda_7, \lambda_3, \lambda_8, \lambda_1, \lambda_9, \lambda_2) \\
& \star (\hat{\mathcal{C}} \, \hat{\Phi})(\lambda_5, \lambda_8, \lambda_{10}, \lambda_7, \lambda_4, \lambda_3) \star (\hat{\mathcal{C}} \, \hat{\Phi})(\lambda_9, \lambda_{10}, \lambda_6, \lambda_5, \lambda_1, \lambda_8) \\
& \star (\hat{\mathcal{C}} \, \hat{\Phi})(\lambda_4, \lambda_6, \lambda_2, \lambda_9, \lambda_7, \lambda_{10}) \\
= \int \mathrm{d}\lambda^{30} \, & \Big(\hat{\mathcal{V}}(\{\lambda_{\alpha;i}\}) \star \Big((\hat{\mathcal{C}} \, \hat{\Phi})(\lambda_{1;1}, \lambda_{1;2}, \lambda_{1;3}, \lambda_{1;4}, \lambda_{1;5}, \lambda_{1;6}) \, (\hat{\mathcal{C}} \, \hat{\Phi})(\lambda_{2;1}, \lambda_{2;2}, \lambda_{2;3}, \lambda_{2;4}, \lambda_{2;5}, \lambda_{2;6}) \\
& (\hat{\mathcal{C}} \, \hat{\Phi})(\lambda_{3;1}, \lambda_{3;2}, \lambda_{3;3}, \lambda_{3;4}, \lambda_{3;5}, \lambda_{3;6}) \, (\hat{\mathcal{C}} \, \hat{\Phi})(\lambda_{4;1}, \lambda_{4;2}, \lambda_{4;3}, \lambda_{4;4}, \lambda_{4;5}, \lambda_{4;6}) \\
& (\hat{\mathcal{C}} \, \hat{\Phi})(\lambda_{5;1}, \lambda_{5;2}, \lambda_{5;3}, \lambda_{5;4}, \lambda_{5;5}, \lambda_{5;6}) \Big) \Big) \,,
\end{aligned}$$

is the *interaction term* whose amplitude is given by

$$\begin{aligned}\hat{\mathcal{V}} = &\Big(\delta(\lambda_{1;1}\lambda_{2;4}^{-1})\,\delta(\lambda_{1;1}\lambda_{4;5}^{-1})\Big)\,\Big(\delta(\lambda_{1;2}\lambda_{2;6}^{-1})\,\delta(\lambda_{1;2}\lambda_{5;3}^{-1})\Big)\,\Big(\delta(\lambda_{1;3}\lambda_{2;2}^{-1})\,\delta(\lambda_{1;3}\lambda_{3;6}^{-1})\Big)\\ &\Big(\delta(\lambda_{1;4}\lambda_{3;5}^{-1})\,\delta(\lambda_{1;4}\lambda_{5;1}^{-1})\Big)\,\Big(\delta(\lambda_{1;5}\lambda_{3;1}^{-1})\,\delta(\lambda_{1;5}\lambda_{4;4}^{-1})\Big)\,\Big(\delta(\lambda_{1;6}\lambda_{4;3}^{-1})\,\delta(\lambda_{1;6}\lambda_{5;2}^{-1})\Big)\\ &\Big(\delta(\lambda_{2;1}\lambda_{3;4}^{-1})\,\delta(\lambda_{2;1}\lambda_{5;5}^{-1})\Big)\,\Big(\delta(\lambda_{2;3}\lambda_{3;2}^{-1})\,\delta(\lambda_{2;3}\lambda_{4;6}^{-1})\Big)\,\Big(\delta(\lambda_{2;5}\lambda_{4;1}^{-1})\,\delta(\lambda_{2;5}\lambda_{5;4}^{-1})\Big)\\ &\Big(\delta(\lambda_{3;3}\lambda_{4;2}^{-1})\,\delta(\lambda_{3;3}\lambda_{5;6}^{-1})\Big)\,,\end{aligned} \tag{5.4.34}$$

that is associated with a combination of five tetrahedra (expressed in terms of their edge vectors) with the combinatorics of a 4-simplex[5].

As we explained, the tetrahedron wave function is related to the functions on the Lorentz group by a non-commutative Fourier transform, which in turn can be decomposed in the Fourier modes using the Plancharel decomposition or in the modes of the translation group. Therefore, using appropriately such decomposition with the non-commutative Fourier transform, it should not be hard to convince ourselves that also the propagator (5.4.33) and 4-simplex (5.4.34) amplitudes can be related to the usual GFT amplitudes. As in standard group field theory, the Feynman amplitudes of our GFT model are given by an arbitrary combination of 4-simplex amplitudes merged through propagator amplitudes. The partition function can thus be expanded as a sum over the Feynman amplitudes associated with four dimensional triangulations. A given triangulation Γ, is thus associated to the amplitude

$$\mathcal{A}_\Gamma = \int \mathrm{d}\alpha \mathrm{d}\alpha' \prod_{\tau\subset\Gamma} \mathcal{A}_\tau(\alpha,\alpha') \prod_{s\subset\Gamma} \mathcal{A}_s(\alpha,\alpha')\,. \tag{5.4.35}$$

The amplitude $\mathcal{A}_\tau$ associated to each tetrahedron of the triangulation is given by the propagator amplitude

$$\mathcal{A}_\tau(\alpha,\alpha') = \int \mathrm{d}\lambda^6\, T^{\alpha'_{1;\nu}}_{\alpha_{1;\nu}}(\lambda_2,\lambda_3)\, T^{\alpha'_{2;\nu}}_{\alpha_{2;\nu}}(\lambda_3,\lambda_5)\, T^{\alpha'_{3;\nu}}_{\alpha_{3;\nu}}(\lambda_6,\lambda_5)\, T^{\alpha'_{4;\nu}}_{\alpha_{4;\nu}}(\lambda_2,\lambda_6)\,, \tag{5.4.36}$$

while the amplitude $\mathcal{A}_s$, given by the interaction term, is associated to each 4-simplex of the triangulation

$$\begin{aligned}\mathcal{A}_s(\alpha,\alpha') = \int \mathrm{d}\lambda^{10}\, &T^{\alpha'_{1;\nu}}_{\alpha_{1;\nu}}(\lambda_2,\lambda_3)\, T^{\alpha'_{2;\nu}}_{\alpha_{2;\nu}}(\lambda_3,\lambda_5)\, T^{\alpha'_{3;\nu}}_{\alpha_{3;\nu}}(\lambda_6,\lambda_5)\, T^{\alpha'_{4;\nu}}_{\alpha_{4;\nu}}(\lambda_2,\lambda_6)\\ &T^{\alpha'_{5;\nu}}_{\alpha_{1;\nu}}(\lambda_3,\lambda_8)\, T^{\alpha'_{6;\nu}}_{\alpha_{2;\nu}}(\lambda_8,\lambda_9)\, T^{\alpha'_{7;\nu}}_{\alpha_{3;\nu}}(\lambda_2,\lambda_9)\, T^{\alpha'_{1;\nu}}_{\alpha_{4;\nu}}(\lambda_3,\lambda_2)\\ &T^{\alpha'_{8;\nu}}_{\alpha_{1;\nu}}(\lambda_8,\lambda_{10})\, T^{\alpha'_{9;\nu}}_{\alpha_{2;\nu}}(\lambda_{10},\lambda_4)\, T^{\alpha'_{2;\nu}}_{\alpha_{3;\nu}}(\lambda_3,\lambda_4)\, T^{\alpha'_{5;\nu}}_{\alpha_{4;\nu}}(\lambda_8,\lambda_3)\\ &T^{\alpha'_{10;\nu}}_{\alpha_{1;\nu}}(\lambda_{10},\lambda_6)\, T^{\alpha'_{3;\nu}}_{\alpha_{2;\nu}}(\lambda_6,\lambda_1)\, T^{\alpha'_{6;\nu}}_{\alpha_{3;\nu}}(\lambda_8,\lambda_1)\, T^{\alpha'_{8;\nu}}_{\alpha_{4;\nu}}(\lambda_{10},\lambda_8)\\ &T^{\alpha'_{4;\nu}}_{\alpha_{1;\nu}}(\lambda_6,\lambda_2)\, T^{\alpha'_{7;\nu}}_{\alpha_{2;\nu}}(\lambda_2,\lambda_7)\, T^{\alpha'_{9;\nu}}_{\alpha_{3;\nu}}(\lambda_{10},\lambda_7)\, T^{\alpha'_{10;\nu}}_{\alpha_{4;\nu}}(\lambda_6,\lambda_{10})\,.\end{aligned} \tag{5.4.37}$$

[5]Recall that in the above expressions we used the symbol $\star$ to emphasize that the field are non-commutative functions on $\mathbb{R}^4 \wedge \mathbb{R}^4$ with the noncommutativity arising by the canonical commutators between the creation and annihilation operators (5.1.15) of the harmonic oscillator.

As we hinted in (5.4.27), using a combination (5.3.15) with coefficients (5.1.25) for each field, plus a (non-commutative) Fourier transform, one can make contact between the amplitudes above and those of ordinary group field theory based on the Lorentz group. , realizes an explicit GFT duality between SF models and simplicial gravity path integrals. It also makes explicit how simplicial geometry is encoded in the GFT formalism.

5.5 Conclusion

We outlined the main steps and concepts towards the construction of a new SF model based on the quantization of edge vectors as the fundamental degrees of freedom. We first identified the relation between the infinite dimensional unitary irreducible representations of the Lorentz group with that of the translation group that becomes manifest in the harmonic oscillator basis. Using these tools, we sketched the classical picture of a triangle and that of a tetrahedron, where we identified the necessary constraints to be imposed on the set of edge vectors characterizing such geometric entities. We emphasized that the subspace of states identifying the bivector-tetrahedra is obtained by projecting on the skew-symmetric sector of the full space of the edge-tetrahedron, where the explicit expression of the change of variables is obtained via the same transformation defined (via expansors) at the level of single triangles. The obtained amplitude expression is in terms of edge vectors and we showed that we recover the BC model as a sector of this more general one. This is realized once we identify the skew symmetric part of the model and express it in terms of bivectors, as well in terms of unitary irreducible representations of the Lorentz group (at the quantum level). Let us stress that, the new model is not equivalent to the BC model, it is equivalent, as it is made clear in (5.4.2) to a combination of BC amplitudes with additional combinatorial relations. These can be viewed as gluing constraints. Finally, we showed that one can obtain the full amplitude also via GFT formulation based on the translation group. The obvious advantage in this construction is that the simplicial geometry is certainly fully encoded and manifest thanks to the edge length degrees of freedom.

The work outlined above is merely the first step towards tackling the problems plaguing the standard SF models. We list a few of them now. As we emphasized throughout this chapter, the formulation of the quantum geometry in terms of bivectors is lacking some geometrical input due to the restriction of the Hilbert space of states to the skew symmetric part. Whereas if we consider the construction of the triangle based on the edge vectors instead, we see there is no need to make any drastic restrictions and we have access to the full geometric content of the theory. In fact, this prescription brings a new element to the game, namely that of the *normal vector* to the tetrahedron. This additional degree of freedom should really be understood as encoding the extrinsic geometric information of the simplicial geometry and more importantly, relevant information to ensure $4d$ covariance of the intrinsic geometry. We will point out further research directions in chapter 8.

Chapter 6

Entanglement in superpositions of spin network states with different graph structures

The notion of spin networks popped up several times throughout this thesis. In chapter 3 as well in chapter 4 (section 4.3) we discussed how these quantum states of geometry enter the kinematical Hilbert space of the theory and explored several aspects they exhibit. In fact, in those chapters, we explored only their relevance to QG theories, but the scope of spin network states goes beyond that. As a matter of fact, they arise naturally in many fields of physics since they form a basis of gauge invariant functionals in Yang-Mills-like theories [185]. The cases we focused on so far handled only spin network states associated with a single graph structure. In this chapter, we study a generalization thereof, namely that of a superposition of spin networks with different graph structures. In fact, a striking feature of most QG approaches is that spacetime can be in a superposition of geometries [22, 186]. This is a genuine quantum gravitational sequel. As a matter of fact, it is also present at non-relativistic speeds and with gravity in the Newtonian regime [187–189]. Moreover, superpositions of graphs are naturally produced by the quantum dynamics of QG theories and thus we should expect these generic states to encode the full content of the quantum geometry at the microscopic kinematical level.
In this chapter and based on section 4.3, we explore further the quantum information content of such QG states for a bipartite system. In particular, we are interested in studying states involving superpositions of spin networks with various combinatorial structures, defining therefore the connectivities of the underlying graphs. These states represent the most general ones that live in the Hilbert space of GFT (and in some sense that of LQG). We start in section 6.1 by providing the general construction of a bipartite entanglement graph states that are in superposition. In particular, we focus on the GFT pre-Fock space, where the vertices of the graph, characterizing the spin network states, are *labeled* and thus *distinguishable*. In section 6.2, we investigate the quantification of the induced entanglement within such a superposition of quantum gravity states which is provided by the von

Neumann entropy (entanglement entropy). More precisely, we started by studying a simple example of the superposition of a pair of spin network entanglement graphs describing a bipartite system in section 6.2.1. We then generalized the discussion to include an arbitrary number of superpositions in section 6.2.2 and how they are related to those in LQG. Furthermore, we explore the quantum information characterization of the corresponding correlations. Up to this point, the language in which we construct the bipartite entanglement graph states is the pre-Fock one, therefore to take into consideration the Hilbert space of the full theory, we perform the second quantization of the derived superposed states in section 6.3 under certain assumptions.

6.1 Construction of bipartite quantum gravity states

The general approach to studying the entanglement entropy of states in bipartite quantum systems [190–192] and similarly in quantum gravity models relies on studying the tensor product structure of Hilbert spaces [28, 193–195]. However, particularly in a quantum gravity setting, one can distinguish two different approaches to studying the entanglement entropy of quantum states of geometry within a bipartite system [27, 196]. The first one relies on the standard tensor product of the Hilbert space of each region without including in the picture their respective boundary regions as well the associated degrees of freedom. Whereas the second route is more involved and does take such boundary- considerations into account. Hereby the Hilbert space of the bipartite system is different, which naturally results in contrasting entanglement entropies. In what follows, we briefly describe the two different decompositions of the bipartite Hilbert space and why we are more inclined to work with the tensor product one. Before delving into this comparison, we set the notation straight to describe a bipartite setting.
The quantum degrees of freedom of a system composed of two subsystems A and B live on a Hilbert space, that is given by the tensor product:

$$\mathcal{H} = \mathcal{H}_A \otimes \mathcal{H}_B \,. \tag{6.1.1}$$

For a state $|\psi\rangle$ in $\mathcal{H}$ given by the tensor product $|\psi_A\rangle \otimes |\psi_B\rangle$, the reduced density matrix of the subsystem A is defined by the partial trace over the subsystem B:

$$\rho_A = \mathrm{Tr}_B \, |\psi\rangle\langle\psi| \,, \tag{6.1.2}$$

and the entanglement entropy of the subsystem A is defined as the von Neumann entropy of the reduced density matrix in (6.1.2):

$$S_A = -\,\mathrm{Tr}\,(\rho_A \log \rho_A) \ . \tag{6.1.3}$$

Now, there are several reasons why we chose for the purposes of this work the tensor product structure of a given bipartite Hilbert space. To explore this point, let us first discuss the second common approach which is the edge modes decomposition [197, 198]. The basic

idea behind it is to consider bipartition of the vertices, where the degrees of freedom live on the latter; the Hilbert space associated with any set of vertices is, therefore, the tensor product of the Hilbert spaces of each individual one that reproduces the tensor product given in (6.1.1). In a lattice gauge theory, the degrees of freedom live on the links, so there is not such a simple tensor product decomposition. However, we can define a Hilbert space $\mathcal{H}_A$ first introduced in [199] where one can split the links that cross the boundary.

Through this cutting of the links, we end up with one endpoint in region A and another in region B and we are able to insert a new vertex on the boundary separating the two regions. This splitting of, what we will call the *boundary-crossing links*, induces a change on the level of the Hilbert spaces $\mathcal{H}_A$; the nodes in the interior are the only ones that reflect gauge invariance, whereas the boundary nodes are not. In restricting the gauge symmetry, degrees of freedom that were previously pure gauge are promoted to physical degrees of freedom. The Hilbert space $\mathcal{H}$ is not equal to $\mathcal{H}_A \otimes \mathcal{H}_B$, since the former is invariant under all gauge transformations, and the latter is invariant under only those gauge transformations that act trivially on the boundary. Thus instead of an isomorphism of Hilbert spaces, we have the embedding:

$$\mathcal{H} \to \mathcal{H}_A \otimes \mathcal{H}_B \,. \tag{6.1.4}$$

The entanglement entropy of any state in $\mathcal{H}$ can be defined by embedding the state into $\mathcal{H}_A \otimes \mathcal{H}_B$. In this case, there is a local boundary contribution due to these edge modes and a non-local contribution due to intertwiner entanglement [196, 200].

In our setting, as we highlighted in section 4.3 and section 3.3, the ordering of the spin network states in the GFT Hilbert space is different than that in the LQG one, this is summarized in Box 3.2 and the above inclusion of the boundary degrees of freedom in the structure of the Hilbert is still poorly understood in GFT. Therefore, as a first step towards understanding the properties of the general states of the theory, being in a superposition, their characteristics, and their versatility in computing expectation values of observables, we consider the conceptually simplest case of a tensor product of Hilbert space given by (6.1.1). Of course, this implies we are neglecting the contribution of the local degrees of freedom at the boundaries, however, we postpone such investigations to future work.

6.1.1 Bipartite Hilbert space and quantum states

In this section we start by presenting the construction of a GFT bipartite Hilbert space for the simplest set of states containing $N_{A/B}$ vertices, then we move on to studying the more general case of a *superposition of graph states* starting from the simplest case of a single entanglement graph state presented in section 4.3. For simplicity, we will work only with finite graphs having a finite number of nodes. We are interested in quantifying the entanglement between two regions, a region A defined by the set of graphs $\{\gamma\}$ and region B with a set of graph $\{\delta\}$, through their respective set of combinatorial structures. We denote the set of vertices that belong to the region A by $V_A = \{x_1 \cdots x_{N_A}\}$ and those

that belong to B by $W_B = \{y_1 \cdots y_{N_B}\}$, where N_A and N_B denote the total number of vertices (particles) in the respective regions (Hilbert spaces). The Hilbert spaces of the spin network graph state for these two regions yield:

$$\mathcal{H}_A = L^2\left(G^{d\times N_A}/G^{N_A}\right) = \bigotimes_{x=1}^{N_A} \mathcal{H}_x\,, \quad \mathcal{H}_B = L^2\left(G^{d\times N_B}/G^{N_B}\right) = \bigotimes_{y=1}^{N_B} \mathcal{H}_y\,, \tag{6.1.5}$$

where $\mathcal{H}_x$ and $\mathcal{H}_y$ are given by the single-vertex Hilbert space as in (4.3.4). Elements of these two Hilbert spaces ($\mathcal{H}_A$ and $\mathcal{H}_B$) can be represented in the spin basis by the following states:

$$|\psi_A\rangle = \bigotimes_{N_A} |f_x\rangle = \bigotimes_{N_A} \left(\bigoplus_{\vec{j}} \sum_{\vec{n}\iota} f^{\vec{j}}_{\vec{n}\iota}\, |\vec{j}\vec{n}\iota\rangle\right), \quad |\psi_B\rangle = \bigotimes_{N_B} |f_y\rangle = \bigotimes_{N_B} \left(\bigoplus_{\vec{j}'} \sum_{\vec{n}'\iota'} f^{\vec{j}'}_{\vec{n}'\iota'}\, |\vec{j}'\vec{n}'\iota'\rangle\right). \tag{6.1.6}$$

The Hilbert space of the bipartite system is then given by the tensor product:

$$\mathcal{H}_{AB} = \mathcal{H}_A \otimes \mathcal{H}_B\,. \tag{6.1.7}$$

Consequently, a state that lives on $\mathcal{H}_{AB}$ is then constructed by the following operation:

$$|\psi_A\rangle \otimes |\psi_B\rangle = \bigotimes_{N_A} |f_x\rangle \otimes \bigotimes_{N_B} |f_y\rangle\,. \tag{6.1.8}$$

We can also express the above state in the group representation and this reads:

$$|\psi_A\rangle \otimes |\psi_B\rangle = \int \prod_x \mathrm{d}\mathbf{g}^x \prod_y \mathrm{d}\mathbf{k}^x \psi\left(\mathbf{g}^1, \ldots, \mathbf{g}^{N_A}\right) \psi\left(\mathbf{k}^1, \ldots, \mathbf{k}^{N_B}\right) \otimes_x |\mathbf{g}^x\rangle \bigotimes \otimes_y |\mathbf{k}^y\rangle\,. \tag{6.1.9}$$

where $\mathbf{g}^x = \mathrm{g}^x_1, \ldots, \mathrm{g}^x_d$, and $|\mathbf{g}^x\rangle$ provide a basis for the single-vertex Hilbert space $\mathcal{H}^x$ and $\mathbf{k}^y = \mathrm{k}^y_1, \ldots, \mathrm{k}^y_d$, and $|\mathbf{k}^y\rangle$ provide a basis for the single-vertex Hilbert space $\mathcal{H}^y$.

Separability and entanglement. We emphasize here the notion of separability and entanglement in the constructed states. The N-particle wave function appearing in (6.1.8) cannot be written in a factorized form (as a product of single-vertex states), hence it is not separable and by definition *it is* entangled. This can be traced back to the fact that entanglement in our framework is translated into correlating the degrees of freedom living on the different vertices. Now, if for instance, we take the case of several nodes interconnecting through a superposition of spin states, the form of the resulting intertwiners wave function is in general *not* factorizable [35, 201]. However, it is possible to consider special cases where it is possible. This is the case when we consider fixed spins (not in superposition) attached to the vertices. In the spin representation, the vertices wavefunction takes the simplified form [36]:

$$\varphi^{\vec{j}_1\ldots\vec{j}_N}_{\vec{n}_1\ldots\vec{n}_{N_A}\iota_1\ldots\iota_{N_A}} = \prod_{x=1}^{N_A} (f_x)^{\vec{j}_x}_{\vec{n}_x\iota_x}\,, \tag{6.1.10}$$

where $(f_x)^{\vec{j}_x}_{\vec{n}_x \iota_x}$ is the wave function representing the vertex x as in (4.3.1). In our analysis, we will focus on graph states constructed out of this type of many-body wave function. This factorization plays an important role when we perform the explicit computations of the entanglement entropy captured by the reduced density matrix of the subsystems. Even though it simplifies the entropic calculation we present in the next sections, this simple case we are considering will not have any direct impact on the following more general conceptual point that we will raise.

Superposition and biadjacency matrix. The tensor product in (6.1.8) is the basis for constructing a class of states in which the set of vertices in the two graphs are connected according to a combination of patterns. Note that for each set of graphs, we consider certain patterns, where the connectivity for the graphs $\{\gamma\}$ is dictated by the respective adjacency matrices), that orchestrate the gluing of links with colors i. For the graphs $\{\delta\}$, it is encoded in the combinatorial set gluing links with colors j. This gluing mechanism naturally induces two types of connectivity, namely one that takes place between edges that belong only to the graphs $\{\gamma, \delta\}$ and another one that entangles links belonging to γ and links in δ. They have of course to share the same combinatorics, in the sense that there is an overlap in the respective patterns (γ, δ) or equivalently, they belong to the same class (or category) of combinatorics. This way, the set of bi-connecting links belongs to the two graphs. We denote such overlapping connectivity by a bracket of the respective patterns, where the reference graph comes always in first position. This bracket will appear as an index for the respective parameters[1].
After assigning an orientation to the set of edges where the group elements $\{g_i, k_j\}$ are associated with the outgoing direction of the spins, the operation of gluing vertices is made evident through forming three categories of entangled links:

1. For vertices (x_a and x_b)$\in \{V_{N_A}\}$ that are connected through a link of color i; they then form an internal link between the two vertices $l_x = (x_a, x_b; i)$, carrying the group element $g_{l_x} = g_i^{x_a x_b^{-1}}$.

2. For vertices (y_a and y_b)$\in \{V_{N_B}\}$ that are connected through a link of color j; they then form an internal link between the two vertices $l_y = (y_a, y_b; j)$, carrying the group element $k_{l_y} = k_j^{y_a y_b^{-1}}$.

3. For vertices (x_a and y_b)$\in \{V_{N_A}, V_{N_B}\}$ that are connected through a link of color $[i, j]$; they then form an internal link between the two vertices $l_z = (x_a, y_b; [i, j])$, carrying the group element $q_{l_z} = g_c^{x_a y_b^{-1}}$.

The construction of a superposition of graph states for a bipartite system is now presented. It is very important to understand the superposition of this class of states in terms of

[1]For instance if we take the graph γ_A for the region A as the reference graph governed by the pattern γ, then the bracket reads $[\gamma, \delta]$.

combinatorial structures. Each region is assigned a Hilbert space, where it is allowed to have a superposition of graph states endowed with different connectivity patterns. Then, the bipartite class of combinatorial states can be constructed using techniques borrowed from graph theory based on the notion of an adjacency- along with a *biadjacency* matrices for graphs, underlying the three types of entanglement governing the total system. The information about the connectivity of the graph is then implemented at the level of the gluing map as we will see shortly.

Biadjacency matrix. Let us consider a region A given by a graph defined through its combinatorial pattern γ and a region B and its graph δ. Then the combined total graph Γ_{AB} is specified by a matrix M_{AB}, called the *biadjanceny* matrix. Formally, let $G = (A, B, E)$ be a bipartite graph with distinct sub-graph $A = \{a_1, \ldots, a_r\}, B = \{b_1, \ldots, b_s\}$ and edges E. The biadjacency matrix is the $r \times s$ $(0-1)$ matrix M_{AB} such that the block matrix C has entries $c_{i,j} = 1$ if and only if $(u_i, v_j) \in E$. This is given by the following matrix:

$$M_{AB} = \begin{pmatrix} 0_{r,r} & C \\ C^{\top} & 0_{s,s} \end{pmatrix}, \tag{6.1.11}$$

where here C is an $r \times s$ matrix, and $0_{r,r}$ and $0_{s,s}$ represent the off diagonal $r \times r$ and $s \times s$ zero matrices. In this case, the block matrix C uniquely represents the bipartite graph. The total graph matrix including the internal connectivity between the set of vertices in the subgraphs γ and γ is then given by

$$G_{AB} = \begin{pmatrix} A_{r,r} & C \\ C^{\top} & B_{s,s} \end{pmatrix}, \tag{6.1.12}$$

where $A_{r,r}$ and $B_{r,r}$ are the $r \times r$ and $s \times s$ adjacency matrices for the graphs Γ_A and Γ_B respectively and they are given by

$$A_{x_a+i,x_b+j} = \begin{cases} a^i_{x_a x_b} & i = j \\ 0 & i \neq j \end{cases}, \quad B_{y_c+i,y_d+j} = \begin{cases} b^i_{y_c y_d} & i = j \\ 0 & i \neq j \end{cases} \tag{6.1.13}$$

where the indices (a, b) and (c, d) label the vertices in the graphs γ and γ and they run from $(a, b) \in \{1 \cdots N_A\}$ and $(c, d) \in \{1 \cdots N_B\}$.
In order to establish a bipartite entanglement within such graph structures, we rely on a gluing procedure (section 4.3) performed between links of the two subgraphs γ and γ manifesting the same combinatorial pattern. In this case, we introduce the bipartite gluing map which acts on the links belonging to the Hilbert spaces $\mathcal{H}_A$ and $\mathcal{H}_B$ that connect two vertices by gluing their open links of color i is equivalent to the projection map $\mathbb{P}_i^{x\otimes y} : \mathcal{H}_A^{x_i} \otimes \mathcal{H}_B^{y_i} \to \mathrm{Inv}_R\left(\mathcal{H}_A^{x_i} \otimes \mathcal{H}_B^{y_i}\right)$ defined as follows:

$$\mathbb{P}_i^{x\otimes y} := \int dh_i^{xy} dg_i^x dg_i^y \, |g_i^x\rangle \langle g_i^x h_i^{xy}| \otimes |g_i^y\rangle \langle g_i^y h_i^{xy}|, \tag{6.1.14}$$

where $h_i^{xy} = h_i^{yx}$. Allowing internal gluing (connectivity) is translated into applying this gluing map on the bipartite wavefunction in (6.1.8) which will act on the internal links in each Hilbert space $\mathcal{H}_A$ or $\mathcal{H}_B$ through the specific implementation of the adjacency matrix, where the map then reads

$$\mathbb{P}_{\mathcal{B}} = \prod_{x_a<x_b} \prod_{y_c<y_d} \prod_{i:a_{x_a x_b}=1} \prod_{j:b_{y_c y_d}=1} \mathbb{P}_i^{x_a \otimes x_b} \mathbb{P}_j^{y_c \otimes y_d} \,. \tag{6.1.15}$$

For those links that are shared between the two sets of graphs, we consider the data encoded in the biadjacency matrix M_{AB} in (6.1.11) and refer to it as the boundary gluing map

$$\mathbb{P}_{\partial} = \prod_{p:c_{z_e z_f}=1} \prod_{z_e<z_f} \mathbb{P}_c^{z_e \otimes z_f} \,. \tag{6.1.16}$$

where the set of vertices $\{z_e, z_f\}$ belong either to γ or δ. Here we also introduce the new pattern notation $p_c \in [\gamma_i, \delta_j]$. The connected bipartite state is obtained after successfully having operated with the maps (6.1.16) and (6.1.15) yields:

$$|\Psi\rangle = \mathbb{P}_{\mathcal{B}} \mathbb{P}_{\partial} |\psi\rangle \,. \tag{6.1.17}$$

6.1.2 Superposition of entangled bipartite graph states

Now that we are well equipped with the appropriate Hilbert space and quantum states, we can address the case of an arbitrary superposition of states containing a fixed number of quanta of space and then proceed to derive its entanglement entropy. As we described in section 4.3, each individual state entering the superposition corresponds, generically, to an inhomogeneous discrete (simplicial) geometry[2] which is also evident at the level of the total Hilbert space of the theory. In this section, we present the construction of entangled bipartite quantum states of geometry that are in superposition. We illustrate roughly the procedure in figure 6.1.

As we argued in section 4.3, we realize the calculations in the case where the corresponding bipartite Hilbert space is a tensor product and the states take the following form:

$$|\Psi\rangle = |\psi_A\rangle \otimes |\psi_B\rangle \in \mathcal{H}_{AB} \,. \tag{6.1.18}$$

Let us denote by $\mathcal{N}_A$ the total number of combinatorial patterns γ_i governing the set of graphs of the region A and by $\mathcal{N}_B$ the total number of the ones governing region B[3]. We will refer to these numbers as *the degrees of combinatorial structure* of the graphs, which should not be confused with the total number of the graph vertices. Since we are

[2]This is considered true with some exceptions. In fact, the superposed graph states may also include states associated with triangulations of regular combinatorial structure as well as homogeneous assignment of discrete data [22, 131].

[3]We can also understand the combinatorial degree as the cardinality of the set of the superposed graphs.

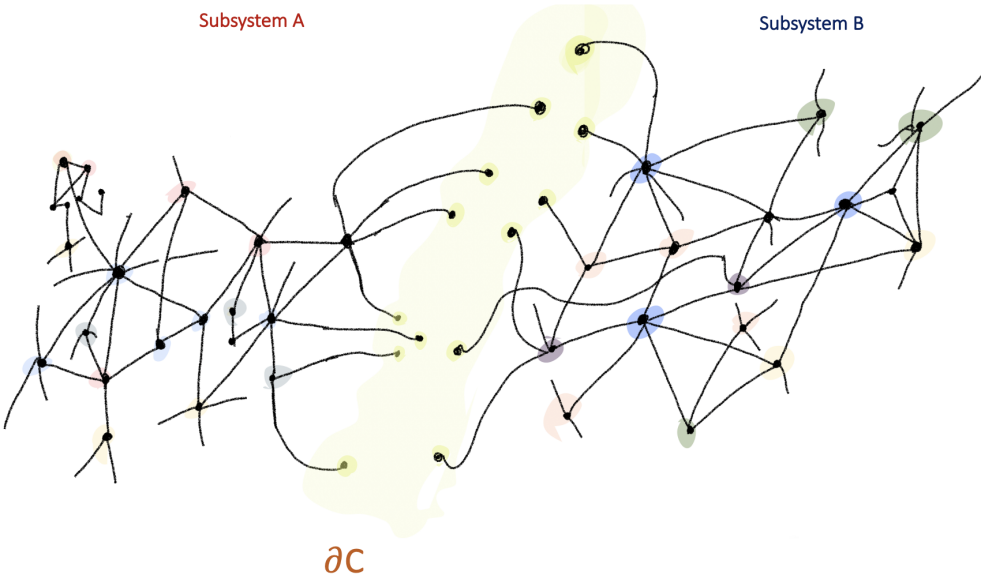

Figure 6.1: Bipartite system consisting of region A and region B. Each region entails a superposition of different connectivity patterns, that can be internally correlated along common edges. The bipartite boundary ∂C is defined as the overlapping sector of the correlations such that it does not coincide with the internal gluing data.

considering a superposition of states in each subsystem and their connectivity properties, we can write $|\psi_A\rangle$ and $|\psi_B\rangle$ with arbitrary combinatorial degrees living on $\mathcal{H}_A$ and $\mathcal{H}_B$ as

$$|\psi_A\rangle = \sum_{\gamma} \alpha_{\gamma_i} |\psi_i\rangle \ , \quad |\psi_B\rangle = \sum_{\delta} \beta_{\delta_j} |\psi_j\rangle \ , \tag{6.1.19}$$

where α_{γ_i} are the coefficients encoding the information of the wave function of each graph γ_i entering the superposition. Note that states entering such superpositions are not a priory entangled. This can be implemented by performing the link-entangling procedure discussed in section 6.1.1 that we will perform shortly. First, let us write down the most generic state that describes the total bipartite system, which is given by the tensor product of the subregion's superposition

$$|\Psi\rangle = \sum_{k=0}^{\mathcal{N}_A+\mathcal{N}_B} \sum_{s=0}^{k} \alpha_{\gamma_s}\beta_{\delta_{k-s}} |\psi_s\rangle |\psi_{k-s}\rangle \equiv \sum_{k=0}^{\mathcal{N}_A+\mathcal{N}_B} \tilde{\xi}_k |\tilde{\Gamma}_k\rangle \ , \tag{6.1.20}$$

where k and s are Cauchy product indices keeping track of the different summation over the products and the state $|\tilde{\Gamma}_k\rangle$ is an element of the total Hilbert space $\mathcal{H}_{AB}$. Now, before proceeding to the entangling procedure, let us mention that there are two ways to establish it in such a class of states:

1. The first possibility we encounter is, we could entangle pair of states entering the superposition in the respective Hilbert space $\mathcal{H}_{A/B}$ by applying the gluing map in

(6.1.15) according to the connectivity pattern characterized by the adjacency matrix, and do that for each degree of combinatorial structure. Once this step of *internal gluing* in each subsystem is achieved, we proceed in a similar manner to entangling the bipartite total state given by the tensor product in (6.1.18) of the system by gluing *common links* in the two subsystems. This is of course obtained by acting with the map (6.1.16) encoding the biadjacency matrix entries (M_{AB}).

2. As for the second option, we could take the entire graph states (6.1.20) living in $\mathcal{H}_{AB}$ and entangle them directly and randomly (using the maps (6.1.15) and (6.1.16)). However, this procedure does not allow us to keep track of the gluing operation. Hence, the complexity level of the task rises for no apparent useful reason.

The two methods should theoretically keep the same degrees of freedom intact and we assume that no information is lost in both processes. Therefore, we follow the first proposition (1) of connecting the graphs in the two subsystems and then proceed to entangle the entire bipartite system.
To be more precise and concrete, let us consider for instance the superposition of $\mathcal{N}_A$ states in the $A-$system and proceed to entangle these. This amounts to working with states $|\psi_A\rangle \in \mathcal{H}_A$, where we use the gluing operation (6.1.14). Consequently, in the group basis, the connectivity is mirrored in the group averaging procedure and the entangled state reads:

$$|\psi_A\rangle = \sum_{\gamma_i} \mathbb{P}_{\mathcal{B}}\left(\alpha_{\gamma_i} |\psi_{\gamma_i}\rangle\right) = \sum_{\gamma_i} \int \prod_x \mathrm{d}g^x \int \prod_{x<t_{\gamma_i}} \mathrm{d}h^{xt_{\gamma_i}} \psi_i \left(\left\{g^x_{\gamma_i} h^{xt_{\gamma_i}}_{t_{\gamma_i}}\right\}\right) \otimes_x |g^x_{\gamma_i}\rangle \ ,$$

where the sum is over the different combinatorial patterns $\{\gamma_i\}$ (i is the index running from $1, \cdots, \mathcal{N}_A$), $\mathrm{dh}^{yt_\gamma(x)} := \mathrm{dh}_1^{xt^1_{\gamma_i}} \cdots \mathrm{dh}_{d_A}^{xt^d_{\gamma_i}}$, and the gluing map acts according to the adjacency matrix characterizing the entanglement on the vertices $\{x_a, x_b\} \in \{1, \cdots, V_{N_A}\}$: consequently encoded in the tensor[4] $t_{\gamma_i}(x)$. In the spin network basis the resulting state is given by:

$$|\psi_A\rangle = \sum_{\gamma_i} \sum_{\vec{n}_{\partial\gamma_i}} \sum_{\vec{\iota}} (\psi_{\gamma_i})^{\vec{\iota}}_{\vec{n}_{\partial\gamma_i}} \bigotimes_{l\in\partial\gamma_i} |\vec{j}_l \vec{n}_l\rangle \otimes \bigotimes_x |\vec{j}_x \vec{\iota}_x\rangle \ , \tag{6.1.21}$$

where $\vec{n}_{\partial\gamma_i}$ are the magnetic indices associated with the open semi-links defining the boundary of the graphs associated with the combinatorial degree γ_i, $\vec{\iota} = \{\iota_1, \cdots, \iota_{N_A}\}$ are the intertwiners identified with the vertices, whereas the internal connectivity is encoded in the coefficients $(\psi_{\gamma_i})^{\vec{\iota}}_{\vec{m}_{\partial\gamma_i}}$ which entail the gluing formula encoded in the product of the delta functions:

$$(\psi_{\gamma_i})^{\vec{\iota}}_{\vec{n}_{\partial\gamma_i}} = \sum_{\{n_{e\in L_A}\}} \sum_{\{p\}} \prod_{x=1}^{N_A} \left(\phi^{\vec{j}}_{\vec{n}\iota}\right)^x \prod_{l_{\gamma_i}\in L_A} \delta_{n^i_x p^{xx'}_i} \delta_{n^i_{x'} p^{xx'}_i} \ . \tag{6.1.22}$$

[4]Recall that this is the tensor encoding the combinatorial pattern of the graph such that $t_{\gamma_i}(x_a) = x_b$ if $a^i_{x_a x_b} = 1$, and $t_{\gamma_i}(x) = 0$ if $a^i_{x_a x_b} = 0$; the gluing elements $h_i^{xt_{\gamma_i}}$ are such that $h_i^{x_a x_b} = h_i^{x_{ab}}$, and $h_i^{x0} = e$.

The resulting wavefunction of the state $|\psi_A\rangle$ is then associated to graphs with

$$\text{Internal links:} \quad L_A = \sum \ell_{\gamma_i} = (x, t_{\gamma_i}(x); \{\gamma_i\}) \ , \tag{6.1.23}$$

$$\text{Boundary open links:} \quad L_{\partial A} = \sum \ell_{\partial\gamma_i} = (x, t_{\gamma_i}(x); \{\gamma_i\}) \ . \tag{6.1.24}$$

Note that these boundary links (yet open) carry the quantum data to realize the boundary gluing with region B later on. In the same manner, the entangled $\mathcal{N}_B$ superposition of states $|\psi_B\rangle \in \mathcal{H}_B$ is constructed according to all the combinatorial patterns $\{\delta_j\}$ encoded in the adjacency matrix in $B_{r,r}$ given in (6.1.13) and it yields

$$|\psi_B\rangle = \sum_{\delta_j} \sum_{\vec{m}_{\partial\delta_j}} \sum_{\vec{\iota}'} \left(\psi_{\delta_j}\right)^{\vec{\iota}}_{\vec{m}\partial_{\delta_j}} \bigotimes_{l\in\partial\delta_j} |\vec{j}_l \vec{m}_l\rangle \otimes \bigotimes_y |\vec{j}_y \vec{\iota}'_y\rangle \ , \tag{6.1.25}$$

where similarly, the wavefunction of the resulting state $|\psi_B\rangle$ is then identified with the graph having internal links $L_B = \sum \ell_{\delta_j} = \left(y, t_{\delta_j}(y); \{\delta_j\}\right)$. Notice once again, the coefficients encode the internally correlated vertices of the graphs and they are given by:

$$\left(\psi_{\delta_j}\right)^{\vec{\iota}}_{\vec{m}\partial\delta_j} = \sum_{\left\{m_{e\in L_B}\right\}} \sum_{\{r\}} \prod_{y=1}^{N_B} \left(\phi^{\vec{j}}_{\vec{m}\iota}\right)^y \prod_{l_{\delta_j}\in L_B} \delta_{m^j_y r^{yy'}_j} \delta_{m^j_y r^{yy'}_j} \ . \tag{6.1.26}$$

The bipartite (unentangled) state is given by the tensor product of the states (6.1.21) and (6.1.25). Now, by applying the map (6.1.16) to the state (6.1.18), namely that $|\Psi_\Gamma\rangle = \mathbb{P}_\partial |\Psi\rangle$, we obtain the final bipartite entangled state:

$$\begin{aligned} |\Psi_\Gamma\rangle = \sum_{s=0}^{\mathcal{N}^A+\mathcal{N}^B} \sum_{k=0}^{s} \Bigg(\sum_{\vec{m}_{\partial\gamma_i}} \sum_{\vec{\iota}_{\gamma_s}} \sum_{\vec{m}_{\partial_{[sk]}}} \sum_{\vec{\iota}_{[sk]}} \left(\psi^{\vec{\iota}}_{m_{\partial_{[sk]}}}\right)_{[sk]} \bigotimes_{l\in\partial\gamma_i} |\vec{j}_{l_{\gamma_s}} \vec{m}_{l_{\gamma_s}}\rangle \bigotimes_{l\in\partial_{[sk]}} |\vec{j}_{l_{[sk]}} \vec{m}_{l_{[sk]}}\rangle \otimes \bigotimes_x |\vec{j}_x \vec{\iota}_x\rangle \Bigg) \\ \times \left(\sum_{\vec{m}_{\partial\delta_k}} \sum_{\vec{\iota}'} \left(\psi^{\vec{\iota}}_{\vec{m}\partial_{\delta_k}}\right)_{\delta_k} \bigotimes_{l\in\partial\delta_k} |\vec{j}_{l_{\delta_k}} \vec{m}_{l_{\delta_k}}\rangle \otimes \bigotimes_y |\vec{j}_y \vec{\iota}'_y\rangle \right) \ , \end{aligned} \tag{6.1.27}$$

where we considered the graphs in region A as the reference ones with which we connect the vertices to those in the region B, hence the compact notation in the wavefunction's coefficients is given by

$$\left(\psi^{\vec{\iota}}_{m_{\partial_{[sk]}}}\right)_{[sk]} = \sum_{\left\{n_{l\in L_A}\right\}} \sum_{\left\{n_{l\in L_A\cup L_B}\right\}} \sum_{\{p\}} \sum_{\{r\}} \prod_x (\phi)^{\vec{j}_x}_{\vec{n}_x \iota_x} \prod_{l_{\gamma_i}\in L_A} \delta_{n^i_x p^{xx'}_i} \delta_{n^i_{x'} p^{xx}_i} \prod_{l_{\gamma_i}\in L_A\cup L_B} \delta_{n^i_x r^{xy}_i} \delta_{n^j_y r^{xy}_j} \ , \tag{6.1.28}$$

and the numbers s, k are running indices. s runs from γ_1 till $\gamma_{\mathcal{N}_A}$, whereas k takes values from δ_1 till $\delta_{\mathcal{N}_B}$. We recall that $[i, j]$ denotes the set of overlapping connected edges belonging simultaneously to both graphs constructed out of the respective entanglement pattern (biadjacency matrix).
Let us define by $\partial C_{[\gamma_i,\delta_j]}$ the outer boundary of the bipartite graph, that contains the open

links resulting from the gluing according to the patterns $(\gamma_i, \delta_j, [\gamma_i, \delta_j])$. The bipartite superposition of entangled states in (6.1.27) can be expressed as:

$$\begin{aligned}|\Psi_\Gamma\rangle &= \sum_{k=0}^{\mathcal{N}^A+\mathcal{N}^B} \sum_{s=0}^{k} \sum_{m_{l\in\partial C_{[\gamma_i\delta_j]}}} \sum_{\vec{\mathcal{J}}} \left(\psi^{\vec{\iota}}_{m_{l\in\partial C_{[\gamma_i\delta_j]}}}\right)_{s,k} \bigotimes_{l\in\partial C_{[\gamma_i\delta_j]}} |\partial_{\gamma_i\delta_j}\rangle \otimes \bigotimes_{x,y} |\vec{j}_{x,y}\vec{\mathcal{J}}_{x,y}\rangle \\ &= \sum_{k=0}^{\mathcal{N}_A+\mathcal{N}_B} \xi_k \, |\Gamma_k\rangle \ , \end{aligned} \tag{6.1.29}$$

where we denoted by $\vec{\mathcal{J}}_{x,y}$ the set of all intertwiners living on the bipartite Hilbert space. The index k is equivalent to the one running in the second sum representing the graph data in the region B with the combinatorial degrees $\{\delta\}$. For completeness, we identify the bipartite spin basis:

$$\begin{aligned}|\Gamma_k\rangle &= \bigotimes_{l\in\partial\gamma_i} |j_{l_{\gamma_i}} n_{l_{\gamma_i}}\rangle \bigotimes_{l\in\partial_{[ik]}} |j_{l_{[ik]}} n_{l_{[ik]}}\rangle \bigotimes_{l\in\partial\delta_k} |j_{l_{\delta_k}} m_{l_{\delta_k}}\rangle \otimes \bigotimes_{x} |\vec{j}_x \vec{\iota}_x\rangle \otimes \bigotimes_{y} |\vec{j}_y \vec{\iota}'_y\rangle \\ &= \bigotimes_{l\in\partial C_{[\gamma_i\delta_j]}} |\partial_{\gamma_i\delta_j}\rangle \otimes \bigotimes_{y,x} |\vec{j}_{x,y}\mathcal{J}_{x,y}\rangle \ , \end{aligned} \tag{6.1.30}$$

and the coefficients functions are given by (6.1.27). In the last step, one should keep track of the summation over the different labeling of the graph wavefunction, since we are dealing with polynomial indexing.

Now, let us briefly comment on the constructed states underlying the internal and bipartite connectivity of the graphs in (6.1.21), (6.1.25), and (6.1.27). Notice that there are different patterns braiding the boundary-crossing edges. One can distinguish the subset that carries $\{\gamma_i\}$, an other one is associated to the combinatorics of $\{\delta_j\}$ and obviously another subset with $[\gamma_i, \delta_j]$. This distinguishability on the level of boundary degrees of freedom induces further subtleties on the level of the respective intertwiners. Indeed, the wavefunction of N-vertices might bear a mixture of intertwiners that simultaneously encode the entanglement of one subset of the above-mentioned links or a combination of them. This in return is still in accordance with the non-separability criteria, any entangled state should obey. However, as we already mentioned in section 6.1, we will focus on vertices-factorized form for the sake of computational simplicity. It is then worth emphasizing that the usual criteria of non-separability, in this case, is automatically insured in the very definition of the gluing procedure. This is also clearly manifest in the gluing formula that results from such an entangling step. Moreover, it is important to mention for later use, that at the level of the graph matrices depicting the entangled superposition of the bipartite states, the matrix in (6.1.11) is also to be considered in superposition. The class of superposed states constructed above depicts spin network states with open ends that live on the GFT Hilbert space (4.3.6). The same construction can also be discussed for the case of LQG square integrable functions. The kinematical Hilbert space of the latter is built out of these graph-based Hilbert spaces, for all possible graphs and modulo some equivalence relations by imposing cylindrical consistency conditions [157] (see section 4.3), where the Hilbert

space of a single graph is given by $\mathcal{H}_{LQG} = L^2(G^L/G^V)$. As we mentioned in chapter 4 and also in section 3.3.2, it is possible to embed such structures in the GFT Hilbert space by means of the group averaging technique. For the bipartite state derived above, this will then reads for the internal glued version

$$\Psi_\gamma\left(\left\{g_{\ell_\gamma} = g_i^{x_a} g_i^{x_b^{-1}}, k_{\ell_\delta} = k_j^y k_j^{y_b^{-1}}\right\}\right) = \sum_\gamma \sum_\delta \int \left(\prod_{\ell_x \in \gamma} \mathrm{d}h_{\ell_\gamma} \prod_{\ell_y \in \delta} \mathrm{d}h'_{\ell_\delta}\right) \psi\left(\ldots, g_i^{x_a} h_\ell, \ldots, g_i^{x_b} h_\ell, \ldots, k_j^{y_a} h'_\ell, \ldots, k_i^{y_b} h'_\ell, \ldots\right), \tag{6.1.31}$$

where the gluing is performed over the set of links l_y and l_x belonging in the set graphs $\{\gamma\}$ and $\{\delta\}$ respectively. The bipartite boundary gluing can also be carried out for the superposition. Recall that we denoted for simplify p_c the gluing pattern taking place at the boundary, this us be then implemented,

$$\Psi_{LQG}\left(\{g_{\ell_\gamma}\}, \{k_{\ell_\delta}\}, \{z_{p_c}\}\right) = \sum_\gamma \sum_\delta \sum_{p_c} \int \prod_{\ell_x \in \gamma} \mathrm{d}h_{\ell_\gamma} \prod_{\ell_y \in \delta} \mathrm{d}h'_{\ell_\delta} \mathrm{d} \prod_{p_c} h''_{\ell_{p_c}}$$
$$\psi\left(\ldots, g_i^{x_a} h_\ell, \ldots, g_i^{x_b} h_\ell, \ldots, k_j^{y_a} h'_\ell, \ldots, k_i^{y_b} h'_\ell, \ldots, q_c^{z_b} h''_\ell, \ldots, q_c^{z_b} h''_\ell, \ldots\right), \tag{6.1.32}$$

This form of the wave function is then the embedding of the LQG bipartite superposed spin network state in the GFT Hilbert space 4.3.6. It is merely the generalization of the case of a single entanglement graph studied in [36]. Now that we constructed superposed spin network states that can be interpreted as a superposition of entanglement graphs, let us investigate the quantification of the correlations in such a case.

6.2 Interference of quantum geometries

In this section, we derive the entanglement entropy associated with the above-described bipartite system, where each subsystem A and B is considered to be in a superposed quantum state of geometries. The superposition of quantum gravity state characterized by the total number of combinatorial $\mathcal{N} = \mathcal{N}_A + \mathcal{N}_B$ is given by (6.1.29). Due to the peculiar properties of quantum superposition, we will see in this section how the von Neumann entropy is affected by it and the advantages we end up with when we consider the GFT entanglement graph states. We start by deriving from the density matrix of the state (6.1.29) the corresponding entropy, whereby we distinguish two cases, namely that of equal graph size in the bipartition and that of different size one.
In order to clearly grasp the combinaotrial nature of this class of states characterizing the GFT theory, we start by a toy model where step by step build a superposition of two states in each region of the bipartite system, keeping track of the different kinds of connectivities defining the entangled bigrahs.

6.2.1 Toy model for a superposition of bipartite states

Bipartite entanglement entropy. Let us consider the simplest case where we have a single vertex in the region A and another one in the region B and study the entanglement measure induced by gluing a single shared link between them. For now, we focus on the case of four valent vertices and comment on its generalization to d valent ones. The procedure of connecting the two vertices amounts to gluing one of the four links associated with them as illustrated in figure 4.3. In the spin network basis, this reads

$$\int \mathrm{d}h\, \psi(g^1,\dots,g^4h,k^1,\dots,k^4h) = \sum_{\vec{j}\vec{j}'} \sum_{\vec{n}\vec{n}'\iota\iota'} \psi^{\vec{j}\vec{j}'}_{\vec{n}\vec{n}',\iota\iota'} \int \mathrm{d}h\, S^{\vec{j}}_{\vec{n},\iota}(g^1,\dots,g^4h)\, S^{\vec{j}'}_{\vec{n}',\iota'}(k^1,\dots,k^4h)\,, \tag{6.2.1}$$

where g^i and k^j for $(i,j)=(0,\cdots 4)$ are the group elements decorating the links in each region and the wavefunction of the r.h.s is the bipartite wavefunction. In the above equation, the integration is performed over the gluing element h and after having explicitly exploited the expression for the spin network basis given by (6.1.30). As we already mentioned in section 4.3, this is equivalent to the operation of group averaging at the level of the GFT bipartite wavefunction, which is, in turn, equivalent to projecting the associated state onto a maximally entangled link-states given by (4.3.12).
Now, in this simple case, it is easy to show that on this basis, entangling degrees of freedom living on the vertices is equivalent to gluing links that share the same color. If we consider for instance gluing the spin $j=4$ we get

$$\int dh\, \psi(g^1,\dots,g^4h,q^1,\dots,k^4h) = \sum_{\vec{j}\vec{j}'} \sum_{\vec{n}\vec{n}'\iota\iota'} \sum_{pp'} \left(\psi^{\vec{j}\vec{j}'}_{\vec{n}\vec{n}',\iota\iota'}\delta_{jj'}I_{nn'}\right) S^{jj}_{\vec{n}_{123}p,\iota}(\vec{g}) S^{j'j}_{\vec{n}'_{123}p',\iota'}(\vec{k}) I_{pp'} \tag{6.2.2}$$

and after integration over the system B degrees of freedom, it is easy to show that the entanglement entropy of the reduced density matrix reads

$$S(\rho_A) = S(\rho_B) = \log D_j\,, \tag{6.2.3}$$

where D_j is the dimension of the representation space V^j of the glued link. Let us push this further, and glue another link in this bipartite graph, the entropy increases with another factor associated with the dimension of the representation space of the second glued link. Therefore we can detect a systematic increment for a generic d-valent vertex contribution to the entropy which can be formally described in terms of the links ℓ carrying a color i and connecting a vertex x (in A) and y (in B) through

$$\ell : (x,y:i) \to \log\left(D_{j_i}\right)\,, \tag{6.2.4}$$

$$\forall i \in \{0\cdots d\}\,, \ell_i : (x,y:\{i\}) \to \log\left(\prod_i D_{j_i}\right) = \sum_i \log\left(D_{j_i}\right)\,. \tag{6.2.5}$$

Now that was for the case of a *single* vertex. The situation changes drastically if we consider an arbitrary number of them, since the dimension of the intertwiner space, labeling the

vertices, will also play an important role in the entangling procedure. If we have for instance N_A vertices in the region A, we get a contribution in the entropy coming from each vertex of the form

$$D[\mathcal{I}_x] \equiv D_{\vec{j}} \times d_{j_1} \times \cdots \times d_{j_d} \,, \quad \to \log\left(D[\mathcal{I}_x]\right) \,, \tag{6.2.6}$$

This can be further generalized a the level of each graph by means of the adjacency matrix. The entries of such a matrix as binary ones of the nature $(0,1)$ and they are sort of the manual that encodes all the information we need to know about the connectivity of a graph, let's say γ. Using these tools we can right (6.2.6) in the more general way for each graph localized in the system A (and similarly also for the B)

$$D[\gamma] \equiv \prod_{a^i_{x_a,x_b}} D[\mathcal{I}_x] = \prod_{a^i_{x_a,x_b}} D_{\vec{j}} \prod^{d} d_{j_i} \,, \to \log\left(D[\gamma]\right) \,, \tag{6.2.7}$$

where now we denote the dimension of intertwiners space underlying the graph by $D[\gamma]$. Notice that it is only because we are considering the case of factorized graph wavefunctions over the single vertex one that we are able to write the above implications. It can be generalized to the case the vertex wavefunctions are not factorized, however, this is very poorly understood for the case of a superposition. Moreover, it is clear that in the above case, and through the operation of group averaging the resulting entanglement entropy for an entanglement graph in GFT and LQG coincide. This is not always the case as we will see below.

Superposing entanglement graph states. Let us consider the more complicated case of superposing two entanglement graph states in each region A and B. As we discussed in the above section, we start by constructing the bipartite entangled state. The first step is to entangle each state in each region separately. Therefore we let the gluing map (6.1.14) act on the graphs γ_1 and γ_2 in the system A. This amounts to working with states $|\psi_A\rangle \in \mathcal{H}_A$ of the form:

$$|\psi_A\rangle = \mathbb{P}_{\mathcal{B}}\left(\alpha_{\gamma_1}|\psi_1\rangle + \alpha_{\gamma_2}|\psi_2\rangle\right) \tag{6.2.8}$$

$$= \sum_{\left\{n_{l\in\partial\gamma_1}\right\}} \sum_{\vec{\iota}} \left(\psi_{\gamma_1}\right)_{\{m_l\in\partial\gamma_1\}\vec{\iota}} \bigotimes_{l\in\partial\gamma_1} |j_l n_l\rangle \otimes \bigotimes_x |\vec{j}_x \vec{\iota}_x\rangle + \sum_{\left\{m'_{l\in\partial\gamma_2}\right\}} \sum_{\vec{\iota}} \left(\psi_{\gamma_2}\right)_{\{m_l\in\partial\gamma_2\}\vec{\iota}} \bigotimes_{l\in\partial\gamma_2} |j_l m_l\rangle \otimes \bigotimes_{x'} |\vec{j}_{x'} \vec{\iota}_{x'}\rangle \tag{6.2.9}$$

where the tensor product defined above $\bigotimes_{l\in\partial\gamma_i}$ defines the projection onto the maximally entangling link state of the edge specifying the combinatorial pattern of the graph γ_i. The set of magnetic indices associated with the internal links are denoted by $m_{l\in\gamma_i}$ and the open ones living (basically defining) the boundary are labeled by $m_{l\in\partial\gamma_i}$. In the same manner, the entangled superposition of graphs in B is obtained from the graphs δ_1 and δ_2. The

wavefunction of the resulting state $|\psi_{\delta_1}\rangle$ is then identified with the graph having internal links $\ell_{\delta_1} = (y, t_{\delta_1}(y); j)$ and the same applies for δ_2. The bipartite state is given by the tensor product of the above states and we can then proceed to performing the boundary gluing procedure.

This can be realized by applying the gluing map again according to the biadjacency matrix encoded in C:

$$|\Psi_\Gamma\rangle = \prod_{c:m_{z_e z_f}=1} \prod_{\{z_e<z_f\}} \mathbb{P}_c^{z_e\otimes z_f} |\Psi\rangle = \mathbb{P}_\partial |\Psi\rangle \ . \tag{6.2.10}$$

Note that we introduced p_c the class of patterns that overlap or belong to the same class of connectivity. In the case of a simple superposition of two states for each Hilbert space, we can write all possible combinations of such patterns as $p_c = [P[\gamma_i], P[\delta_j]] = [\gamma_1\delta_1, \gamma_1\delta_2, \gamma_2\delta_1, \gamma_2\delta_2]$. This is translated in the wave function of the bipartite graph implementing the boundary gluing, we obtain the more general entangled bipartite state

$$\begin{aligned}
|\Psi_\Gamma\rangle = &\sum_{\{m_{l\in\partial\gamma_1}\}} \sum_{\vec{\iota}_{\gamma_1}} \sum_{\{m_{l\in\partial_{[11]}}\}} \sum_{\vec{\iota}_{[11]}} \left(\left(\psi_{[11]}\right)^{\vec{\iota}_{[11]}}_{\{m_l\in\partial\}} \right) \bigotimes_{l\in\partial\gamma_1} |j_{l_{\gamma_1}} m_{l_{\gamma_1}}\rangle \bigotimes_{l\in\partial_{[11]}} |j_{l_{[11]}} m_{l_{[11]}}\rangle \otimes \bigotimes_x |\vec{j}_v \iota_x\rangle \\
&\times \left(\sum_{\{m_{l\in\partial\delta_1}\}} \sum_{\vec{\iota}_{\delta_1}} (\psi_{\delta_1})^{\vec{\iota}_{\delta_1}}_{\{m_l\in\partial\gamma\}} \bigotimes_{l\in\partial\delta_1} |j_{l_{\delta_1}} m_{l_{\delta_1}}\rangle \otimes \bigotimes_y |\vec{j}_y \iota_y\rangle \right) \\
&+ \left(\sum_{\{m_{l\in\partial\gamma_2}\}} \sum_{\vec{\iota}_{\gamma_2}} \left(\left(\psi_{[21]}\right)^{\vec{\iota}_{[21]}}_{\{m_l\in\partial\}} \right) \bigotimes_{l\in\partial\gamma_2} |j_{l_{\gamma_2}} m_{l_{\gamma_2}}\rangle \bigotimes_{l\in\partial_{[21]}} |j_{l_{[21]}} m_{l_{[21]}}\rangle \otimes \bigotimes_{x'} |\vec{j}_{x'} \iota_{x'}\rangle \right) \\
&\left(\sum_{\{m_{l\in\partial\delta_1}\}} \sum_{\vec{\iota}_{\delta_1}} (\psi_{\delta_1})^{\vec{\iota}_{\delta_2}}_{\{m_l\in\partial\delta_1\}} \bigotimes_{l\in\partial\delta_1} |j_{l_{\delta_1}} m_{l_{\delta_1}}\rangle \otimes \bigotimes_{y'} |\vec{j}_{y'} \iota_{y'}\rangle \right) + (\delta_1 \to \delta_2)
\end{aligned}$$

where we have

$$\left(\psi_{[ij]}\right)^{\vec{\iota}_{[ij]}}_{\{m_l\in\partial\}} = \sum_{\{m_{l\in L_A}\}} \sum_{\{m_{l\in L_A\cup L_B}\}} \sum_{\{p\}} \sum_{\{q\}} \prod_x (f_x)^{\vec{j}_x}_{\vec{n}_x \iota_x} \prod_{l_{\gamma_i}\in L_A} \delta_{m^i_x p^{xy}_i} \delta_{m^i_y p^{xy}_i} \prod_{l_{\gamma_i}\in L_A\cup L_B} \delta_{m^i_x q^{xy}_i} \delta_{m^j_y q^{xy}_j} \tag{6.2.11}$$

and $[ij]$ denote the bracket i-th pattern belonging to γ class of connectivity and j-th pattern of the δ one and denoting the set of overlapping connected edges belong simultaneously to both graphs constructed out of the respective entanglement pattern (adjacency matrix). Notice that we considered the graphs in region A as the reference ones with we connect the vertices to those in the region B, hence the compact notation above.

Let us denote by $\partial C_{[\gamma\delta]}$ the inner boundary of the bipartite graph that contains the open links that resulted from the gluing according to the patterns $p_c \in [\gamma_1\delta_1, \gamma_1\delta_2, \gamma_2\delta_1, \gamma_2\delta_2]$. We can construct the density matrix of the above bipartite system and in order to do this

in a compact manner and transparent to the combinatorial nature of the states, let us introduce the notation with the implicit sum of the representation labels

$$\sum_{\left\{m_{l\in\partial\gamma_1}\right\}}\sum_{\vec{\iota}_{\gamma_1}}\sum_{\left\{m_{l\in\partial_{[11]}}\right\}}\sum_{\vec{\iota}_{[11]}}\left(\left(\psi_{[11]}\right)^{\vec{\iota}_{[11]}}_{\{m_l\in\partial\}}\right)\sum_{\left\{m_{l\in\partial\delta_1}\right\}}\sum_{\vec{\iota}_{\delta_1}}\left(\psi_{\delta_1}\right)^{\vec{\iota}_{\delta_2}}_{\{m_l\in\partial\delta_1\}}\equiv\sum\psi\left(\gamma_1,\delta_1,[\gamma_1\delta_1]\right) \tag{6.2.12}$$

$$\bigotimes_{l\in\partial\gamma_1}|j_{l_{\gamma_1}}m_{l_{\gamma_1}}\rangle\bigotimes_{l\in\partial_{[11]}}|j_{l_{[11]}}m_{l_{[11]}}\rangle\otimes\bigotimes_{x}|\vec{j}_v\iota_x\rangle\bigotimes_{l\in\partial\delta_1}|j_{l_{\delta_1}}m_{l_{\delta_1}}\rangle\otimes\bigotimes_{y'}|\vec{j}_{y'}\iota_{y'}\rangle\equiv|\gamma_i\,,\delta_j\,,[\gamma_i\,,\delta_j]\rangle\ . \tag{6.2.13}$$

Assuming that the pairs of graphs in each "layer" of the superposed bipartite state we are considering are of equal size but have different combinatorial patterns, the density matrix entails terms of the form

$$\sum|\psi\left(\gamma_1,\delta_1,[\gamma_1\delta_1]\right)|^2\,|\gamma_1\,,\delta_1\,,[\gamma_1\,,\delta_1]\rangle\,\langle\gamma_1\,,\delta_1\,,[\gamma_1\,,\delta_1]|\ , \tag{6.2.14}$$

applied to the set of the four connectivity patterns of the bigraph. Hence, we can write it as

$$\rho_I=\sum_{i=j=1}^{4}|\psi\left(\gamma_i,\delta_j,[\gamma_i\delta_j]\right)|^2\,|\gamma_i\,,\delta_j\,,[\gamma_i\,,\delta_j]\rangle\,\langle\gamma_i\,,\delta_j\,,[\gamma_i\,,\delta_j]|\ . \tag{6.2.15}$$

Bear in mind the above expressions still do encode the data labeling the open links and connected ones. As in the simple case we encountered above (with no superposition) we can define the dimension of the intertwiners that contain the links connecting vertices in the region A and B by means of the biadjacency matrix, namely

$$D[\gamma,\delta]\equiv\prod_{c^i_{z_e,z_e}}D[\mathcal{I}_z]=\prod_{c^i_{z_e,z_e}}D_{\vec{j}}\prod^{d}d_{j_i}\,,\to\log\left(D[\gamma,\delta]\right)\ , \tag{6.2.16}$$

One can then trace over the region B degrees of freedom, namely the internally connected vertices to obtain the reduced density matrix ρ^A_I. The entanglement entropy for the above state can be computed

$$S_A=\sum_{i=1}^{4}\log\left(\sum_i\prod_j D[\gamma_i]D[\gamma_i,\delta_j]\right)\ . \tag{6.2.17}$$

Let us see in the next section how can we generalize this to any number of superpositions and not only a pair of them in the bipartite system.

6.2.2 Generalization to an arbitrary number of superposition

We are now interested in generalizing the above case of graph superposition to include an arbitrary number of superpositions. To this scope, we rely on the broad construction

in section 6.1.2 In order to make the notation more compact, we work in the spin basis following the labeling defined in (6.1.30). In the spin graph basis, the density matrix is given by:

$$\rho_{AB} = |\Psi_\Gamma\rangle\langle\Psi_\Gamma| = \left(\sum_{k=0}^{\mathcal{N}} \xi_k |\Gamma_k\rangle\right)\left(\sum_{k=0}^{\mathcal{N}} \xi_k^* \langle\Gamma_k|\right) ,$$

where the explicit form of the states are given in (6.1.29). Recall that the open links decorated with the combinatorial patterns live on the boundary ∂C of the regions A and B (see figure 6.1). Furthermore, the sum over the spin basis degrees of freedom is implicit and defined in section 6.1. This is again a Cauchy product including complex wavefunction coefficients. The bipartite density takes the form:

$$\rho_{AB} = \sum_{q'=0}^{2\mathcal{N}} \left(\sum_{q'=1}^{2\mathcal{N}} \left(\psi^{\vec{\iota}}_{m_l\in\partial C_{[\gamma_i\delta_j]}}\right)_{q'} \sum_{s=0}^{q'} \overline{\left(\psi^{\vec{\iota}}_{m_l\in\partial C_{[\gamma_i\delta_j]}}\right)}_{q'-s}\right) \tag{6.2.18}$$
$$\left(\sum_{p_c} \bigotimes_{l\in\partial C_{[\gamma_i\delta_j]}} |\partial_{\gamma_i\delta_j}\rangle \otimes \bigotimes_{y,x} |\vec{j}_{x,y}, \vec{\mathcal{J}}_{x,y}\rangle\right)_{q'} \left(\sum_{p_c} \bigotimes_{l\in\partial C_{[\gamma_i\delta_j]}} \langle\partial_{\gamma_i\delta_j}| \otimes \bigotimes_{y,x} \langle\vec{j}_{x,y}, \vec{\mathcal{J}}_{x,y}|\right)_{q'-s} ,$$

where the bar notation refers to considering the complex conjugate. Notice that the coefficients appearing in the above state can be stored in the following matrix

$$D_{AB} = \begin{bmatrix} d_{11} & d_{12} & \dots \\ \vdots & \ddots & \\ d_{\mathcal{N}1} & & d_{\mathcal{N}\mathcal{N}} \end{bmatrix} = \begin{bmatrix} \xi_1\xi_1^* & \xi_1\xi_2^* & \dots \\ \vdots & \ddots & \\ \xi_{\mathcal{N}}\xi_1^* & & \xi_{\mathcal{N}}\xi_{\mathcal{N}}^* \end{bmatrix} \tag{6.2.19}$$

The above product reflects the peculiar property that a quantum superposition of states puts on the table, which is that of *interference*. Indeed, the expression of the state in (6.2.18) is nothing but an entity that encodes the interference of all possible superposition of the quantum states of geometry. In fact, it decomposes into two types of series of products, namely that of coherent and incoherent superposition that we will denote respectively by $\mathcal{C}$ and $\mathcal{I}$. The terms that will contribute to $\mathcal{C}$ are the off-diagonal ones, whereas those entering $\mathcal{I}$ appear in the diagonal of the matrix D. This distinct separation can be traced back to the structure of the GFT Hilbert space we working with. As we emphasized earlier in section 6.1, entanglement states with different combinatorial patterns are not necessarily orthogonal as in the case of the LQG ones, where in the latter, the incoherent term will not appear due to such orthogonality. In particular, only terms that carry the index $2q' = s$ enter the incoherent contribution $\mathcal{C}$ and it reads:

$$\mathcal{I} = \sum_{2q'=s}^{2\mathcal{N}} \left|\left(\psi^{\vec{\iota}}_{m_l\in\partial C_{[\gamma_i\delta_j]}}\right)_{q'}\right|^2 \left[\sum_{p_c} \bigotimes_{l\in\partial C_{[\gamma_i\delta_j]}} |\partial_{\gamma_i\delta_j}\rangle \otimes \bigotimes_{y,x} |\vec{j}_{x,y}\rangle\right]_{q'} \left[\sum_{p=0}^{q'} \bigotimes_{l\in\partial C_{[\gamma_i\delta_j]}} \langle\partial_{\gamma_i\delta_j}| \otimes \bigotimes_{y,x} \langle\vec{j}_{x,y}|\right]_{q'-s} \tag{6.2.20}$$

where we end up with a generic sum over the square modules of all possible wavefunctions entering the superposition. On the other hand, in the case $2q' \neq s$, we come across the case of incoherent states. This additional cross-term is rather more involved. Notice that for the above-constructed state (6.2.18), we encounter a very interesting critical crossroad where we have to distinguish between two situations:

1. We are dealing with different numbers of vertices and hence the mixed terms including the graph coefficients with different patterns and sizes will vanish and we end up with all terms for the coherent possible combination of states.

2. We are dealing with a graph of equal size since graph states with different combinatorial patterns and equal size are *not* orthogonal.

Furthermore, notice that the state ρ of the bipartite system already has a form that will facilitate the computation of the von Neumann entropy.

Incoherent interference

Let us start by investigating the entanglement entropy we could extract from the first case mentioned above. The crucial part to not be ignored in this case is the size of the graph in consideration. It has been extensively studied in [36, 131]. Since we are dealing with different numbers of vertices, the coherent term $\mathcal{C}$ governs the quantum geometries and in this case, it is simply a sum over the modulus square of the linear combination of the graphs states in (6.2.20). To proceed to the computation of the von Neumann entropy for so far studied bipartite system, we explicitly define the operation of the trace, since we have an overcounting of degrees of freedom, namely that of the shared links between the two graphs. Let us consider a set of basis states in $\mathcal{H}_B$ and we trace out the system B degrees of freedom. The resulting reduced density matrix then reads ρ reads:

$$\rho_A = \sum_s^{2\mathcal{N}} \left| \left(\psi^{\vec{\iota}}_{m_l \in \partial C_{[\gamma_i \delta_j]}} \right)_s \right|^2 \left[\bigotimes_{l \in \partial C_{[\gamma_i \delta_j]}} |\partial_{\gamma_i \delta_j}\rangle \otimes \bigotimes_x |\vec{j}_x \vec{\iota}_x\rangle \right]_s \left[\bigotimes_{l \in \partial C_{[\gamma_i \delta_j]}} \langle \partial_{\gamma_i \delta_j}| \otimes \bigotimes_x \langle \vec{j}_x \vec{\iota}_x| \right]_s . \tag{6.2.21}$$

We can write the above-reduced density matrix in a simpler form, where we make a distinction between the state describing the boundary and that of the bulk

$$\rho_A = \sum_s^{2\mathcal{N}} \left| \left(\psi^{\vec{\iota}}_{m_l \in \partial C_{[\gamma_i \delta_j]}} \right)_s \right|^2 \left(\bigotimes_{l \in \partial C_{[\gamma_i \delta_j]}} \rho^A_\partial \right)_s \left(\bigotimes_x \rho^{bulk}_A \right)_s . \tag{6.2.22}$$

Notice that the above decomposition is only possible since we are considering the case of fixed spins, allowing the factorization of the vertex wavefunctions. Before proceeding to derive the entanglement measure for the above states, let us set the dimensional notation straight.

- We denote the dimension of the representation space V_j associated to a link carrying the color i with D_{j_i} and it reads $D_{j_i} = 2j_i + 1$ (we replace i with j for the system B).
- We denote the dimension or representation of a connected graph by $D[\gamma_i]$ and $D[\delta_j]$, for the subsystems A and B respectively, this is basically the intertwiner dimensions, since the after applying the gluing procedure, we end up with a maximally entangled state. The exact expression thereof can be extracted only in special cases, such as 4-valent vertices.

Furthermore, let us recall that in the special case of the factorized wave function over the single-vertex, we are dealing with frozen boundary spin for each graph entering the superposition. Now, let us introduce what we will call the weight of a graph with characterizing combinatorial pattern γ_i with respect to the total set of graphs

$$q_{\gamma_i} = \frac{\left|\psi^{\vec{\iota}}_{m_l \in \partial C_{[\gamma_i \delta_j]}}\right|^2}{\sum_{\gamma_i}\left|\psi^{\vec{\iota}}_{m_l \in \partial C_{[\gamma_i \delta_j]}}\right|^2}\,, \tag{6.2.23}$$

which can be interpreted as the weight of a state associated with the wave function in the numerator. We define the dimension functions:

$$\omega(D[\gamma_i]D[\gamma_i, \delta_j]) \equiv \omega(D[\gamma_i])\omega(D[\gamma_i, \delta_j]) = \sum_{\gamma_i} \sum_{[\gamma_i, \delta_j]} D[\gamma_i] \prod_j D[\gamma_i, \delta_j]\,, \tag{6.2.24}$$

Computing the von Neumann entropy amounts to:

$$S^I(\rho_A) = S\left(\sum_s^{\mathcal{N}} q_{\gamma_i}\right) + \sum_s^{\mathcal{N}} \frac{q_{\gamma_i}}{\omega(D[\gamma_i]D[\gamma_i, \delta_j])} \log\left[\sum_s^{\mathcal{N}} \frac{q_{\gamma_i}}{\omega(D[\gamma_i]D[\gamma_i, \delta_j])}\right] \tag{6.2.25}$$

$$= S(Q_{\gamma_i}) + Q_{\gamma_i}\omega(D_x) \log\left[Q_{\gamma_i}\omega\left(\omega(d_{j_{\gamma_i}} d_{j_{[ij]}})\right)\right]\,, \tag{6.2.26}$$

where we introduced $Q_{\gamma_i} = \sum_s^{\mathcal{N}} q_{\gamma_i}$. Spin network states have probability interpretation as well. The first term appearing in the entropy can be interpreted as the probability of finding a state with the weight q_{γ_i}. The above entanglement entropy contains the correlation of the bulk degrees of freedom, including those that reflect the internal connectivity and that which threads the bipartite system. In the more generic case, when one considers states that are not factorized over the single vertex wave functions, one can observe that one can distinguish between spin- and vertices-correlations since the intertwiner entanglement would depend on the special form of the vertices wave function. Recall that we made the assumption of separating boundary-crossing vertices with those who undertook the role of internal connectivity. Now, if we ignore this restriction, one can expect a further complicated expression for the intertwiners entanglement entropy. In the sense that, we would have correlations between the intertwiner in the bulk of region A with those in the region B.

The expression in (6.2.25) is very similar to the LQG calculations for a superposition of graph states [193]. The entropy depends on the bulk degrees of freedom since they reflect those of glued links and hence the degrees of freedom responsible for the correlations. As we will see in the following the situation is different when we are dealing with the same number of vertices entering each superposition.

Coherent superposition

Let us define some entropic notions that we will use to formally write down an expression for the off-diagonal terms contributing to the entropy of ρ_{AB} in (6.2.18) borrowed from QIT [37–39]. The coherent term appearing in the density reflects the interdependence and interconnectivity within each subsystem as well as the total system. In the following, we define first the joint entropy and marginal entropy in order to facilitate the computation of the entanglement entropy within the superposition of the graphs in the case of coherent interference.

Entropic notions from Quantum information theory. We exploit the definition of the multivariate entropy also called the interaction information. This is basically the generalization of the mutual information in QIT. To facilitate the comprehension of this entropy, we can consider the states that are elements of the coherent term of the density as an ensemble that reflects their interconnectivity despite the fact of being characterized by different combinatorial patterns.

Definition 10. *The joint overlapping connectivity over the gluing elements described by two entanglement graphs characterized by the pair of quantum combinatorial patterns is given by*

$$S\left[\gamma_1\,,\delta_1\right] = -\sum_{\gamma_1\,,\delta_1} P\left(\psi_{\gamma_1}\,,\psi_{\delta_1}\right)\log P\left(\psi_{\gamma_1}\,,\psi_{\delta_1}\right)\,, \tag{6.2.27}$$

where

$$P\left(\psi_{\gamma_1}\,,\psi_{\delta_1}\right) = \sum_{\gamma_1\,,\delta_1}\int\prod_x \mathrm{dg}\prod_y \mathrm{dk}\;\Psi^{\vec{\iota}}_{m_l\in\partial C_{[\gamma_1\delta_1]}}\overline{\Psi^{\vec{\iota}}_{m_l\in\partial C_{[\gamma_1\delta_1]}}}\,|\psi_{\gamma_1}\rangle\,\langle\psi_{\delta_1}|\,. \tag{6.2.28}$$

The generalization to an arbitrary $\mathcal{N}_A$ and $\mathcal{N}_B$ is straightforward and it is given by

$$S\left[\{\gamma_i\},\{\delta_j\}\right] = -\sum_{\{\gamma_i\},\{\delta_j\}} P\left(\psi_{\gamma_1},\cdots,\psi_{\gamma_i}\,;\psi_{\delta_1},\cdots,\psi_{\delta_j}\right)\log P\left(\psi_{\gamma_1},\cdots,\psi_{\gamma_i}\,;\psi_{\delta_1},\cdots,\psi_{\delta_j}\right)\,. \tag{6.2.29}$$

The marginal entropy associated with a set of superposition of states is nothing but the entropy $S[\delta_j]$, $S[\gamma_i]$ and all possible combinations of i,j given in $S[\{\gamma_i\}\,,\{\delta_j\}]$. Now the interaction information is defined as:

Definition 11. *Given a collection of combinatorial patterns* $\{\gamma_i\}$, $\{\delta_j\}$ *and* $\{[\gamma_i, \delta_j]\}$, *the wavefunction whose quantum parameters are labeled by such a collection defines a probability distribution. The multivariate mutual information is equal to an alternating signed sum of all the marginal entropies and is called in this case the interaction information:*

$$\mathrm{I}\left(\gamma_1 : \gamma_1 : \cdots : \gamma_{N_A}\right) := -\sum_{z \in \mathcal{P}(\mathcal{N}_A)} (-1)^{|z|} S\left[\gamma_1, \gamma_1, \cdots, \gamma_z^{|z|}\right] \tag{6.2.30}$$

where $\mathcal{P}(\mathcal{N}_A)$ *is the power set of the set of connectivity patterns* $\{\gamma_i\}$. *We drop the explicit reference to the state and content of the notation solely to the pattern of the underlying graph.*

Notice that this is already expressed in the superposition of spin network graph states due to the Cauchy product. The single pattern case (where a bipartite system is absent) is equal to the entropy, $I(\gamma) = S(\gamma)$, and the binary case is equal to the standard mutual information between two systems with different classes of combinatorial structures, and the ternary case is for example

$$I(\gamma_1 : \gamma_2 : \gamma_3) := \sum P\left(\gamma_1, \gamma_2, \gamma_3\right) \log \frac{P\left(\gamma_1, \gamma_2\right) P\left(\gamma_1, \gamma_3\right) P\left(\gamma_2, \gamma_3\right)}{P\left(\gamma_1, \gamma_2, \gamma_3\right) P\left(\gamma_1\right) P\left(\gamma_2\right) P\left(\gamma_3\right)} \,. \tag{6.2.31}$$

It is still unclear if the mutual information can be negative as in the case of sets in quantum information theory. Now, let us take a closer look on the coherent contribution in the density ρ_{AB}. As we already emphasized, the terms defining coherent interference are of the shape

$$\int \prod_x \mathrm{dg} \prod_x \mathrm{dk} \Big(\cdots \Psi^{\vec{\iota}}_{m_l \in \partial C_{[\gamma_i \delta_j]}} \overline{\Psi^{\vec{\iota}}_{m_l \in \partial C_{\gamma_i}}} \left|\psi_{\gamma_i}\right\rangle \left\langle\psi_{[\gamma_i \delta_j]}\right| + \cdots \Psi^{\vec{\iota}}_{m_l \in \partial C_{\gamma_i}} \overline{\Psi^{\vec{\iota}}_{m_l \in \partial C_{\gamma_k}}} \left|\psi_{\gamma_i}\right\rangle \left\langle\psi_{\gamma_k}\right| + \tag{6.2.32}$$

$$\cdots \Psi^{\vec{\iota}}_{m_l \in \partial C_{\gamma_i}} \overline{\Psi^{\vec{\iota}}_{m_l \in \partial C_{\delta_k}}} \left|\psi_{\gamma_i}\right\rangle \left\langle\psi_{\delta_k}\right| + \cdots \Big) \,,$$

For the case of the same number of vertices we are dealing with the coherent terms that appear in the density matrix are the ones corresponding to the off-diagonal entries. This is a direct manifestation of the superposition of the states we are working with and more importantly, the GFT Hilbert space which allows it. Indeed, in the LQG case, this term appearing at the level of the density is prohibited due to the orthogonality of states with different connectivity. The von Neumann entropy in this case will have additional contributions coming from it. The degrees of freedom from region B can be traced out

from the state in (6.2.18) and we can write the density matrix as

$$\rho_A = \prod_{\gamma_i, p_{[ij]}} |\psi(\gamma_i, [\gamma_i \delta_j])|^2 \, |\gamma_i, [\gamma_i, \delta_j]\rangle \langle \gamma_i, [\gamma_i, \delta_j]| \tag{6.2.33}$$

$$\left(\frac{\sum_{\gamma_i, p_{[ij]}} |\psi(\gamma_i, [\gamma_i \delta_j])|^2 \, |\gamma_i, [\gamma_i, \delta_j]\rangle \langle \gamma_i, [\gamma_i, \delta_j]|}{\prod_{\gamma_i, p_{[ij]}} |\psi(\gamma_i, [\gamma_i \delta_j])|^2 \, |\gamma_i, [\gamma_i, \delta_j]\rangle \langle \gamma_i, [\gamma_i, \delta_j]|} + \frac{\sum_{\gamma_i, p[ij], i \neq j} \psi(\gamma_i, [\gamma_i, \delta_j]) \, \psi^* \left(\gamma_i, p_{[ij]}\right) |\gamma_i, [\gamma_i, \delta_j]\rangle \langle \gamma_i, [\gamma_i, \delta_j]|}{\prod_{\gamma_i, p_{[ij]}} |\psi(\gamma_i, [\gamma_i \delta_j])|^2 \, |\gamma_i, [\gamma_i, \delta_j]\rangle \langle \gamma_i, [\gamma_i, \delta_j]|} \right). \tag{6.2.34}$$

Rearranging the above expression of the entropy and using the notation defined in (6.2.29) along with the definition of interaction information entropy defined in (6.2.30)) we can compute the correlations between the regions A and B and the internal ones as well. This yields

$$S^C(\rho_A) = S(Q_{\gamma_i}) + Q_{\gamma_i} \omega(D_x) \log \left[Q_{\gamma_i} \omega \left(\omega(d_{j_{\gamma_i}} d_{j_{[ij]}}) \right) \right] + \mathrm{I}(\gamma_1 : \gamma_2 : \cdots : \gamma_{\mathcal{N}_A}) \tag{6.2.35}$$

$$= S_A^I + \mathrm{I}(\gamma_1 : \gamma_2 : \cdots : \gamma_{\mathcal{N}_A}) \, . \tag{6.2.36}$$

The interaction information obtained above specifically quantifies the amount of information depicting the entanglement entropy of the degrees of freedom inside region A and the overlap with region B, hence the product appearing in the log function. The additional third term arises due to the entanglement of the superposition of states we considered. Notice that this disappears the more the connectivity patterns in the overlapping regions are similar, till the coherent contribution "collapses" and we return to the incoherent entanglement density. Such a process can be dynamical or kept track by introducing an operator that can count the closeness of graph connectivities. In this sense, one can also regard the above entanglement entropy as a tool to measure how close the states are in our superposition, hinting at the description of a *pre-metric*. We leave this inquiry for future work and how we can compute observables based on such superposed states.

6.2.3 Observables in bipartite regions

The superposition of entanglement graph states we constructed in section 6.1 are the most generic state that are elements of the full Hilbert space of the theory. In a bipartition of Hilbert space, we encountered in section 6.2 that density state ρ_{AB} is controlled by two contributions, namely that of coherent and incoherent states. This was also detected at the level of the entanglement entropy of the reduced density states, containing all the information needed about the correlation between the subregions A and B and within each one. Now, using this prescription provided by the superposed density states and the powerful information reduced densities provide, we can derive the expectation value of an operator $\mathcal{O}_A$ in the region A and its action on the entangled bipartite state.
Due to the tensor product structure of the bipartite Hilbert space $\mathcal{H}_{AB}$, we can write the

operator $\mathcal{O}_A$ acting on the degrees of freedom in $\mathcal{H}_A$ as

$$\mathcal{O}_A = \mathcal{O}_A \otimes 1_B \,, \tag{6.2.37}$$

where 1_B is the identity operator acting in the Hilbert space $\mathcal{H}_B$. The expectation value of this observable in the superposed state ψ_{AB} then reads

$$\langle \mathcal{O}_A \rangle = \langle \psi_{AB} | \, \mathcal{O}_A \otimes 1_B \, | \psi_{AB} \rangle = \mathrm{Tr} \left(\mathcal{O}_A \rho_A \right) = \mathrm{Tr} \left(\mathcal{O}_A^I + \mathcal{O}_A^C \right) \,, \tag{6.2.38}$$

where introduced the coherent thanks to (6.2.33) and incoherent (6.2.21) decomposition of the expectation value of the observable in the reduced state ρ_A

$$\mathcal{O}_A^I = \mathcal{O}_A \mathcal{I} \,, \quad \mathcal{O}_A^C = \mathcal{O}_A \mathcal{C} \,. \tag{6.2.39}$$

The consideration of a superposition of spin network states with different combinatorial structures allows us to introduce the notion of *ensemble*. The expectation value of an operator is then perceived as being averaged over this ensemble. Then quantum effects are expected to be present due to the coherent contribution, underlying the interference phenomena.

6.3 Second quantization of superposition of entangled graph states

Labeling vertices is merely a tool that allowed us to some extent to keep track of the entanglement calculations we presented and physically it is void of any meaning. This is the reason why up to this point, we considered graphs with vertices that are distinguishable to keep in some sense control of the connectivity and complexity of the graph. As was already mentioned in section 4.3, in the context of group field theories, working with graph states and in particular their superposition is equivalent to dealing with a labeled fixed number of vertices in the pre-Fock space of the theory (4.3.6). In such quantum gravity models, considering the full theory is translated to studying an arbitrary number of vertices of a graph instead of a fixed one and symmetrizing over them at the level of the respective wavefunctions. This transitions the states living in the pre-Fock space of the theory to a first-quantized one, which is the needed step towards introducing the GFT Fock space whose elements are characterized by wavefunctions that are symmetric under permutations of the vertex set.
We are interested in translating the so-far developed tools of bipartite wavefunctions to a second quantized one since the full theory is endowed with a Fock-structure for the Hilbert space. Therefore, in section 6.3.1 we render our labeled superposed graph states unlabeled by symmetrizing over the set of vertex labels. In section 6.3.2, we present a proposal for describing the superposition within the GFT Fock space. More importantly, we focus on the trails of the superposition within the expression of the density operator.

6.3.1 Bipartite wavefunction symmetrization

In the following, we present the main results of the symmetrization procedure that we are implementing in the bipartite system considered so far. Let us recall that the Hilbert space of multi-particle states for two regions is given by (6.1.5), where the N-particle states that constitute these spaces are depicted in the expression (6.1.6). The pre-Fock space of the theory is given by pre-$\mathcal{F}(\mathcal{H}) = \oplus_{N=1}^{\infty}\mathcal{H}_N$, within which the superposition of graph states (6.1.27) live. In the group representation, the corresponding wave functions read

$$\Psi\left(\{g_{l_x}\},\{k_{l_y}\}\right) = \sum_{i=0}^{\mathcal{N}^A+\mathcal{N}^B}\sum_{k=0}^{i}\int\prod_{x<t_{\gamma_i}}\mathrm{d}h^{xt_{\gamma_i}}\prod_{y<t_{\delta_{j_l}}}\mathrm{d}h^{yt_{\delta_j}}\,\psi_i\left(\left\{g^x_{\gamma_i}h^{xt_{\gamma_i}}_{t_{\gamma_i}}\right\}\right)\psi_{j_l}\left(\left\{k^k_{\delta_{j_l}}h^{yt_{\delta_j}}_{t_{\delta_{j_l}}}\right\}\right). \tag{6.3.1}$$

Clearly, we are dealing with two different sets of vertices, namely that belonging to the graphs $\{\Gamma_A\}$ and $\{\Gamma_B\}$ which pose two ways of performing the symmetrization. One can proceed by symmetrizing over each set of vertices separably and then gluing the superposition of states living on the two Hilbert spaces, underlying therefore the entanglement between the two regions. However, this operation should commute with the one where we entangle the two graphs as discussed in section 6.1 to obtain the set of the bipartite states and then symmetrize the wavefunction of the bipartite system. In the following, we proceed with the latter. There are many reasons why this is more convenient for the purposes of this thesis, maybe the most important one is, in some way, to make evident which degrees of freedom are entangled and according to which combinatorial pattern. This is reasonable since we are symmetrizing only *after* having implemented the gluing procedure. Moreover, following this approach underlines the importance of the quantum information-combinatorial feature that governs the graph structure in promoting some degrees of freedom over others.
Let us now consider the symmetrization map acting on the two sets of vertices $(N_A\,,N_B)$ that reads

$$\mathbb{P}_\pi : \{x,y\} \to \pi(x,y)\,, \tag{6.3.2}$$

where the permutation operator $\mathbb{P}_\pi$ acts on $\{x,y\} \in (N_A\,,N_B)$ vertices. Notice that the unlabeling operation once it acts on every single graph, transforms the superposition-notion of the graph states we studied so far. Indeed, once we symmetrize over the vertices of each graph with certain combinatorial patterns $\{\gamma_i\}$, the induced indistinguishably will collect all those graphs that belong to the same class $[A_\gamma]$, that are characterized by the invariance of the adjacency matrix (see section 4.3). Thus the superposition is not over all possible connectivity patterns, but rather over a selected set of adjacency classes. Under the symmetrization operation, the graph wave function (6.3.1) reads

$$\mathbb{P}_\pi\Psi\left(\{g_{l_x}\},\{k_{l_y}\}\right) = \sum_{\pi\in S_N}\sum_{i=0}^{[\mathcal{N}]}\sum_{k=0}^{i}\int\prod_{x<t_{\gamma_i}}\mathrm{d}h^{xt_{\gamma_i}}\prod_{y<t_{\delta_{j_l}}}\mathrm{d}h^{yt_{\delta_{j_l}}}\,\psi\left(\left\{g^{\pi(x)}_{\gamma_i}h^{xt_{\gamma_i}}_{t_{\gamma_i}}\right\},\left\{k^{\pi(y)}_{\delta_j}h^{yt_{\delta_j}}_{t_{\delta_j}}\right\}\right), \tag{6.3.3}$$

where the map $\mathbb{P}_\pi$ is responsible for the projection of the labeled graphs onto an invariant subspace under N vertex relabeling S_N and $[\mathcal{N}]$ is the sum of the various graph classes present in the subsystems A and B. The above symmetrization defines the GFT Fock space in the case of a bipartite system. More precisely, symmetrizing the above-superposed graph states leads to the indistinguishability of particles, and true entanglement can no longer be separated from fake one.
It is in fact possible to express the symmetrized bipartite state in terms of the permanent of graph matrix entailing the connectivity. The permanent of an $n \times n$ matrix $A = (a_{i,j})$ is defined as

$$\mathcal{P} = \mathrm{perm}(A) = \sum_{\sigma \in S_n} \prod_{i=1}^{n} a_{i,\sigma(i)}. \tag{6.3.4}$$

The sum above is extended over all elements σ of the symmetric group S_n; i.e. over all permutations of the numbers $1, \ldots, n$. For the case of the superposition of the graph states of interest, this generalizes to a sum over the permanent of all graph matrices encoding the connectivity of each superposition. In particular, the permanent will keep track of the internal (off-diagonal) and boundary-crossing connectivity. The above-symmetrized states become

$$|\Psi\rangle = \sum_{k=0}^{[\mathcal{N}_k]} \mathbb{P}_\pi \sum_{\sigma \in S_n} \prod_{i=1}^{n} a_{i,\sigma(i)} [\mathcal{N}] \, |\psi_{AB}\rangle \ . \tag{6.3.5}$$

6.3.2 Superposition of graph states in the GFT Fock space

Several assumptions are needed in order to second quantize the bipartite pre-Fock Hilbert space. We assume that we can introduce two families of creation and annihilation operators. This should correspond to a tower-like decomposition of the creation/ annihilation operator constituting the GFT field. Each family is a superposition of operators that create a number x of particles that carry certain combinatorial structures belonging to either $\{\gamma, \delta\}$. The symmetrization over the set of vertices can be discarded in this case, since it is insured by the commutation relation of the operators. This way we could to some extent and in some sense survey the combinatorial pattern. However, we need to assume that the creation/annihilation operators can be decomposed in a set of combinatorial modes and that in order to create/annihilate a vertex (with a set of d links, that indirectly in this picture carry the connectivity patterns) the superposition of these modes act on the vacuum state $|0\rangle$. Practically, this amounts to writing the

$$\hat{c}^\dagger_a = \sum_i \hat{c}^\dagger_{a^{\gamma_i}} \ , \quad \hat{d}^\dagger_a = \sum_j \hat{d}^\dagger_{a^{\delta_j}} \ . \tag{6.3.6}$$

To each set of creation/annihilation operators, we can introduce the corresponding pseudo number operator

$$\hat{N}_{\hat{c}} = \sum_i \hat{c}^\dagger_{a^{\gamma_i}} \hat{c}_{a^{\gamma_i}} \ , \quad \hat{N}_{\hat{d}} = \sum_i \hat{d}^\dagger_{a^{\delta_i}} \hat{d}_{a^{\delta_i}} \ . \tag{6.3.7}$$

Entangling the respective particles amounts to considering the set of operators:

$$t^{\dagger}=\sum_{i}\hat{c}^{\dagger}_{a^{\gamma_i}}\sum_{j}\hat{d}^{\dagger}_{a^{\delta_j}}\,, \tag{6.3.8}$$

such that $\hat{c}^{\dagger}_{a}$ and $\hat{d}^{\dagger}_{a}$ commute, acting on the vacuum state. If we were to consider the other scenario where we perform the gluing at the very end of the symmetrization which leads to introduce a single set of creation and annihilation operators, it should be in principle equivalent to the above product in (6.3.8). However, this is only valid once we take seriously the above assumptions. An entangled bipartite state in the second quantized language then read:

$$|\Psi\rangle=t^{\dagger}\,|0\rangle=\left(\sum_{i}\hat{c}^{\dagger}_{a^{\gamma_i}}\sum_{j}\hat{d}^{\dagger}_{a^{\delta_j}}\right)|0\rangle\,. \tag{6.3.9}$$

From this construction, one can write also work in the particles number basis, where we have now (6.3.7) by

$$|\Psi\rangle=\sum_{n}\mathcal{C}_{n}\,|n_1\cdots,n_T\rangle\,, \tag{6.3.10}$$

where $\mathcal{C}_n$ is the wavefunction encoding the information coming from the first quantization procedure and T is the total number in the bipartite system. From the tower-like decomposition of the creation and annihilation operators, one can define the bosonic field operators:

$$\hat{\varphi}\left(g_1,\cdots,g_d;k_1,\cdots,k_{d'}\right)\equiv\hat{\varphi}(\{g_i\},\{k_j\})=\sum_{S^{ij}}\hat{t}\,\psi_{S^{ij}}(\{g_i\},\{k_j\})\,, \tag{6.3.11}$$

$$\hat{\varphi}^{\dagger}\left(g_1,\cdots,g_d;k_1,\cdots,k_{d'}\right)\equiv\hat{\varphi}^{\dagger}(\{g_i\},\{k_j\})=\sum_{S^{ij}}\hat{t}^{\dagger}\,\psi^{*}_{S^{ij}}(\{g_i\},\{k_j\})\,, \tag{6.3.12}$$

where S^{ij} denotes the set of all graphs and their respective quantum numbers characterizing the field modes. They satisfy the commutation relations:

$$\left[\hat{\varphi}(\vec{g},k),\hat{\varphi}^{\dagger}\left(\vec{g}',k'\right)\right]=\mathbb{I}_{G}\left(g_i,g'_i,\right)\mathbb{I}_{G}\left(k_j,k'_j,\right)\,, \tag{6.3.13}$$

$$\left[\hat{\varphi}(\vec{g},k),\hat{\varphi}\left(\vec{g}',k'\right)\right]=\left[\hat{\varphi}^{\dagger}(\vec{g},k),\hat{\varphi}^{\dagger}\left(\vec{g}',k'\right)\right]=0 \tag{6.3.14}$$

where $\mathbb{I}_{G}\left(g_i,g'_i\right)\equiv\int_{G}dh\prod_{1}^{d}\delta\left(g_i h\left(g'_i\right)^{-1}\right)$ is the identity operator on the space of gauge invariant fields, that is encoding the gauge invariance condition at the spin network vertices. Note that we are dealing with a second quantized version of the already entangled labeled graph states, which is made clear once we examine the resulting group element obtained after the group averaging operation that appears as an argument in the field operators. This can be made evident when we write down the second quantized bipartite state:

$$|\Psi\rangle=\sum_{S^{ij}}\int\prod_{\delta_j}\mathrm{d}h^{yt_{\delta_j}}\prod_{\gamma_i}\mathrm{d}h^{xt_{\delta_i}}\,\hat{\varphi}^{\dagger}\left(g^{x}h^{xt_{\gamma_i}},k^{y}h^{yt_{\delta_j}}\right)|0\rangle\,. \tag{6.3.15}$$

The density matrix $\rho=|\Psi\rangle\langle\Psi|$ in second quantization reads

$$\rho_{AB}=\sum_{S^{ij}}\int\prod_{\delta_j}d\mathbf{h}^{yt_{\delta_j}}\prod_{\gamma_i}d\mathbf{h}^{xt_{\delta_i}}\,\hat{\varphi}^{\dagger}\left(g^{x}h^{xt_{\gamma_i}},k^{y}h^{yt_{\delta_j}}\right)\hat{\varphi}\left(g^{x}h^{xt_{\gamma_i}},k^{y}h^{yt_{\delta_j}}\right)|0\rangle\langle 0|\,. \tag{6.3.16}$$

Bipartite density matrix in the number-basis Let us denote the bipartite number basis of the Fock space by

$$\mathcal{C}_n \left|n_1 \cdots, n_T\right\rangle = \left|n_{ab}\right\rangle = \left|n_a^1\right\rangle \left|n_b^1\right\rangle \cdots \left|n_a^N\right\rangle \left|n_b^N\right\rangle \ ,$$

and write the density state in this basis:

$$\rho = \sum_{S^{ij}} \mathcal{C}\left(n_{ab}^1, \cdots n_{ab}^t\right) \mathcal{C}^*\left(n_{ab}^1, \cdots n_{ab}^t\right) \left|n_{ab}\right\rangle \left\langle n_{ab}\right| \ . \tag{6.3.17}$$

where the same information content of the wave function is stored in different coefficients $\mathcal{C}\left(n_1^i, \ldots, n_f^i, \ldots\right)$ that will keep track only of the occupation numbers of a certain combinatorial pattern, i.e. the number of times each single-vertex with a certain combinatorial degree of labels appears. To compute the partial trace we have to define a product operation between bra and ket of different numbers of particles. The degrees of freedom of the bipartite system in the Fock picture are encoded in the occupation number states. On the level of the operation performed entering the entropy calculations, this means the information we are interested in is stored in this type of state, which simultaneously depicts the same information formulated in the first quantized language of the states but with a peculiar reordering and classification. Following this line of reasoning, the partial trace operation that is conducted in order to map out the degrees of freedom that defines states living on $\mathcal{H}_B$ can be understood as tracing out all the number of particles endowed with the same degrees of freedom (with possibly very different storage of that information) over the bipartite density states[5].

In order to properly define this step, it is necessary to underline the combinatorial aspect of the theory. In fact, the different ways in which the quanta can fill the modes in the states of (6.3.17) can be expressed in terms of the combinatorial pattern that governs the bipartite graph. For instance, we can examine the kth particle state that admits k building blocks and where we are ignorant which particle carries one of the entanglement patterns $\{\gamma_i, \delta_j\}$ depicting, therefore, an element of the adjacency matrices set. In this context, a k-permutation of $\{\gamma_i\}$ is an ordered arrangement of k elements of $\{\gamma_i\}$, where different orderings of elements of this type are not distinguished. This is an ordered multiset and repetition numbers $s_1, \ldots, s_{|\{\gamma_i\}|}$ such that $s_i \leq r_i, 1 \leq i \leq |\{\gamma_i\}| = \mathcal{N}_\gamma$, and $\sum_{i=1}^{\mathcal{N}_\gamma} s_i = k$. Recall that $\sum_{a=1} n_a = N_A$ and $\sum_{b=1} n_b = N_B$ such that the total number of particles is $T = N_A + N_B$. We can express each particle state in a different, more convenient way making evident the combinatorial pattern present in each state. This is equivalent to relabeling the occupation number basis with the set of permutations over the possible connectivity:

$$\left|n_1, \cdots, n_a\,, \mathbb{P}_\gamma\right\rangle = \binom{n_a}{\mathcal{N}_\gamma} \frac{1}{\sqrt{n_a!}} \left(c^\dagger\right)^a \left|0\right\rangle \ , \quad \mathbb{P}_\gamma = 1, 2, \ldots, \binom{n_a}{\mathcal{N}_\gamma} , \tag{6.3.18}$$

$$\left|n_1, \cdots, n_b\,, \mathbb{P}_\delta\right\rangle = \binom{n_b}{\mathcal{N}_\delta} \frac{1}{\sqrt{n_b!}} \left(d^\dagger\right)^b \left|0\right\rangle \ , \quad \mathbb{P}_\delta = 1, 2, \ldots, \binom{n_b}{\mathcal{N}_\delta} . \tag{6.3.19}$$

[5] As long as not mentioned otherwise, we work in the case of fixed spin at the shared boundary between the two regions.

The bipartite basis states then read:

$$|n_1, \cdots, n_t\rangle = |n_1, \cdots, n_a, \mathbb{P}_\gamma\rangle \otimes |n_1, \cdots, n_b, \mathbb{P}_\delta\rangle \tag{6.3.20}$$
$$= |\{n_a, \mathbb{P}_\gamma\}, \{n_b, \mathbb{P}_\delta\}, \mathbb{P}_T\rangle \ , \tag{6.3.21}$$

where $\mathbb{P}_T = \binom{T}{k}$. We can now rewrite the density state in a more explicit way

$$\rho = \sum_{S^{ij}} \sum_{\mathbb{P}_\gamma, \mathbb{P}_\delta} \mathcal{C}(n_1, \cdots n_t)\, \mathcal{C}^*(n_1, \cdots n_t)\, |\{n_a, \mathbb{P}_\gamma\}, \{n_b, \mathbb{P}_\delta\}, \mathbb{P}_T\rangle \langle\{n_a, \mathbb{P}_\gamma\}, \{n_b, \mathbb{P}_\delta\}, \mathbb{P}_T| \ . \tag{6.3.22}$$

This in fact allows us to introduce the assumption the number basis wavefunction can be decomposed into a purely combinatorial factor (that can also explain the Shannon-term present in the entropic calculations) and a reduced one that encodes the rest of the information each particle in that basis pertains.
Now, let us define the tracing out operation in this case. If we are interested in the quantum entanglement in the region A expressed by the von Neumann entropy, we should be able to remove the B-particle degrees of freedom. These are encoded in the occupation basis- states exhibiting the combinatorial feature spanning the Hilbert space $\mathcal{H}_B$ given by (6.3.19):

$$\mathrm{Tr}\,\rho_{AB} = \sum_{\mathcal{N}_b} \sum_{N_{\mathbb{P}_\delta}} \Big(\langle\{n_b\}, \mathbb{P}_\delta| \sum_{n_{ij}} \sum_{\mathbb{P}_\gamma, \mathbb{P}_\delta} \mathcal{C}(n_1, \cdots n_t)\, \mathcal{C}^*(n_1, \cdots n_t) \tag{6.3.23}$$
$$|\{n_a, \mathbb{P}_\gamma\}, \{n_b, \mathbb{P}_\delta\}, \mathbb{P}_T\rangle \langle\{n_a, \mathbb{P}_\gamma\}, \{n_b, \mathbb{P}_\delta\}, \mathbb{P}_T| \Big) |\{n_b\}, \mathbb{P}_\delta\rangle \ .$$

This tracing operation can be understood as follows:

- *The case where each vertex has at least one link.* This is only possible if there are at least as many vertices as links ($N > k$). This is the same as the number of partitions of $[N]$ into k non-empty parts which we also call *Stirling Numbers* of the second kind and write as $s_k^{II}(N)$.

- *The Arbitrary number of patterns per particle.* The case of an arbitrary number of patterns per vertex is allowed. To count all arrangements, we first choose the number i of vertices that should be non-empty ($0 \leq i \leq k$), then we can count the number of arrangements of n patterns into the i vertex such that non of them are empty. This gives a total of:
$$\sum_{i=0}^{k} s_i^{II}(N)\,.$$

- *Noncrossing partitioning and counting of vertices* Imagine the elements of $[N_T]$ to be laid out in a circular way. Two disjoint sets $A, B \subseteq [n]$ are crossing if there are numbers $i < j < k < l \in [n]$ such that $\{i, k\} \subseteq A, \{j, l\} \subseteq B$. A non-crossing partition is a partition in which the parts are pairwise noncrossing. We denote the

number of non-crossing partitions of $[n]$ by NC_n.. This number NC_n is equal to C_n, the n -th Catalan number given by

$$\mathrm{NC}_n = C_n = \frac{1}{n+1}\left(\begin{array}{c} 2n \\ n \end{array}\right). \tag{6.3.24}$$

One can apply the above counting techniques for graph states carrying a set of different patterns in the number basis, by assigning with each operation such as tracing out the B degrees of freedom or the entanglement entropy calculation by the appropriate combinatorial counting coefficient (as the ones introduced above). As it is clear from the above cases, this is rather more involved if we were to compare with the labeled graph and postpone it to future work.

6.4 Conclusion

In this chapter, we considered for the first time the generic case of a superposition of spin network states with different combinatorial structures. More precisely, we studied their characteristics and the prescription to construct such states within a bipartite system in section 6.1. The superposition is carried out in each region of the bipartition and then works with the tensor product of the respective states. Our agenda of entangling these states were carried out on two levels; first, we achieved internal gluing within each subsystem of the bipartition and then performed the same operation on the level of the boundary degrees of freedom. To accomplish this we relied on the notion of biadjacency matrix borrowed from graph theory. We also discussed how these bipartite graph states enter the LQG Hilbert space. We then illustrated the elementary steps to quantify such correlations in section 6.2.1, where we emphasized that correlating two vertices in a bipartition produces an increase in the entanglement entropy proportional to the representation space of the connecting link between the vertices. This is then generalized in section 6.2.2 to extract the entanglement measure (von Neumann entropy) for the generic case of superpositions of spin network graph states. The main result of this step is the appearance of coherent and incoherent terms in the bipartite density state that led to *an interference* of quantum geometries. The coherent contribution appeared only in the GFT Hilbert space since it allows spin network states with different combinatorial structures not-be orthogonal, as opposed to the LQG Hilbert space. This gave rise to an additional term in the entanglement entropy that is called *interaction information*. This is interesting since this quantity characterizes the interconnectivity of the entire superposition of the quantum states. This term vanishes the more the connectivities patterns get closer to each other, which hints towards a definition of *pre-metric* in this context. After these entropic reflections, we exposed how we can use these states to compute observables and associated it with the idea of averaging over an ensemble of quantum geometries. Finally, we presented a proposal for a second quantization program for this class of states in section 6.3. In particular, we stumbled upon the same issues raised in condensed matter physics [202]. Therefore, several

assumptions were needed to be introduced in order to be able to formulate the idea of a bipartition, bipartite density, and the operation of tracing out degrees of freedom. In turn, this highlighted the complexity of the unlabeling operation of the superposition of graphs. A last, let us mention that summing over graph structure is most likely an ingredient of any coarse-graining procedure for the quantum gravity states and the asymptotic behavior of it should be investigated. The work presented in this chapter is only the first step in a broader research direction that we will explore in chapter 8.

Chapter 7

Cosmological group field theories as a field theory on curved spacetime

Only a fundamental theory of QG, that has survived some consistency checks can deliver answers to the open physical problems concerning the physics of early cosmology. A viable model should depict the transition from the fundamental building blocks of the theory up to the emergence of continuum structures and therefore it is *necessary* to extract effective macroscopic dynamics of geometry and matter. This is precisely what we explore in this chapter. In chapter 5 and 6 we discussed two approaches to addressing the microscopic quantum geometry from the GFT point of view, where we pursued the covariant approach of SF and provided a new model encoding the full geometric content of $4d$ geometry, whereas in chapter 6 we initiated the investigation of the kinematical aspects of the GFT full theory quantum states, namely the entanglement graph states with different combinatorial structures that are superposed. Despite their intriguing and appealing features from a mathematical and QG point of view, it is so far unclear how to extract from them continuum geometries and physical predictions, which would usually imply some process of coarse-graining of the relevant degrees of freedom. However, a more successful route to tackle such issues is the mean field theory approach. In particular, to reproduce cosmological scenarios, the mean field approach was successfully implemented within the dynamics of the GFT condensate [203–205], which are a class of coherent states characterized by the collective behavior of the fundamental GFT quanta as we discussed in section 4.4 [206, 207]. The dynamics are then defined in this setting in a relational manner [77, 167], namely with respect to massless scalar fields that play the role of a relational reference frame [162, 163, 165], where the evolution of observables is taken with respect to such fields (see section 4.4.2). Such notion of dynamical relationalism [208] is then defined only for emergent quantities.

In this chapter we study in detail the resulting dynamics and the coupling of matter to the GFT condensate entering two levels of the theory; when the background data is

homogeneous and then when scalar perturbations are introduced.

In fact, the line of reasoning in this chapter is very simple and we lay it out in the following. Since we know that the program of any background independent theory of QG is a top-down approach [80], it is then widely believed to identify it at the semi-classical level with some Extended Theories of Gravity (ETG) or Modified Gravity Theories (MGT) [209, 210]. Indeed, in the absence of a full well-tested theory of QG, several research fields initiated frameworks departing from the GR construction by adding corrections and further degrees of freedom to the EH action [211–213]. The logic behind it consists in studying the additional information coming from considering higher order curvature invariants as well minimally- or non-minimally- coupled scalar fields within the GR dynamics. This is in turn perceived to be the extracted physics from an *effective* QG action that *still* needs to be identified.

More importantly, a category of ETG that has had remarkable success in semi-classical gravity and especially inflationary cosmology are modified theories of gravity that rely on higher order corrections in curvature invariants and non-minimal couplings. In fact, this turned out to be extremely related to the formalism of a QFT propagating on a curved spacetime. Such description of matter exhibits its powerful predictions when faced with small-scale physics, while, unlike the case of describing matter as the universe in the language of a fluid [86, 214], we associate matter with quantum field theories instead of living on a fixed gravitational curved background.

We show in this chapter how GFT predictions are *indeed* at the crossroads of QG theories (see chapter 3), phenomenology of QG and MGT. The main objective of this chapter is then to bridge the effective description of the GFT framework, with MGT (and QFT) in the cosmological sector. Therefore, we will investigate the following problematic

1. Can we provide a formulation of a field theory propagating on a curved background starting from the background independent GFT model? and what kind of field theory does it describe?

2. How does this field theory behave at early- and late- times of the universe? In a second stage, how does it affect the scalar perturbation?

To answer these questions we make use of the key elements provided by GFT incorporating pre-matter degrees of freedom, their kinematical aspects as well the dynamics that were presented in section 4.4. In section 7.1.1 we go through the following points

* We provide solutions to the condensate dynamics at the level of the background variables in terms of the scale factor. In particular, we focus on early time and late time cosmologies.

* We then proceed with the same program to treat the dynamics of the inhomogeneities in section 7.1.2 relying on several Analog Gravity (AG) techniques after having embedded them within the GFT setting.

In section 7.2, we proceed with the scheme of formulating a quantum field theory on a curved background starting from the GFT model. To this end, we derive a relation connecting the dynamics of the scalar field to the GFT condensate parameters. We do this again for early time cosmologies and late times. In section 7.3, we analyze the treatment of the scalar perturbation from a field theory living on a curved background point of view and show how it is affecting the relational dynamics of the perturbed scalar field, where we derive its dispersion relation. We close the chapter by summarizing the main results of this work and we discuss its outlook in chapter 8.

7.1 Solving GFT effective dynamics

In this section, we show the demarche of solving the effective dynamics of the GFT condensate at the background level as well the perturbed one pointed out in section 4.4.2.
As already emphasized earlier, we are interested in extracting an effective formulation of a quantum field theory on an emergent curved background for homogeneous geometries and investigating how this affects the treatment of inhomogeneities. This is carried out in a homogeneous isotropic cosmological setting, where we will formulate all the extracted physical equations encoding the geometric- and matter-content of the universe in terms of the scale factor. In order to dive into this, we work at the mean-field level of the extracted dynamics of the GFT condensate by rewriting the evolution equations in terms of the scale factor that can be identified with $a = \langle \hat{V} \rangle^{1/3}$, where the volume operator is given by (4.4.4) and the expectation value, as mentioned in section 4.4.2, is taken with respect to the coherent states (4.4.14). We perform this step for the background as well the perturbed condensate evolution equations. To this aim, we rely on the extracted dynamics presented in section 4.4.2 where we illustrate the solutions depicting the background and perturbed dynamics encoded in the GFT condensate quantum gravity parameters.

7.1.1 The dynamics of homogeneous GFT

As already emphasized, the first step towards a formulation of a QFT on cosmological curved background from a quantum gravitational origin is to express the GFT condensate parameters in terms of the scale factor $a(x^0, \pi_\phi)$, that stems from the expectation value of the volume operator. Hence, in the following, we present the formulation of the background dynamics in terms of the scale factor. Moreover, we focus mainly on the simplest case of a dominant spin value denoted by j_v, since several studies indicated that this is the most relevant case to reproduce results compatible with the predictions of general relativity and cosmology, leaving the more involved case of including all possible values of spins for future work. The explicit expression of the expectation value of the GFT volume operator was already derived using the CPS in [77, 168] and it reads for the general case of a sum over

different spin values:

$$\langle \hat{V} \rangle \simeq \sum_j V_j \rho_j^2 \left(x', \pi_\phi\right). \tag{7.1.1}$$

One way of interpreting the above expression for the volume operator is the following; the total volume is given by the sum over j of the average number of isotropic atoms associated to spin j at a certain time χ_0, and that are weighted by their particular volume contribution V_j. Since we are focusing on the case where the volume expectation value is dominated by a single j_v contribution, (7.1.1) simplifies to $\langle \hat{V} \rangle = V_{j_v} \rho_{j_v}^2$. This is the case in which all the spins are identically zero except for a non-zero j_v. One justification for this assumption is the fact that the background evolution is exponential for each spin value j hence, the evolution of macroscopic observables such as the volume will be dominated by j_v. Several studies also support this assumption [76, 161, 215]. Taking into account these considerations, the scale factor then reads

$$\langle V \rangle = a^3(x^0, \pi_\phi), \quad a(x^0, \pi_\phi) = \tilde{V}_{j_v} \left(\rho_{j_v}(x^0, \pi_\phi)\right)^{(2/3)}, \tag{7.1.2}$$

here we defined $\tilde{V}_{j_v} = V_{j_v}^{1/3}$. For notation simplicity, we drop the spin label v from now on, as well as the function's dependence and refer to background quantities by the subscript 0. In the first part of this section, we will be dealing with data of a *homogeneous* cosmological background that our quantum gravity model provides at mean field level. Therefore, the arguments of most of the functions we will encounter are always in terms of the relational clock and/or the momentum π_ϕ of the coupled scalar field. We first reformulate the background evolution equation of the GFT condensate variables ρ_0 and θ_0 in terms of the scale factor a and solve the associated dynamical equations. As we will see when we study the matter content of the model (section 7.2 and 7.3), depending on such solutions and their behavior in different regimes (early- and late- time cosmology), we can extract information about the behavior of the matter scalar field and its coupling to the gravitational degrees of freedom. Furthermore, such a perspective generates several insights about the parameters characterizing the relational clock and rods.

Small GFT background density. Let us start with the density ρ_0 as a function of the scale factor (7.1.2) and derive it twice with respect to the relational clock χ^0 to deliver the ratio $\ddot{\rho}_0/\rho_0$. We are then able to recast the background equations appearing in (4.4.25) in terms of $a(x^0)$ as the fundamental evolution equations for the background GFT condensate phase θ_0 namely;

$$D[\theta_0] \equiv (\dot{\theta}_0)^2 - \gamma \dot{\theta}_0 + \eta = \frac{3}{4}\left(\frac{2\ddot{a}}{a} + \frac{\dot{a}^2}{a^2}\right), \tag{7.1.3}$$

$$\ddot{\theta}_0 + \frac{3\dot{a}}{a}\left(\dot{\theta}_0 - \frac{\gamma}{2}\right) - \beta_j = 0. \tag{7.1.4}$$

In the following we work in the case where $\beta = 0, \alpha_i = 0$ (assumption EL.5 (hence negligible) and EL.6). The motivation behind this approximation was studied in [164],

where it was found that the regime for small β_j is compatible with the decoupling regime for first order perturbations and that is equivalent to setting $\alpha_i = 0$ since $\beta_j \propto \alpha_i$. The roots for the above quadratic equation $D[\theta_0]$ are given by

$$\left(\dot{\theta}_{0_{1,2}} - \frac{\gamma}{2}\right) = \pm\sqrt{\frac{\gamma^2}{4} - \left(\eta - \frac{3}{4}\left(\frac{2\ddot{a}}{a} + \frac{\dot{a}^2}{a^2}\right)\right)}\,. \tag{7.1.5}$$

The evolution equation for the background phase θ_0 in (7.1.3) can be solved exactly. This can be obtained once we render the second order differential equation appearing in (7.1.3) to a first order one. More precisely, let us consider the change of variable $\Theta_0 = \dot{\theta}_0$, then the second equation in (7.1.3) becomes

$$\dot{\Theta}_0 + \frac{3\dot{a}}{a}\Theta_0 - \frac{3\gamma}{2}\frac{\dot{a}}{a} = 0\,. \tag{7.1.6}$$

Notice that the coefficients appearing in this differential equation are time dependent. The general solution for such first order differential equation is given in terms of an integrating factor $\nu(x^0, \pi_\phi)$ by

$$\Theta_0 = \left(\int \nu(x^0)\frac{3\gamma}{2}\frac{\dot{a}}{a}\,dx^0 + c_2\right)\nu^{-1}(x^0)\,, \quad \nu = e^{\int \frac{3\dot{a}}{a}dx^0}\,. \tag{7.1.7}$$

In our case the integrating factor is computed to be $\nu = e^{\int p(x^0)dx^0} = e^{c_1}a^3$ and the solution for Θ_0 is simply given by $\Theta_0 = \frac{\gamma}{2} + c_2(e^{-c_1}a^{-3})$ with $(c_1\,, c_2)$ being integration constants. Once we go back to the initial variable θ_0, we find that the general solution of the background phase reads

$$\theta_0(x^0\,, \pi_\phi) = \frac{\gamma}{2}x^0 + c_2 e^{-c_1}\left(\int \frac{dx^0}{a^3(x^0, \pi_\phi)}\right) + c_3\,, \tag{7.1.8}$$

where c_3 is an integration factor and it is important to mention that a priori, all introduced constants can have a dependence on the scalar field momentum π_ϕ. The solution for the background condensate density was derived in [168]. The differential equation for the density (once we write it in terms of conserved quantities of the GFT condensate [77, 156], namely Q_j and energy $\mathcal{E}_j$) is given in (4.4.30) whose roots yield

$$\dot{\rho}_0 = \pm\sqrt{\mathcal{E}_j - \frac{Q_j^2}{\rho_0^2} + \mu_j^2\rho_0^2}\,.$$

The general solution[1] for such a differential equation is given by

$$\rho_0^2 = -\frac{\mathcal{E}_j}{2\mu_j^2} + A_j e^{2\mu_j x^0} + B_j e^{-2\mu_j x^0}\,, \tag{7.1.9}$$

[1]Notice that late time solution (large volume values), depends on the sign we attribute to μ_j. In this case, the solution for ρ_0 simplifies further as we will discuss later on.

where A_j and B_j are integration constants. By defining x^0_m as the point at which the density parameter reaches a minimum $\partial_0\left(\rho_0^2\right)\left(x^0_m\right)=0$, we see that we are able to parametrize the above expression for the squared density and it takes the form

$$\rho_0^2=-\frac{\alpha_j}{2}+\frac{\sqrt{\alpha_j^2+4\beta_j^2}}{2}\cosh\left(2\mu_j\left(x^0-x^0_m\right)\right)\,,\quad \alpha_j\equiv\mathcal{E}_j/\mu_j^2\,,,\quad \beta_j^2\equiv Q_j^2/\mu_j^2\,. \tag{7.1.10}$$

Recall that we are working in the case of a dominant spin value j_v and hence the conserved quantities are associated with this value only. Previous studies of the volume operator and the derived modified Friedman equations from it showed that if at least one of the conserved charges Q_j's is different from zero, or at least one of the conserved condensate energies $\mathcal{E}_j$ is strictly negative, then the expectation value of the volume operator never vanishes. Obviously, this case leads to a bouncing scenario replacing therefore the cosmological big bang singularity in the very early universe [204]. We will further discuss this point once we explore the matter content near the bounce within the GFT framework. Using the relation between the scale factor a and ρ_0 we can write down the explicit expression for the scale factor in terms of the solution for the background density, namely

$$a(x^0,\pi_\phi)=V_j\left(-\frac{\mathcal{E}_j}{2\mu_j^2}+A_je^{2\mu_j(x^0-x^0_m)}+B_je^{-2\mu_j(x^0-x^0_m)}\right)^{1/3}\,. \tag{7.1.11}$$

In order to avoid ambiguities that can be associated with the above expression of the GFT scale factor, it is important to recall that we are considering early times effective cosmologies and hence the variable x^0, in this case, is always the clock value near the bouncing event, i.e. $x^0-x^0_m$. Now, we can compute the exact form of the phase in (7.1.8) using the expression above for the scale factor. This explicitly reads

$$\begin{aligned}\theta_0=\frac{\gamma}{2}x^0+\frac{c_2e^{-c_1}}{V_j}&\frac{1}{2\mu_j\sqrt{\left(\frac{\mathcal{E}_j}{2\mu_j}\right)^2-4A_jB_j}}\\ &\times\left(i\log\left(\frac{\sqrt{\left(\frac{\mathcal{E}_j}{2\mu_j}\right)^2-4A_jB_j}-i(2A_je^{2\mu_j(x^0-x^0_m)}+\frac{\mathcal{E}_j}{2\mu_j^2})}{\sqrt{\left(\frac{\mathcal{E}_j}{2\mu_j}\right)^2-4A_jB_j}+i(2A_je^{2\mu_j(x^0-x^0_m)}+\frac{\mathcal{E}_j}{2\mu_j^2})}\right)+c_4\right)\,.\end{aligned} \tag{7.1.12}$$

where c_4 is an integration constant. This is the general solution for θ_0 for a dominant spin $j\equiv j_v$, for small densities ρ_0, characterizing, therefore, the background phase dynamics at early times. Before proceeding to the case of large-density-solution of θ_0, which indicates late time cosmological predictions, let us define the following functions for notation simplicity

$$\Delta_1(\pi_\phi)=\sqrt{\left(\frac{\mathcal{E}_j}{2\mu_j}\right)^2-4A_jB_j}\,,\quad n(\pi_\phi)=\frac{c_2e^{-c_1}}{V_j}\,,\quad b(\pi_\phi)=\frac{\mathcal{E}_j}{2\mu_j^2}\,, \tag{7.1.13}$$

$$X(\pi_\phi\,,(x^0-x^0_m))=i\log\left[\frac{\Delta_1-2iA_je^{2\mu_j(x^0-x^0_m)}-ib(\pi_\phi)}{\Delta_1+2iA_je^{2\mu_j(x^0-x^0_m)}+ib(\pi_\phi)}\right]\,. \tag{7.1.14}$$

Note that, a priori there is no physical reason for the constant $n(\pi_\phi)$ not to depend on the scalar field momentum π_ϕ, and this also applies to all integration constants. The background phase takes then a simpler form:

$$\theta_0(x^0\,,(\pi_\phi)) = \frac{\gamma}{2}x^0 + \frac{n(\pi_\phi)}{2\mu_j\Delta_1(\pi_\phi)}\left(X(\pi_\phi\,,(x^0 - x^0_m) + c_4\right)\,. \tag{7.1.15}$$

As we will see in the next section, the behavior of the background phase encoded in (7.1.12) and the form of the scale factor (7.1.11) will allow us to study the dynamical evolution of the matter content of the scalar field ϕ_0. They play a crucial role since they will enable the interpretation of the GFT matter content in the relational setting as an effective field theory propagating on curved spacetimes, stemming from the full QG theory.

Large GFT background density. Let us briefly discuss how the above solution for the background phase changes once we consider the case of large density ρ_0 [164,166,215]. The differential equation satisfied by ρ_0 for the large volume limit can be precisely derived once we neglect the first term including the conserved quantities $\mathcal{E}_j$ and Q_j appearing in (4.4.30). More concretely, the simplified evolution equation for the density reads

$$(\dot{\rho}_0)^2 \approx \mu_j^2\,(\pi_\phi)\,\rho_0^2\,, \tag{7.1.16}$$

whose solution is given by $\rho_0 = A_j e^{\pm 2\mu_j x^0}$. A precise solution thereof demands that we choose an appropriate sign for the parameter μ_j as well a specific root for (7.1.16). Such a choice can be made depending on the classical (or semi-classical) physical theory we are interested in reproducing.
Now, after having solved the differential equation for the background phase in (4.4.25), we end up with the general solution of θ_0 for large densities

$$\theta_0 = \frac{\gamma}{2}x^0 - \frac{Q_j V_j}{2\mu_j}e^{\pm 2\mu_j x^0} + c_5\,, \tag{7.1.17}$$

where c_5 is an integration constant that in principle can depend on the scalar field momentum π_ϕ.

Reintroducing β_j and α_i. In the following we perform the same analysis presented above without neglecting the contribution of the parameters β_j and α_i for the general solution of the background scale factor (density ρ_0) and then comment on how the solution changes the case of large volume. The first modification that surfaces is at the level of the solution for the background phase. In fact, if we consider the change of variables $\Theta_0 = \dot{\theta}_0 - \gamma/2$ we can derive the solution for the homogeneous differential equation $\dot{\Theta}_0 + 3\mathcal{H}\Theta = 0$, where we define $\mathcal{H} = \dot{a}/a$ as the Hubble parameter. The solution in this case yields $\Theta_0 = \tilde{c}_1 a^{-3}$. Since the inhomogeneous part of the differential equation is a constant,

namely β_j, the final Ansatz in this case for the variable $\Theta_0 = \tilde{c}_1 a^{-3} + \beta_j$. Going back to the initial variable θ_0, we end up with the solution

$$\theta_0 = \left(\frac{\gamma}{2} + \beta_j\right) x^0 + c_1 \int \frac{1}{a^3} dx^0 \,. \tag{7.1.18}$$

The integration over the scale factor can be carried out once we use the usual solution for the background density. The only change at this level is the appearance of the constant β_j in front of the clock. Moreover, for large densities, matching the volume background dynamics (expressed in terms of the scalar field clock) requires an exponential expression for it, since such dynamics are mainly dictated by ρ_0^2. In this case, if we consider an exponential Ansatz for ρ_0^2 and we derive the equation of motion for the phase we obtain, for large densities (and thus for large values of the clock, given our exponential Ansatz), $\theta_0 = (\gamma\mu_j + \beta_j) / (2\mu_j)$. To see if this solution is viable, we plug it in the evolution equation for the density in (4.4.25), where we can clearly see that it is not consistent, exactly because of the presence of β_j. This naturally supports our choice of restricting to small values of β_j.

7.1.2 The dynamics of inhomogeneities in GFT

The treatment of inhomogeneity conducted with the GFT condensate framework is rather involved since the dynamics of the perturbation are coupled and are dependent on the data entering the background. However, we are able to inspect several solutions to $\delta\theta$ and $\delta\rho$ once we explore inversion relations intertwining the respective dynamics. This procedure is commonly used in AG models based on Bose Einstein Condensate (BEC)-systems [11,12,216,217]. We proceed analogous to such employed schemes and present the detailed derivation of GFT perturbed phase dynamics, where the coupled perturbation of $\delta\rho$ and $\delta\theta$ are investigated. Once we do this, we devote the remaining of this section to analyzing the simpler case of the decoupling regime, namely by neglecting the contributions coming from β_j and α_i (assumption EL.6 and EL.5). Analogously to what we did for the background dynamics, we study the scale factor dependence of the perturbed geometry, provided we make the distinction between small and large background densities.

The AG treatment to the GFT perturbations In this section, we derive the inversion equation of the perturbed density that leads to the dynamical equation for the phase $\delta\theta$ inspired by the treatment of AG to BEC. We present the general case without neglecting the contribution of the parameter α_i. Let us then consider the equations of first

order perturbations given by the equations

$$\delta\ddot{\rho}\left(x,\pi_\phi\right)+\alpha_r\nabla^2\delta\rho\left(x,\pi_\phi\right)-\eta_j\left(\pi_\phi\right)\delta\rho\left(x,\pi_\phi\right) \tag{7.1.19}$$
$$-\left[\delta\dot{\theta}\left(x,\pi_\phi\right)\left(2\dot{\theta}_0\left(x^0,\pi_\phi\right)-\gamma\right)-\alpha_i\nabla^2\delta\theta\left(x,\pi_\phi\right)\right]\rho_0\left(x^0,\pi_\phi\right)=0\,,$$
$$\delta\ddot{\theta}\left(x,\pi_\phi\right)\rho_0\left(x^0,\pi_\phi\right)+\ddot{\theta}_0\left(x^0,\pi_\phi\right)\delta\rho\left(x,\pi_\phi\right)+2\delta\dot{\theta}\left(x,\pi_\phi\right)\dot{\rho}_0\left(x^0,\pi_\phi\right)+2\dot{\theta}_0\left(x^0,\pi_\phi\right)\delta\dot{\rho}\left(x,\pi_\phi\right)$$
$$-\gamma\delta\dot{\rho}+\alpha_r\left[\nabla^2\delta\theta\left(x,\pi_\phi\right)\right]\rho_0-\beta\delta\rho\left(x,\pi_\phi\right)+\alpha_i\nabla^2\delta\rho\left(x,\pi_\phi\right)=0\,. \tag{7.1.20}$$

Notice that we can write the first equation above (7.1.19) in a simpler form once we use the modified d'Alembert operator

$$\tilde{\Box}=\partial_0^2+\alpha_r\nabla^2\,. \tag{7.1.21}$$

and this yields explicitly

$$\left(\tilde{\Box}-\delta\eta\right)\rho\left(x,\pi_\phi\right)=\mathcal{D}\left[\delta\theta\left(x,\pi_\phi\right)\right]\,, \tag{7.1.22}$$

where we define the differential operator acting of the perturbed phase $\theta\left(x,\pi_\phi\right)$

$$\mathcal{D}\left[\delta\theta\left(x,\pi_\phi\right)\right]=\rho_0\left(x^0,\pi_\phi\right)\left(\left(2\dot{\theta}_0\left(x^0,\pi_\phi\right)-\gamma\right)\partial_0-\alpha_i\nabla^2\right)\delta\theta\left(x,\pi_\phi\right)\,. \tag{7.1.23}$$

Let us drop the argument of functions for the sake of notation simplicity. If we assume that the defined modified d'Alembert operator in (7.1.21) admits an inverse, one can invert the above equation for $\delta\rho$ and this reads

$$\delta\rho=\left(\tilde{\Box}-\eta_j\right)^{-1}\mathcal{D}[\delta\theta]\,. \tag{7.1.24}$$

We then proceed to the second equation in the perturbations. Once we set $\beta=0$ this equation yields

$$0=\rho_0\left[\delta\ddot{\theta}+2\delta\dot{\theta}\frac{\dot{\rho}_0}{\rho_0}+\alpha_r\nabla^2\delta\theta\right]+\delta\rho\left[\ddot{\theta}_0+\left[2\dot{\theta}_0-\gamma\right]\frac{\delta\dot{\rho}}{\delta\rho}\right]+\alpha_i\nabla^2\delta\rho\,. \tag{7.1.25}$$

Again using the defined d'Alembert operator and (7.1.24), the above evolution equation for the perturbation is recast in the following form

$$\tilde{\Box}\delta\theta+2\delta\dot{\theta}\frac{\dot{\rho}_0}{\rho_0}+\mathcal{L}[\delta\rho]=0\,, \tag{7.1.26}$$

where we defined the operator acting on the GFT perturbed density (after having multiplied (7.1.25) by ρ_0^{-1})

$$\mathcal{L}=\frac{2\dot{\theta}_0-\gamma}{\rho_0}\partial_0+\alpha_i\rho_0^{-1}\nabla^2+\frac{\ddot{\theta}_0}{\rho_0}\,. \tag{7.1.27}$$

This operator depends only on the background data. The equation of motion of the perturbed phase in (7.1.26) can be written solely in terms of the background data without the perturbed density appearing in it by plugging (7.1.24) and this reads

$$\tilde{\Box}\delta\theta + 2\dot{\delta}\theta\frac{\dot{\rho}_0}{\rho_0} + \mathcal{L}\Big[\left(\tilde{\Box}-\eta\right)^{-1}\mathcal{D}[\delta\theta]\Big] = \alpha_r\nabla^2\delta\theta\,. \tag{7.1.28}$$

This is the evolution equation of the perturbed phase of the GFT condensate on the (sort of) background encoded in (ρ_0,θ_0) whose equations of motion are dictated by (4.4.27). One can write down explicitly the relational dynamics provided by the background data of the condensate given in section 7.1.1. The explicit equation of motion for the perturbation yields

$$\begin{aligned}&\partial_0^2\delta\theta + \alpha_r\nabla^2\delta\theta + 2\frac{\dot{\rho}_0}{\rho_0}\partial_0\delta\theta + \frac{D^{-1}\left[\rho_0(2\dot{\theta}_0-\gamma)(2\ddot{\theta}_0-\gamma)\right]}{\rho_0}\partial_0\delta\theta - \frac{D^{-1}\alpha_i(2\dot{\theta}_0-\gamma)}{\rho_0}\partial_0\nabla^2\delta\theta\\ &+ D^{-1}\alpha_i(2\ddot{\theta}_0-\gamma)\nabla^2\delta\theta - \alpha_i^2 D^{-1}\nabla^2.\nabla^2\delta\theta + \frac{D^{-1}\ddot{\theta}_0(\rho_0(2\theta_0-\gamma))}{\rho_0}\delta\theta - \frac{D^{-1}\ddot{\theta}_0\alpha_i}{\rho_0}\nabla^2\delta\theta = 0\,,\end{aligned} \tag{7.1.29}$$

where we defined $D^{-1} = \left(\tilde{\Box}-\eta\right)^{-1}$ as the compact notation for the inverse operator associated with the perturbed density. Let us stress that there are two terms that are still there without any obvious association, therefore, we assume they cancel each other

$$D^{-1}\alpha_i^2\nabla^2.\nabla^2\delta\theta = D^{-1}\theta_0''(2\theta_0-\gamma)\delta\theta\,. \tag{7.1.30}$$

This provides an equation that probably can fix the coefficient α_i and hence deliver more insight into its physical interpretation. Let us work out the solutions of the perturbation in the assumption EL.6 of α_i set to zero. In this case (7.1.29) reads

$$\partial_0^2\delta\theta + \alpha_r\nabla^2\delta\theta + \frac{\dot{\rho}_0}{\rho_0}\partial_0\delta\theta + \frac{D^{-1}\left[\rho_0(2\theta_0-\gamma)(2\ddot{\theta}_0-\gamma)\right]}{\rho_0}\partial_0\delta\theta + \frac{D^{-1}\ddot{\theta}_0(\rho_0(2\theta_0-\gamma))}{\rho_0}\delta\theta = 0\,. \tag{7.1.31}$$

Denoting time derivative by dots, spatial ones by $'$, and defining the clock dependent functions

$$\lambda_1 = 2\frac{\dot{\rho}_0}{\rho_0} + D^{-1}\left[(2\theta_0-\gamma)(2\ddot{\theta}_0-\gamma)\right]\,, \tag{7.1.32}$$

$$\lambda_2 = D^{-1}\ddot{\theta}_0((2\theta_0-\gamma))\,, \tag{7.1.33}$$

we can then write (7.1.31) in a simpler form

$$\delta\ddot{\theta} + \lambda_1\delta\dot{\theta} + \lambda_2\delta\theta = -\alpha_r\delta\theta''\,. \tag{7.1.34}$$

Solutions to the above equation can be obtained using the variable separation techniques (the spatial translation symmetry allows the spatial dependence to be separated from the

time dependence). Notice also that the time dependent part of the evolution equation is similar to that of a damped harmonic oscillator whose solution we denote by $C(t)$. A general solution for a single mode momentum k_θ is then given by

$$\delta\theta = C(t, \pi_i, \pi_\phi) e^{i\pi_i \cdot x^i} . \tag{7.1.35}$$

This is the general procedure to extract relational dynamics of the perturbed phase without any direct reference of $\delta\rho$. We now focus on the regime where these perturbations decouple for the case of small and large perturbed GFT densities.

Small background density. The strategy we are adapting in what follows is simple; from the two equations in (7.1.19) we derive an inversion relation to express the perturbed density $\delta\rho$ in terms of the phase $\delta\theta$ for small- and later on for large- background density ρ_0. This requires, as we saw above, an assumption to be made on the differential operator that acts on the perturbed density $\delta\rho$, namely that it has to be invertible. Then one can reformulate the perturbation equations solely in terms of the phase $\delta\theta$, where now, the background data appearing in the coefficients are a function of the scale factor. Let us proceed with this approach.Noticing that the second evolution equation for the background phase θ_0 can be written as

$$\ddot{\theta}_0 = -3\mathcal{H}\left(\dot{\theta}_0 - \frac{\gamma}{2}\right) , \tag{7.1.36}$$

and using the general solution for the background GFT condensate phase (7.1.8), this can be further simplified to

$$\ddot{\theta}_0 = -3c\mathcal{H}a^{-3} . \tag{7.1.37}$$

The inversion equation for the perturbed density in (7.1.24) yields

$$\left(\tilde{\Box} - \eta_j\right) \delta\rho\left(x, \pi_\phi\right) = \mathcal{D}\left[\delta\theta\left(x, \pi_\phi\right)\right] , \tag{7.1.38}$$

$$\delta\rho = \left(\tilde{\Box} - \eta_j\right)^{-1} \mathcal{D}[\delta\theta] , \tag{7.1.39}$$

where $\tilde{\Box}$ is the modified d'Alembert operator (7.1.21) and the differential operator $\mathcal{D}[\theta]$ acting of the perturbed phase as in (7.1.23) reads

$$\mathcal{D}_a\left[\delta\theta\left(x, \pi_\phi\right)\right] = \left(2\left(\frac{a}{\tilde{V}_j}\right)^{3/2}\left(\dot{\theta}_0 - \gamma/2\right)\right) \partial_0 \delta\theta\left(x, \pi_\phi\right) . \tag{7.1.40}$$

It is important to notice that (7.1.38) is a second order inhomogeneous wave equation. The usual treatment in this case is to derive the solution to the homogeneous differential equation $\left(\tilde{\Box} - \eta_j\right) \delta\rho\left(x, \pi_\phi\right) = \delta(x^0 - y^0)\delta^3(x^i - y^i)$ by means of a Green function [218]. Once this is obtained, we can derive the general solution to the inhomogeneous evolution equation. It is worth emphasizing that in order to specify a unique Green function or

fundamental solution for the wave equation, one must pose some boundary and initial conditions. This involves considering the different types of boundary conditions, namely Dirichlet, Neumann, and Cauchy's initial boundary conditions. For the purpose of this work, we will suppress the implications of such a detail, and solve the inhomogeneous wave equation for a general Green function (assumption EL.7). In fact, the well-posedness of the problem comes from imposing boundary- and initial- conditions. Local solutions can always be found and this is indeed our case since we are not specifying any boundary conditions. The fundamental solution to the homogeneous PDE can be exactly solved once we work in momentum space by means of the Fourier transform. The Green function associated with the homogeneous evolution equation of the perturbed density must then satisfy a Klein-Gordan-like equation with a mass-like term (the constant η_j appearing in (7.1.38)), namely

$$\left(\partial_0^2 + \alpha_r \nabla^2 - \eta_j\right) G(x^0 - y^0)(x^i - y^i) = \delta(x^0 - y^0)\delta^3(x^i - y^i)\,, \tag{7.1.41}$$

where $\delta(x^0 - y^0)\delta^3(x - y)$ is the Dirac function. Recall that π_0 and π_i are the momenta of the clock and rods scalar fields. The Green function in momentum space then yields

$$G = \frac{1}{\pi_0^2 + \alpha_r \pi_i^2 - \eta_j}\,. \tag{7.1.42}$$

Thus the perturbed density takes the following form in field (coordinate) and momentum space respectively

$$\delta\hat{\rho}_h(\pi_0, \pi_i) = \int_{\mathbb{R}} \int_{\mathbb{R}^3} \delta\rho(x^i, x^0) e^{-2\pi i(\mathbf{x^i}\cdot\pi_\mathbf{i} + x^0\cdot\pi_0)} d\mathbf{x^i} dx^0\,, \tag{7.1.43}$$

$$\delta\rho_h(x^0, x^i) = \int_{\mathbb{R}} \int_{\mathbb{R}^3} \delta\hat{\rho}(\pi_\mathbf{i}, \pi_0) e^{2\pi i(\mathbf{x^i}\cdot\pi_\mathbf{i} + x^0\cdot\pi_0)} d\pi_i d\pi_0\,, \tag{7.1.44}$$

where we denote the inverse transform with the hat, the index h stands for the homogeneous wave equation and the bold letters refer to vector notation of the spatial directions. To solve the inhomogeneous wave equation $\delta\ddot{\rho} + \alpha_r \nabla^2 \delta\rho - \eta_j \delta\rho = \mathcal{D}_a[\delta\theta]$, we simply apply the Fourier transform to the equation to obtain

$$\pi_0^2 \hat{\rho} + \alpha_r |\pi_i|^2 \hat{\rho} - \eta_j \hat{\rho} = \hat{\mathcal{D}}_a[\theta]\,, \tag{7.1.45}$$

$$\delta\hat{\rho} = \frac{\hat{\mathcal{D}}_a[\delta\theta]}{\pi_0^2 + \alpha_r |\pi_i|^2 - \eta_j}\,. \tag{7.1.46}$$

We would then recover $\delta\rho$ via the inverse Fourier transform. The Fourier transform of the operator $\mathcal{D}_a$ can be derived after recalling that $\rho_0\left(2\dot{\theta}_0 - \gamma\right) = 2c_2 e^{-c_1} a^{-3/2}/V_j^2$ and after performing an integration by part

$$\begin{aligned}\hat{\mathcal{D}}_a[\delta\theta(\pi_0, \pi_i)] &= \int_{\mathbb{R}} \int_{\mathbb{R}^3} \left(\rho_0(x^0)\left(2\dot{\theta}_0(x^0) - \gamma\right)\right) \delta\dot{\theta}(x^i, x^0) e^{-2\pi i(\mathbf{x^i}\cdot\pi_\mathbf{i} + x^0\cdot\pi_0)} d\mathbf{x^i} dx^0 \\ &= \frac{c_2 e^{-c_1}}{V_j^2} \int_{\mathbb{R}} \int_{\mathbb{R}^3} 3\mathcal{H} a^{-3/2} \delta\theta(x^0, x^i) e^{-2\pi i(\mathbf{x^i}\cdot\pi_\mathbf{i} + x^0\cdot\pi_0)} d\mathbf{x^i} dx^0\,,\end{aligned} \tag{7.1.47}$$

which is basically a convolution of two functions. Now let us study the second equation encoding the perturbation (7.1.25) and write the counterpart of the operator $\mathcal{L}$ defined in (7.1.27) in terms of the scale factor. To this aim, we use the evolution equation of the background phase given in (7.1.36), this yields

$$\mathcal{L}_a = \left(\frac{a}{V_j}\right)^{-3/2} \left(\left(\dot{\theta}_0 - \frac{\gamma}{2}\right)(2\partial_0 - 3\mathcal{H})\right) , \tag{7.1.48}$$

and (7.1.28) in the decoupling regime describing the dynamics of the perturbed GFT phase is then given by

$$\tilde{\Box}\delta\theta + 3\mathcal{H}\delta\dot{\theta} + \mathcal{L}_a\left[\left(\tilde{\Box}_j - \eta_j\right)^{-1}\mathcal{D}_a[\delta\theta]\right] = 0 , \tag{7.1.49}$$

The effective dynamical equation for the perturbed phase can be derived using the relation (7.1.37) and expressed in terms of the effective Hubble parameter $\mathcal{H}$ and scale factor a, this reads

$$\delta\ddot{\theta} + \lambda_1(x^0, \pi_{\phi_0})\delta\dot{\theta} + \lambda_2(x^0, \pi_{\phi_0})\delta\theta = -\alpha_r\nabla^2\delta\theta . \tag{7.1.50}$$

where we introduced the time dependent functions appearing in the differential equation for the perturbation in terms of the scale factor:

$$\lambda_1(x^0, \pi_{\phi_0}) = 3\mathcal{H} + 3\mathcal{H}c^2a^{-6} , \tag{7.1.51}$$

$$\lambda_2(x^0, \pi_{\phi_0}) = 6\dot{\mathcal{H}}c^2a^{-6} - 18c^2\mathcal{H}^2a^{-6} , \tag{7.1.52}$$

where for notation simplicity, we defined the constant $c = \frac{c_2 e^{c_1}}{V_j}$. In the case where we neglect the contribution coming from the density propagator given by the Green function G in (7.1.42) (assumption(EL.9)). One could write down an Ansatz for the perturbed $\delta\theta$ and it reads

$$\delta\theta = \mathcal{C}(x^0, \pi_\phi)e^{i\pi_j . x^j} , \tag{7.1.53}$$

where $\mathcal{C}(x^0, \pi_\phi)$ is the solution to the damped harmonic oscillator-type equation for the perturbed phase. The dynamics encoded in (7.1.50) are thus the fundamental evolution equations of the phase $\delta\theta$ encapsulating inhomogeneities for small background densities.
It is in principle possible to solve the above equation if we assume that $\lambda_1(x^0, \pi_{\phi_0})$ obeys the following approximation (assumption EL.8)

$$3\mathcal{H}c^2a^{-6} \gg \frac{1}{2} - 3\mathcal{H} , \tag{7.1.54}$$

we can then replace $\lambda_1(x^0, \pi_{\phi_0})$ simply with $6\mathcal{H}c^2a^{-6}$. In this case, the solution to the damped harmonic oscillations reads

$$\mathcal{C}(x^0, \pi_{\phi_0}) = c^2\mathcal{A}(\pi_\phi)\exp\left(-a^{-6}(x^0, \pi_\phi)\right) , \tag{7.1.55}$$

where $\mathcal{A}(\pi_\phi)$ is an integration constant, that can depend on the scalar field momentum.

Large background density. The decoupling regime of the perturbations for which a sufficient condition is established by setting $\beta_j = 0$ corresponds to the limit in which the parameter

$$|\alpha_i| = \frac{2}{3}\frac{\pi_x^2 \delta_r \, |\delta_i|}{\epsilon^2 \pi_0^2} \ll 1, , \tag{7.1.56}$$

where the background density ρ_0 is taken to be very large. Indeed, using the background equation, The differential operator acting on $\delta\rho$ can be written as

$$\left(\tilde{\Box} - \eta_j\right) \delta\rho \simeq \frac{2Q_j}{\rho_0}\delta\dot{\theta} \, , \tag{7.1.57}$$

For large enough background densities ρ_0, the above equations simplify and we end the following decoupled evolution equations for the perturbations[2]

$$\delta\ddot{\rho}\,(x,\pi_\phi) + \alpha_r \nabla^2 \delta\rho\,(x,\pi_\phi) - \eta_j^2\,(\pi_\phi)\,\delta\rho\,(x,\pi_\phi) \simeq 0\,, \tag{7.1.58}$$

$$\delta\ddot{\theta}\,(x,\pi_\phi) + 3\mathcal{H}\left(x^0,\pi_\phi\right)\delta\dot{\theta}\,(x,\pi_\phi) + \alpha_r \nabla^2 \delta\theta\,(x,\pi_\phi) \simeq 0\,, \tag{7.1.59}$$

which are clearly decoupled. Obviously, the perturbed density obeys a modified wave equation as we encountered in the previous case, however, homogeneous. Its explicit solution can then be derived by means of the Green function. In momentum space, this is simply given by

$$\delta\hat{\rho} = \frac{1}{\pi_0^2 + \alpha_r |\pi_i|^2 - \eta_j} \, . \tag{7.1.60}$$

If we set $\alpha_r = -1$ we end up with a Klein Gordan equation for $\delta\rho$ with a mass-like term given by η_j. An interesting feature of the above equations is that any Lorentz property of the second order differential operator in the perturbed equations is in fact only a result of the features of the peaking functions, rather than the fundamental symmetries imposed on the GFT action $S_{\rm GFT}$ in section 4.4.2. Indeed, we can observe the parameter λ appearing in (4.4.19) that is in principle responsible whether the matter variables enter the fundamental GFT action in a Lorentz ($\lambda = 1$) or Euclidean ($\lambda = -1$) invariant form, only enters in η_j. The above dynamical equations are clearly not affected by this. This insinuates that only a certain class of states is able to effectively reproduce local Lorentz signature as was discussed in [164].

The solution for the perturbed phase in (7.1.59) can be formally derived using the integration factor method and it reads

$$\delta\theta\,(x,\pi_\phi) = \left(c_6 x^0 + \int dx^0 (a^{-3})\right) e^{\pi_i x^i} \, . \tag{7.1.61}$$

[2]One can see that $\rho \sim \theta/\rho_0$, and for large enough ρ_0, the right-hand-side can be neglected. Similarly, using that $\ddot{\theta}_0 = -2Q_j\rho_0^{-2}\,(\dot{\rho}_0/\rho_0) \sim -2Q_j\mu_j\rho_0^{-2}$, we deduce that the first term at the second line of equation (4.4.31) is of order $\delta\rho/\rho_0^2$, while the first term at the first line of equation (4.4.31)is of order $\rho_0\theta$, so for large enough ρ_0, only he latter is important.

In the above solution, for simplicity, we considered the case where the parameter α_r coincides with -1 to reproduce the standard d'Alembert operator. The relational clock dependence in this solution for $\delta\theta$ is of the same type as the background θ_0 once we identify the integration constant c_6 with $\gamma/2$. This case will play an important role, when we study the scalar perturbation affecting the matter field $\delta\phi$ for large background densities in section 7.3.

7.2 Background scalar field dynamics

Previous studies showed that the big-bang singularities of classical FLRW spacetimes that occur generically in GR are resolved within the GFT condensate framework presented here [166]. The solution for ρ_0^2 in (7.1.10) clearly shows that it will reach a minimal value at which point they will bounce (and it is clear that there is only a single bounce has only one turning point), and thus the cosmological spacetime that emerges from the GFT condensate state is that of what we call a bouncing FLRW spacetime at late times. It is important to recall that such a bounce occurs when the density is relatively small. Bearing this in mind, enriching the model with matter degrees of freedom and perturbation-treatment (section 4.4.2 and 7.1.2) raises more questions about the additional physical predictions we could extract from it. In this section, we study the matter content of a scalar field near the bounce and then later on for a sufficiently large density to reproduce GR physics at the background level. Therefore, we examine the evolution equations of such a field from the very dynamics of the GFT phase, given such a condition on the density.
The evolution equation for the background matter field can be derived from the expectation value of the corresponding GFT field operator (4.4.5) with respect to the CPS state, as was done for the volume operator. Using the tools we developed in section 7.1.1, we then derive the dynamical equation of the scalar field by getting rid of the condensate parameters dependence (ρ_0 and θ_0). More concretely, we highlight the relation between the phase of the GFT condensate θ_0 and ϕ_0, which allows us to obtain a closed relational dynamical equation for the scalar field starting from that of θ_0. We will compare it to the results concerning alternative theories of gravity for ϕ_0 given in [219, 220]. We then analyze the behavior of the background scalar field in the regime where the GFT density is large, following the same line of reasoning to extract its evolution equation. This is important for the perturbed case since ϕ_0 also enters the equations of motion for the perturbed matter content (section 7.3) in $\delta\phi$.

7.2.1 Early times scalar field dynamics

In section 7.1.1, we were able to determine the explicit form of the background quantity θ_0 depending on large or small values of ρ_0^2. We now study the matter content of the scalar field ϕ_0 and its evolution through the different cosmological regimes. The expression for the background scalar field ϕ_0 and its momentum were already derived in [164] and they

read

$$\langle\hat{\Phi}\rangle = \phi_0 = N_0\partial_{\pi_\phi}\theta_0\,, \tag{7.2.1}$$

$$\langle\hat{\Pi}_\phi\rangle \simeq \tilde{\pi}_\phi\rho_0^2\,(x,\tilde{\pi}_\phi) = \tilde{\pi}_\phi N_0\,(x,\tilde{\pi}_\phi)\ . \tag{7.2.2}$$

where the exact solution for θ_0 is given[3] by (7.1.12). The matter content of the theory is encoded in the above equations and its relational dynamics with respect to the clock are determined through the evolution equation of the GFT phase. On the other hand, the geometry content is given by the expectation value of the GFT volume operator (4.4.4). Using the expression for ϕ_0 and the dynamics dictated by the evolution equation of the condensate phase θ_0, we are able to write down the evolution equations for the background scalar field, that is inasmuch interpreted as an effective quantum field theory propagating on a curved background, after taking into consideration all the assumptions made so far. This has also to accommodate the geometric prediction that the effective volume delivers, which is encoded in the scale factor.

Before proceeding with this scheme, it is important to mention that even though the effective evolution equation will be describing a matter field living on a minisuperspace, parametrized by a clock and rods, we need to keep in mind that classically [164,219], the set of the four scalar fields is governed by the action in (B.1.1), where the adapted coordinates to such a set are given by

$$\chi^\mu \equiv \kappa^\mu x^\mu\,, \tag{7.2.3}$$

where κ^μ is an arbitrary constant and these coordinates also satisfy $\nabla^a\nabla_a x^\mu = 0$. This clearly leads to the relation $\frac{\partial_\mu\chi^\mu}{\partial_\mu x^\mu} = \kappa^\mu$. Hence, we can write the parametrized equation of the scalar field in a deparametrized form where the sole change that will appear overall is a constant. It is only thanks to the properties and settings we assigned to peaking states and the relational frame, we are then able to discuss the possibility of deriving an effective metric in a familiar manner. Indeed, (7.2.3) and (4.4.14) is the direct proof of the indirect assumption that our clock and rods are ideal, which is the simplest case one could take into consideration for its direct relation to classical theories of spacetimes.

Let us now proceed with the derivation of the dynamics of ϕ_0 on a homogeneous background. The key idea behind such a program is to establish a relation between $\partial_{\pi_\phi}\theta_0$ (hence the scalar field ϕ_0) and the initial expression of θ_0. In fact, in our case, one can show that the following holds

$$\partial_{\pi_\phi}\theta_0 = \left(\theta_0 - \frac{\gamma x^0}{2}\right)\left(-\frac{n\partial_{\pi_\phi}(\mu_j\Delta_1)}{2\mu_j\Delta_1} + \frac{n\partial_{\pi_\phi}X(\pi_\phi\,,x^0)}{X(\pi_\phi,x^0)}\right)\,. \tag{7.2.4}$$

[3]Notice that in the expression for (7.1.12) only the parameters V_j and γ do not depend on the scalar field momentum π_ϕ.

Using (7.2.1) we could express the GFT condensate phase θ_0 in terms of the scalar field ϕ_0 as follows

$$\theta_0 = \left(\frac{V_j}{a^3 \left(-\frac{n\partial_{\pi_\phi}(\mu_j \Delta_1)}{2\mu_j \Delta_1} + \frac{n\partial_{\pi_\phi} X(\pi_\phi, x^0)}{X(\pi_\phi, x^0)} \right)} \right) \phi_0 + \frac{\gamma x^0}{2} \equiv \left(a^3 f(\pi_\phi, x^0) \right)^{-1} \phi_0 + \frac{\gamma x^0}{2} \,. \quad (7.2.5)$$

We then compute $\dot{\theta}_0$ and $\ddot{\theta}_0$, recalling that they obey the dynamical equation, $\ddot{\theta}_0 + \frac{3\dot{a}}{a}\left(\dot{\theta}_0 - \frac{\gamma}{2}\right) = 0$. The above relation between the background phase and scalar field can be considered as an inversion formula that translates the condensate parametrization and dynamical content to field one. It is then clear that following this line of reasoning, we obtain a *closed* evolution equation for the matter field on a minisuperspace[4]. The effective field equation of the background scalar field

$$\left(a^3 f\right)^{-1} \ddot{\phi}_0 - \left(3\frac{\dot{a}}{a^4 f} + 2\frac{\dot{f}}{a^3 f^2} \right) \dot{\phi}_0 - \left(-3\frac{\dot{a}^2}{a^5 f} + 3\frac{\ddot{a}}{a^4 f} - 3\frac{\dot{a}\dot{f}}{a^4 f^2} - 2\frac{\dot{f}^2}{a^3 f^3} + \frac{\ddot{f}}{f^2 a^3} \right) \phi_0 = 0 \,. \quad (7.2.6)$$

In order to provide a consistent interpretation of the above field equation within our framework, we need to consider two different types of assumptions that are necessary to exploit the physical predictions of (7.2.6). To be more precise about the assumptions and predictions that we will present shortly, we first write down the d'Alembertian operator $\Box$ acting on a scalar field

$$\Box = \frac{1}{\sqrt{-g}} \partial_\mu \left(\sqrt{g} g^{\mu\nu} \partial_\nu \phi_0 \right) \,, \quad (7.2.7)$$

where $g^{\mu\nu}$ is the inverse metric of the curved spacetime. Looking at (7.2.6) it seems only natural to consider it as a classical field theory on a homogeneous curved background and therefore extract an effective metric describing spacetime time on top of which it is propagating. However, choosing this path insinuates the assumption that the spacetime metric (after deparameterizing the relational frame in the minisuperspace) is fixed, meaning that the latter does not react to the state of the field theory. On the other hand, if we discard such an assumption and consider instead, that the background geometry reacts to the matter fields, we are faced with the program of modified theories of gravity such as the scalar-tensor theories or $f(R)$ theories [220]. Let us investigate the differences and the consistency of the assumptions we are making for each path.

Classical field theory on curved spacetime. The formalism of a field theory on curved spacetimes assumes by construction a fixed classical background, where the evolution equation in the simplest case of a scalar field is given by the d'Alembert operator (7.2.7) in addition to some mass or potential terms, i.e. the Klein Gordon equation. The

[4]It is important to bear in mind for what follows that the above-introduced function f contains an imaginary part. This is evident since it bears the derivative of the function $X(\pi_\phi, t)$ defined in (7.1.13).

field equation is obtained after varying the action (for instance (B.1.5)) with respect to the field. Furthermore, in strong gravitational fields, the field theory could be non-minimally coupled to the Ricci scalar, which hints to the dominance of the gravitational effects over the matter ones. In the beforehand situation, we can extract what we will call effective metric, once we convert (7.2.6) from vector notation to index one, where in this case we encounter only the time indexed part of the metric, namely ∂_0 since we are working on a homogeneous universe. This explicitly yields

$$\left(a^3 f\right)^{-1} \partial_0 \left(a^3 f^2 \partial_0 \phi_0\right) + \left(a^3 f\right)^{-1} \left(3\frac{\dot{a}^2}{a^2} - 3\frac{\ddot{a}}{a} + 3\frac{\dot{a}\dot{f}}{af} + 2\frac{\dot{f}^2}{f^2} - \frac{\ddot{f}}{f}\right)\phi_0 = 0\,. \tag{7.2.8}$$

It is important to mention that in order to identify an effective metric[5] for the above field theory, we need to assume that there is a relation between the power of the scale factor entering the spatial metric component and that of the time one. The key term that encodes all the metric entries we are seeking is given by $\partial_0 \left(a^3 f^2 \phi_0\right)$, since formally it should entail $\partial_0 \left(\sqrt{-g} g^{00} \phi_0\right)$. The g^{00} component can be read off from whatever function multiplying $\partial_0^2 \phi_0$ which in our case should be of the form $\left(a^3 f\right)^{-1}$. Now that we know the time component of the metric, the only option we are left with for the homogeneous space contribution is $g^{ij} = a(x^0)^2 f(x^0, \pi_\phi)$ that conforms the power counting of the scale factor and the function f in the term $\sqrt{-g} g^{00}$ appearing in the above evolution equation. Notice the space components of the metric enter the determinant, even though the space is homogeneous. However, this consideration does not lead to the same volume element stemming from the GFT volume operator in (7.1.2), which was our starting point. Therefore, to stay consistent with the contribution coming from the geometric content of the theory, the time component g_{00} should contain all the powers of the function f. Hence, we can consider the effective metric instead

$$g_{\mu\nu} = \begin{pmatrix} a^3 f^2 & 0 & 0 & 0 \\ 0 & a^2 & 0 & 0 \\ 0 & 0 & a^2 & 0 \\ 0 & 0 & 0 & a^2 \end{pmatrix}. \tag{7.2.9}$$

Now, the Ricci scalar R associated with such a homogeneous isotropic metric and the additional term appearing in the above field equation (after having multiplied with the g_{00} component[6]) takes the form

$$a^3 f^2 R = 6\mathcal{H}\frac{\dot{f}}{f} + 9\mathcal{H}^2 - 6\dot{\mathcal{H}}\,, \tag{7.2.10}$$

$$a^3 f^2 M^2 = \left(\frac{3}{2}\mathcal{H}^2 + 2\frac{\dot{f}^2}{f^2} + \frac{\ddot{f}}{f}\right), \tag{7.2.11}$$

[5] As we already emphasized, going from the relational fields minisuperspace to manifold one is a linear map, due to the properties of the quantum states we used to derive the effective dynamics of the theory.

[6] It might seem clear how the metric and inverse metric transform, namely that way which is similar to the standard case. However, in our setting which is that of an effective theory originating from a specific quantum gravity model, such a fact should be assumed.

which we can identify in the closed evolution equation (7.2.8). The latter then can be written as

$$\ddot{\phi}_0 - \left(3\mathcal{H} + 2\frac{\dot{f}}{f}\right)\dot{\phi}_0 + a^3 f^2 \left(\frac{R}{2}\right)\phi_0 + \left(\frac{3}{2}\mathcal{H}^2 - 2\frac{\dot{f}^2}{f^2} - \frac{\ddot{f}}{f}\right)\phi_0 = 0\,. \tag{7.2.12}$$

We mention that the signature of the effective metric can be extracted from the sign of function f since it enters only the time component g_{00} and is the only function that depends on the quantum gravity parameter η_j responsible for the emergence of such a signature at early times. Furthermore, the effective Ricci scalar will pick up a different sign only in terms coming from the g_{00}-contributions. In our case and for the present being, we avoided specifying any signature. This dynamical equation is obviously the result of varying an effective action with respect to the scalar field, where such an action is given by

$$\frac{\delta S}{\delta \phi_0} = 0\,, \quad S = \frac{1}{2}\int d^4x\sqrt{g}\left(\partial_\mu\phi_0\partial_\nu\phi_0 - \frac{R}{2}\phi_0^2 + M^2\phi_0^2\right)\,. \tag{7.2.13}$$

The solution of the scalar field satisfying the above evolution equation is extracted from the expectation value of the underlying GFT operator[7]. For completeness, we write down the explicit form of ϕ_0

$$\phi_0 = \frac{ia^3}{(2\mu_j)^2\Delta_1^2}\left(\frac{2\mu_j\Delta_1\left(2x^0\tilde{\mu}_j(\Delta_1 - ib) + i\tilde{b} - \tilde{\Delta}_1\right)}{2iA_j e^{2\mu_j x^0} + ib - \Delta_1} + \frac{2\mu_j\Delta_1\left(2\tilde{\mu}_j x^0(ib + \Delta_1) - i\tilde{b} - \tilde{\Delta}_1\right)}{2iA_j e^{2\mu_j x^0} + ib + \Delta_1}\right. \tag{7.2.14}$$

$$\left. - \left(\Delta_1\tilde{\mu}_j + 2\mu_j\tilde{\Delta}_1\right)\log\left(\frac{2\Delta_1}{2iA_j e^{2\mu_j x^0} + ib + \Delta_1 - 1}\right)\right)\,,$$

where the $\tilde{}$ notation refers to the derivatives with respect to the field momentum ∂_{π_ϕ} and the parameters appearing above were introduced in (7.1.13). The dynamics of the scalar field derived above (7.2.6) at early times can be used to write down the associated Friedman equations. Recall that we can write the stress energy tensor

$$T_{\mu\nu} \equiv -\frac{2}{\sqrt{-g}}\frac{\delta S}{\delta g^{\mu\nu}}\,, \tag{7.2.15}$$

Using the field equation (7.2.8) and the GFT phase differential equation (7.1.4) along with the effective metric in (7.2.9), the first Friedmann equation reads

$$3\mathcal{H}^2 = \dot{\phi}_0^2 + \frac{3}{2}\mathcal{H}^2\phi_0^2 + \frac{a^3 f^2}{2}\phi_0^2 - a^3 f^2 M^2\,, \tag{7.2.16}$$

The second Friedman equation is then

$$2\mathcal{H}^2 - \dot{\mathcal{H}} - 2\mathcal{H}\frac{\dot{f}}{f} = a^3 f^2\frac{M^2}{1 - \dot{\phi}_0^2/2}\,, \tag{7.2.17}$$

[7]Bear in mind that even when we make the transition from the minisuperspace to the manifold picture, the field expression will pick up the entries in the constant κ^μ.

where the left-hand side of this set of equations is encoding the geometric part of the universe, and they rely on the expectation value of the GFT volume operator and the relation (7.1.2).
There are several remarks that we can make at this stage. The field equation of the matter field, ϕ_0 at early times reinforces the claim that it is only natural to expect different emergent quantities than those predicted by GR. The QG modifications to the geometry and matter in the universe at early times are precisely captured by the modified scale factor (stemming from the GFT volume operator) and the dynamics of the scalar field ϕ_0, which allow us to interpret it as a non-minimally coupled effective theory in a cosmological setting. The first deviation from GR is the quantum bounce that occurs at the condensate level [156, 160, 166, 206, 215, 221], underlying the quantum gravity origin for the extracted effective physics. Moreover, this claim is further underpinned by the modified Friedmann equations that can take a familiar form as in the studies of modified gravity theories [211], once we fix the GFT quantum gravity parameters listed in (4.4.19). Before proceeding to examine the behavior of the matter content at late times, let us make some conclusive remarks for the matter content near the bounce. Under the assumption EL.10, we are faced with some kind of a field theory propagating on a fixed background and we can reflect from the dynamics in (7.2.6) on several issues and remarks

1. *Gauge:* it is clear from section (B.1.1) that we do not obtain a line element for the geometry at hand that should be in harmonic gauge, meaning that the powers of the scale factor and the additional modification coming from the function f are in discrepancy with the one described in QFT on curved background in harmonic gauge. It is in fact natural since we are still at the action level of the theory and did not perform a Hamiltonian analysis of it. In fact, this is the key difference between the derived metric in (7.2.9) and that of (B.1.1), since it is obtained only after having specified a lapse function that is equal to a^3 that we can recover the line element in the Harmonic gauge.

2. *Emergent mass:* The above emergent parameter that we denote by M^2 is not present at the level of the GFT action which was our starting point. We suggest to interpreted as an effective mass that the field theory acquires at early times, or equivalently an effective potential. In the latter case, we are led to believe that our model naturally incorporates inflation driving the expansion of the universe. This is also related to the Starobinsky model and Higgs inflation, also due to their relevance to $f(R)$ theories [222, 223]. To shed more light on which case our framework reproduces, we need to further constrain the QG parameters of the underlying relational GFT formalism. Despite this and for the sake of simplicity we will refer to this emergent quantity as the effective mass. This is further backed up by the so-called "chameleon mechanism", which was introduced as a mere concept in gravitational physics. The basic idea behind it is that, for theories with a non-minimally coupled scalar field, then in the presence of other matter fields these scalars can acquire an effective mass parameter that is environmentally dependent. This is exactly the case at hand since

one can deduce such a feature from the expression (7.2.11), which is basically a function relating the momenta of the scalar field to the underlying relational frame.

3. *Non-Minimal coupling:* the fact that we end up with non-minimal coupling to gravity through the presence of the Ricci scalar, standard field theory on curved spacetime [47,224] [46,225] tells us that such coupling to gravity occurs due to the natural presence of strong gravitational interaction between the geometrical degrees of freedom and those of matter. This claim is further enhanced once we observe the field expression, actually manifesting such a relation between the dynamics of geometry and matter. In fact, this is expected to be the case at early times, when the energy scale is high. Moreover, it is of great importance to have obtained such a coupling to gravity, since if we were to interpret the additional terms as an interacting potential for the scalar field, usually the appearance of the term $R\phi_0$ is necessary for the good definition of the QFT and its renormalization. This direction of investigation will be left for future work.

4. *Effective metric:* notice that the function $f(x^0, \pi_\phi)$ seems to depend on the scale of the extracted physics, since at early times, it presents itself as a clock-dependent function that runs to become a constant at late time (as we will see later on, this function becomes constant at late times and can be matched to the scalar field momentum). This function can be the starting point to present the EFT treatment to the extracted QFT from our GFT model, since the power of Effective Field Theory (EFT) lies in principle on the scaling of operators and coupling constants. We will discuss this further once we explore the direction of alternative theories of gravity.

5. *Scalar field:* The exact expression of the scalar field (7.2.14) originating from the effective treatment of the associated GFT operator (7.2.1) along with inversion relations derived above, show explicitly the interplay between the matter- and geometric degrees of freedom. In fact, (7.2.5) not only proves itself useful to derive the dynamics of the scalar field, but it also pinpoints the exchange between the two sets of degrees of freedom. Moreover, the natural presence of the Ricci scalar tells us that the matter degrees of freedom are non minimally coupled to the gravitational ones and that as we will discuss below, this model can be regarded as a mimetic gravity [226,227] one.

Modified theories of gravity. The main motivation behind such an approach, is the argument that there is no reason to think the field equations of gravity should not contain other fields. Hence, we are in general free to speculate on the existence of such additional fields[8]. Such a modification is usually affecting the geometry sector of the Einstein equations, leaving the matter one intact, or assuming that the metric is conformally invariant under transformations that contain the additional field degrees of freedom. The simplest

[8]This approach is valid in the regime of high energies only and the effects of such additional fields hast to be suppressed at the validity scales of GR.

case is to consider a scalar field coupled to the Ricci scalar on the gravity side of the equation. A priori there is no apparent reason to not think of the scalar field ϕ_0 in our setting as a field modifying the Einstein equations at high energy scales, rather than a matter field contributing to the stress-energy tensor in the picture. The function f in this case will similarly to the QFT one, play the role of the effective gravitational coupling parameter.

Mimetic gravity: If we were to compare the obtained result for the matter field ϕ_0 with the derived in [227], the effective potential vanishes and the mimetic field $\chi = \Box\psi$ (ψ in this context is the preferred foliation and the scalar field minimally coupled to gravity) and indeed be identified without matter field ϕ_0. Furthermore, we have the presence of the term M^2, and modification to the classical effective metric, endorsed by the quantum parameters stemming from the relational frame. Thus the resulting action differs from the results of mimetic gravity. This can be traced back to the assumption usually made of dominating energy density of the relational clock at early times considered in the calculation. In our framework, we see such dominance at late times, where the dynamics reduce to the predictions of GR. In any case, the formulation of the derived matter content either in a MGT frame or that of a QFT one does not change the fact, that the fundamental dynamical information of the scalar field are encoded in (7.2.8).

7.2.2 Late times scalar field dynamics

In the mesoscopic regime where the scalar field evolution equation (7.2.6) holds, the expectation value of the volume operator and hence the scale factor never reaches zero, as long as at least one of the conserved charges Q_j is non-zero. In [164], it was argued that in order to get both meaningful relational dynamics and a proper FLRW spacetime (rather than a Minkowski spacetime), the energy density of the massless scalar field has to be non-zero, in turn implying that the expectation value of the massless scalar field momentum has to be non-zero as well.

We study now the dynamics of the background scalar field ϕ_0 for large GFT densities. For simplicity, we will choose the path of formulating the results in the language of a QFT on a curved background. This option is most appealing since, previous studies showed that in such a regime and under certain sufficient as well as necessary conditions, the obtained dynamics of the matter field produce the results predicted by GR with minimal coupling. We follow the same line of reasoning as in the early time case and proceed by deriving an inversion relation for ϕ_0 and θ_0. Using the relations derived in section 7.1.1 for the density (assumed to be large), namely that it obeys the differential equation; $(\dot{\rho}_0)^2 (x^0, \pi_\phi) = \mu_j^2 (\pi_\phi) \rho_0^2 (x^0, \pi_\phi)$ whose solution is given by $\rho_0^2 = A_j e^{-2\mu_j x^0}$, where we assumed, for now, a negative value for the parameter μ_j. The associated solution for the phase and the simple

inversion expression for the background scalar field read

$$\theta_0\left(x^0,\pi_\phi\right)=\frac{\gamma}{2}x^0+\frac{A_jQ_j\left(\pi_\phi\right)}{2\mu_j}e^{2\mu_jx^0}\,, \tag{7.2.18}$$

$$\phi_0\left(x^0,\pi_\phi\right)=\frac{a^3}{V_j}\left(\partial_{\pi_\phi}\log\left(\frac{A_jQ_j\left(\pi_\phi\right)}{2\mu_j}\right)+2\partial_{\pi_\phi}\mu_j\right)\left(\theta_0-\frac{\gamma}{2}x^0\right)\,. \tag{7.2.19}$$

Notice that the corresponding dynamical equation will be of the shape (7.2.6) where the defined function f in this case takes the simpler form $\left(\partial_{\pi_\phi}\log\left(\frac{A_jQ_j\left(\pi_\phi\right)}{2\mu_j}\right)+2\partial_{\pi_\phi}\mu_j\right)$ and the background field equation yields

$$\ddot{\phi}_0-3\mathcal{H}\dot{\phi}_0-\left(\frac{2}{3}R+M^2\right)\phi_0=0\,, \tag{7.2.20}$$

where we identified the respective entries of the background metric, namely that

$$g_{00}=a^3\,,\quad g_{ij}=a^2\,, \tag{7.2.21}$$

and the Ricci scalar and effective mass term appearing in (7.2.20) reads respectively

$$R=9\mathcal{H}^2-6\dot{\mathcal{H}}\,,\quad M^2=\dot{\mathcal{H}}\,. \tag{7.2.22}$$

Furthermore, if we follow the same steps as in section 7.2.1 to derive a corresponding effective metric in this case, we are faced with the same subtlety concerning the function f and the matching with the expectation value of the volume operator. Since we already know that according to [164],GR predictions can be matched to the GFT ones at late times, we will shortly show that what we claimed to be an effective gravitational coupling at early times turns out to be the gravitational constant at late times. We can see this once we consider the term f and assume the same approximations made in [164] to successfully reproduce GR, namely

$$f=\left(\partial_{\pi_\phi}\log\left(\frac{A_jQ_j\left(\pi_\phi\right)}{2\mu_j}\right)+2\partial_{\pi_\phi}\mu_j\right)\approx-\partial_{\pi_\phi}\mu_j+2\partial_{\pi_\phi}\mu_j\equiv G\,, \tag{7.2.23}$$

where we identify $2Q_j$ as the inverse of the constant A_j and we implemented the classical matching condition $2\partial_{\pi_\phi}\mu_j\approx\tilde{\pi}_\phi\equiv G$. The gravitational constant enters the action of a quantum field theory and the variation of the latter with respect to the field, there is no surprise that G enters the field equations as well. Thus, the corresponding action reads

$$\frac{\delta S}{\delta\phi_0}=0\,,\quad S=\frac{1}{2f}\int d^4x\sqrt{g}\left(\partial_\mu\phi_0\partial_\nu\phi_0+\frac{2R}{3}\phi_0^2+M^2\phi_0^2\right) \tag{7.2.24}$$

For completeness, the background matter field takes a simpler form, which also allows a plane wave decomposition

$$\phi_0=N_0\left(\partial_{\pi_\phi}\left(\frac{A_jQ_j}{2\mu_j}\right)+\frac{A_jQ_j}{4\mu_j\partial_{\pi_\phi}\mu_j}\right)e^{2\mu_jx^0}\,. \tag{7.2.25}$$

This is the most general solution for the scalar field ϕ_0 propagating on a homogeneous isotropic background. The field equations for this field are clearly not those of a massless scalar field minimally coupled to gravity, which is the starting assumption implemented at the level of the GFT action. It is then worth noting that unless we don't specify the classical matching of the quantum gravity parameters and identify the necessary conditions for it to happen, the extracted effective physical results are clearly those of an alternative theory of gravity (QFT on a curved background, modified gravity), to which we have a non-minimal coupling of the matter field ϕ_0. This becomes more obvious once we write down the Friedmann equations, and in this case, they read

$$3\mathcal{H}^2 = \frac{\dot{\phi}_0^2}{2} - \frac{a^2}{2}\left(\dot{\phi}_0^2 + M^2\right) + 2\mathcal{H}^2\frac{2}{3}a^2\dot{\phi}^2\,, \tag{7.2.26}$$

$$-2\dot{\mathcal{H}} + 3\mathcal{H}^2 = \frac{\dot{\phi}_0^2}{2} - \frac{a^3}{2}\left(M^2\right) + \frac{2}{3}\left(-2\dot{\mathcal{H}} + 3\mathcal{H}^2\right)\phi_0^2\,. \tag{7.2.27}$$

In what follows, we focus on the matching conditions that will present necessary and/or sufficient conditions constraining the effective model at hand to produce the physics of an FLRW universe. With this in mind, it is then important to mention that the classical expression for the scalar field in this case is a linear function in the relational clock. This is essential since in the classical theory, the matter field ϕ_0 is minimally coupled and hence there is no Ricci scalar appearing in (7.2.20). This requires imposing further constraints on the scalar field momentum ad integration constants and was derived in [164]. In particular, in order for the effective theory to match the classical one, the scalar field momentum had to be identified with μ_j in deriving the Friedmann equations. The above dynamical equation for ϕ_0 then becomes

$$\phi_0 = -c + \tilde{\pi}_\phi x^0\,, \tag{7.2.28}$$

where c is a constant that should be different from zero to distinguish the dynamics of the scalar field from that of the clock.
Before proceeding, let us reflect on the role the constant f plays in our theory. If we relax the assumption that $2Q_j = A_j^{-1}$, we claim that we can extract the QG counterpart of the Planck constant in a QFT setting. In fact, in $4d$ the Newton constant is equal to the Planck length; $G = l_p^2$ which can justify such a claim.

7.3 Scalar perturbations in GFT

The theory of cosmological perturbations is based on expanding Einstein equations to linear order about the background metric [228, 229]. This type of perturbation induces similar expansion of the same order in the stress-energy tensor, mirroring the geometrical counterpart of the Einstein tensor. Clearly, this consequently induces several changes at the level of the action describing the dynamics of the matter content in the universe [230],

where the explicit form of such action is gauge dependent. This picture changes considerably when we enter the quantum gravity sector. As we will shortly see in this section, identifying an action for the extracted perturbed scalar field and an effective metric is not as straightforward as in the semi-classical case. We will discuss why this is not an easy task in our case and derive the dispersion relation for the perturbed scalar field.
In what follows we study the evolution equation of the perturbed scalar field $\delta\phi$ at early times and then at late times. The derivation for the perturbed metric component can be obtained in a similar manner as in the case of the background under several drastic assumptions. We will assume that the metric takes a similar shape to the classical one in (B.1.11), i.e. we can factor out the background metric from the Bardeen potentials. Furthermore, we deliver the dispersion relation for $\delta\phi$ and reflect on it before proceeding to section 7.4. In this section, we will work in the case where the inverse of the differential operator acting on the density can be neglected. We start by discussing the general case, where the GFT perturbations are still coupled which implies $\alpha_i \neq 0$, are derived in the section 7.1.2. The implications of this more general consideration will be discussed when we derive the dispersion relation for the scalar field $\delta\phi$ at early times.

The expression of the second quantized scalar field operator is obtained from $\delta\phi = \delta\langle\hat{\Phi}\rangle_\sigma$ and it yields

$$\delta\phi = \delta\langle\hat{\Phi}\rangle_\sigma = \left[\frac{\delta N}{N_0}\phi_0 + N_0\partial_{\pi_\phi}\delta\theta\right]_{\pi_\phi=\tilde{\pi}_\phi} . \tag{7.3.1}$$

The dynamical equation satisfied by $\delta\phi$ can be easily determined by noticing that $\delta N/N_0 = 2\delta\rho/\rho_0$, which allows us to derive the following function, using the inversion relation (7.1.38) for the perturbed density. The above expression then becomes

$$\delta\phi(x^0,\pi_\phi) = \frac{2D^{-1}}{\rho_0(x^0,\pi_\phi)}\phi_0(x^0,\pi_\phi)\delta\theta(x^\mu,\pi_\phi) + \rho_0^2(x^0,\pi_\phi)\left(\frac{\tilde{C}_{\pi_\phi}(x^0,\pi_\phi)}{C(x^0,\pi_\phi)} + \tilde{\pi}_i(\pi_\phi)\right)\delta\theta(x^\mu,\pi_\phi) \tag{7.3.2}$$

where the $\tilde{}$ notation refers to the logarithmic derivative with respect to the scalar field momentum π_ϕ. Notice that, we also did not make any assumptions on the dependence of the rods momenta to not be dependent on π_ϕ. We further define the following functions

$$\Psi \equiv \frac{2D^{-1}}{\rho_0}\phi_0\,, \quad \Phi = \rho_0^2\left(\frac{\tilde{C}_{\pi_\phi}}{C} + \tilde{\pi}_i(\pi_\phi)\right)\,, \tag{7.3.3}$$

where for notation simplicity we drop the argument of the function Φ and Ψ. Now, taking as solution for the perturbed GFT phase (7.1.35), the inversion relation relating $\delta\phi$ to $\delta\theta$ yields

$$\delta\theta \equiv \left(\Psi\left(x^0,\pi_\phi\right) + \Phi(x,\pi_\phi)\right)^{-1}\delta\phi\,. \tag{7.3.4}$$

where the expression for $\delta\theta$ is given by (7.3.13). The derivatives of the perturbed phase till the second order yields

$$\delta\dot{\theta} = \frac{\delta\dot{\phi}}{(\Psi+\Phi)} - \delta\phi\frac{\left(\dot{\Psi}+\dot{\Phi}\right)}{(\Psi+\Phi)^2}\,, \tag{7.3.5}$$

$$\delta\ddot{\theta} = \frac{\delta\ddot{\phi}}{(\Psi+\Phi)} - 2\delta\dot{\phi}\frac{\left(\dot{\Psi}+\dot{\Phi}\right)}{(\Psi+\Phi)^2} - \delta\phi\frac{\left(\ddot{\Psi}+\ddot{\Phi}\right)}{(\Psi+\Phi)^2} + 2\delta\phi\frac{\left(\dot{\Psi}+\dot{\Phi}\right)^2}{(\Psi+\Phi)^3}\,. \tag{7.3.6}$$

Plugging these equations in the dynamical equation of $\delta\theta$ in (7.1.50), we obtain the evolution equation for the perturbed scalar field

$$\delta\ddot{\phi} - \left(2\frac{\dot{\Psi}+\dot{\Phi}}{\Psi+\Phi} - \lambda_1\right)\delta\dot{\phi} - \left(\frac{\ddot{\Psi}+\ddot{\Phi}}{\Psi+\Phi} - 2\frac{(\dot{\Psi}+\dot{\Phi})^2}{(\Psi+\Phi)^2} + \lambda_1\frac{\dot{\Psi}+\dot{\Phi}}{\Psi+\Phi} - \lambda_2\right)\delta\phi = \frac{-\alpha_r}{\Phi+\Psi}\nabla^2\delta\phi\,.$$

Bear in mind that in the above equations, the λ_i are functions of the background scale factor and hence time dependent. This is the full evolution equation for the perturbed scalar field. It describes an effective field theory propagating on a curved background. It is important to notice that the obtained evolution equation predicts a diagonal stress energy tensor for the scalar field and even more probably a diagonal Einstein tensor since the perturbations we introduced are performed on top of a homogeneous background. In what follows we study the emergent effective metric and the behavior of the scalar perturbation formally in this general setting. The basis for deriving the perturbed metric component can be performed in a similar manner as in the case of the background metric in section 7.2. In fact, it is clear that in terms of the defined functions Ψ and Φ and neglecting the function λ_1 the simplest perturbed metric (including the background one) reads

$$\tilde{g}_{00} = (\Psi+\Phi)^2\,, \quad \tilde{g}_{ij} = \alpha_r\,(\Psi+\Phi) \tag{7.3.7}$$

where the Ricci scalar for such a metric takes the following form

$$R = \frac{3}{2}\left(-2\frac{\ddot{\Psi}+\ddot{\Phi}}{\Psi+\Phi} + \frac{(\dot{\Psi}+\dot{\Phi})^2}{(\Psi+\Phi)^2} - 2\alpha_r\frac{\nabla^2\Phi}{\Phi+\Psi} + \alpha_r\frac{(\nabla\Psi)^2}{(\Psi+\Phi)^2} + \alpha_r\frac{\nabla^2\Psi}{(\Psi+\Phi)^2}\right)\,, \tag{7.3.8}$$

and an additional term that can be written as

$$M = 3\frac{\ddot{\Psi}+\ddot{\Phi}}{\Psi+\Phi} - 3\frac{(\dot{\Psi}+\dot{\Phi})^2}{(\Psi+\Phi)^2} + \lambda_1\frac{\dot{\Psi}+\dot{\Phi}}{\Psi+\Phi} - \lambda_2 - 3\alpha_r\frac{(\nabla\Psi)^2}{(\Psi+\Phi)^2} + 3\alpha_r\frac{\nabla^2\Phi}{\Phi+\Psi}\,. \tag{7.3.9}$$

The dynamical evolution equation of the perturbed scalar field can then be recast as

$$\delta\ddot{\phi} - \left(2\frac{\dot{\Psi}+\dot{\Phi}}{\Psi+\Phi} - \lambda_1\right)\delta\dot{\phi} - \left(\frac{2}{3}R + M\right)\delta\phi = \frac{-\alpha_r}{\Phi+\Psi}\nabla^2\delta\phi\,. \tag{7.3.10}$$

7.3.1 Perturbed scalar field at early times

The matter content of the perturbed scalar field at early times is analyzed in the following. We derive the respective evolution equation by inverting the relation between the perturbed GFT phase $\delta\theta$ and the perturbed scalar field $\delta\phi$. The general derivation of the evolution equations for the perturbed scalar field was derived above. We now analyze it for small and large perturbed GFT densities. We fix the background data by entering what we will call a perturbed effective metric to that of the background scalar field propagating on the homogeneous background derived in the previous section. We then study the behavior of the perturbed matter at late times for large volume values (hence large densities).
The expression of the second quantized scalar field operator is obtained from $\delta\phi = \delta\langle\hat{\Phi}\rangle_\sigma$ in (7.3.1). As already mentioned since the dynamical equation satisfied by $\delta\phi$ can be easily determined through $\delta N/N_0 = 2\delta\rho/\rho_0$, we can derive the following function, using the inversion relation (7.1.38) for the perturbed density, namely

$$\frac{2\delta\rho}{\rho_0} = 6\mathcal{H}a^{-3}\delta\theta\,, \tag{7.3.11}$$

where the formal solution for ρ is given by (7.1.45). The expression of the perturbed matter field then yields

$$\delta\phi(x,\pi_\phi) = a^{-3}\left(6c\mathcal{H}\phi_0 + \frac{\tilde{\mathcal{A}}}{A} + 6\frac{\tilde{a}}{a}\right)\delta\theta(x,\pi_\phi) \equiv \left(\Psi\left(a,\phi_0,x^0\right) + \Phi(\pi_\phi,x^0)\right)\delta\theta(x,\pi_\phi)\,, \tag{7.3.12}$$

where the $\tilde{}$ notation refers to the derivatives with respect to the field momentum and $\Psi\left(a,\phi_0,x^0\right) = a^{-3}6c\mathcal{H}\phi_0$. Since we are interested in obtaining the evolution equation for the perturbed scalar field, we proceed analogously to the case of the background scalar field, by computing the first and second order derivatives of the perturbed phase $\delta\theta$ in (7.3.12) and then plugging it in (7.1.50). Let us then write down the equation of the perturbed phase as a function of the scalar field $\delta\phi$. We start with the simplest case, where we assume the content of the scale factor and the constant $\mathcal{A}$ depending on the scalar field momentum are negligible, namely that

$$\delta\theta(x,\pi_\phi) \approx \Psi\left(x^0,\pi_\phi\right)^{-1}\delta\phi(x,\pi_\phi)\,, \quad \frac{\tilde{\mathcal{A}}(x,\pi_\phi)}{A(x,\pi_\phi)} \ll 1\,, \quad 6\frac{\tilde{a}(x,\pi_\phi)}{a(x,\pi_\phi)} \ll 1\,. \tag{7.3.13}$$

where now the above inversion relation depends only on the background matter content ϕ_0 and the scale factor a. The evolution equation for the perturbed scalar field using (7.1.50) yields

$$\delta\ddot{\phi} - \left(2\frac{\dot{\Psi}}{\Psi} - \lambda_1\right)\delta\dot{\phi} - \left(\frac{\ddot{\Psi}}{\Psi} - 2\frac{\dot{\Psi}^2}{(\Psi)^2} + \lambda_1\frac{\dot{\Psi}}{\Psi} - \lambda_2\right)\delta\phi = \Psi\nabla^2\delta\phi\,, \tag{7.3.14}$$

where for simplicity we work in the approximation where $\alpha_r = -1$. Bear in mind that in the above equations, the λ_i are functions of the background scale factor and hence time

dependent. This is the full evolution equation for the perturbed scalar field.
The derivation of a perturbed metric, in this case, is more involved than in comparison with the background case. This can be traced back to the fact that the obtained dynamical equation contains the final further-simplified metric which itself contains the terms entering the background metric and the perturbations affecting them. Moreover, we have no knowledge of the shape of the perturbed action, as well as the raising and lowering of the perturbed metric indices [230]. However, we can proceed as follows; from the above equation, we assume as usual that the perturbed field obeys as in the background case in (B.1.6) an evolution described by a Klein-Gordon-like equation, and after formulating it in index notation, we derive the terms entering the δg_{00} and $\sqrt{\delta g}$. To reproduce the above time dependent coefficients entering the standard $\Box$ operator acting on $\delta\phi$, we then obtain

$$\delta g_{00} = \Psi = a^3 f^2 \left(6c\mathcal{H}/f\right) , \quad \delta g_{ii} = \Psi e^{-a^{-6}/3} = a^2 \left(6c\mathcal{H}\Delta_1\phi_0 X^{-1} \exp\left(-c^2 a^{-6}/3\right) a^{-5}\right) . \tag{7.3.15}$$

Notice that it is only natural to end up with a diagonal metric since the background is a homogeneous one. These functions harbor the background components of $g_{\mu\nu}$ in (7.2.9), and this is evident in (7.3.15). The Ricci scalar for such a metric takes the following form

$$\delta R = -9c\mathcal{H}a^{-6}\frac{\dot{\Psi}}{\Psi} + \frac{3}{2}\frac{\dot{\Psi}^2}{\Psi^2} - 3\left(\frac{\ddot{\Psi}}{\Psi} + 12c^2a^{-6}\mathcal{H}^2 + 2c^2a^{-6}\dot{\mathcal{H}}\right) , \tag{7.3.16}$$

The above perturbed Ricci scalar and metric is only viable once we assume that $\delta\phi$ satisfies the same action principle as the background, namely a field theory that is propagating on a curved background, non-minimally coupled to gravity. Notice that the standard treatment to the cosmological perturbation conducted at the level of geometry and matter can also be associated with a perturbed action capturing such perturbation. This is usually carried out by expanding the action incorporating matter and gravity to second order [230, 231]. The standard treatment then relies on considering the second order in the linearized equation of the perturbed action. This is itself interesting, let alone when the considered action is stemming from a quantum gravity origin.

7.3.2 Perturbed scalar field at late times

In this section, we study the general solution for the perturbed scalar field in light of large values of the background density ρ_0. The expression for $\delta\phi$ is given by the same expectation value in (7.3.1). The dynamical equation satisfied by $\delta\phi$ can be easily determined by noticing that $\delta\theta$ satisfies the differential equation (7.1.59) whose solution is given by (7.1.61)[9]. As we already observed, the solution for the perturbed GFT phase coincides

[9] Already from this equation, in particular from the behavior of the spatial derivative term (scaling as $V^{4/3}$) we can conclude that the evolution equation for the scalar field perturbations does not match, in general, with the GR one.

with the background one once we identify the integration constants with each other. In this case, the perturbations at the level of the scalar field can be recast as

$$\frac{\delta\phi}{\phi_0} = \left(\frac{2\delta\rho}{\rho_0}\right) . \tag{7.3.17}$$

Defining $\delta N/N_0 = 2\delta\rho/\rho_0 \equiv 2\delta_\rho$ as the density contrast, obeying the equation

$$\delta''_\rho + 2\mu_j\delta'_\rho + \alpha_r\nabla^2\delta_\rho = 0\,, \tag{7.3.18}$$

we can highlight two facts; first the above equation points to the possibility that the perturbed scalar field admits a plane-wave solution since $\delta\rho$ is a solution to the wave equation (7.1.60) and ρ_0 admits an exponential solution. Secondly, according to the above equation, $\delta\phi$ satisfied the same evolution equations as the GFT density-contrast perturbation namely (7.1.58) and we obtain

$$\delta\ddot{\phi} + \delta\dot{\phi}\left(2\frac{\dot{\phi}_0}{\phi_0} + 2\mu_j\right) + \delta\phi\left(2\frac{\dot{\phi}_0^2}{\phi_0^2} - 2\mu_j\frac{\dot{\phi}_0}{\phi_0} - \frac{\ddot{\phi}_0}{\phi_0}\right) = \nabla^2\delta\phi\,, \tag{7.3.19}$$

Now let us recall the plane-wave solution of the averaged background scalar field in (7.2.25), the coefficients in the above equation for $\delta\phi$ are then constant and the term multiplying $\delta\phi$ is identically zero. To proceed with deriving a dispersion relation for the perturbed field, we consider the Ansatz of the form $\delta\phi(x^0, x^i) = \mathcal{C}\exp\left(\pm i(\omega x^0 + \pi_\phi x^i) - (2\mu_j x^0)\right)$, where we used the explicit solution of the densities appearing in the contrast density. The dispersion relation for $\delta\phi$ yields

$$\omega = \frac{i}{2}\left(4\mu_j - 1\right) \pm \frac{1}{2}\sqrt{\left(\pi_\phi^2 + 4\mu_j\right) - \left(4\mu_j - 1\right)^2}\,. \tag{7.3.20}$$

This is clearly a modified dispersion relation for the perturbed scalar field.Due to the damped-like dynamical equation, the dispersion relation picks up the modification which is precisely an imaginary term. In case we are interested in matching the above field equation (7.3.19) to the specific case of a scalar field minimally coupled, the above solution reduces to the results of [164] after imposing the corresponding assumptions to satisfy the Friedman equations in such a regime. In this case, we do not identify the background phase and perturbed one to belong to the same class of solutions and make the distinction between the respective integration constants.
It appears that a modification in the dispersion relation for the scalar field in this context is very natural and is mainly due to the quantum gravity perturbed density dynamics.

In fact, the presence of an imaginary term contributing to the dispersion relation of the scalar field is merely an indicator of the effective approach we are considering for the dynamics. This is a feature of effective field theories [232] originating from quantum gravity as was discussed in several works [233,234]. Moreover, this feature is also present in analog gravity treatments of BEC [12] and the field of thermodynamics of spacetime [225, 235]. Since effective theories are commonly viewed as the low-energy, long-wavelength limit of a more complete and established theory, the dissipative effects are usually attributed to the integrating-out of the high energy parameters.

7.4 Conclusion

Summary: In this chapter, we presented the steps to extract a formulation of a field theory on a curved background within the framework of GFT that incorporates scalar perturbations at the effective level. Effective relational dynamics can be extracted after successfully incorporating relational formalism to reintroduce the notion of reference frames in the context of quantum gravity. The inhomogeneities were already introduced in [164] and were conducted at the level of the matter scalar field distinguished from the set of clock and rods. This can be effectively done with the tools deployed by the coherent states sharply peaked on the values associated with the four massless scalar fields, playing the role of the relational reference matter frame. After having assumed that the GFT condensate wave function can be decomposed into such a peaking part and reduced one, we briefly sketched how the dynamics of the condensate in the mesoscopic regime can be effectively extracted, namely by imposing an averaged form of the quantum many body microscopic GFT dynamics. Relying on the Madelung representation for the GFT condensate, we studied the dynamical equations entering the homogeneous background as well the perturbed one. These steps laid the ground to derive an equivalent formulation of the GFT dynamics in the language of an effective field theory on curved spacetime.
The first part of the chapter was devoted to deriving the solution for the GFT condensate quantum gravity parameters, namely the phase and density. We performed this step for the background as well as the perturbed ones (which itself splits for the case of small/large background densities). This was the fundamental step toward the investigation of the matter content within our framework.
We explore first the main interpretation of the results obtained at the level of the background perturbation and postpone the outlook on possible research direction to chapter 8. Based on the information encoded in the GFT phase, an inversion relation, allowing the parametrization of the effective dynamical equations in terms of the background scalar field ϕ_0, was obtained. Thanks to this relation, we were able to extract an effective background metric at early times as well late times in our cosmological setting. More precisely, for the case of early time cosmologies, we obtained the field equations of the scalar field, from which we extracted an effective spacetime metric on top of which it is propagating. This was possible under the necessary assumption that the kinematical evolution of the scalar field is dictated by the standard d'Alembert differential operator after having employed the variational principle to action. What is intriguing about this result is, the dynamics of the scalar field in this case incorporates also non-minimal coupling to gravity, which was not present at the level of the GFT action. Along with the coupling to the Ricci scalar, we obtained an emergent mass term (or equivalently potential term) that is clearly dependent on the quantum gravity parameters related to the underlying geometry and reference frame. From this point on, there are several options we are faced with. One of them is to consider it as a potential term and study the inflationary implications it bears behind. Another option would be to investigate further its relation to the chameleon mechanism that appears in modified theories of gravity.

At late Late times, we took into consideration large background densities and derived the inversion relation between the scalar field and the background phase. However, also, in this case, we spotted the behavior of a field theory on a curved background, non minimally coupled to gravity. In the case where, we are aiming to match the obtained physical results to GR ones (with minimal coupling), necessary and sufficient conditions constraining the several quantum gravity parameters can be fixed. This was already done in [164]. One of the main observations that we can make at this level is that the dynamical equation of the scalar field and the effective metric expression do not match in any case the GR ones (in harmonic gauge). This can be further discussed, affecting mainly the semi-classical CPS states we are working with, the non-matching between the expectation value of the GFT volume operator and the extracted metric (the power of the scale factor appearing in the results is in discrepancy with what GR predicts). Another explanation for the observed properties of such results is; there is a *preferred* gauge (not the harmonic one) that is naturally selected at the effective level.

At the level of the scalar perturbation introduced in the scalar field and the GFT condensate parameters, we followed the same line of reasoning as in the background case, where now we took into consideration the contribution coming from the background geometry and matter content. One can distinguish two cases, the first one is when the background GFT condensate is small (predicting the presence of the quantum bounce, replacing, therefore, the classical singularity). The second case is when we studied the behavior of the perturbed scalar field for large GFT background densities, that predicts an FLRW universe. After having assumed that the perturbed matter content obeys the same type-of evolution equation encoded in the d'Alembert operator, we find that in both cases, the perturbed field depicts the behavior of a field theory on a perturbed background. We extracted the respective metric encoding such perturbations. We emphasize that this assumption is rather radical and rigid, hence requiring further investigations. Indeed, as we argued in section 7.3, in cosmological perturbation theory, the action from which the evolution equations are derived for the perturbed scalar field, is usually obtained after imposing a $3+1$ decomposition of the action and expanding it to second order. This further implies the selection of a preferred foliation (and the perturbed one as well), which should be consistent with perturbations induced at the level of the Einstein (as well the energy momentum) tensor. Implementing such a program to our formalism is rather involved and we leave it to future work. However, we reserve the possibility that it would probably incorporate or reproduce the case we considered for the perturbed matter content at early times, provided we impose the appropriate constraints.
Moreover, since we have at hand the exact expression for the perturbed scalar field at early- and late- times, we were able to derive the explicit expression of the dispersion relation. This exhibits a modified behavior, where imaginary contributions appeared. This is rather intriguing and interesting since it predicts a dissipative effect that is very well predicted in the field of the phenomenology of quantum gravity. Not only, do we have an explicit effective relation between the microscopic degrees of freedom and the emergent

ones (thanks to the GFT scalar field operator and volume), but we also spot such relation (and hence interaction) between these two sets of degrees of freedom at the effective level, formulated in a language we are familiar with, namely that of a field theory on a curved background. This naturally bridges the two fields of research to provide concrete and direct observational constraints.

7.5 Approximations and assumptions

We can distinguish three different levels, where several kinds of assumptions and approximations enter our derivations and physical predictions. These are the fundamental QG level of the underlying model, the effective level, and the classical matching one. Of course, at each level, the approximations are of different kinds, i.e. kinematical, dynamical, or structural, where for instance at the QG level, kinematical approximations are directly related to the properties of the states we are considering.

The assumptions made at the fundamental level

QL.1 The QG states (4.4.7) are considered to be the condensate states [22, 166]. There are several reasons why we promote this class of states over others, probably the most important one is that GFT condensate states are one of the promising coarse grained states that can be associated with emergent continuum geometries under the appropriate approximations.

QL.2 *CPS states*: for the sake of implementing the relational formalism at the fundamental level of the model, we assumed that the GFT condensate wavefunction can be decomposed into a reduced part and a peaking part which depends solely on the reference frame degrees of freedom. The use of coherent peaked states allows for concretely implementing a notion of relational evolution with respect to the frame scalar field variables so that their wavefunction represents a distribution of spatial geometries for each point of the physical manifold labeled by the reference frame fields.

QL.3 *Isotropy*: this condition implemented at the fundamental level can be considered as the counterpart of the classical part of the emergent physics we are seeking.

QL.4 *GFT action and symmetries*: the relation between the GFT action and the classical symmetries we are considering are related through the discrete gravity path integral associated with the classical system we are interested in reproducing from a quantum gravity origin.

QL.5 *Single-spin dominance*: this assumption drastically simplifies the calculations in any QG model. In fact, assuming that only one quantum label ($j_v \equiv j$) dominates the

evolution can be traced back to the observation that the macroscopic evolution of the volume is dominated by a single spin (valid at late times).

The assumptions made at the effective level

EL.1 We assume that the extracted dynamics can be derived using mean-field techniques. More precisely, we use the QG states obeying all the assumptions made and we derive the expectation value of the quantum evolution equations derived from the GFT action.

EL.2 *Neglecting interactions*: interaction terms in the effective dynamics are assumed to be negligible with respect to kinetic terms. At the mean-field level, this approximation can only be satisfied for the condensate densities which are not arbitrarily large.

EL.3 *Classical actions for the scalar field*: the contribution of the frame fields is classically assumed to have negligible impact on the energy-momentum budget of the universe. Besides making these fields behave as frame-like as possible i.e. as ideal clock and rods, this condition allows us to define unambiguously perturbative inhomogeneities with respect to the rods fields.

EL.4 *Mesoscopic regime*: we take the averaged number of particles of the system to be large enough to allow for both a continuum interpretation of the expectation values of the considered operators. However, it shouldn't be too large to avoid the dominance of the interactions. Moreover, in this regime it was possible to decouple the equations for the linear perturbation.

EL.5 $\beta_j = 0$: this assumption facilitates the computations for the background phase and allows matching the obtained physical predictions to the GR ones.

EL.6 $\alpha_i = 0$: assuming that the imaginary term of α to be smaller than the identity imposes further constraints on the CPS parameters, allows the matching process with GR and facilitated the decoupling of the linear perturbation at the level of the perturbed GFT parameters.

EL.7 *Initial boundary conditions:* To specify a unique Green function for a homogeneous as well inhomogeneous second order differential equation, initial boundary conditions need to be specified for the solution to be unique. Furthermore, this issue touches upon various programs in quantum cosmologies [236, 237]. In this paper, we discard this for computational simplicity and leave its involvement in the derived physical prediction for future work.

EL.8 The assumption that $\mathcal{H}c^2a^{-6} \gg \frac{1}{2} - 3\mathcal{H}$ drastically simplifies the process of solving the dynamics for $\delta\theta$. In fact, this condition also constrains the background scale factor at early times for the perturbation to be meaningful. Of course, a proper sign

for the Hubble parameters should be chosen, and in this case, for it to be consistent with the dynamical solution it has to be positive. This further implies that $\mathcal{H}c^2a^{-6}$ has to be considerably larger than the Hubble scale.

EL.9 *GFT perturbed density Green function:* In this paper and analogously to the works carried in analog gravity in [11], we discard the contribution of the inverse operator appearing in the inversion relations relating the perturbed density to the perturbed phase. The main reason behind this assumption is to facilitate the computations. Moreover, at early times, the contribution of the perturbed densities is naturally assumed to be small similar to the background case.

EL.10 *Field theory on curved background*: in this paper, we assume that the matter fields obey a kinetic term encoded in $\Box$ in (7.2.7), which is the one deployed in the standard QFT on a curved background. This enables us to derive the fixed background on top of which matter propagates, and hence the emergent spacetime within such a quantum gravity model. Moreover, there is no reason to expect that the *shape* of the $\Box$ operator from a QG origin (at an effective level) to be different from the standard one. The only possible modification we detected was regarding the inhomogeneities at the level of spatial derivatives, where we have the additional factor α_r and α_i at the coupled regime.

Assumptions for classical matching

This is the main assumption we mentioned in this paper, for the full set of assumptions that one can implement in order to recover GR results, we refer to [164].

CL.1 Effective coupling constant: in this paper, for the case of large GFT background densities, we assumed that $\mu_v\left(\pi_\phi\right) \propto \pi_\phi$. This is a necessary condition to match the obtained results from our model to GR ones.

Chapter 8

Conclusion and outlook

Summary

In recent years, the field of QG experienced promising and compelling progress touching its various facets, bringing it one step further to extracting continuum physics. In this thesis, we targeted three questions tackled with the technology furnished by GFT and we can list them according to their level of emergence. The first two questions concern the "how" to solve the prominent problem with the current BC model listed in Box 3.1, and the "how" to exploit the entanglement within the generic superposition of spin network states with different graph structures. This is relevant at the *microscopic* (pre-geometric) level of the theory. The third question was more concerned with extracting continuum gravitational predictions in a cosmological setting and with perturbation treatment included, that can be put in contact with the current standard formulation. Let us then summarize the main results obtained after the investigation of these problems.

After having exposed the essential ingredients that ought to be present in every theory of QG in chapter 2, such as background independence and relationalism, the fundamentality of discreteness and how they can be combined to give rise to the standard continuum geometry, we presented several approaches in chapter 3. They are based on different ways of implementing these ingredients and we focused on the BC model in quantizing Lorentzian geometries formulated as a constrained BF theory. As we emphasized in Box 3.1, this is due to encoding the geometric in the bivectors instead of the edge vectors of the tetrahedron (the elementary building block in $4d$ from which the SF is computed). This was the main motivation behind deriving the new SF model in chapter 5 and its equivalent GFT dynamics. The steps that made this possible are very simple; starting from the prescription initially proposed by Barret and Yetter, we identified the edge vector as the entity that fully defines the geometry in $4d$, where triangles, tetrahedra, and simplices are constructed out of it, provided we implement correctly constraints (at the classical and quantum level). Quantizing such geometric quantities amounted to exploiting the $\mathrm{SL}(2,\mathbb{C})$ representation theory and its possible expression in terms of Lorentzian harmonic oscillators, which are

in turn representations of the translation group. Consequently, we were able to derive a prescription for the quantum analog of the triangle, tetrahedron, and finally the evaluation of the SF amplitude. This new SF amplitude bears the full causal structure of the geometry. Moreover, the obtained SF reduced to a non-trivial combination of BC amplitude as explained in section 5.4.2. We then translated all the derived tools in the language of GFT in section 5.4.3 at the kinematical and dynamical levels of the theory. This is merely the first step towards curing the issues present in SF and we will mention several future research directions below.
In chapter 6 we explored the entanglement property of the generic superposition of spin networks. As we mentioned several times throughout the thesis and in section 3.3. Spin network states arise in the kinematical sector of the GFT setting as entanglement graphs, where this entangled state of the quantum geometry is equivalent to gluing $d-1$ simplices along their common faces. The common approach to studying such states and their coarse-graining is to work with a single graph underlying the spin network. However, it is in fact a very strong truncation of the degrees of freedom of the quantum geometry. Therefore, in that part of the thesis we provided the prescription for constructing a generic superposition of spin network states with different connectivity patterns proliferating the tower of the quantum geometric states. Furthermore, we investigated the induced correlation within a bipartite system described by such a class of states. This produced remarkable results at the level of entanglement entropy, where we can explore coherent and incoherent contributions in the interference of the correlations of the quanta of spacetime. Pushing the analysis further to study observables we are then led to think of these superpositions as a quantum ensemble that allows the averaging of QG observables. Finally, we derived the second quantization expression for these states.
Working at the effective relational level of the framework of the GFT condensate, continuum gravitational physics was successfully extracted. In particular, this covered the reproduction of an FLRW homogeneous universe with the resolution of the singularity by a quantum bounce. The results derived in chapter 7 aim to contribute to bringing the GFT condensate model closer to cosmological observations. In particular, we were able to provide an inversion relation allowing the bi-directional transitioning between the GFT condensate parameters and the matter scalar field. This in turn allows us to study matter content as well as the geometric content of the theory. Indeed, we successfully extracted a formulation of the GFT matter field as field theory propagating on a curved spacetime, exhibiting peculiar features at the dynamical level. This was performed for a matter scalar field living on a homogeneous background and also for the case of a perturbed one, where scalar perturbations are present.

Outlook

New SF model based on edge vectors. As we already spoiled in chapter 5, a thorough study of the infinities and the adequate normalization scheme should be carried out for the proposed model. In the standard BC models, this is usually done by considering the

corresponding deformed quantum group [2]. In particular, this should accommodate the following points

* As was conjectured in [115], it is possible that degenerate states of the old model will carry now measure 0 since they do not correspond to any assignment of edge lengths. Indeed, this seems as a robust presumption and hints towards the possible existence of a more global constraint that must be satisfied by the quantum edge data on a 4-simplex. This has to be addressed for this new SF model and see how it can be avoided or formulated within a GFT setting.

* A further observation concerns the geometrical operators. Let us stress that we can associate the length variables in our model with discrete quantum numbers which is a result of the quantization of the Minkowski space in terms of the translation group, whereas the area operator will possess a continuous spectrum because the decomposition of the tensor product of the irreducible unitary representations is a direct integral.

* Among the shared features, we mention the fact that the new SF model can be of the form of noncommutative simplicial gravity path integrals when expressed in the Lie algebra representation. It would be interesting to study how this enters their semi-classical analysis and explore the non-commutative feature and when it breaks down to restore commutativity. Along the same line, it could be interesting to compare the extracted results from the Ginzburg-Landau (GL) approach and renormalization group analyses of the area variable models with those with edge vector variables to see if they fall in the same/or different universality classes from the continuum gravitational physics point of view.

Indeed, concerning the last point mentioned above, we saw in chapter 5 that the non-commutative plane waves encode the correct non-trivial combinations of the edge vector representation. Despite being phrased in terms of simplicial geometry and in seemingly classical terms, as appropriate for a path integral quantization, also this method of quantization necessarily relies on a certain choice of quantization map (which dictates, for example, choices of operator orderings. The one that seems to be at the root of the non-commutative Fourier transform and star product on which these results rely is the Duflo quantization map [100]. It is then interesting to compare and study the relation between the resulting quantum geometry that is produced from the geometric quantization prescription and that resulting from the Duflo map. We also found out that, once we rely on a quantization scheme of the simplicial geometry based on edge lengths, one is able a priori, to define a quantum reference frame as was suggested by Crane and Yetter in their original paper [115]. This can be implemented once a labeling (or equivalently an ordering) of vertices of a 4-simplex is introduced (decorated by the appropriate group elements and representations). This vertex is naturally associated with a set of six triangles in such a simplex, which in turn is associated (as we saw in section 5.2) is isomorphic to the space of a pair of edges. Consequently, a vertex can be equivalently perceived as the meeting

point of a set of four edge vectors. The rest of the four triangles (and their representations) can be directly obtained by means of the switching map (5.2.5). This in turn requires a thorough investigation of the explicit expression for such an operator, which in some sense ensures the notion of diffeomorphism of the theory on the quantum level. In fact, the action of the switching operator from the GFT perspective is equivalent to a first quantization program of the model, where the wave function of the fundamental building blocks (tetrahedron) is invariant under relabeling. Moreover, there is an indirect relation to the categorial 2-groups point and their relation to the Poincaré group, this then would be a further advancement in pointing out the quantization procedure relying on the symmetries of spacetime.

Another research direction is to attempt to extract physical consequences (e.g. as in GFT cosmology). The standard path followed in this direction usually relies on working with a GFT whose perturbative expansion reproduces the EPRL model. On this account, it is possible to proceed similarly with our new SF model and compare the resulting predictions. Moreover, one would have to think of writing the volume operator starting from edge vectors instead of what is usually done, in terms of fluxes.

Superposition of spin network states with different combinatorial structures. The construction presented in chapter 6 is just the first step to accomplish the proposal of the emergence of continuum physics from the quantum entanglement of the fundamental building block of quantum geometry by utilizing the tools supplied by QIT. The main result of section 6.2 is the purely quantum phenomena of quantum interference that arise due to the superposition of the spin network states. Indeed we were only able to point out the correlation in such a case only for a very simple and special class of states where the labeling spins are fixed allowing the associated wave function to factorize. The next step would be to generalize the construction and go beyond the wavefunction of the entanglement graphs factorized over the single vertices ones. This requires a better understanding of the intertwiner dimensional space and how it enters the definition of entangled states in a superposition context. Along the same lines, it would be of great interest to converge to other QG approaches by extending the superposition of the spin network states to express them as Tensor Networks (TN) and eventually explore the possibility of relating them to the AdS/CFT formalism. We expect this to generate a GFT-TN-AdS/CFT dictionary. Moreover, as we emphasized in section 6.1.2, the structure of the considered bipartite Hilbert space is of a tensor product nature. It is indeed a simple setting that enabled the derivation of the entanglement measure for the superposed states. However, it does not take into account the boundary degrees of freedom between the bipartite regions. We know that these degrees of freedom are valuable, and this is usually formulated with the techniques of an edge-modes decomposition promoting the *boundary* symmetries degrees of freedom over others since that is all that is needed to glue local regions of quantum spacetime. These are a few points that can be pursued further at the *kinematical* level of the theory. At the dynamical level, we list the following open questions:

* How can we derive a unitary operator that implements the connectivity in a systematic way at the dynamical level with the tools borrowed from QIT, graph theory?

* What are the techniques needed to be developed to control the divergence of the sum over graphs and its scaling/renormalizability?

* Define a coarse-graining procedure through the introduction of an entanglement witness to this class of states. This calls for defining an entanglement witness for them first. Explore the ensemble idea as coarse graining and its results in computing the effective expectation value of the observables.

* Study the approximation or regime where this class of states coincides with the condensate one (superfluidity?) to bridge the gap between effective (mean-field) and coarse graining.

The bipartite idea can be used to mimic the situation of the interior and exterior regions of a black hole. We can use this setup to study such cases and if we want to be ambitious, we could derive an attempt to derive the Hawking radiation from a QG origin.

GFT as a field theory on a curved background. The main focus for the future research direction of the extracted results in chapter 7 is prioritizing bringing in contact with the GFT predictions to sensitive observational tests in cosmology. This falls into two topical units:

* *Background scalar field physics*: From this point on, there are several options we are faced with. One of them is to consider it as a potential term and study the inflationary implications it bears behind. Another option would be to investigate further its relation to the chameleon mechanism that appears in modified theories of gravity. Study the symmetry of the field at early time, since that is the regime where we expect deviations from classical GR. Furthermore, we could with scrutiny investigate the relation of the derived formalism to MGT theories and in which regime what theory our model produces. This is in fact important to make contact with observations. With the same token, since we now are endowed with the usual machinery of field theories, we could program it in a way to explain the CMB spectrum from the QG point of view, even at this effective level. We can even perform the canonical quantization of the background scalar field and study all phenomena that a standard QFT theory faces in this QG context. Construct a tentative quantum operator for the curvature/ metric by tracing back the QG nature of the extracted effective one.

* *Perturbed scalar field physics*: Quantization of the theory and performing the standard analysis of modern cosmology in this regard is required at this stage and with the technology derived in chapter 7. This could also naturally enable us to study the phenomena of particle creation. Furthermore, quantum gravitational extrapolation between early times cosmology and late times one must be further investigated. The

very presence of the Ricci scalar near the bounce and then its vanishing when we are in the regime of recovering GR is indeed puzzling and hints at a mysterious mechanism that takes place in between. It is also of great interest to study the behavior of cosmological GFT once we reintroduce the interaction of the fundamental building block of the quantum space. Would we be able to extract effectively in a systematic way? How will this contribution affect gravitational physics? The interaction term is present to include more and more degrees of freedom at the microscopic level of the theory, but from an effective point of view, will they play an important role in comparison with the kinematics of the theory or not?

Generally, effective GFT cosmologies are promising QG models that are at the forefront of extracting continuum physics that allows a possible dialog with the field of cosmological observations. In fact, if we pursue the goal of including the tensorial perturbation treatment in this framework we have, we could possibly bridge a connection with the other branch of observational physics, namely that of gravitational waves.

Appendix A

Representation theory of the Lorentz group

A.1 Infinite dimensional unitary representations of the Lorentz group

We first recall the realization of the infinite dimensional unitary representations of the Lorentz group and its algebra in the space of homogeneous functions, and finally, explore the Plancharel decomposition of the various classes of such representations. We then present the alternative representation of the Lorentz group in terms of expansors, first introduced by Dirac in [177, 179].
Finite dimensional representations of the $\mathrm{SL}(2,\mathbb{C})$ (double cover of the Lorentz group), i.e. tensor, spinor representations [238–241], are not *unitary* and the problem of identifying finite unitary representations remains unsolved [141, 178]. However, as we already mentioned in chapter 5 the case of the infinite dimensional representations of the Lorentz group has been extensively studied in [105, 179], and unitary irreducible representations were first derived in [177]. An element $g \in \mathrm{SL}(2,\mathbb{C})$ can be described by the matrix:

$$g = \begin{pmatrix} \alpha & \beta \\ \gamma & \delta \end{pmatrix}, \tag{A.1.1}$$

with $\alpha, \beta, \gamma, \delta \in \mathbb{C}$ satisfying the relation $\alpha\delta - \beta\gamma = 1$. A representation of the group denoted $R_\chi(g)$, can then be given by its action on the set of homogeneous polynomial functions ϕ of two complex variables $z_1, z_2 \in \mathbb{C}$ of order $n_1 - 1$ in z_1 and $n_2 - 1$ in z_2. We denote by χ the pair of numbers $\chi = (n_1, n_2)$. Such action takes the form:

$$R_\chi(g)\,\phi(z_1, z_2) = \phi(\alpha z_1 + \gamma z_2, \beta z_1 + \delta z_2)\,. \tag{A.1.2}$$

Among the $\mathrm{SL}(2,\mathbb{C})$ infinite dimensional representations, we can distinguish the *unitary* ones, which are the so-called *principal series*. Such representations are denoted by $R_{j\,\mu}(g)$,

labelled by the half integer j and the real number $\mu \in \mathbb{R}$, and again the $\mathrm{SL}(2,\mathbb{C})$ transformations are specified by the action of $R_{i\,\bar{\mu}}$ on the polynomials of degree $(\frac{1}{2}(\mu+j), \frac{1}{2}(\mu-j))$. The only isomorphism between such representations is the one depicted by $R_{j\,\mu} = R_{-j\,-\mu}$. The representations in the principal series are further classified according to the value of j: the representations labeled by j integer are called *bosonic*, whereas those with j being half-integer are referred to as the *fermionic* ones. The bosonic irreducible representations are unitary infinite dimensional representations of the Lorentz group. Throughout this paper, when discussing the unitary infinite dimensional representations of the Lorentz group, we will thus refer to the bosonic representations in the principal series of $\mathrm{SL}(2,\mathbb{C})$.

We also note that the irreducible representations of the principal series $R_{j\,\mu}$ correspond to the canonical D-matrices $D^{j\,\mu}_{\ell,m;\ell',m'}$. These can be realized as the expectation value of a general unitary operator $U(g)$ associated with the transformation $g \in \mathrm{SO}(1,3)$, in the (canonical) orthogonal basis $|\, j, \mu; \ell', m'\rangle$ of the Lorentz group

$$D^{j\,\mu}_{\ell,m;\ell',m'}(g) = \langle j, \mu; \ell, m\,|U(g)|\, j, \mu; \ell', m'\rangle\,. \tag{A.1.3}$$

where $(j\,,\mu)$ are the representation labels, whereas $(l\,,m)$ are the angular momentum- and magnetic quantum numbers.

In the following, the so-called *balanced* representations among the principal series of the Lorentz representations will play a central role. As we will see in section 5.2.2, we are interested in triangles whose geometry is encoded by a *simple* bivector [114, 184]. On the level of the associated representation, it is obtained by setting the representation labels $j = 0$ or $\mu = 0$. According to [105, 114, 124], a natural expression for such representations is given by the Gelfand-Graev transformations on the hyperboloid in Minkowski space. Let $x_\mu \in \mathbb{R}^4$ be the embedding coordinates for such hyperboloid, with scalar product $x \cdot x = x_0^2 - \mathbf{x}^2$, with $\mathbf{x}^2 = x_1^2 + x_2^2 + x_3^2$. Let us consider the three hyperboloids; Q_1 given by $x \cdot x = 1$ and $x_0 > 0$, the null positive cone Q_0 given by $x \cdot x = 0$ and $x_0 > 0$, and the de-Sitter space Q_{-1} given by $x \cdot x = -1$. The Fourier decomposition for the square integrable functions on the three hyperboloids is given by the Plancherel theorem:

$$\begin{aligned} L^2[Q_1] &= \bigoplus_{\mu} R_{0\,\mu}\, \mathrm{d}\mu\, \mu^2\,, \\ L^2[Q_0] &= 2 \bigoplus_{\mu} R_{0\,\mu}\, \mathrm{d}\mu\, \mu^2\,, \\ L^2[Q_{-1}] &= \left(2 \bigoplus_{\mu} R_{0\,\mu}\, \mathrm{d}\mu\, \mu^2\right) \bigoplus \left(\bigoplus_{j} R_{j\,0}\right), \end{aligned} \tag{A.1.4}$$

where $\mathrm{d}\mu\,\mu^2$ is the Plancherel measure for $j = 0$. The Plancherel theorem thus provides a definition of the Hilbert spaces of the three hyperboloids based on a combination of the Lorentz balanced representations.

For completeness, looking at the Lorentz algebra, we can notice that it is isomorphic to $\mathfrak{sl}(2,\mathbb{C})$ or $\mathfrak{so}(3,\mathbb{C})$, both considered as real algebras. Hence, the Lorentz algebra generators can be written as a combination of a rotation J and a boost N. In components, this

translates to writing a general element of the algebra as $L_{ab} = J_{ab} + \mathrm{i}N_{ab}$. Furthermore, there exist two invariant inner scalar products on this Lie algebra given by:

$$\langle L\,,\, L\rangle = J^2 - N^2\ , \quad \langle L\,,\, *L\rangle = 2\, J\cdot N\,, \tag{A.1.5}$$

where the symbol $*$ denotes the Hodge dual: $*L_{ab} = \frac{1}{2}\varepsilon_{ab}{}^{cd}L_{cd}$. They lead to the Casimir elements with eigenvalues:

$$C_1 = j^2 - \mu^2 - 1\ , \quad C_2 = 2j\,\mu\,, \tag{A.1.6}$$

which can be recast as the real and imaginary parts of the complex quantity $\omega^2 - 1 = C_1 + \mathrm{i}C_2$, with $\omega = j + \mathrm{i}\mu$. This implies that the eigenvalue of the Casimir C_2 for a simple bi-vector vanishes. The eigenvalue associated instead to the Casimir $C_1 + 1$, $|b| = \rho^2 - n^2$, gives instead its length (note a change of sign respect to (A.1.6) due to the Hodge operator $*$). In particular, the sign of such eigenvalue leads to the notion of time-like, null, and space-like surfaces spanned by the bi-vector: for $n = 0$ and $\rho \neq 0$ the bi-vector b spans a space-like wedge and is labeled by a balanced representation $R_{0\,\rho}$, for $n \neq 0$ and $\rho = 0$ the bi-vector b spans a time-like wedge and is labeled by a balanced representation $R_{n\,0}$, and if both the quantum numbers vanish, $n = \rho = 0$, the bi-vector b spans a null surface and is labeled by a trivial representation $R_{0\,0}$. We summarize these results in the table A.1. We

$C_2 = 2\,n\rho = 0$	$C_1 + 1 = \rho^2 - n^2$	**Representation**
$n = 0\,,\ \rho \neq 0$	$\lvert b\rvert > 0$: *space-like wedge*	$R_{0\,\rho}$
$n \neq 0\,,\ \rho = 0$	$\lvert b\rvert < 0$: *time-like wedge*	$R_{n\,0}$
$n = 0\,,\ \rho = 0$	$\lvert b\rvert = 0$: *null wedge*	$R_{0\,0}$

Table A.1: The simplicity condition for the bi-vector $b = *L$ is given by the vanishing of the Casimir C_2. The sign of the Casimir C_1 gives its length. The two conditions together lead to the notion of time-like, space-like, and null surfaces spanned by the bi-vector b. This is reflected by the representations used to decorate the bi-vector.

derived that simple bi-vectors (given as the wedge product of edges) are only labeled by the balanced irreducible representation of the Lorentz group.

A.2 Four dimensional Lorentzian harmonic oscillators

We present here the solutions of the four dimensional Lorentzian harmonic oscillator in different basis formulations that we used for deriving the results in chapter 5. The isotropic four dimensional harmonic oscillator is described by the Hamiltonian

$$\mathcal{H} = -\frac{1}{2}\Delta + \frac{1}{2}(t^2 - x^2 - y^2 - z^2)\,, \tag{A.2.1}$$

with associated Schrödinger equation $\mathcal{H}\,\Psi = E\,\Psi$, where Δ is the four dimensional Lorentzian Laplacian operator $\Delta = \partial_t^2 - \partial_x^2 - \partial_y^2 - \partial_z^2$. Following [180,182], we solve such wave equation in the Minkowskian, cylindrical, spherical, and hyperbolic coordinates.

(i) *Minkowskian coordinates.* The Minkowskian basis is $|n_t, n_x, n_y, n_z\rangle$, with $n_x, n_y, n_z \in \mathbb{N}$ and $n_t \in \mathbb{R}$. It is associated to the eigenvalue $E = (n_t + 1/2) - (n_x + n_y + n_z + 3/2)$ with eigenbasis

$$\Psi_{n_t,n_x,n_y,n_z}(t,x,y,z) = \psi_{n_t}(t)\,\psi_{n_x}(x)\,\psi_{n_y}(y)\,\psi_{n_z}(z)\,, \tag{A.2.2}$$

where ψ_n are the Hermite functions.

(ii) *Cylindrical coordinates.* The cylindrical basis is $|n_t, n_\rho, m, n_z\rangle$, with $n_t, n_\rho, n_z \in \mathbb{N}$, $n_t \in \mathbb{R}$ and $m \in \mathbb{Z}$. It is associated to the eigenvalue $E = (n_t + 1/2) - (2n_\rho + |m| + n_z + 3/2)$ with eigenbasis

$$\Psi_{n_t,n_\rho,m,n_z}(t,\rho,\phi,z) = \psi_{n_t}(t)\frac{(-1)^{n_\rho}}{\sqrt{\pi}}\sqrt{\frac{n_\rho!}{\Gamma(n_\rho + |m| + 1)}}e^{-\frac{1}{2}\rho^2}\rho^{|m|}L_{n_\rho}^{(|m|)}(\rho^2)e^{im\phi}\psi_{n_z}(z)\,, \tag{A.2.3}$$

where $L_n^{(\alpha)}$ are the Laguerre polynomials with the proper renormalization.

(iii) *Spherical coordinates.* The spherical basis is $|n_t, n_R, \ell, m\rangle$, with $n_t, n_R, \ell \in \mathbb{N}$, $n_t \in \mathbb{R}$ and $m \in -\ell, \dots, \ell$. It is associated to the eigenvalue $E = (n_t + 1/2) - (2n_R + \ell + 3/2)$ with eigenbasis

$$\Psi_{n_t,n_R,\ell,m}(t,R,\theta,\phi) = \psi_{n_t}(t)(-1)^{n_R}\sqrt{\frac{n_R!}{\Gamma(n_R + \ell + 3/2)}}\,e^{-\frac{1}{2}R^2}R^\ell L_{n_R}^{(\ell+1/2)}(R^2)Y_\ell^m(\theta,\phi)\,, \tag{A.2.4}$$

where Y_ℓ^m are the spherical harmonics.

(iv) *Hyperbolic coordinates.* The hyperbolic basis is $|n_r, \mu, \ell, m\rangle$, with $n_r, \ell \in \mathbb{N}$, $m \in -\ell, \dots, \ell$ and $n_t, \mu \in \mathbb{R}$. It is associated to the eigenvalue $E = 2n_r + i\mu + 1$ with eigenbasis

$$\Psi_{n_r,\mu,\ell,m}(r,\eta,\theta,\phi) = (-1)^{n_r}\sqrt{\frac{n_r!}{\Gamma(n_r + \mu + 1/2)}}\,r^{\mu-1}e^{-\frac{1}{2}r^2}\,L_{n_r}^{(\mu)}(r^2) \times \frac{1}{\sinh\eta}\,Q_\ell^{i\mu}(\coth\eta)\,Y_\ell^m(\theta,\phi)\,, \tag{A.2.5}$$

where Q_λ^α are the Legendre function with the proper normalization constant

Note that by our choice of hyperbolic coordinates, we assumed the energy to be positive. This amounts to requiring that the solutions Ψ are time-like.

For completeness, we show the details of the derivation of the eigenbasis in the hyperbolic coordinates. Let us consider the change of coordinates:

$$\begin{cases} t = r\cosh\eta \\ x = r\sinh\eta\sin\theta\cos\phi \\ y = r\sinh\eta\sin\theta\sin\phi \\ z = r\sinh\eta\cos\theta \end{cases} \qquad \text{with} \qquad \begin{bmatrix} \eta \in \mathbb{R} \\ \theta \in [0,\pi] \\ \phi \in [0,2\pi] \end{bmatrix} \tag{A.2.6}$$

In these coordinates the Laplacian writes

$$\begin{aligned} \Delta &= \partial_t^2 - \partial_x^2 - \partial_y^2 - \partial_z^2 \\ &= \frac{\partial_r}{r^3}\left(r^3\partial_r\right) - \frac{1}{r^2\sinh^2\eta}\partial_\eta\left(\sinh^2\eta\partial_\eta\right) - \frac{1}{r^2\sinh^2\eta\sin\theta}\partial_\theta(\sin\theta\partial_\theta) - \frac{1}{r^2\sinh^2\eta\sin^2\theta}\partial_\phi^2. \end{aligned} \tag{A.2.7}$$

We are looking for a separable solution for the above differential equation, namely of the type $\Psi(r,\eta,\theta,\phi) = u_r(r)\,u_\eta(\eta)\,u_\theta(\theta)\,u_\phi(\phi)$. First, we note that the non-radial part of the differential equation is exactly the Laplacian equation for the Casimir C_1 (5.1.17). The time-like solutions are the eigenfunctions with eigenvalue $-1-\mu^2$:

$$\Big(C_1 - (1+\mu^2)\Big)\left(u_\eta(\eta)\,u_\theta(\theta)\,u_\phi(\phi)\right) = 0\,. \tag{A.2.8}$$

Therefore, the rotational part gives the usual spherical harmonics $u_\theta(\theta)\,u_\phi(\phi) = Y_\ell^m(\theta,\phi)$. While the radial and the hyperbolic contribution instead satisfy the equations

$$\begin{aligned} &\partial_\eta^2\,u_\eta + 2\coth\eta\,\partial_\eta\,u_\eta - \frac{\ell(\ell+1)}{\sinh^2\eta}\,u_\eta = -(1+\mu^2)\,u_\eta\,, \\ &\partial_r^2\,u_r + \frac{3}{r}\partial_r\,u_r + \frac{1}{r^2}(1+\mu^2)\,u_r - r^2\,u_r = -2E\,u_r\,. \end{aligned} \tag{A.2.9}$$

Two solutions for the hyperbolic part are given by the Legendre functions of the first or second kind. According to [180], we take the solution of the second kind, given by:

$$u_\eta(\eta) = \frac{1}{\sinh\eta}\,Q_\ell^{i\mu}(\coth\eta)\,. \tag{A.2.10}$$

A solution for the radial part is instead given in terms of the generalized Laguerre polynomials:

$$u_r(r) = r^{i\mu-1}e^{-\frac{1}{2}r^2}\,L_{n_r}^{(i\mu)}(r^2)\,, \tag{A.2.11}$$

with $E = 2n_r + i\mu + 1$. The general (non-normalized) eigenfunction of the four dimensional isotropic Lorentzian harmonic oscillators in the hyperbolic basis is thus given by

$$\Psi_{n_r,\mu,\ell,m}(r,\eta,\theta,\phi) = r^{i\mu-1}e^{-\frac{1}{2}r^2}\,L_{n_r}^{(i\mu)}(r^2)\,\frac{1}{\sinh\eta}\,Q_\ell^{i\mu}(\coth\eta)\,Y_\ell^m(\theta,\phi)\,. \tag{A.2.12}$$

The eigenfunction in the spherical coordinates in terms of the eigenfunction in the Minkowskian coordinates [181] writes

$$\Psi_{n_t,n_R,\ell,m}(t,R,\theta,\phi) = \sum_{n_\rho,n_x,n_y,n_z} \frac{i^{m+|m|}(-1)^{\tilde{n}_x+n_\xi}(\sigma_m i)^{n_y}}{2^{(1-\delta_{m,0})/2}} \times \mathcal{C}^{\frac{1+|m|}{2},\frac{1}{4}+\frac{q_z}{2},\frac{\ell}{2}+\frac{3}{4}}_{n_\rho,\tilde{n}_z,n_R} \mathcal{C}^{\frac{1}{4}+\frac{q_x}{2},\frac{1}{4}+\frac{q_y}{2},\frac{1+|m|}{2}}_{\tilde{n}_x,\tilde{n}_y,n_\rho} \Psi_{n_t,n_x,n_y,n_z}(t,x,y,z)\,. \tag{A.2.13}$$

Here $\sigma_m = sign(m)$ and $\mathcal{C}^{\nu_1,\nu_2,\nu_{12}}_{n_1,n_2,n_{12}}$ is the $\mathfrak{su}(1,1)$ Clebsh-Gordan coefficient defined as

$$\mathcal{C}^{\nu_1,\nu_2,\nu_{12}}_{n_1,n_2,n_{12}} = \left(\frac{(2\nu_1)_{n_1}(2\nu_2)_{n_2}(2\nu_1)_{n_1+n_2-n_{12}}}{n_1!n_2!n_{12}!(n_1+n_2-n_{12})!(2\nu_2)_{n_1+n_2-n_{12}}(2\nu_{12})_{n_{12}}(\nu_1+\nu_2+\nu_{12}-1)_{n_1+n_2-n_{12}}}\right)^{1/2} \times (n_1+n_2)!\,{}_3F_2\left(\begin{matrix}-n_1,\,-n_1-n_2+n_{12},\,\nu_1+\nu_2+\nu_{12}-1\\ 2\nu_1,\,-n_1-n_2\end{matrix};1\right) \tag{A.2.14}$$

where ${}_mF_n$ is the generalized hypergeometric function.

Realization of $\mathfrak{su}(1,1)$ and $\mathfrak{so}(1,3)$ algebras. Let us first remind the $\mathfrak{su}(1,1)$ structure. Let $J_0, J_\pm$ be the $\mathfrak{su}(1,1)$ generators obeying the commutation relations:

$$[J_0\,,\,J_\pm] = \pm J_\pm\,, \quad [J_+\,,\,J_-] = -2J_0\,, \tag{A.2.15}$$

with Casimir operator $Q = J_0^2 - J_+J_- - J_0$. The $\mathfrak{su}(1,1)$ irreducible representations are labelled by an integer $n \in \mathbb{N}$ and a real number $\nu \in \mathbb{R}$, where the action of the generators on it yields

$$\begin{aligned} J_0\,|\nu;n\rangle &= (\nu+n)\,|\nu;n\rangle\,,\\ J_+\,|\nu;n\rangle &= \sqrt{(n+1)(n+\nu)}\,|\nu;n+1\rangle\,,\\ J_-\,|\nu;n\rangle &= \sqrt{n(n+\nu-1)}\,|\nu;n-1\rangle\,,\\ Q\,|\nu;n\rangle &= \nu(\nu-1)\,|\nu;n\rangle\,. \end{aligned} \tag{A.2.16}$$

In [180] it was pointed that each one dimensional harmonic oscillator can be mapped into an $\mathfrak{su}(1,1)$ sub-algebra. For the space-like oscillators in the $\{x,y,z\}$ directions, the map between each of them and the $\mathfrak{su}(1,1)$ basis is provided by $|n_a\rangle \cong |1/4+q_a/2\,;\,\tilde{n}_a\rangle$, with $a = x,y,z$ and $n_a = 2\tilde{n}_a + q_a$. We show below how to derive such map for the harmonic oscillator in the t direction. To this scope we use Dirac's work [177]; from this, we know that infinite dimensional representations of the Lorentz group are realized on homogeneous polynomials on Minkowski space with coordinates ξ_μ, where the Lorentzian signature is implemented as a negative power of the time coordinate. Such polynomials can be recast as a four dimensional Lorentzian harmonic oscillator with constant energy[1]. From Dirac's construction, we have the relation (5.1.8) between the harmonic oscillator ladder

[1]The request of constant energy for the harmonic oscillator is equivalent to the homogeneity condition of the polynomials.

operators, the coordinates on Minkowski space ξ_μ and the harmonic oscillator coordinates x_μ. In order to derive the map between the quantum oscillator and the $\mathfrak{su}(1,1)$ irreducible representations, we first consider the realization of the $\mathfrak{su}(1,1)$ generators in the harmonic oscillator basis

$$J_0 = \frac{1}{2}(a_0^\dagger a_0 + 1/2) \ , \quad J_+ = \frac{1}{2}(a_0^\dagger)^2 \ , \quad J_- = \frac{1}{2}(a_0)^2 \, . \tag{A.2.17}$$

The $\mathfrak{su}(1,1)$ irreducible representation basis is diagonal with respect the operators J_0, Q, whose action is

$$\begin{aligned} J_0 \, |\nu; n\rangle = (\nu + n) \, |\nu; n\rangle \ &:= \ \frac{1}{2}(a_0^\dagger a_0 + 1/2) \, |n_t\rangle = \frac{1}{2}(n_t + 1/2) \, |n_t\rangle \\ Q \, |\nu; n\rangle = \nu(\nu - 1) \, |\nu; n\rangle \ &:= \ \Big(\frac{1}{4}(a_0^\dagger a_0 + 1/2)^2 - \frac{1}{4}(a_0^\dagger)^2 (a_0)^2 - \frac{1}{2}(a_0^\dagger a_0 + 1/2)\Big) \, |n_t\rangle \\ &= -\frac{3}{16} \, |n_t\rangle \, . \end{aligned}$$

Solving the system of equations $n + \nu = n_t/2 + 1/4$ and $\nu(\nu - 1) = -3/16$, one derives the map

$$|\nu; n\rangle \cong |1/4 + q_t/2 \, ; \, \tilde{n}_t\rangle \, . \tag{A.2.18}$$

Notice that this map relates the $\mathfrak{su}(1,1)$ sub-algebra characterized by $\nu = \{1/4, 3/4\}$ to the time-oriented harmonic oscillator whose real contribution $\bar{n}_t$ is restricted to the set of even numbers.

Hyperbolic vs Minkowskian basis. We would like now to obtain the basis of the four dimensional harmonic oscillator in the hyperbolic coordinates, as the tensor product between the three dimensional harmonic oscillator (in the spherical basis $|n_R, \ell, m\rangle \cong |\ell/2 + 3/4 \, ; \, n_R\rangle$) and the time oriented harmonic oscillator $|n_t\rangle \cong |1/4 + q_t/2 \, ; \, \tilde{n}_t\rangle$. Both can be mapped to an $\mathfrak{su}(1,1)$ basis, thus, following again [180], we use the $\mathfrak{su}(1,1)$ Clebsh-Gordan coefficients to derive their tensor product. Concretely, we aim to obtain the relation

$$|n_r, \mu; \ell, m\rangle = \sum_{n_t, n_R} \langle n_t, n_R, \ell, m | n_r, \mu; \ell, m\rangle \, |n_t, n_R, \ell, m\rangle \, , \tag{A.2.19}$$

for states with the same energy given by:

$$2n_r + i\mu + 1 = (n_t + 1/2) - (2n_R + \ell + 3/2) \, , \tag{A.2.20}$$

along with the ℓ, m parameters which label the three dimensional rotational part that remains unchanged from the spherical to the hyperbolic basis. We thus have to express the basis in the hyperbolic coordinates (written as an $\mathfrak{su}(1,1)$ basis $|\nu; n\rangle$) as a combination of the tensor product

$$|n_t\rangle \otimes |n_R, \ell, m\rangle \cong |1/4 + q_t/2 \, ; \, \tilde{n}_t\rangle \otimes |\ell/2 + 3/4 \, ; \, n_R\rangle \, . \tag{A.2.21}$$

To this aim, we write the generators of the tensor product basis as the difference[2] of the generators of the two initial basis

$$J_0 = J_0^t \otimes 1 - 1 \otimes J_0^{xyz} \,, \quad J_\pm = J_\pm^t \otimes 1 - 1 \otimes J_\mp^{xyz} \,. \tag{A.2.22}$$

It is straightforward to check that each set of generators $\{J_0, J_\pm\}$, $\{J_0^t, J_\pm^t\}$ and $\{J_0^{xyz}, J_\pm^{xyz}\}$ satisfy the commutation relations (A.2.15) with respective Casimir operators Q, Q^t, Q^{xyz} and actions (A.2.16) on the respective basis. The tensor product basis $|n;\nu\rangle = |n_r, \mu; \ell, m\rangle$ is completely determined by requiring it to be diagonal with respect to the tensor product operators J_0 and Q. Using (A.2.20), the first gives the condition

$$n + \nu = \frac{1}{2}(n_t + 1/2) - \frac{1}{2}(2n_R + \ell + 3/2) = n_r + \frac{1}{2}(i\mu + 1) \,. \tag{A.2.23}$$

Moreover, we demand the solutions $|n_r, \mu; \ell, m\rangle$ to be a basis for the principal series of the irreducible representation of the Lorentz group. We recall that the Lorentz algebra with generators L_a, N_a has two Casimir operators [2]:

$$C_1 = J^2 - N^2 \,, \quad C_2 = 2J \cdot N \,, \tag{A.2.24}$$

with respective eigenvalues of the principal series of the irreducible representation $C_1 = j^2 - \mu^2 - 1$ and $C_2 = 2j\mu$. Using (5.1.18), one can directly check that the Casimir C_2 automatically vanishes. According to [113], the vanishing of $C_2 = 2j\mu$ means that $|n_r, \mu; \ell, m\rangle$ is a basis for the balanced representations of the Lorentz group. In particular, since we assumed the energy of the harmonic oscillator to be positive, the Casimir C_1 has to be negative, and thus $k = 0$ which implies $C_1 = -1 - \mu^2$. Hence, the basis $|n_r, \mu; \ell, m\rangle$ provides a quantization for the space-like bivectors. Using (5.1.18), from a direct computation one can check that

$$Q = \frac{1}{4} C_1 \,. \tag{A.2.25}$$

By enforcing this equation on the basis $|n_r, \mu; \ell, m\rangle$ together with (A.2.23), we end up with the system of equations

$$\begin{cases} n + \nu = n_r + \dfrac{1}{2}(i\mu + 1) \,, \\ \nu(\nu - 1) = -\dfrac{1}{4}(1 + \mu^2) \,, \end{cases} \quad \Rightarrow \quad n = n_r \,, \quad \nu = \frac{1}{2}(1 + i\mu) \,. \tag{A.2.26}$$

This gives the Clebsh-Gordan coefficients in (A.2.19) for the harmonic oscillator from the spherical coordinates to the hyperbolic coordinates (the time-like principal series of the irreducible representations of the Lorentz group):

$$\langle n_t, n_R, \ell, m \,|\, n_r, \mu; \ell, m\rangle = e^{i\varphi}\, \mathcal{C}^{1/4+q_t/2,\, \ell/2+3/4,\, (1+i\mu)/2}_{\tilde{n}_t+\bar{n}_t/2,\, n_R,\, n_r} \,, \tag{A.2.27}$$

[2]The minus sign of the linear combination reflects the Lorentzian signature.

where $e^{i\varphi}$ is a phase factor that can be fixed by requiring that the expansion (A.2.19) holds also for the solutions (A.2.5). The overall map of the four dimensional oscillator, between the Minkowskian basis and the hyperbolic basis is thus

$$\Psi_{n_r,\mu,\ell,m}(r,\eta,\theta,\phi) = \sum_{n_t,n_x,n_y,n_z} \mathcal{C}_{n_r,\,\mu,\,\ell,\,m}^{n_t,\,n_x,\,n_y,\,n_z}\, \Psi_{n_t,n_x,n_y,n_z}(t,x,y,z)\,, \tag{A.2.28}$$

with

$$\begin{aligned}\mathcal{C}_{n_r,\,\mu,\,\ell,\,m}^{n_t,\,n_x,\,n_y,\,n_z} &:= \langle n_t,n_x,n_y,n_z|n_r,\mu;\ell,m\rangle \\ &= \sum_{n_R,n_\rho} \frac{i^{m+|m|}(-1)^{\tilde{n}_x+n_\xi}(\sigma_m i)^{n_y}}{2^{(1-\delta_{m,0})/2}}\, e^{i\varphi}\, \mathcal{C}_{n_\rho,\tilde{n}_z,n_R}^{\frac{1+|m|}{2},\frac{1}{4}+\frac{q_z}{2},\frac{\ell}{2}+\frac{3}{4}}\, \mathcal{C}_{\tilde{n}_x,\tilde{n}_y,n_\rho}^{\frac{1}{4}+\frac{q_x}{2},\frac{1}{4}+\frac{q_y}{2},\frac{1+|m|}{2}} \\ &\times \mathcal{C}_{\tilde{n}_t+\bar{n}_t/2,\,n_R,\,n_r}^{1/4+q_t/2,\,\ell/2+3/4,\,(1+i\mu)/2}\,.\end{aligned} \tag{A.2.29}$$

A.3 Algebra of representation functions

In this section, we present some notions from the representation theory that we used throughout the thesis. We work with a finite group or a compact Lie group G. The *representation* ρ of G on a finite-dimensional complex vector space V^ρ is defined as being a group homomorphism such that

$$\rho : G \to \mathrm{Aut}\,[V^\rho]\,, \tag{A.3.1}$$

where $\mathrm{Aut}\,[V^\rho]$ is the automorphism group of the space V^ρ. An *invariant subspace* for the representation ρ is a vector subspace U such that, for all $u \in U$, $\rho(g)u \in U$ for all $g \in G$. A representation is called *irreducible* if its only closed invariant subspaces are $\emptyset$ and V^ρ. Whereas, a representation is *unitary* if, for every $g \in G$, $\rho(g)$ is unitary. Moreover, two representations ρ and ρ' are *equivalent* if there exist an isomorphism $Iso : V^\rho \to V^{\rho'}$ such that $Iso\,\rho(g) = \rho'(g)\,Iso$ for all $g \in G$. We set $\rho = 0$ as the *trivial representation* which maps every element of G to 1 (hence $V^0 \cong \mathbb{C}$).

• *Unitary representations.* One can show that Every finite-dimensional representation is equivalent to a unitary representation. This enables us to restrict the attention to a set $\tilde{\mathcal{U}}$ of unitary representations, one for each equivalence class of finite-dimensional representations of G [105]. Now, every finite-dimensional representation ρ of G can be decomposed into a direct sum of irreducible representations $\rho_1,\ldots,\rho_k$ [141, 240]:

$$V^\rho = V^{\rho_1} \oplus \cdots \oplus V^{\rho_k} \tag{A.3.2}$$

and we can make use of the notion of the unitary representations here as follows; we denote by $\mathcal{U} \subset \tilde{\mathcal{U}}$ the subset of irreducible representations and we can perceive it as the elementary not dividable unit of generic representations. We explore now the notion of a

dual representation. Let $V^{\rho *}$ be the vector space dual to V^{ρ}, given a subspace of unitary irreducible representations $\rho \in \tilde{\mathcal{U}}$, the dual representation we define the *dual representation*

$$\rho^* : G \to \mathrm{Aut}\left[V^{\rho *}\right] , \tag{A.3.3}$$

is such that, for each element in this space $\eta \in V^{\rho *}$ we have

$$\left(\rho^*(g)\eta\right)(v) = \eta\left(\rho(g^{-1})v\right) , \quad \forall v \in V^{\rho} . \tag{A.3.4}$$

• *Scalar product and representation function.* There is a natural scalar product $\langle\cdot|\cdot\rangle$ induced in the representation spaces V^{ρ}, where $\rho \in \tilde{\mathcal{U}}$, and the duality between two orthonormal basis $\{a_i\}$ (not to be confused with the ladder operator discussed in chapter 5) of V^{ρ} and $\{\alpha^i\}$ of $V^{\rho *}$ is given by

$$\langle a_i|a_j\rangle = \beta^i(a_j) = \delta_{ij} , \quad \langle \alpha^i|\alpha^j\rangle = \alpha^j(b_i) = \delta_{ji} . \tag{A.3.5}$$

We can now introduce the notion of representation function. For $\rho \in \tilde{\mathcal{U}}$, $v \in V^*$ and $\eta \in V^{\rho *}$, the functions

$$\begin{aligned} f^{\rho}_{\eta,v} &: G \to \mathbb{C} , \\ & g \to f^{\rho}_{\eta,v}(g) \coloneqq \langle \eta|\rho(g)v\rangle , \end{aligned} \tag{A.3.6}$$

are called representation functions of G and form a commutative and associative unital algebra over $\mathbb{C}$, denoted by $C_{\mathrm{alg}}(G)$. We can perform the following operations

$$\left(f^{\rho}_{\eta,v} + f^{\rho'}_{\eta',v'}\right)(g) \coloneqq f^{\rho\oplus\rho'}_{\eta+\eta',v+v'}(g), \tag{A.3.7}$$

$$\left(f^{\rho}_{\eta,v} \cdot f^{\rho'}_{\eta',v'}\right)(g) \coloneqq f^{\rho\otimes\rho'}_{\eta\otimes\eta',v\otimes v'}(g) . \tag{A.3.8}$$

The null elements are given by $f^{(0)}_{0,0}$ satisfying $f^{(0)}_{0,0}(g) = 0\ \forall g \in G)$ whereas the unit element by $f^{(0)}_{\eta,v}$, such that $f^{(0)}_{\eta,v}(g) = 1\ \forall g \in G)$. Considering the orthonormal basis, one can obtain their representation functions, and this yields

$$f^{\rho}_{mn}(g) \coloneqq f^{\rho}_{\alpha^m,a_n}(g) = \langle \alpha^m|\rho(g)a_n\rangle , \tag{A.3.9}$$

We can present the Fourier analysis of these decompositions for their usefulness for our discussions in almost every chapter of the thesis.

• *The Peter-Weyl decomposition* The Peter-Weyl theorem implements a Fourier analysis for compact groups, where the matrix coefficients $f^{\rho}_{mn}(g)$ of all irreducible unitary representations $\rho \in \mathcal{U}$ of G form an orthogonal basis of $L^2(G)$, where the following equality holds

$$\langle f^{\rho}_{mn}|f^{\rho'}_{m'n'}\rangle = \int_G dg\ \overline{f^{\rho}_{mn}(g)} f^{\rho'}_{m'n'}(g) = \frac{1}{\dim V^{\rho}}\delta_{\rho\rho'}\delta_{mm'}\delta_{nn'} . \tag{A.3.10}$$

where $\mathrm{d}g$ is the Haar measure on G. Any function $\varphi \in L^2(G)$ can therefore be written as

$$\varphi(g) = \sum_{\rho\in\mathcal{U}} \sum_{mn} b^{\rho}_{mn} f^{\rho}_{mn}(g) . \tag{A.3.11}$$

where

$$b^{\rho}_{mn} = \dim V^{\rho} \int_G dg \varphi(g) \overline{f^{\rho}_{mn}(g)} \,. \tag{A.3.12}$$

On the level of the space of square integrable functions this yields

$$L^2(G) \cong \bigoplus_{\rho \in \mathcal{U}} \left(V^{\rho *} \otimes V^{\rho} \right) \,. \tag{A.3.13}$$

• *Intertwiner map* We now introduce the intertwiner map, one the most important ingredients to spin network states as we encounter in section 3.3. Given a representation $\sigma \in \tilde{\mathcal{U}}$ endowed with the orthogonal decomposition

$$V^{\sigma} \cong \bigoplus_{i=1}^{q} V^{\tau_k} \quad \tau_k \in \mathcal{U}, q \in \mathbb{N} \,, \tag{A.3.14}$$

where the first p components $\tau_1, \ldots, \tau_p$, with $0 \leq p \leq q$, are equivalent to the trivial representation, and considering the projector $P^{\sigma;k}$ such that $P^{\sigma;k} : V^{\sigma} \to V^{\tau_k}$ and $P^{\sigma;k}_m := P^{\sigma;k} |a_m\rangle$; we can write

$$\int_G \mathrm{d}g f^{\sigma}_{mn}(g) = \sum_{k=1}^{p} \overline{P^{\sigma;k}_m} P^{\sigma;k}_n \,, \tag{A.3.15}$$

where the right-hand side is the orthogonal decomposition of the identity in the subspace of V^{σ} of invariant vectors. Let us generalize this equation to include the tensor product of N representations given by

$$V^{\rho_1} \otimes \cdots \otimes V^{\rho_N} \cong \bigoplus_{i=1}^{q} V^{\tau_k} \quad \tau_k \in \mathcal{U}, q \in \mathbb{N} \,, \tag{A.3.16}$$

and, if $\tau_1, \ldots, \tau_p$ (with $0 \leq p \leq q$) are equivalent to the trivial representation, then

$$\int_G \mathrm{d}g \; f^{\rho_1}_{m_1 n_1}(g) \ldots f^{\rho_N}_{m_N n_N}(g) = \sum_{k=1}^{p} \overline{P^{\rho_1 \ldots \rho_N ;k}_{m_1 \ldots m_N}} P^{\rho_1 \ldots \rho_N ;k}_{n_1 \ldots n_N} \,, \tag{A.3.17}$$

where $P^{\rho_1 \cdots \rho_N ;k}$ is the projector from $V^{\rho_1} \otimes \cdots \otimes V^{\rho_N}$ onto $\mathrm{Inv}_G \left[V^{\rho_1} \otimes \cdots \otimes V^{\rho_N} \right]$, i.e. the subspace of G-invariant tensors, also called *intertwiner space*. Equivalently the above operation can be written as

$$\int_G dg \; f^{\rho_1}_{m_1 n_1}(g) \ldots f^{\rho_N}_{m_N n_N}(g) = \mathbb{I} \in \mathrm{Inv}_G \left[V^{\rho_1} \otimes \cdots \otimes V^{\rho_N} \right] \,. \tag{A.3.18}$$

As already mentioned, the intertwining operation and the decomposition into a direct sum at the level of representations is at the core of the spin network state definition. Let us then go a bit further and explore the notion of *intertwiners*. Given two representations ρ and σ, a linear map $I : V^{\rho} \to V^{\sigma}$ such that

$$I \rho(g) = \sigma(g) I \tag{A.3.19}$$

is called *intertwiner*. We also say that I *intertwines* the two representations. We can make several comment on these quantities:

- If the map I is bijective, then (A.3.19) provides the definition of equivalence of the representations ρ and σ.
- Relying on $V^{\rho *} \cong V^{\rho}$, the intertwiner can be regarded as a map $I : V^{\rho} \otimes V^{\sigma} \to V^{0} \cong \mathbb{C}$, i.e. as an *invariant tensor* on $V^{\rho} \otimes V^{\sigma}$.
- the projector $P^{\rho_1 \cdots \rho_N ; k}$ defined in (A.3.17) is an intertwiner.

A.4 Representation and recoupling theory of SU(2)

We can study the above notion in the case of the SU(2) group, since we make use of them extensively in several chapters. $SU(2)$ is a 3-dimensional compact Lie group corresponding to the group of 2×2 unitary matrices with a

$$h = \begin{pmatrix} a & -\bar{b} \\ b & \bar{a} \end{pmatrix} \quad |a|^2 + |b|^2 = 1 \quad a, b \in \mathbb{C} \,. \tag{A.4.1}$$

The Lie algebra of this group is $\mathfrak{su}(2)$ and its generators are $\tau_i := i\frac{\sigma_i}{2}$, where σ_i being the Pauli matrices. They satisfy the following commutation relations

$$[\tau_i, \tau_j] = -\varepsilon_{ijk}\tau_k \,. \tag{A.4.2}$$

The representations of $SU(2)$ are labeled by a half-integer $j \in \frac{\mathbb{N}}{2}$ called *spin*. The representation space V^j is a Hilbert space of dimension $d_j := 2j + 1$.
The angular momentum $\hat{J}_i := \frac{\sigma_i}{2}$ satisfy the following commutations

$$[\hat{J}_i, \hat{J}_j] = i\varepsilon_{ijk}\hat{J}_k \,. \tag{A.4.3}$$

The standard basis of V^j is composed of the eigenstates of both the $\mathfrak{su}(2)$ Casimir $\hat{J}^2 := \hat{J}_i\hat{J}^i$ and the generator $\hat{J}_3$, labeled by the spin j and the magnetic momentum m and this yields

$$\hat{J}^2 \,|jm\rangle = j(j+1)\,|jm\rangle \ , \tag{A.4.4}$$

$$\hat{J}_3 \,|jm\rangle = m\,|jm\rangle \ , \tag{A.4.5}$$

with the magnetic numbers running from $m = -j, \ldots, j$. By means of (A.3.9) the representation matrices $D^j(g)$ are called *Wigner matrices* Tand they are the j-representation matrix of $g \in SU(2)$ is denoted by $D^j(g)$, and has coefficients

$$D^j_{mn}(g) := \langle jm|g|jn\rangle \,. \tag{A.4.6}$$

On the other hand exploiting (A.3.17) we end up with

$$\int_G dg \ D^{j_1}_{m_1 n_1}(g) D^{j_2}_{m_2 n_2}(g) D^{j_3}_{m_3 n_3}(g) D^{j_4}_{m_4 n_4}(g) = \sum_{\iota} I^{j_1 j_2 j_3 j_4 ; \iota}_{m_1 m_2 m_3 m_4} I^{j_1 j_2 j_3 j_4 ; \iota}_{n_1 n_2 n_3 n_4} \,, \tag{A.4.7}$$

where $I^{j_1 j_2 j_3 j_4 ; \iota}$ is the intertwiner recoupling fours representations $j_1, \ldots, j_4$. This naturally defines its as an element of the space $\mathrm{Inv}_{\mathcal{G}}\left[V^{j_1} \otimes \cdots \otimes V^{j_4}\right]$.

Holonomies Here we present several properties of the holonomy that enters the derivation in section 3.3:

- *E* Under a local gauge transformation generated by the Gauss constraint the connection A_a transforms as
$$A'_a = gA_a g^{-1} + g\partial_a g^{-1} \tag{A.4.8}$$
- ✣ Under a gauge transformation the holonomy $h_e[A]$ becomes
$$h'_e[A] = g(s_e)h_e[A]g^{-1}(t_e) \tag{A.4.9}$$
- ✣ The densitized triad E^a_i transforms, under the action of the local gauge group, as follows:
$$E^{a\prime} = gE^a g^{-1} \tag{A.4.10}$$
Since E^a_i encodes the spatial geometry of Σ, any geometrical quantity on Σ can thus be written in terms of it. Important examples are the area of a two-dimensional surface $S \subset \Sigma$,
$$A_S[E] \coloneqq \int_S d\sigma^1 d\sigma^2 \sqrt{E^a_i E^b_j \delta^{ij} n_a n_b}\,, \tag{A.4.11}$$
- ✣ The volume of a three-dimensional region $R \subset \Sigma$:
$$V_R[E] = \int_R d^3x \sqrt{\left|\frac{1}{3!}\varepsilon_{abc} E^a_i E^b_j E^c_k \varepsilon^{ijk}\right|}\,. \tag{A.4.12}$$

Appendix B

Field theories in cosmology and scalar perturbations

B.1 Scalar field in QFT and scalar perturbation

Classically, the coupled reference matter fields playing the role of the clock and rods in our framework are governed by the action

$$S_m\left[\chi^\mu,\phi\right] = -\frac{1}{2}\int \mathrm{d}^4x\sqrt{-g}g^{ab}\partial_a\chi^0\partial_b\chi^0 + \frac{\lambda}{2}\sum_{i=1}^{d}\int \mathrm{d}^4x\sqrt{-g}g^{ab}\partial_a\chi^i\partial_b\chi^i \tag{B.1.1}$$

$$-\frac{\alpha_\phi}{2}\int \mathrm{d}^4x\sqrt{-g}g^{ab}\partial_a\phi\partial_b\phi \tag{B.1.2}$$

$$=\frac{1}{2}\int \mathrm{d}^4x\sqrt{-g}M^{(\lambda)}_{\mu\nu}g^{ab}\partial_a\chi^\mu\partial_b\chi^\nu - \frac{\alpha_\phi}{2}\int \mathrm{d}^4x\sqrt{-g}g^{ab}\partial_a\phi\partial_b\phi \tag{B.1.3}$$

However, as we encountered in section 7.2, this is not the action we recover for small background densities ρ_0 but rather that of a non minimally coupled QFT. Therefore in the following, we present the field equations of a QFT on a curved background, minimally coupled to gravity. We work in the harmonic gauge.

B.1.1 Quantum field theory on curved spacetime in the harmonic gauge

The line element for a homogeneous isotropic universe in the harmonic gauge reads

$$\mathrm{d}s^2 = -a^6(t)\mathrm{d}t^2 + a^2(t)\delta_{ij}\,\mathrm{d}x^i\,\mathrm{d}x^j. \tag{B.1.4}$$

The action of a non minimally coupled QFT on a classical fixed background yields

$$S[\varphi] = \int d^4x\sqrt{|g|}\frac{1}{2}\left(g^{\mu\nu}\partial_\mu\varphi\partial_\nu\varphi - \left(m^2+\xi R\right)\varphi^2\right), \tag{B.1.5}$$

where $g_{\mu\nu}$ of the spacetime metric, g its determined, R is the Ricci scalar, ξ is a constant and m^2 the mass associated to the field φ. The equation of motion of the scalar field is obtained by varying the action with respect to the field φ and it is given by

$$\left(\Box + m^2 + \xi R\right)\varphi = 0, \quad \Box = |g|^{-1/2}\partial_\mu |g|^{1/2} g^{\mu\nu}\partial_\nu \,, \tag{B.1.6}$$

where for the above line element this takes the simpler form

$$-a^{-6}\ddot{\varphi} + a^{-2}\nabla^2\varphi + a^{-6}\xi\left(-12\frac{\dot{a}^2}{a^2} + 6\frac{\ddot{a}}{a}\right)\varphi + m^2\varphi = 0\,, \tag{B.1.7}$$

The stress energy tensor can be obtained by varying the action (B.1.5) and its general expression reads

$$T_{\mu\nu} = \nabla_\mu\varphi\nabla_\nu\varphi - \frac{1}{2}g_{\mu\nu}\left[\nabla_\delta\varphi\nabla^\delta\varphi + V(\varphi)\right] + \xi\varphi^2 G_{\mu\nu} + \xi\left(g_{\mu\nu}\nabla_\delta\nabla^c - \nabla_a\nabla_\delta\right)\left(\varphi^2\right)\,, \tag{B.1.8}$$

where $G_{\mu\nu}$ is the Einstein tensor. The Friedmann equations then read

$$3\mathcal{H}^2 = \dot{\varphi}^2 + \frac{a^6}{2}\left(\nabla^2\varphi + m^2\right) + 3\xi\mathcal{H}^2\varphi^2 + \xi\left(a^6\nabla^2 - \partial_0^2\right)\varphi^2\,, \tag{B.1.9}$$

$$-2\dot{\mathcal{H}} + 3\mathcal{H}^2 = \nabla^2\varphi^2 - \frac{a^2}{2}\left(\dot{\varphi}^2 + m^2\right) + \xi(-2\dot{\mathcal{H}} + 3\mathcal{H}^2)\varphi^2 + \xi\left(a^2\partial_0^2 - \nabla^2\right)\varphi^2\,. \tag{B.1.10}$$

Scalar perturbation. In the following we are considering the scalar perturbation at the level of the metric that is diagonal, since this is the only relevant form that we could compare our results with from section 7.3. The line element that includes scalar perturbations in the harmonic gauge reads

$$ds^2 = -a^6(1+2A)\mathrm{d}t^2 + a^2(t)\left[(1-2\psi)\delta_{ij}\right]\mathrm{d}x^i\ \mathrm{d}x^j, \tag{B.1.11}$$

$$\phi = \phi(t)_0 + \delta\phi(t,x) \tag{B.1.12}$$

At the linear order, the scalar perturbations present at the level of Einstein- and the scalar field equations can be reduced to the following set of equations in Fourier space:

$$0 = \frac{1}{2}\bar{\phi}'\delta\phi' + 3\mathcal{H}\psi' + k^2a^4\psi\,, \quad 0 = \mathcal{H}A + \psi' - \frac{1}{2}\bar{\phi}'\delta\phi \tag{B.1.13}$$

Perturbed volume equations. It is useful to recast the above equations for the metric perturbations in terms of quantities that we have access to from the fundamental quantum gravity theory. The most important one in this context is the local volume element associated to an infinitesimally small patch of spacetime. At the classical level, this can be compared to the local volume element

$$V_c \equiv \sqrt{\det{}_3\, g} = \sqrt{\det a^2\left[(1-2\psi)\delta_{ij}\right]} = a^3\sqrt{\det\left[\delta_{ij} - 2\psi\delta_{ij}\right]}.$$

The perturbed part, at first order in ψ and E, is therefore given, in Fourier transform, by

$$\delta V_c = \bar{V}_c\left(k^2E - 3\psi\right), \quad \bar{V}_c \equiv a^3$$

Using that, by definition, $\mathcal{H} = \bar{V}'/(3\bar{V})$, we find

$$\delta V_c'' - 6\mathcal{H}\delta V_c' + 9\mathcal{H}^2\delta V_c - a^4\nabla^2\delta V_c = 0.$$

Bibliography

[1] Oriti, D. Spin foam models of quantum spacetime (2003). arXiv:gr-qc/0311066.

[2] Barrett, J. W. and Crane, L. *Relativistic spin networks and quantum gravity*. *J. Math. Phys.*, **39** (1998), 3296. arXiv:gr-qc/9709028, doi:10.1063/1.532254.

[3] de Boer, J. et al. Frontiers of Quantum Gravity: shared challenges, converging directions. (2022). arXiv:2207.10618.

[4] Butterfield, J. and Bouatta, N. Emergence and reduction combined in phase transitions (2011).

[5] Anderson, E. The problem of time in quantum gravity (2012). arXiv:1009.2157.

[6] Curiel, E. On the Existence of Spacetime Structure. *Brit. J. Phil. Sci.*, **69** (2018), 447. arXiv:1503.03413, doi:10.1093/bjps/axw014.

[7] Wüthrich, C., Le Bihan, B., and Huggett, N. *Philosophy Beyond Spacetime: Implications from Quantum Gravity*. Oxford University Press (2021). ISBN 9780198844143. Available from: https://doi.org/10.1093/oso/9780198844143.001.0001, doi:10.1093/oso/9780198844143.001.0001.

[8] Seoane, P. A. et al. Astrophysics with the Laser Interferometer Space Antenna. *Living Rev. Rel.*, **26** (2023), 2. arXiv:2203.06016, doi:10.1007/s41114-022-00041-y.

[9] Moresco, M. et al. Unveiling the Universe with emerging cosmological probes. *Living Rev. Rel.*, **25** (2022), 6. arXiv:2201.07241, doi:10.1007/s41114-022-00040-z.

[10] Alonso-Serrano, A. and Liška, M. Quantum Gravity Phenomenology from the Thermodynamics of Spacetime. *Universe*, **8** (2022), 50. doi:10.3390/universe8010050.

[11] Barceló, C., Liberati, S., and Visser, M. Analogue gravity. *Living Reviews in Relativity*, **8** (2005). Available from: https://doi.org/10.129422Flrr-2005-12, doi:10.12942/lrr-2005-12.

[12] Liberati, S. and Maccione, L. Astrophysical constraints on planck scale dissipative phenomena. *Physical Review Letters*, **112** (2014). Available from: https://doi.org/10.1103%2Fphysrevlett.112.151301, doi:10.1103/physrevlett.112.151301.

[13] Amelino-Camelia, G. *Quantum-Spacetime Phenomenology. Living Rev. Rel.*, **16** (2013), 5. arXiv:0806.0339, doi:10.12942/lrr-2013-5.

[14] Rovelli, C. *Loop quantum gravity. Living Rev. Rel.*, **1** (1998), 1. arXiv:gr-qc/9710008, doi:10.12942/lrr-1998-1.

[15] Thiemann, T. Introduction to modern canonical quantum general relativity. (2001). arXiv:gr-qc/0110034.

[16] Perez, A. *The Spin Foam Approach to Quantum Gravity. Living Rev. Rel.*, **16** (2013), 3. arXiv:1205.2019, doi:10.12942/lrr-2013-3.

[17] Baez, J. C. An introduction to spin foam models of quantum gravity and bf theory. (1999). Available from: https://arxiv.org/abs/gr-qc/9905087, doi:10.48550/ARXIV.GR-QC/9905087.

[18] Loll, R. Quantum Gravity from Causal Dynamical Triangulations: A Review. *Class. Quant. Grav.*, **37** (2020), 013002. arXiv:1905.08669, doi:10.1088/1361-6382/ab57c7.

[19] Freidel, L. Group field theory: An overview. *International Journal of Theoretical Physics*, **44** (2005), 1769. Available from: https://doi.org/10.1007%2Fs10773-005-8894-1, doi:10.1007/s10773-005-8894-1.

[20] Kiritsis, E. *String theory in a nutshell*. Princeton University Press, USA (2019). ISBN 978-0-691-15579-1, 978-0-691-18896-6.

[21] Oriti, D. Levels of spacetime emergence in quantum gravity (2018). arXiv:1807.04875.

[22] Oriti, D. *Spacetime as a quantum many-body system*. (2017). arXiv:1710.02807.

[23] Van Raamsdonk, M. Comments on quantum gravity and entanglement. (2009). arXiv:0907.2939.

[24] Van Raamsdonk, M. Building up spacetime with quantum entanglement. *Gen. Rel. Grav.*, **42** (2010), 2323. doi:10.1007/s10714-010-1034-0,10.1142/S0218271810018529.

[25] Cao, C., Carroll, S. M., and Michalakis, S. Space from hilbert space: Recovering geometry from bulk entanglement. *Physical Review D*, **95** (2017). Available from: https://doi.org/10.11032Fphysrevd.95.024031, doi:10.1103/physrevd.95.024031.

[26] Hohenberg, P. and Krekhov, A. An introduction to the ginzburg–landau theory of phase transitions and nonequilibrium patterns. *Physics Reports*, **572** (2015), 1. Available from: https://doi.org/10.1016%2Fj.physrep.2015.01.001, doi:10.1016/j.physrep.2015.01.001.

[27] Livine, E. R. and Terno, D. R. Entanglement of zero angular momentum mixtures and black hole entropy. (2005).

[28] Livine, E. R. Intertwiner entanglement on spin networks. (2017). Available from: http://arxiv.org/abs/1709.08511http://dx.doi.org/10.1103/PhysRevD.97.026009, doi:10.1103/PhysRevD.97.026009.

[29] Freidel, L., Geiller, M., and Wieland, W. Corner symmetry and quantum geometry (2023). arXiv:2302.12799.

[30] Donnelly, W., Timmerman, S., and Valdés-Meller, N. Entanglement entropy and the large n expansion of two-dimensional yang-mills theory. (2019). Available from: http://arxiv.org/abs/1911.09302http://dx.doi.org/10.1007/JHEP04(2020)182, doi:10.1007/JHEP04(2020)182.

[31] Maldacena, J. M. The Large N limit of superconformal field theories and supergravity. *Adv. Theor. Math. Phys.*, **2** (1998), 231. arXiv:hep-th/9711200, doi:10.1023/A:1026654312961.

[32] Hubeny, V. E. The AdS/CFT Correspondence. *Class. Quant. Grav.*, **32** (2015), 124010. arXiv:1501.00007, doi:10.1088/0264-9381/32/12/124010.

[33] Chirco, G., Colafranceschi, E., and Oriti, D. Bulk area law for boundary entanglement in spin network states: entropy corrections and horizon-like regions from volume correlations. (2021). Available from: http://arxiv.org/abs/2110.15166.

[34] Chirco, G., Mele, F. M., Oriti, D., and Vitale, P. Fisher metric, geometric entanglement and spin networks. (2017). Available from: http://arxiv.org/abs/1703.05231http://dx.doi.org/10.1103/PhysRevD.97.046015, doi:10.1103/PhysRevD.97.046015.

[35] Colafranceschi, E., Chirco, G., and Oriti, D. Holographic maps from quantum gravity states as tensor networks. (2021). Available from: http://arxiv.org/abs/2105.06454.

[36] Colafranceschi, E. and Oriti, D. Quantum gravity states, entanglement graphs and second-quantized tensor networks. *Journal of High Energy Physics*, **2021** (2021). Available from: https://doi.org/10.1007%2Fjhep07%282021%29052, doi:10.1007/jhep07(2021)052.

[37] Renes, J. M. *Quantum Information Theory*. De Gruyter (2022). ISBN 978-3-11-057024-3.

[38] Ghassami, A. and Kiyavash, N. Interaction information for causal inference: The case of directed triangle.

[39] Srinivasa, S. A review on multivariate mutual information.

[40] Gielen, S., Oriti, D., and Sindoni, L. Cosmology from Group Field Theory Formalism for Quantum Gravity. *Phys. Rev. Lett.*, **111** (2013), 031301. arXiv:1303.3576, doi:10.1103/PhysRevLett.111.031301.

[41] Marchetti, L., Oriti, D., Pithis, A. G. A., and Thürigen, J. Phase transitions in TGFT: a Landau-Ginzburg analysis of Lorentzian quantum geometric models. *JHEP*, **02** (2023), 074. arXiv:2209.04297, doi:10.1007/JHEP02(2023)074.

[42] Oriti, D., Pranzetti, D., and Sindoni, L. Horizon entropy from quantum gravity condensates. *Phys. Rev. Lett.*, **116** (2016), 211301. arXiv:1510.06991, doi:10.1103/PhysRevLett.116.211301.

[43] Castelvecchi, D. and Witze, A. Einstein's gravitational waves found at last. *Nature*, (2016). Available from: https://doi.org/10.1038/nature.2016.19361, doi:10.1038/nature.2016.19361.

[44] Abbott, B., et al. Observation of gravitational waves from a binary black hole merger. *Physical Review Letters*, **116** (2016). Available from: https://doi.org/10.1103%2Fphysrevlett.116.061102, doi:10.1103/physrevlett.116.061102.

[45] Gandolfi, G., Lapi, A., and Liberati, S. Empirical Evidence of Nonminimally Coupled Dark Matter in the Dynamics of Local Spiral Galaxies? *Astrophys. J.*, **929** (2022), 48. arXiv:2203.00572, doi:10.3847/1538-4357/ac5970.

[46] Ford, L. H. Quantum field theory in curved spacetime (1997). Available from: https://arxiv.org/abs/gr-qc/9707062, doi:10.48550/ARXIV.GR-QC/9707062.

[47] N. D. Birrell, P. C. W. D. *Quantum fields in curved space*. Cambridge Monographs on Mathematical Physics. Cambridge University Press, cup edn. (1984). ISBN 9780521278584; 0521278589. Available from: libgen.li/file.php?md5=926e0805c7542cecdd017f6b2a912cd8.

[48] Zinn-Justin, J. *Quantum Field Theory and Critical Phenomena*. Oxford Science Publications (2002). International Series of Monographs on Physics.

[49] Anderson, E. Beables/observables in classical and quantum gravity. *Symmetry, Integrability and Geometry: Methods and Applications*, (2014). Available from: https://doi.org/10.3842%2Fsigma.2014.092, doi:10.3842/sigma.2014.092.

[50] Wheeler, J. and Ford, K. Geons, black holes and quantum foam: A life in physics. *American Journal of Physics*, **68** (2000). doi:10.1119/1.19497.

[51] Wald, R. M. *General relativity*. Chicago Univ. Press, Chicago, IL (1984). Available from: https://cds.cern.ch/record/106274.

[52] Arnowitt, R. L., Deser, S., and Misner, C. W. The Dynamics of general relativity. *Gen. Rel. Grav.*, **40** (2008), 1997. arXiv:gr-qc/0405109, doi:10.1007/s10714-008-0661-1.

[53] Einstein, A. A Generalized Theory of Gravitation. *Rev. Mod. Phys.*, **20** (1948), 35. doi:10.1103/RevModPhys.20.35.

[54] Einstein, A. A generalization of the relativistic theory of gravitation. *Annals Math.*, **46** (1945), 578. doi:10.2307/1969197.

[55] Einstein, A., Infeld, L., and Hoffmann, B. The Gravitational equations and the problem of motion. *Annals Math.*, **39** (1938), 65. doi:10.2307/1968714.

[56] Rovelli, C. The century of the incomplete revolution: Searching for general relativistic quantum field theory. *Journal of Mathematical Physics*, **41** (2000), 3776. Available from: https://doi.org/10.1063%2F1.533327, doi:10.1063/1.533327.

[57] Maggiore, M. 744Bibliography. In *Gravitational Waves: Volume 2: Astrophysics and Cosmology*. Oxford University Press (2018). ISBN 9780198570899. arXiv:https://academic.oup.com/book/0/chapter/369015050/chapter-ag-pdf/45458208/book_43950_section_369015050.ag.pdf, doi:10.1093/oso/9780198570899.001.0001.

[58] Emparan, R., Barakovic, E., Dekhil, R., and Rescic, F. Black holes in the classical and quantum world (2023). arXiv:2306.11139.

[59] Oriti, D. The complex timeless emergence of time in quantum gravity. (2021). arXiv:2110.08641.

[60] Kiefer, C. Conceptual Problems in Quantum Gravity and Quantum Cosmology. *ISRN Math. Phys.*, **2013** (2013), 509316. arXiv:1401.3578, doi:10.1155/2013/509316.

[61] Kiefer, C. *Quantum Gravity*. Oxford University Press (2004).

[62] Kowalski-Glikman, J. and Nowak, S. *Noncommutative space-time of doubly special relativity theories*. *Int. J. Mod. Phys. D*, **12** (2003), 299. arXiv:hep-th/0204245, doi:10.1142/S0218271803003050.

[63] Addazi, A. et al. Quantum gravity phenomenology at the dawn of the multi-messenger era—A review. *Prog. Part. Nucl. Phys.*, **125** (2022), 103948. arXiv:2111.05659, doi:10.1016/j.ppnp.2022.103948.

[64] Isham, C. J. Structural issues in quantum gravity. In *14TH INTERNATIONAL CONFERENCE ON GENERAL RELATIVITY AND GRAVITATION (GR14)*, pp. 167–209 (1995). arXiv:gr-qc/9510063.

[65] Oriti, D. and Williams, R. M. Gluing 4-simplices: a derivation of the barrett-crane spin foam model for euclidean quantum gravity. *Physical Review D - Particles, Fields, Gravitation and Cosmology*, **63** (2000), 13. Available from: http://arxiv.org/abs/gr-qc/0010031http://dx.doi.org/10.1103/PhysRevD.63.024022, doi:10.1103/PhysRevD.63.024022.

[66] Ashtekar, A., Reuter, M., and Rovelli, C. From General Relativity to Quantum Gravity. (2014). arXiv:1408.4336.

[67] Gaul, M. and Rovelli, C. Loop quantum gravity and the meaning of diffeomorphism invariance (1999). arXiv:gr-qc/9910079.

[68] PADMANABHAN, T. FROM GRAVITONS TO GRAVITY: MYTHS AND REALITY. *International Journal of Modern Physics D*, **17** (2008), 367. Available from: https://doi.org/10.1142%2Fs0218271808012085, doi:10.1142/s0218271808012085.

[69] Gomes, H. and Butterfield, J. The Hole Argument and Beyond: Part I: The Story so Far. *J. Phys. Conf. Ser.*, **2533** (2023), 012002. arXiv:2303.14052, doi:10.1088/1742-6596/2533/1/012002.

[70] Gambini, R. and Pullin, J. Relational physics with real rods and clocks and the measurement problem of quantum mechanics. *Foundations of Physics*, **37** (2007), 1074. Available from: https://doi.org/10.1007%2Fs10701-007-9144-6, doi:10.1007/s10701-007-9144-6.

[71] Höhn, P. A., Smith, A. R. H., and Lock, M. P. E. Trinity of relational quantum dynamics. *Phys. Rev. D*, **104** (2021), 066001. Available from: https://link.aps.org/doi/10.1103/PhysRevD.104.066001, doi:10.1103/PhysRevD.104.066001.

[72] Bojowald, M., Hoehn, P. A., and Tsobanjan, A. An Effective approach to the problem of time. *Class. Quant. Grav.*, **28** (2011), 035006. arXiv:1009.5953, doi:10.1088/0264-9381/28/3/035006.

[73] Bojowald, M. *Canonical Gravity and Applications: Cosmology, Black Holes, and Quantum Gravity*. Cambridge University Press (2010). doi:10.1017/CBO9780511921759.

[74] Barbour, J. The nature of time (2009). arXiv:0903.3489.

[75] Tambornino, J. Relational observables in gravity: a review. *Symmetry, Integrability and Geometry: Methods and Applications*, (2012). Available from: https://doi.org/10.3842%2Fsigma.2012.017, doi:10.3842/sigma.2012.017.

[76] Gielen, S., Marchetti, L., Oriti, D., and Polaczek, A. Effective cosmology from one-body operators in group field theory. *Classical and Quantum Gravity*, **39** (2022), 075002. Available from: https://doi.org/10.1088%2F1361-6382%2Fac5052, doi:10.1088/1361-6382/ac5052.

[77] Marchetti, L. and Oriti, D. Quantum fluctuations in the effective relational GFT cosmology. *Frontiers in Astronomy and Space Sciences*, **8** (2021). Available from: https://doi.org/10.3389%2Ffspas.2021.683649, doi:10.3389/fspas.2021.683649.

[78] Williams, R. M. Discrete quantum gravity. *Journal of Physics: Conference Series*, **33** (2006), 38. Available from: https://dx.doi.org/10.1088/1742-6596/33/1/004, doi:10.1088/1742-6596/33/1/004.

[79] Witten, E. *(2+1)-Dimensional Gravity as an Exactly Soluble System. Nucl. Phys. B*, **311** (1988), 46. doi:10.1016/0550-3213(88)90143-5.

[80] Oriti, D. The bronstein hypercube of quantum gravity (2018). arXiv:1803.02577.

[81] Freidel, L. and Louapre, D. Diffeomorphisms and spin foam models. *Nuclear Physics B*, **662** (2003), 279. Available from: https://doi.org/10.1016%2Fs0550-3213%2803%2900306-7, doi:10.1016/s0550-3213(03)00306-7.

[82] Huggett, N. and Wüthrich, C. Emergent spacetime and empirical (in)coherence. *Studies in History and Philosophy of Science Part B: Studies in History and Philosophy of Modern Physics*, **44** (2013), 276. Available from: https://www.sciencedirect.com/science/article/pii/S1355219812000676, doi:https://doi.org/10.1016/j.shpsb.2012.11.003.

[83] Butterfield, J. Emergence, reduction and supervenience: A varied landscape. *Foundations of Physics*, **41** (2011), 920. doi:10.1007/s10701-011-9549-0.

[84] Krajewski, T. Group field theories (2012). Available from: https://arxiv.org/abs/1210.6257, doi:10.48550/ARXIV.1210.6257.

[85] Oriti, D. *The Group field theory approach to quantum gravity*. (2006), 310. arXiv:gr-qc/0607032.

[86] Oriti, D. *The universe as a quantum gravity condensate. Comptes Rendus Physique*, **18** (2017), 235. arXiv:1612.09521, doi:10.1016/j.crhy.2017.02.003.

[87] Oriti, D. *Tensorial Group Field Theory condensate cosmology as an example of spacetime emergence in quantum gravity* (2021). arXiv:2112.02585.

[88] Ambjørn, J., Durhuus, B., and Jonsson, T. *Quantum Geometry: A Statistical Field Theory Approach*. Cambridge Monographs on Mathematical Physics. Cambridge University Press (1997). doi:10.1017/CBO9780511524417.

[89] Kitaev, A. and Suh, S. J. *Statistical mechanics of a two-dimensional black hole*. *JHEP*, **05** (2019), 198. arXiv:1808.07032, doi:10.1007/JHEP05(2019)198.

[90] Raamsdonk, M. V. Building up spacetime with quantum entanglement. (2010). Available from: http://arxiv.org/abs/1005.3035http://dx.doi.org/10.1007/s10714-010-1034-010.1142/S0218271810018529, doi:10.1007/s10714-010-1034-010.1142/S0218271810018529.

[91] Perez, A. *Spin foam models for quantum gravity*. *Class. Quant. Grav.*, **20** (2003), R43. arXiv:gr-qc/0301113, doi:10.1088/0264-9381/20/6/202.

[92] Goeller, C., Livine, E. R., and Riello, A. Non-Perturbative 3D Quantum Gravity: Quantum Boundary States and Exact Partition Function. *Gen. Rel. Grav.*, **52** (2020), 24. arXiv:1912.01968, doi:10.1007/s10714-020-02673-3.

[93] Goeller, C., Hoehn, P. A., and Kirklin, J. Diffeomorphism-invariant observables and dynamical frames in gravity: reconciling bulk locality with general covariance. (2022). arXiv:2206.01193.

[94] Freidel, L., Goeller, C., and Livine, E. R. The quantum gravity disk: Discrete current algebra. *J. Math. Phys.*, **62** (2021), 102303. arXiv:2103.13171, doi:10.1063/5.0051647.

[95] Oriti, D. Spacetime geometry from algebra: spin foam models for non-perturbative quantum gravity. *Reports on Progress in Physics*, **64** (2001), 1703. Available from: https://doi.org/10.1088%2F0034-4885%2F64%2F12%2F203, doi:10.1088/0034-4885/64/12/203.

[96] Krasnov, K. *Formulations of General Relativity : Gravity, Spinors and Differential Forms*. Cambridge Monographs on Mathematical Physics. Cambridge University Press (2020). ISBN 9781108481649; 1108481647. Available from: libgen.li/file.php?md5=dc289e6e4c739dd3bedee0724b12585d.

[97] Cartan, H. *Differential Calculus*. Houghton Mifflin (1971). ISBN 0395120330; 9780395120330. Available from: libgen.li/file.php?md5=c01641b044140c66448602e381445178.

[98] Gaul, M. and Rovelli, C. Loop quantum gravity and the meaning of diffeomorphism invariance. (1999). Available from: https://arxiv.org/abs/gr-qc/9910079, doi:10.48550/ARXIV.GR-QC/9910079.

[99] Pietri, R. D. and Freidel, L. Plebanski action and relativistic spin-foam model. *Classical and Quantum Gravity*, **16** (1999), 2187. Available from: https://doi.org/10.1088%2F0264-9381%2F16%2F7%2F303, doi:10.1088/0264-9381/16/7/303.

[100] Finocchiaro, M. and Oriti, D. *Spin foam models and the Duflo map. Class. Quant. Grav.*, **37** (2020), 015010. arXiv:1812.03550, doi:10.1088/1361-6382/ab58da.

[101] Barbieri, A. Quantum tetrahedra and simplicial spin networks. *Nuclear Physics B*, **518** (1998), 714. Available from: https://doi.org/10.1016%2Fs0550-3213%2898%2900093-5, doi:10.1016/s0550-3213(98)00093-5.

[102] Baez, J. C. and Barrett, J. W. The quantum tetrahedron in 3 and 4 dimensions. (1999). arXiv:gr-qc/9903060.

[103] Marc Levine, F. M. *Algebraic Cobordism*. Springer monographs in mathematics. Springer, 1 edn. (2007). ISBN 9783540368229; 3540368221. Available from: libgen.li/file.php?md5=20d75154f7200465e1b2018a742b48d6.

[104] F., P. *Lectures on cobordism theory*. Kinokuniya (1968). Available from: libgen.li/file.php?md5=9153102ceb05f4381aad19761cd9223a.

[105] I.M. Gel'fand, M. G. *Geometry of homogeneous spaces, representations of groups in homogeneous spaces and related questions of integral geometry.*

[106] Livine, E. R. *Hamiltonian flows of Lorentzian polyhedra: Kapovich-Millson phase space and SU(1, 1) intertwiners. Journal of Mathematical Physics*, **60** (2019), 012301. Available from: http://dx.doi.org/10.1063/1.5048980, doi:10.1063/1.5048980.

[107] Chen, Z., Stiçnon, M., and Xu, P. *Poisson 2-Groups. J. Differential Geom.*, **94** (2013), 209. Available from: https://doi.org/10.4310/jdg/1367438648, doi:10.4310/jdg/1367438648.

[108] Misner, C. W. Feynman quantization of general relativity. *Rev. Mod. Phys.*, **29** (1957), 497. Available from: https://link.aps.org/doi/10.1103/RevModPhys.29.497, doi:10.1103/RevModPhys.29.497.

[109] Reisenberger, M. P. and Rovelli, C. *'Sum over surfaces' form of loop quantum gravity. Phys. Rev. D*, **56** (1997), 3490. arXiv:gr-qc/9612035, doi:10.1103/PhysRevD.56.3490.

[110] Hawking, S. W. *THE PATH INTEGRAL APPROACH TO QUANTUM GRAVITY*, pp. 746–789 (1980).

[111] Rovelli, C. and Smolin, L. Spin networks and quantum gravity. *Physical Review D*, **52** (1995), 5743. Available from: https://doi.org/10.1103%2Fphysrevd.52.5743, doi:10.1103/physrevd.52.5743.

[112] Rovelli, C. *Quantum Gravity*. Cambridge Monographs on Mathematical Physics. Cambridge University Press (2004). ISBN 9780521837330. Available from: https://books.google.ca/books?id=HrAzTmXdssQC.

[113] Baez, J. C. Spin foam models. *Classical and Quantum Gravity*, **15** (1998), 1827. Available from: https://doi.org/10.1088%2F0264-9381%2F15%2F7%2F004, doi:10.1088/0264-9381/15/7/004.

[114] Barrett, J. W. and Crane, L. A lorentzian signature model for quantum general relativity. *Classical and Quantum Gravity*, **17** (1999), 3101. Available from: http://arxiv.org/abs/gr-qc/9904025http://dx.doi.org/10.1088/0264-9381/17/16/302, doi:10.1088/0264-9381/17/16/302.

[115] Crane, L. and Yetter, D. *A More sensitive Lorentzian state sum*. (2003). arXiv:gr-qc/0301017.

[116] Baez, J. C., Christensen, J. D., and Egan, G. Asymptotics of 10j symbols. *Classical and Quantum Gravity*, **19** (2002), 6489. Available from: https://doi.org/10.1088/0264-9381/19/24/315, doi:10.1088/0264-9381/19/24/315.

[117] Perez, A. and Rovelli, C. 3+1 spinfoam model of quantum gravity with spacelike and timelike components. *Physical Review D*, **64** (2000). Available from: http://arxiv.org/abs/gr-qc/0011037http://dx.doi.org/10.1103/PhysRevD.64.064002, doi:10.1103/PhysRevD.64.064002.

[118] Crane, L. and Yetter, D. N. *Measurable categories and 2-groups*. (2003). arXiv:math/0305176.

[119] Baez, J. C. *Spin network states in gauge theory*. *Adv. Math.*, **117** (1996), 253. arXiv:gr-qc/9411007, doi:10.1006/aima.1996.0012.

[120] Jercher, A. F., Oriti, D., and Pithis, A. G. Complete barrett-crane model and its causal structure. *Physical Review D*, **106** (2022). Available from: https://doi.org/10.1103%2Fphysrevd.106.066019, doi:10.1103/physrevd.106.066019.

[121] Jercher, A. F., Oriti, D., and Pithis, A. G. A. *Emergent cosmology from quantum gravity in the Lorentzian Barrett-Crane tensorial group field theory model*. *JCAP*, **01** (2022), 050. arXiv:2112.00091, doi:10.1088/1475-7516/2022/01/050.

[122] Baratin, A. and Oriti, D. *Group field theory with non-commutative metric variables*. *Phys. Rev. Lett.*, **105** (2010), 221302. arXiv:1002.4723, doi:10.1103/PhysRevLett.105.221302.

[123] Engle, J., Livine, E., Pereira, R., and Rovelli, C. *LQG vertex with finite Immirzi parameter*. *Nucl. Phys. B*, **799** (2008), 136. arXiv:0711.0146, doi:10.1016/j.nuclphysb.2008.02.018.

[124] Perez, A. and Rovelli, C. *Spin foam model for Lorentzian general relativity*. *Phys. Rev. D*, **63** (2001), 041501. arXiv:gr-qc/0009021, doi:10.1103/PhysRevD.63.041501.

[125] Jercher, A. F., Oriti, D., and Pithis, A. G. A. The Complete Barrett-Crane Model and its Causal Structure. (2022). arXiv:2206.15442.

[126] Ashtekar, A. and Lewandowski, J. Quantum theory of geometry ii: Volume operators (1997). arXiv:gr-qc/9711031.

[127] Thiemann, T. *Modern Canonical Quantum General Relativity*. Cambridge Monographs on Mathematical Physics. Cambridge University Press (2007). doi:10.1017/CBO9780511755682.

[128] Bianchi, E., Doná, P., and Speziale, S. *Polyhedra in loop quantum gravity*. *Physical Review D*, **83** (2011). Available from: http://dx.doi.org/10.1103/PhysRevD.83.044035, doi:10.1103/physrevd.83.044035.

[129] Oriti, D. The microscopic dynamics of quantum space as a group field theory. In *Proceedings, Foundations of Space and Time: Reflections on Quantum Gravity: Cape Town, South Africa*, pp. 257–320 (2011). Available from: http://inspirehep.net/record/942719/files/arXiv:1110.5606.pdf, arXiv:1110.5606.

[130] Krajewski, T. Group field theories (2012). arXiv:1210.6257.

[131] Oriti, D. *Group Field Theory and Loop Quantum Gravity* (2014). arXiv:1408.7112.

[132] Penrose, R. *Angular momentum: an approach to combinatorial spacetime*. In *Living Reviews in Relativity*, pp. 151–180. University Press (1971).

[133] Dona, P. and Speziale, S. Introductory lectures to loop quantum gravity. In *Gravitation Théorie et Expérience.Proceedings, Troisième école de physique théorique de Jijel: Jijel, Algeria, September 26?October 03, 2009*, pp. 89–140 (2013). Available from: https://inspirehep.net/record/860342/files/arXiv:1007.0402.pdf, arXiv:1007.0402.

[134] Perez, A. Introduction to loop quantum gravity and spin foams. (2004). arXiv:gr-qc/0409061.

[135] Gourgoulhon, E. 3+1 formalism and bases of numerical relativity. (2007). arXiv:gr-qc/0703035.

[136] Freidel, L. *Group field theory: An Overview. Int. J. Theor. Phys.*, **44** (2005), 1769. arXiv:hep-th/0505016, doi:10.1007/s10773-005-8894-1.

[137] Bonzom, V., Gurau, R., and Rivasseau, V. *Random tensor models in the large N limit: Uncoloring the colored tensor models. Phys. Rev. D*, **85** (2012), 084037. arXiv:1202.3637, doi:10.1103/PhysRevD.85.084037.

[138] Gurău, R. *Random Tensors* (2016). Available from: https://oxford.universitypressscholarship.com/view/10.1093/acprof:oso/9780198787938.001.0001/acprof-9780198787938, doi:10.1093/acprof:oso/9780198787938.001.0001.

[139] Rivasseau, V. *The Tensor Track, III. Fortsch. Phys.*, **62** (2014), 81. arXiv:1311.1461, doi:10.1002/prop.201300032.

[140] Barrett, J. W. and Mackaay, M. *Categorical representations of categorical groups.* (2004). arXiv:math/0407463.

[141] Martin-Dussaud, P. A primer of group theory for loop quantum gravity and spin-foams. *General Relativity and Gravitation*, **51** (2019). doi:10.1007/s10714-019-2583-5.

[142] Kapovich, M. and Millson, J. J. *The symplectic geometry of polygons in Euclidean space. J. Differential Geom.*, **44** (1996), 479. Available from: https://doi.org/10.4310/jdg/1214459218, doi:10.4310/jdg/1214459218.

[143] Faraut, J. *Analysis on Lie Groups: An Introduction.* Cambridge Studies in Advanced Mathematics. Cambridge University Press (2008). doi:10.1017/CBO9780511755170.

[144] Dao Vong Duc, N. V. H. *On the theory of unitary representations of the SL(2,C) group. Annales de l'I. H. P., section A, tome 6*, **11** (1967), 17. arXiv:{}, doi:10.1007/BF03159474.

[145] Baratin, A. and Oriti, D. *Quantum simplicial geometry in the group field theory formalism: reconsidering the Barrett-Crane model. New J. Phys.*, **13** (2011), 125011. arXiv:1108.1178, doi:10.1088/1367-2630/13/12/125011.

[146] Tjin, T. *An Introduction to quantized Lie groups and algebras. Int. J. Mod. Phys. A*, **7** (1992), 6175. arXiv:hep-th/9111043, doi:10.1142/S0217751X92002805.

[147] Guedes, C., Oriti, D., and Raasakka, M. Quantization maps, algebra representation, and non-commutative fourier transform for lie groups. *Journal of Mathematical Physics*, **54** (2013), 083508. Available from: https://doi.org/10.1063%2F1.4818638, doi:10.1063/1.4818638.

[148] Oriti, D. and Rosati, G. *Noncommutative Fourier transform for the Lorentz group via the Duflo map*. *Phys. Rev. D*, **99** (2019), 106005. arXiv:1812.08616, doi:10.1103/PhysRevD.99.106005.

[149] Reisenberger, M. and Rovelli, C. Spin foams as feynman diagrams (2000). arXiv:gr-qc/0002083.

[150] Pietri, R. D., Freidel, L., Krasnov, K., and Rovelli, C. Barrett–crane model from a boulatov–ooguri field theory over a homogeneous space. *Nuclear Physics B*, **574** (2000), 785. Available from: https://doi.org/10.1016%2Fs0550-3213%2800%2900005-5, doi:10.1016/s0550-3213(00)00005-5.

[151] Reisenberger, M. P. and Rovelli, C. Spacetime as a feynman diagram: the connection formulation. *Classical and Quantum Gravity*, **18** (2000), 121. Available from: https://doi.org/10.1088%2F0264-9381%2F18%2F1%2F308, doi:10.1088/0264-9381/18/1/308.

[152] Carrozza, S., Gielen, S., and Oriti, D. Editorial for the special issue "progress in group field theory and related quantum gravity formalisms". (2020). Available from: http://arxiv.org/abs/2001.08428http://dx.doi.org/10.3390/universe6010019, doi:10.3390/universe6010019.

[153] Oriti, D. Disappearance and emergence of space and time in quantum gravity. (2013). Available from: http://arxiv.org/abs/1302.2849.

[154] Essam, J. W. and Fisher, M. E. Some Basic Definitions in Graph Theory. *Reviews of Modern Physics*, **42** (1970), 271. doi:10.1103/RevModPhys.42.271.

[155] Meusburger, C. and Wise, D. K. *Hopf algebra gauge theory on a ribbon graph*. *Reviews in Mathematical Physics*, **33** (2021), 2150016. Available from: http://dx.doi.org/10.1142/S0129055X21500161, doi:10.1142/s0129055x21500161.

[156] Oriti, D., Sindoni, L., and Wilson-Ewing, E. Emergent friedmann dynamics with a quantum bounce from quantum gravity condensates. *Classical and Quantum Gravity*, **33** (2016), 224001. Available from: https://doi.org/10.1088%2F0264-9381%2F33%2F22%2F224001, doi:10.1088/0264-9381/33/22/224001.

[157] Oriti, D. Group field theory as the 2nd quantization of loop quantum gravity.

[158] Soni, R. M. and Trivedi, S. P. Aspects of entanglement entropy for gauge theories. *Journal of High Energy Physics*, **2016** (2016), 1. doi:10.1007/JHEP01(2016)136.

[159] Ghassami, A. and Kiyavash, N. Interaction information for causal inference: The case of directed triangle. Available from: https://arxiv.org/abs/1701.08868, doi:10.48550/ARXIV.1701.08868.

[160] Alesci, E., Botta, G., Cianfrani, F., and Liberati, S. Cosmological singularity resolution from quantum gravity: The emergent-bouncing universe. *Physical Review D*, **96** (2017). Available from: https://doi.org/10.1103%2Fphysrevd.96.046008, doi:10.1103/physrevd.96.046008.

[161] Gielen, S. Inhomogeneous universe from group field theory condensate. *Journal of Cosmology and Astroparticle Physics*, **2019** (2019), 013. Available from: https://doi.org/10.1088%2F1475-7516%2F2019%2F02%2F013, doi:10.1088/1475-7516/2019/02/013.

[162] Höhn, P. A. and Vanrietvelde, A. How to switch between relational quantum clocks. *New Journal of Physics*, **22** (2020), 123048. Available from: https://doi.org/10.1088%2F1367-2630%2Fabd1ac, doi:10.1088/1367-2630/abd1ac.

[163] Höhn, P. A., Smith, A. R., and Lock, M. P. Trinity of relational quantum dynamics. *Physical Review D*, **104** (2021). Available from: https://doi.org/10.1103%2Fphysrevd.104.066001, doi:10.1103/physrevd.104.066001.

[164] Marchetti, L. and Oriti, D. Effective dynamics of scalar cosmological perturbations from quantum gravity. *Journal of Cosmology and Astroparticle Physics*, **2022** (2022), 004. Available from: https://doi.org/10.1088%2F1475-7516%2F2022%2F07%2F004, doi:10.1088/1475-7516/2022/07/004.

[165] Li, Y., Oriti, D., and Zhang, M. Group field theory for quantum gravity minimally coupled to a scalar field. *Classical and Quantum Gravity*, **34** (2017), 195001. Available from: https://doi.org/10.1088%2F1361-6382%2Faa85d2, doi:10.1088/1361-6382/aa85d2.

[166] Oriti, D., Pranzetti, D., Ryan, J. P., and Sindoni, L. Generalized quantum gravity condensates for homogeneous geometries and cosmology. *Classical and Quantum Gravity*, **32** (2015), 235016. Available from: https://dx.doi.org/10.1088/0264-9381/32/23/235016, doi:10.1088/0264-9381/32/23/235016.

[167] Gielen, S. and Oriti, D. Cosmological perturbations from full quantum gravity. (2018).

[168] Marchetti, L. and Oriti, D. Effective relational cosmological dynamics from quantum gravity. *Journal of High Energy Physics*, **2021** (2021). Available from: https://doi.org/10.1007%2Fjhep05%282021%29025, doi:10.1007/jhep05(2021)025.

[169] Baez, J. C. *Four-Dimensional BF theory with cosmological term as a topological quantum field theory. Lett. Math. Phys.*, **38** (1996), 129. arXiv:q-alg/9507006, doi:10.1007/BF00398315.

[170] Engle, J. S. Spin foams. In *Springer Handbook of Spacetime*, pp. 783–807. Springer Berlin Heidelberg (2014). Available from: https://doi.org/10.1007%2F978-3-642-41992-8_38, doi:10.1007/978-3-642-41992-8_38.

[171] Barrett, J. W. *Quantum gravity as topological quantum field theory. J. Math. Phys.*, **36** (1995), 6161. arXiv:gr-qc/9506070, doi:10.1063/1.531239.

[172] Crane, L., Kauffman, L. H., and Yetter, D. N. *State sum invariants of four manifolds. 1.* (1994). arXiv:hep-th/9409167.

[173] LAUDA, A. D. and PFEIFFER, H. STATE SUM CONSTRUCTION OF TWO-DIMENSIONAL OPEN-CLOSED TOPOLOGICAL QUANTUM FIELD THEORIES. *Journal of Knot Theory and Its Ramifications*, **16** (2007), 1121. Available from: https://doi.org/10.1142%2Fs0218216507005725, doi:10.1142/s0218216507005725.

[174] Fukuma, M., Hosono, S., and Kawai, H. Lattice topological field theory in two dimensions. *Communications in Mathematical Physics*, **161** (1994), 157. Available from: https://doi.org/10.1007%2Fbf02099416, doi:10.1007/bf02099416.

[175] Moore, M. A. Exactly solved models in statistical mechanics. *Physics Bulletin*, **34** (1983), 167. Available from: https://dx.doi.org/10.1088/0031-9112/34/4/045, doi:10.1088/0031-9112/34/4/045.

[176] Freidel, L. and Louapre, D. *Asymptotics of 6j and 10j symbols. Class. Quant. Grav.*, **20** (2003), 1267. arXiv:hep-th/0209134, doi:10.1088/0264-9381/20/7/303.

[177] Dirac, P. A. M. *Unitary representations of the Lorentz group. Royal Society of London. A183284–295*, **183** (1945). arXiv:{}, doi:http://doi.org/10.1098/rspa.1945.0003.

[178] IRUEHL, W. *The Lorentz group and harmonic analysis. New York, W. A. Benjamin, Inc.*

[179] Chandra, H. *Infinite Irreducible Representations of the Lorentz Group. Royal Society of London. Series A, Mathematical and Physical Sciences 189*, **1018** (1947), 372. arXiv:{}, doi:http://www.jstor.org/stable/97833.

[180] Genest, V. X., Vinet, L., and Zhedanov, A. Interbasis expansions for the isotropic 3d harmonic oscillator and bivariate krawtchouk polynomials. *Journal of Physics A: Mathematical and Theoretical*, **47** (2013). Available from: http://arxiv.org/abs/1307.0692http://dx.doi.org/10.1088/1751-8113/47/2/025202, doi:10.1088/1751-8113/47/2/025202.

[181] Cohl, H. S. and Kalnins, E. G. Fundamental solution of the laplacian in the hyperboloid model of hyperbolic geometry (2012). Available from: https://arxiv.org/abs/1201.4406, doi:10.48550/ARXIV.1201.4406.

[182] Xuegang, Y., Wuming, L., and Junli, G. The four-dimensional hyperbolic spherical harmonics.

[183] Barrett, J. Minkowski space-time and hyperbolic geometry (original 2015 version) (2015).

[184] Reisenberger, M. P. *On relativistic spin network vertices*. *J. Math. Phys.*, **40** (1999), 2046. arXiv:gr-qc/9809067, doi:10.1063/1.532850.

[185] Baez, J. C. *Higher Yang-Mills theory*. (2002). arXiv:hep-th/0206130.

[186] Kiefer, C. Conceptual Issues in Canonical Quantum Gravity and Cosmology. In *Time and Matter 2007*, pp. 131–143. University of Nova Gorica Press (2007).

[187] Giacomini, F. and Brukner, v. Einstein's Equivalence principle for superpositions of gravitational fields and quantum reference frames. (2020). arXiv:2012.13754.

[188] Belenchia, A., Wald, R. M., Giacomini, F., Castro-Ruiz, E., Brukner, v., and Aspelmeyer, M. Information Content of the Gravitational Field of a Quantum Superposition. *Int. J. Mod. Phys. D*, **28** (2019), 1943001. arXiv:1905.04496, doi:10.1142/S0218271819430016.

[189] Giacomini, F. and Brukner, v. Quantum superposition of spacetimes obeys Einstein's equivalence principle. *AVS Quantum Sci.*, **4** (2022), 015601. arXiv:2109.01405, doi:10.1116/5.0070018.

[190] Horodecki, R., Horodecki, P. L., Horodecki, M. L., and Horodecki, K. Quantum entanglement. (2007).

[191] Vidal, G. Entanglement monotones. (1999).

[192] Vidal, G., Dür, W., and Cirac, J. I. Entanglement cost of mixed states. (2002).

[193] Bianchi, E., Dona, P., and Vilensky, I. Entanglement entropy of bell-network states in lqg: Analytical and numerical results. (2018). Available from: http://arxiv.org/abs/1812.10996http://dx.doi.org/10.1103/PhysRevD.99.086013, doi:10.1103/PhysRevD.99.086013.

[194] Livine, E. R. and Terno, D. R. Reconstructing quantum geometry from quantum information: Area renormalisation, coarse-graining and entanglement on spin networks. (2006).

[195] Delcamp, C., Dittrich, B., and Riello, A. On entanglement entropy in non-abelian lattice gauge theory and 3d quantum gravity. *Journal of High Energy Physics*, **2016** (2016). doi:10.1007/JHEP11(2016)102.

[196] Donnelly, W. Entanglement entropy in loop quantum gravity. (2008). Available from: http://arxiv.org/abs/0802.0880http://dx.doi.org/10.1103/PhysRevD.77.104006, doi:10.1103/PhysRevD.77.104006.

[197] Donnelly, W. Entanglement entropy and nonabelian gauge symmetry. (2014). Available from: http://arxiv.org/abs/1406.7304http://dx.doi.org/10.1088/0264-9381/31/21/214003, doi:10.1088/0264-9381/31/21/214003.

[198] Donnelly, W. Decomposition of entanglement entropy in lattice gauge theory. (2011). Available from: http://arxiv.org/abs/1109.0036http://dx.doi.org/10.1103/PhysRevD.85.085004, doi:10.1103/PhysRevD.85.085004.

[199] Buividovich, P. and Polikarpov, M. Entanglement entropy in gauge theories and the holographic principle for electric strings. *Physics Letters B*, **670** (2008), 141. Available from: https://doi.org/10.10162Fj.physletb.2008.10.032, doi:10.1016/j.physletb.2008.10.032.

[200] Riello, A. *Edge modes without edge modes*. (2021). arXiv:2104.10182.

[201] Chen, Q. and Livine, E. R. Intertwiner entanglement excitation and holonomy operator.

[202] Ghirardi, G. and Marinatto, L. Identical particles and entanglement *.

[203] Oriti, D. The universe as a quantum gravity condensate. *Comptes Rendus Physique*, **18** (2017), 235. arXiv:1612.09521, doi:10.1016/j.crhy.2017.02.003.

[204] Gielen, S. and Sindoni, L. Quantum Cosmology from Group Field Theory Condensates: a Review. *SIGMA*, **12** (2016), 082. arXiv:1602.08104, doi:10.3842/SIGMA.2016.082.

[205] Pithis, A. G. A. and Sakellariadou, M. Group field theory condensate cosmology: An appetizer. *Universe*, **5** (2019), 147. arXiv:1904.00598, doi:10.3390/universe5060147.

[206] Gielen, S., Oriti, D., and Sindoni, L. Cosmology from group field theory formalism for quantum gravity. *Physical Review Letters*, **111** (2013). Available from: https://doi.org/10.1103%2Fphysrevlett.111.031301, doi:10.1103/physrevlett.111.031301.

[207] Gielen, S. and Polaczek, A. Generalised effective cosmology from group field theory. (2020).

[208] Rovelli, C. A note on the foundation of relativistic mechanics i: Relativistic observables and relativistic states. (2002).

[209] Hollands, S. and Wald, R. M. Quantum fields in curved spacetime. *Physics Reports*, **574** (2015), 1. Available from: https://doi.org/10.1016%2Fj.physrep.2015.02.001, doi:10.1016/j.physrep.2015.02.001.

[210] Pereira, S. H., Bessa, C. H., and Lima, J. A. Quantized fields and gravitational particle creation in f (r) expanding universes. *Physics Letters, Section B: Nuclear, Elementary Particle and High-Energy Physics*, **690** (2010), 103. doi:10.1016/J.PHYSLETB.2010.05.027.

[211] Clifton, T., Ferreira, P. G., Padilla, A., and Skordis, C. Modified gravity and cosmology. *Physics Reports*, **513** (2012), 1. Modified Gravity and Cosmology. Available from: https://www.sciencedirect.com/science/article/pii/S0370157312000105, doi:https://doi.org/10.1016/j.physrep.2012.01.001.

[212] Langlois, D., Liu, H., Noui, K., and Wilson-Ewing, E. Effective loop quantum cosmology as a higher-derivative scalar-tensor theory. (2017).

[213] Torromé, R. G., Letizia, M., and Liberati, S. Phenomenology of effective geometries from quantum gravity. *Phys. Rev. D*, **92** (2015), 124021. arXiv:1507.03205, doi:10.1103/PhysRevD.92.124021.

[214] Bettoni, D. and Liberati, S. Dynamics of non-minimally coupled perfect fluids. *JCAP*, **08** (2015), 023. arXiv:1502.06613, doi:10.1088/1475-7516/2015/08/023.

[215] Gielen, S. Quantum cosmology of (loop) quantum gravity condensates: an example. *Classical and Quantum Gravity*, **31** (2014), 155009. Available from: https://doi.org/10.1088%2F0264-9381%2F31%2F15%2F155009, doi:10.1088/0264-9381/31/15/155009.

[216] Di Casola, E., Liberati, S., and Sonego, S. Between quantum and classical gravity: Is there a mesoscopic spacetime? *Found. Phys.*, **45** (2015), 171. arXiv:1405.5085, doi:10.1007/s10701-014-9859-0.

[217] Fewster, C. J. and Liberati, S. Quantum fields in curved spacetime, semiclassical gravity, quantum gravity phenomenology, and analogue models: parallel session D4. *Gen. Rel. Grav.*, **46** (2014), 1707. arXiv:1402.3544, doi:10.1007/s10714-014-1707-1.

[218] Huang, J. Green function. In *Perturbation Theory* (edited by D. I. Uzunov), chap. 3. IntechOpen, Rijeka (2017). Available from: https://doi.org/10.5772/68028, doi:10.5772/68028.

[219] Battarra, L., Koehn, M., Lehners, J.-L., and Ovrut, B. A. Cosmological perturbations through a non-singular ghost-condensate/galileon bounce. *Journal of Cosmology and Astroparticle Physics*, **2014** (2014), 007. Available from: https://doi.org/10.1088%2F1475-7516%2F2014%2F07%2F007, doi:10.1088/1475-7516/2014/07/007.

[220] Clifton, T., Ferreira, P. G., Padilla, A., and Skordis, C. Modified gravity and cosmology. *Physics Reports*, **513** (2012), 1. doi:10.1016/J.PHYSREP.2012.01.001.

[221] Oriti, D., Sindoni, L., Wilson-Ewing, E., Adjei, E., Gielen, S., Wieland, W., and Polaczek, A. Classical and quantum gravity you may also like emergent friedmann dynamics with a quantum bounce from quantum gravity condensates cosmological evolution as squeezing: a toy model for group field cosmology generalised effective cosmology from group field theory. *Classical and Quantum Gravity Class. Quantum Grav*, **37** (2020), 35. Available from: https://doi.org/10.1088/1361-6382/ab8f67, doi:10.1088/1361-6382/ab8f67.

[222] Starobinsky, A. A. A new type of isotropic cosmological models without singularity. *Physics Letters B*, **91** (1980), 99. doi:10.1016/0370-2693(80)90670-X.

[223] Broy, B. J. The starobinsky model.

[224] Ford, L. H. Cosmological particle production: a review. *Reports on Progress in Physics*, **84** (2021), 116901. Available from: https://doi.org/10.1088%2F1361-6633%2Fac1b23, doi:10.1088/1361-6633/ac1b23.

[225] Jacobson, T. Introduction to quantum fields in curved spacetime and the hawking effect. *CECS School on Quantum Gravity in*, (2002).

[226] Zheng, Y., Shen, L., Mou, Y., and Li, M. On (in)stabilities of perturbations in mimetic models with higher derivatives. *Journal of Cosmology and Astroparticle Physics*, **2017** (2017), 040. Available from: https://doi.org/10.1088%2F1475-7516%2F2017%2F08%2F040, doi:10.1088/1475-7516/2017/08/040.

[227] de Cesare, M. Limiting curvature mimetic gravity for group field theory condensates. *Physical Review D*, **99** (2019). Available from: https://doi.org/10.1103%2Fphysrevd.99.063505, doi:10.1103/physrevd.99.063505.

[228] Tapia, T. and Rojas, C. Scalar cosmological perturbations (2020). arXiv:2007.04423.

[229] Bretó n, N., Cervantes-Cota, J. L., and Salgado, M. (eds.). *The Early Universe and Observational Cosmology*. Springer Berlin Heidelberg (2004). Available from: https://doi.org/10.1007%2Fb97189, doi:10.1007/b97189.

[230] Mukhanov, V., Feldman, H., and Brandenberger, R. Theory of cosmological perturbations. *Physics Reports*, **215** (1992), 203. Available from: https://www.sciencedirect.com/science/article/pii/037015739290044Z, doi:https://doi.org/10.1016/0370-1573(92)90044-Z.

[231] Mukhanov, V. Quantum theory of cosmological perturbations in r2 gravity. *Physics Letters B*, **218** (1989), 17. Available from: https://www.sciencedirect.com/science/article/pii/037026938990467X, doi:https://doi.org/10.1016/0370-2693(89)90467-X.

[232] Donoghue, J. F. General relativity as an effective field theory: The leading quantum corrections. *Physical Review D*, **50** (1994), 3874. Available from: https://doi.org/10.1103%2Fphysrevd.50.3874, doi:10.1103/physrevd.50.3874.

[233] 't Hooft, G. Determinism and dissipation in quantum gravity, erice lecture (2000). arXiv:hep-th/0003005.

[234] Hu, B. Dissipation in quantum fields and semiclassical gravity. *Physica A: Statistical Mechanics and its Applications*, **158** (1989), 399. Available from: https://www.sciencedirect.com/science/article/pii/0378437189905396, doi:https://doi.org/10.1016/0378-4371(89)90539-6.

[235] Liberati, S., Maccione, L., and di Trieste, S. Astrophysical constraints on planck scale dissipative phenomena.

[236] Tucci, A. D. and Lehners, J.-L. No-boundary proposal as a path integral with robin boundary conditions. *Physical Review Letters*, **122** (2019). Available from: https://doi.org/10.1103%2Fphysrevlett.122.201302, doi:10.1103/physrevlett.122.201302.

[237] Hartle, J. B. and Hawking, S. W. Wave function of the universe. *Phys. Rev. D*, **28** (1983), 2960. Available from: https://link.aps.org/doi/10.1103/PhysRevD.28.2960, doi:10.1103/PhysRevD.28.2960.

[238] Lachièze-Rey, M. and Eze-Rey, M. L. Spin and clifford algebras, an introduction. (2005). Available from: https://hal.archives-ouvertes.fr/hal-00502337, doi:10.1007/s00006.

[239] Shurtleff, R. The lorentz group with dual-translations and the conformal group (2016). Available from: https://arxiv.org/abs/1607.01250, doi:10.48550/ARXIV.1607.01250.

[240] Baez, J. C. and Crans, A. S. *Higher-Dimensional Algebra VI: Lie 2-Algebras* (2010). arXiv:math/0307263.

[241] Livine, E. R. and Tambornino, J. *Spinor Representation for Loop Quantum Gravity*. *J. Math. Phys.*, **53** (2012), 012503. arXiv:1105.3385, doi:10.1063/1.3675465.

Danksagung

I would like to dedicate this work to my grandparents *Rgaya Bent el Bakouch*, *Mohamed Sassi Boukraa* and my brothers *Hamma* and *Houssam*.

The work produced in this thesis would not have been possible without the constant support, mentoring, and guidance of my supervisor Daniele Oriti. It also would not have been possible without the amazing collaboration I got to have with Prof. Stefano Liberti and Matteo Laudonio.

I would like to express eternal gratitude to Andreas Pithis and Christophe Goeller and Luca Marchetti for their constant support, advice, and constructive discussions and aside from this professional side, for being amazing friends! Also many thanks to Simon Langenscheidt for always saving my life when I am not around in Munich.
I was lucky to have met Daniele and Silke Pranzetti a few years ago, who made the Ph.D. journey enjoyable, fruitful, and meaningful. For that, there are no words to portray my gratitude.
Now comes the hidden agents who helped make this journey easier and more exciting on a daily basis. I am without a doubt eternally in debt to my parent *Hamadi*, *Souad*, and *Fatia* for just being the way they are and being my guardian angels. This is extended to my cousins *Djas, Sophie and Celine, Hama and Houssam* (of course!).
Then there is of course *Arij Ben Rejeb*, I can't thank you enough *sadi9i*, you know your place in my heart. Alice my *cicci*, is the most wonderful and amazing person that always knew everything and was there every step of the way!
Eugenia Colafranceschi, my *cara*, thank you for your support and for being an amazing friend despite the ocean separating us.

Schließlich möchte ich *Hanjo Klimpel* dafür danken, dass er so ist, wie er ist: ein verrückter, hilfsbereiter und großherziger Mann. Danke, dass du mich immer unterstützt, egal was ich tun muss, sei es für meine Arbeit, meine Familie oder meine Freunde.

This thesis was financially supported by the Stiftung der Deutschen Wirtschaft.